Production and Characterization of Artificial Spider Silk Fibers with the Same Toughness as Natural Dragline Silk Fibers

Dissertation

zur Erlangung des Grades

Doktor der Naturwissenschaften

im Promotionsprogramm „Molekulare Biowissenschaften" der

Bayreuther Graduiertenschule für Mathematik und Naturwissenschaften (BayNAT)

Universität Bayreuth

Aniela Heidebrecht

M. Sc. Natur- und Wirkstoffchemie

Bayreuth, 2016

Die vorliegende Arbeit wurde in der Zeit von November 2011 bis August 2016 in Bayreuth am Lehrstuhl Biomaterialien, Fakultät für Ingenieurwissenschaften, unter Betreuung von Herrn Prof. Dr. Thomas Scheibel angefertigt.

Vollständiger Abdruck der von der Bayreuther Graduiertenschule für Mathematik und Naturwissenschaften (BayNAT) der Universität Bayreuth genehmigten Dissertation zur Erlangung des akademischen Grades eines Doktors der Naturwissenschaften (Dr. rer. nat.).

Dissertation eingereicht am: 09.08.2016

Zulassung durch Leitungsgremium: 30.08.2016

Wissenschaftliches Kolloquium: 28.10.2016

Amtierender Direktor: Prof. Dr. Stephan Kümmel

Prüfungsausschuss:

Prof. Dr. Thomas Scheibel   (Erstgutachter)

Prof. Dr. Birgitta Wöhrl   (Zweitgutachterin)

Prof. Dr. Stephan Schwarzinger   (Vorsitz)

Prof. Dr. Stefan Geimer

Für meine Familie und Markus

TABLE OF CONTENTS

SUMMARY

Natural spider silk fibers combine extraordinary properties such as strength and flexibility resulting in a toughness no other natural or synthetic fibrous material can accomplish, designating spider silk fibers as an interesting material for various applications in the textile, automotive and biomedical industry. However, the large amount and consistent quality needed for industrial applications cannot be obtained by harvesting spider silk webs or by farming and forcible spider silking. Therefore, the production of artificial spider silk fibers is a prerequisite in order to make spider silk fibers industrially available. Even though spider silk fibers and especially their outstanding mechanical properties have been in the focus of research for decades, the production of artificial fibers mimicking the mechanical properties of natural spider silk fibers is still unsuccessful.

The main objective of this work was to produce fibers based on recombinant spider silk proteins possessing the same toughness as natural spider silk fibers. Firstly, eight recombinant spidroins, called eADF3, which are based on ADF3, one of the spidroins found in the dragline silk of the European garden spider *A. diadematus*, were engineered. Even though the tripartite structure of spidroins, comprising a highly repetitive core and non-repetitive amino- and carboxy-terminal domains, is well known, the influence of the terminal-domains on the mechanical properties is not yet understood. In order to get an insight into their function, the contribution of individual spidroin domains onto assembly and their influence on the mechanical properties of the spun fibers was analyzed. For this purpose, proteins comprising either the repetitive domain in varying lengths ($(AQ)_{12}$ and $(AQ)_{24}$), or additional terminal domains ($N1L(AQ)_{12}$, $N1L(AQ)_{24}$, $(AQ)_{12}NR3$ and $(AQ)_{24}NR3$) or both ($N1L(AQ)_{12}NR3$ and $N1L(AQ)_{24}NR3$) were investigated.

The next step towards fiber production was the preparation of aqueous spinning dopes. In contrast to organic solutions, aqueous dopes enable protein self-assembly and prevent possible health risks when using artificial fibers for biomedical applications. Two aqueous spinning dopes were developed in this work: 1) a "classical" (CSD) and 2) a "biomimetic" spinning dope (BSD). To prepare a CSD, a solution with relatively low spidroin concentration (2-3 % (w/v)) was step-wise concentrated using dialysis against a polyethylene glycol (PEG) solution, yielding protein concentrations between 10-17 % (w/v). In order to achieve a self-assembled spinning dope, diluted spidroin solutions were dialyzed against a phosphate-containing buffer. This self-assembly leads to a liquid-liquid phase separation of the proteins into a low-density and a self-assembled high-density

phase, yielding concentrations between 10-15 % (w/v). Strikingly, only eADF3-variants comprising the carboxy-terminal domain self-assembled upon dialysis against a phosphate-containing buffer. Even though both types of spinning dopes were suitable for wet-spinning recombinant fibers from all proteins (if applicable), the mechanical properties of the spun fibers differed depending on the used type of dope. For fibers wet-spun from CSD, the highest toughness (111 MJ/m^3) was achieved with N1L(AQ)$_{12}$NR3 fibers that were post-stretched to 600 % of their initial length. Determining the mechanical properties of post-stretched (AQ)$_{12}$NR3 and N1L(AQ)$_{12}$NR3 fibers spun from BSD revealed a significant increase in extensibility and toughness compared to the corresponding fibers spun from CSD. The toughness was equal to ((AQ)$_{12}$NR3, 171.6 MJ/m^3) or even slightly exceeded (N1L(AQ)$_{12}$NR3, 189.0 MJ/m^3) that of natural spider silk fibers (167.0 MJ/m^3).

Structural analyses using SAXS measurements of (AQ)$_{12}$NR3 fibers spun from CSD and BSD revealed a β-sheet crystal size of 7.1 nm, which corresponds to the reported size of these crystallites in natural spider silk fibers (5.5-7.3 nm). Another characteristic attribute of natural spider silk fibers is the strong orientation of the crystalline structures along the fiber axis. The orientation of these domains was analyzed using FTIR measurements. In comparison to the crystallites in natural spider silk fibers ($S = 0.89$), the crystallites in artificial spider silk fibers were less oriented along the axis (CSD: $S = 0.32$; BSD: $S = 0.47$). Similar results were obtained when analyzing the low orientation of the amorphous areas, even though the difference in orientation between natural ($S = 0.17$) and artificial (CSD: $S = 0.10$; BSD: $S = 0.13$) spider silk fibers was not as great. Interestingly, the effect of post-stretching on the molecular order in the fibers was higher in fibers spun from BSD than CSD, meaning the foundation for a high structural order is already laid in the spinning dope. The previously determined superior mechanical properties of fibers spun from BSD compared to those spun from CSD can clearly be ascribed to the increased alignment of the nanocrystals in the BSD fibers.

These results indicate that the production of artificial fibers with the mechanical properties as seen in natural silk fibers requires a spinning process that integrates shear forces during formation of the fiber in order to obtain a high order as found in natural silk fibers.

ZUSAMMENFASSUNG

Natürliche Spinnenseidenfasern besitzen außergewöhnliche Eigenschaften wie ihre Kombination aus Stabilität und Dehnbarkeit, die ihnen eine Belastbarkeit verleiht, die kein anderes natürliches oder synthetisches faserförmiges Material erreicht. Aufgrund dieser Eigenschaften stellen Spinnenseidenfasern ein interessantes Material für verschiedene Anwendungen in der Textil-, Automobil- und biomedizinischen Industrie dar.

Die große Menge und gleichbleibende Qualität, die für industrielle Anwendungen benötigt werden, können jedoch nicht durch das Ernten von natürlichen Spinnenseidennetzen oder Spinnenfarmen erhalten werden. Daher ist die Produktion von artifiziellen Spinnenseidenfasern eine Voraussetzung um dieses Material für industrielle Anwendungen verfügbar machen zu können. Obwohl Spinnenseidenfasern und deren außergewöhnliche mechanische Eigenschaften seit Jahrzehnten im Fokus der Forschung stehen, blieb die Produktion von artifiziellen Fasern, die die mechanischen Eigenschaften der natürlichen Spinnenseidenfasern imitieren, bisher erfolglos.

Das Ziel dieser Arbeit war die Produktion von Fasern basierend auf rekombinanten Spinnenseidenproteinen, die dieselbe Zähigkeit wie natürliche Spinnenseidenfasern besitzen. Zunächst wurden acht rekombinante Spinnenseidenproteine, genannt eADF3, konstruiert. Diese Proteine basieren auf ADF3, einem der Spinnenseidenproteine, aus denen der Abseilfaden der Gartenkreuzspinne *A. diadematus* besteht.

Spinnenseidenproteine setzen sich aus einer Zentraldomäne mit repetitiven Sequenzen zusammen, die von kleinen nicht-repetitiven, amino- bzw. carboxyterminalen Domänen flankiert wird. Obwohl diese dreigeteilte Struktur bereits detailliert analysiert wurde, ist der Einfluss der terminalen Domänen auf die mechanischen Eigenschaften der Spinnenseidenfasern nicht vollständig erklärt. Durch Variation der nicht-repetitiven Domänen, sowie der Größe der repetitiven Kerndomäne, wurde deren Einfluss auf das Assemblierungsverhalten der Proteine und auf die mechanischen Eigenschaften der gesponnenen Fasern analysiert. Zu diesem Zweck wurden Proteine untersucht, die entweder die repetitive Domäne in unterschiedlichen Längen ($(AQ)_{12}$ und $(AQ)_{24}$), zusätzlich eine terminale Domäne ($N1L(AQ)_{12}$, $N1L(AQ)_{24}$, $(AQ)_{12}NR3$ und $(AQ)_{24}NR3$) oder beide terminale Domänen enthielten ($N1L(AQ)_{12}NR3$ and $N1L(AQ)_{24}NR3$).

Als nächster Prozessschritt folgte die Herstellung von wässrigen Spinnlösungen. Im Gegensatz zu organischen Lösungen ermöglichen wässrige Spinnlösungen eine Selbstassemblierung der Proteine und beugen möglichen Gesundheitsrisiken vor, falls

artifizielle Fasern für biomedizinische Anwendungen eingesetzt werden sollen. In dieser Arbeit wurden zwei Arten von wässrigen Spinnlösungen entwickelt: 1) eine „klassische" (*classical spinning dope*, CSD) und 2) eine „biomimetische" Spinnlösung (*biomimetic spinning dope*, BSD). Zur Herstellung einer CSD wurde eine Lösung mit relativ geringem Spinnenseidenproteingehalt (2-3 % (m/V)) schrittweise konzentriert. Hierzu wurde die Proteinlösung gegen Polyethylenglykol (PEG) dialysiert und somit Proteinkonzentrationen im Bereich von 10-17 % (m/V) erreicht. Biomimetische Spinnlösungen wurden durch eine Dialyse der Proteinlösung gegen einen phosphathaltigen Puffer hergestellt. Der Phosphatgehalt des Puffers bewirkte eine flüssig-flüssig Phasenseparation der Proteine in eine Phase mit geringer Proteinkonzentration und einer Phase mit einer hohen Proteinkonzentration von 10-15 % (m/V). Diese Selbstassemblierung nach Dialyse gegen einen phosphathaltigen Puffer trat jedoch nur bei eADF3-Varianten auf, die die carboxy-terminale Domäne enthielten. Obwohl sich beide Arten von Spinnlösungen zum Nassspinnen von artifiziellen Fasern aus allen rekombinanten eADF3-Varianten eigneten, variierten die mechanischen Eigenschaften der gesponnenen Fasern in Abhängigkeit von der eingesetzten Spinnlösung.

Die größte Zähigkeit der Fasern die aus CSD gesponnen wurden (111 MJ/m^3), wurde mit 600 % nachgestreckten $N1L(AQ)_{12}NR3$-Fasern erreicht. Im Vergleich zu den korrespondierenden Fasern, die aus CSD gesponnen wurden, zeigten nachgestreckte $(AQ)_{12}NR3$- und $N1L(AQ)_{12}NR3$-Fasern, die aus BSD gesponnen wurden eine signifikant erhöhte Extensibilität und Zähigkeit. Die Zähigkeit dieser Fasern entsprach ($(AQ)_{12}NR3$, 171.6 MJ/m^3) oder überstieg sogar ($N1L(AQ)_{12}NR3$, 189.0 MJ/m^3) die der natürlichen Spinnenseidenfasern (167.0 MJ/m^3).

Strukturanalysen mittels SAXS-Messungen von $(AQ)_{12}NR3$-Fasern die aus CSD und BSD gesponnen wurden, ergaben eine Größe der β-Faltblatt-Kristalle von 7.1 nm, die mit der berichteten Größe dieser Kristalle in natürlichen Spinnenseidenfasern (5.5-7.3 nm) übereinstimmt. Eine weitere charakteristische Eigenschaft natürlicher Spinnenseidenfasern ist die starke Ausrichtung der Kristallstrukturen entlang der Faserachse. Die Orientierung dieser Strukturen wurde mittels FTIR-Messungen analysiert. Im Vergleich zu der starken Ausrichtung der Kristallstrukturen der natürlichen Spinnenseidenfasern ($S = 0.89$), zeigten die Kristalle der artifiziellen Spinnenseidenfasern eine geringere Orientierung entlang der Faserachse (CSD: $S = 0.32$; BSD: $S = 0.47$).

Ähnliche Ergebnisse wurden bei der Analyse der weitestgehend unorientierten amorphen Bereiche erhalten, jedoch fiel der Unterschied der Orientierung dieser Bereiche zwischen natürlichen ($S = 0.17$) und artifiziellen (CSD: $S = 0.10$; BSD: $S = 0.13$) Spinnenseidenfasern geringer aus. Interessanterweise beeinflusste der Effekt des Nachstreckens die molekulare Ordnung der Faser, die aus BSD gesponnen wurden, stärker als die Fasern, die aus CSD gesponnen wurden. Dies weist darauf hin, dass die Grundlage für eine hohe strukturelle Ordnung bereits während der Entstehung der Spinnlösung gelegt wird.

Die zuvor ermittelten, im Vergleich zu Fasern aus CSD gesponnenen, überlegenen mechanischen Eigenschaften der Fasern, die aus BSD gesponnen wurden, können eindeutig der erhöhten Ausrichtung der molekularen Strukturen zugewiesen werden. Diese Ergebnisse weisen darauf hin, dass die Produktion von artifiziellen Fasern mit naturähnlichen mechanischen Eigenschaften einen Spinnprozess benötigen, bei dem die Proteinlösung bereits während der Faserbildung Scherkräften ausgesetzt ist, um eine hohe strukturelle Ordnung wie in natürlichen Spinnenseidenfasern zu generieren.

1. INTRODUCTION

1.1. Silk

The term "silk" is used to describe protein fibers produced by the classes of arachnids, insects and myriapoda, all belonging to the phylum of arthropods (*arthropoda*).[1] Its wide diversity, given by the number of arthropod lineages and the fact that the ability to produce silk has evolved multiple times,[1] complicates a distinct definition.[2] Nevertheless, there are certain features which are common among all silks. Silks are fibers which consist of structural extracorporeal proteins with highly repetitive sequences.[3] In particular, these proteins are rich in alanine, serine, and/or glycine and fold into different secondary structures, resulting in a semicrystalline material.[3] Additionally, processing of silk proteins starts with an aqueous, concentrated solution, also referred to as spinning dope, which are stored in specialized glands. The spinning process involves a highly controlled phase transition of the aqueous, liquid solution to water insoluble solid fiber, which is initiated by shear forces.[4,5]

1.1.1. Insect silk

Many insect species, including dragonflies, crickets, lacewings, bees and moths produce silk for different purposes, such as protective sheltering, offspring protection and reproductive purposes.[1] Insect silk-producing glands are found in different parts of the insect's body, of which labial (also called salivary) glands are the most common, followed by dermal glands and Malpighian tubules (part of the digestive tract). Life stages in which silk is produced also varies between insect types, ranging from silk production being limited to larval stages to producing silk in all life stages. Analyses of different silk producing insects revealed no obvious causal linkages between the gland that produces the silk, the structure of the proteins, and the function of the mature silk.[1]

For the general public, the term "silk" denotes woven fabrics made of fibers produced by the silkworm *Bombyx mori* (*B. mori*), which is the most prominent insect producing silk. Due to the silk fiber's shimmering appearance, it has always been used as a luxury raw material to produce highly valuable and sophisticated fabrics.[6]

Silkworm silk production originated in China around 4000-3000 BC[7] and was confined to this territory until approx. 200 AD when the silk road enabled its trading. During the next millennium silkworm silk cultivation (sericulture) spread around the world and lead to the boom of the silk industry in Western Europe in the 12th century. However, due to the

industrial revolution and epidemics of silkworm diseases, sericulture in Europe declined, helping Japan and China to regain their role in the silk production. Nowadays, China again is the world's largest producer of silkworm silk.[7]

B. mori has been domesticated from the wild moth *B. mandarina* and is nowadays completely dependent on humans.[8,9] Silkworm larvae in their fifth instar (the stage between two successive molts) prepare to enter the pupal stage and therefore weave a cocoon to protect themselves during this vulnerable phase of their lifecycle. Before the silkworm pupae can undergo metamorphosis and moths emerge from the cocoons the latter are immersed in boiling water in order to kill the silkworm pupae. This procedure enables the harvest of the whole cocoon, which can weigh up to several grams, and allows unraveling of the silk as a single continuous thread, its length varying from 600 to 1500 m.[10] The silk produced by *B. mori* silkworm larvae is also known as mulberry silk, since the silkworm larvae feed on the leaves of white mulberry trees. Due to its high durability, pure white color and individual long fibers, *B. mori* silk is considered superior in quality to other types of silk, such as wild silk from *B. mandarina*, whose color and texture is less homogenous. In contrast to *B. mori* silk production, wild silks are only harvested after the moths have cut themselves out of the cocoon, resulting in smaller fiber fragments. Wild silks are often tougher and rougher compared to silk produced by *B. mori* silkworms and impress with their attractive coloring.[6]

In regards to other natural and synthetic fibrous materials, *B. mori* silk fibers display a moderate strength (0.6 GPa) and high extensibility (18 %), resulting in a high toughness (70 MJ/m^3) (Table 1).

Table 1: The mechanical properties of *A. diadematus* dragline silk compared with other fibrous materials (adapted from [11-15])

Material	Stiffness [GPa]	Strength [GPa]	Extensibility [%]	Toughness [MJm^{-3}]
A. diadematus **dragline**	8	1.2	24	167
B. mori **cocoon**	7	0.6	18	70
elastin	0.001	0.002	15	2
nylon 6.6	5	0.95	18	80
kevlar 49	130	3.6	2.7	50
steel	200	1.5	0.8	6
carbon fiber	300	4	1.3	25

B. mori silk is secreted as a double thread (10-25 µm in diameter)[16] from a pair of labial glands in the worms head and consists of the protein fibroin which is covered by glue-like glycoproteins called sericin.[17] Fibroin itself consists of 3 different components: heavy chain (H-chain, approx. 390 kDa), light chain (L-chain, approx. 25 kDa) and a glycoprotein called P25 (30 kDa)[18] with a molar ratio of 6:6:1 in mulberry silk.[19] The inner silk core is made up of bundles of nanofibrils,[20] which have a mean width of 90-170 nm[21] and are oriented parallel to the long axis of the silk fiber. Sericin makes up 25-30 % of weight of the silk protein[22,23] and its stickiness aids the cocoon formation and ensures a cohesion by glueing single silk threads together.[24] It is composed of 5 proteins with ranging molecular weights of 80 – 309 kDa and the preponderant amino acids were determined to be serine (30.7 ± 5.3 %), glycine (13.5 ± 2.4 %) and aspartic acid (13.9 ± 1.3 %).[25,26]

Additionally, the sericin coating acts as a protective coating, shielding the silk thread from oxidation and UV radiation and serving as a fungicidal and bactericidal agent.[27] Besides its helpful properties, sericin has been associated to human's immune response towards silk.[22] Apart from silkworms, spiders (*Araneae*) belong to the most prominent silk producers.[28]

1.1.2.   Spider silk

Due to their outstanding biomedical and mechanical properties, spider silk webs have been used by mankind since ancient times.[29] The ancient Greeks exploited the high biocompatibility and low immunogenicity of webs as they covered wounds to stop the bleeding.[30] Over two thousand years later, in 1710, first scientific studies were performed, showing that a spider's web is capable of supporting the healing process.[22,31,32] Another two centuries later, in 1901, first investigations on natural spider silk fibers as suture materials for surgery were conducted.[33] Apart from its biomedical properties, spider silks mechanical properties have also been exploited throughout history. The fibers extraordinary toughness, a combination of moderate strength and a high extensibility, enabled Australian aborigines to use spider webs as fishing nets. Aside from fishing nets, New Guinea natives produced head gear and bags from spider silk webs.[30] Until today, the high toughness is still unmatched by all natural and modern synthetic fibers (Table 1).[11] Despite the long history of spider silk use, intensive scientific research on spider silk fibers has only been conducted in the last decades. Spider silks mechanical performance, combined with a high biocompatibility, designates spider silk fibers as a highly desirable material for industrial applications, especially in the fields of biomedical applications and high-performance fibers.[34,35] Initial successes were achieved using natural spider silk fibers for biomedical applications. For example, functional recovery of nerve defects in rats and sheep was achieved by employing the fibers as a guiding material.[36,37] Additionally, spider dragline silk woven onto steel frames served as a matrix for three dimensional skin cell culture.[38]

Female orb-weaving spiders produce up to six types of silk fibers and one glue, which they use for different purposes, such as catching prey with a complex web, prey wrapping and offspring protection. Each silk is produced in a specialized gland that provides the name of the corresponding silk type. The mechanical properties (Table 2) of each silk are adapted to their various uses (Figure 1).[39] Even though these glands predominately express one spidroin type, they may also produce small amounts of spidroins normally synthesized by other silk glands and one spidroin type can itself comprise different sub-types (see chapter 1.2.2).[40]
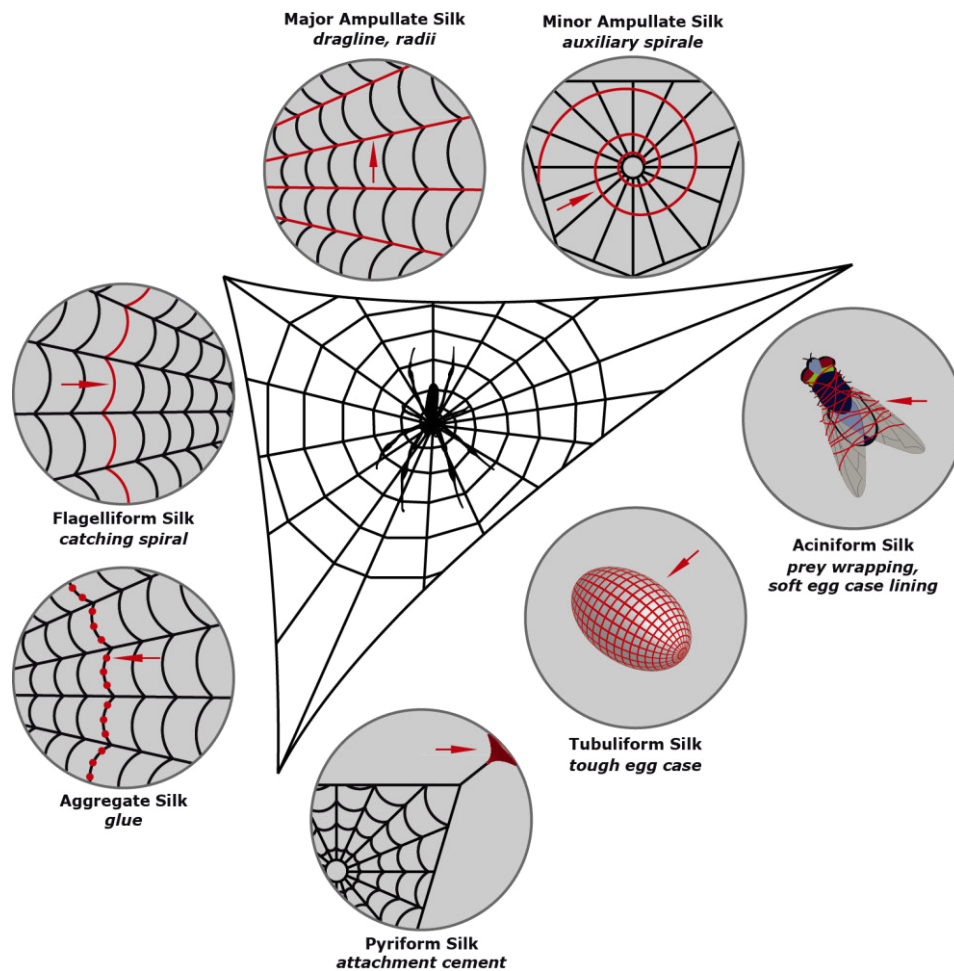
Figure 1: Schematic presentation of the six different types of spider silk fibers and one glue. (modified from [14] by courtesy of the publisher Elsevier)

The outer frame and the radii of a spider web are built up from major ampullate (MA) silk, which has a very high tensile strength.[11,41-47] The spider also uses this silk type as a lifeline, if it has to escape from a predator.[43,47,48] Among all silk types, MA silk fibers are the most intensely studied, because they exhibit a high toughness and are easily obtained by forced silking, since spiders constantly secure themselves using MA fibers. The outstanding mechanical properties of spider silk fibers are based on the hierarchical setup of the fiber and the spidroins ("spidroin" = spider fibroin)[49] involved. MA silk is made up of a core-skin structure (Figure 2). The core consists of proteinaceous fibrils which are oriented along the long axis of the fiber and can itself be divided into an outer and inner region, based on their spidroin content. These fibrils are made up of at least two major ampullate spidroins (MaSp), which have a molecular weight of 200-350 kDa (with an exception of MaSp1s from the dragline fiber of *Cyrtophora moluccensis*, 40 kDa). Two classes of MaSp proteins have been identified: one with a low (MaSp1) and one with a high proline content (MaSp2). Strikingly, in the inner core of MA fibers from *N. clavipes*

both classes of spidroins (MaSp1 and MaSp2) have been identified, whereas in the outer core area only MaSp1 was found.[50]
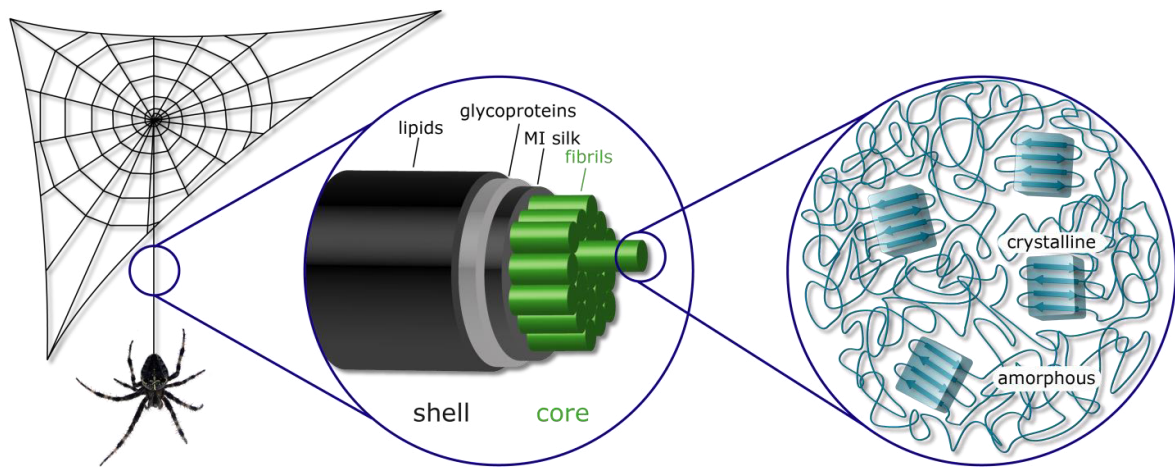

Figure 2: Core-shell structure of the dragline silk (modified from [14]). The core of the fiber comprises fibrils that are oriented along the fiber axis. On a molecular level, these fibrils consist of crystalline areas that are embedded in an amorphous matrix, depending on the amino acid composition. The core is covered by a three-layered shell containing MI silk, glycoproteins, and lipids (By courtesy of the publisher Elsevier)

The 150-250 nm thick three-layered skin[51] comprises minor ampullate (MI) silk, glycoproteins and lipids[50] and each layer serves distinct purposes. The outer lipid layer builds the coat of the fiber[50] and functions as a carrier for pheromones enabling sex and species recognition.[52] This 10-20 nm thick lipid layer is only loosely attached and does not contribute to the mechanical performance of the fiber.[50] In comparison, the 40-100 nm thick glycoprotein-layer[51] is attached more tightly than the lipid layer and thus protects the fiber more profoundly from microorganisms. Additionally, the glycoprotein-layer serves as a water balance regulator and thus influences the mechanical strength of the fiber indirectly, since the water content has a high impact on the contraction state of the fiber.[53] The inner layer of the skin consists of MI spidroins and has a thickness of 50-100 nm. Apart from protecting the fiber against environmental damage, such as microbial activity and chemical agents, this layer also supports the fiber mechanically, because of its plasticity.[50]

MA silk fibers are characterized by their outstanding mechanical properties. Their moderate strength (1.2 GPa) combined with a high extensibility (25 %) result in an outstanding toughness (167 MJ/m^3). The mechanical properties however, vary to a great extent between spider species, as well as in the same thread of one spider. Table 2 gives an overview of the mechanical properties of each silk type from a selection of spider species.

Table 2: Selection of mechanical properties of the different types of spider silk from different spiders (modified from [14,54])

Silk	Stiffness [GPa]	Strength [MPa]	Extensibility [%]	Strength [MPa]	Extensibility [%]	Toughness [MJ/m^3]	Source
		Real values		Engineered values			
Major ampullate							
Araneus diadematus	8.0±2.0	1183±334	24±8	824±10	40±3	167±65	[55,56]
Araneus gemmoides	-	4700±500	23±5	-	-	-	[34]
Araneus sericatus	8.6± -	880± -	22±-	710± -	24± -	106± -	[57]
Argiope argentata	8.0±0.8	1495±65	21±1	1217±56	23±1	136±7	[54]
Argiope trifasciata	6.9±0.4	-	-	600±50	30±2	90±10	[58]
Caerostris darwini	11.5±2.6	1652±208	52±22	-	-	354±93	[59]
Nephila clavipes	13.8± -	1215± -	17± -	-	-	111± -	[60]
Minor ampullate							
Araneus diadematus	-	-	-	-	34± -	-	[61]
Araneus gemmoides	-	1400±100	22±7	-	-	-	[34]
Argiope argentata	10.6±1.2	923±154	33±3	669±113	40±5	137±22	[54]
Argiope trifasciata	8.9±0.5	-	-	483±34	55.6±4	150±12	[62]
Flagelliform							
Araneus diadematus	0.003± -	500± -	270± -	-	-	150± -	[11]
Araneus sericatus	-	1270±45	119±5	296±10	329±32	150±9	
Argiope argentata	0.001±0.0001	534±40	172±5	95±9	465±26	75±6	[54]
Caerostris darwini	-	1400±423	101±14	-	-	270±91	[59]
Tubuliform							
Araneus diadematus	8.7±0.1	-	-	270±3	32±1	-	[63]
Araneus gemmoides	-	2300±200	19±2	-	-	-	[34]
Argiope argentata	11.6±2.1	476±90	29±2	360±70	34±2	95±17	[54]
Argiope bruennichi	9.1± -	390±30	40±7	-	-	129±27	[64]
Aciniform							
Argiope argentata	10.4±1.4	1052±120	40±2	636±78	51±4	230±31	[50]
Argiope trifasciata	9.8±1.1	-	-	687±56	83±6	376±39	[62]

-: no values reported

Additionally, the spider uses MI silk as an auxiliary spiral during web construction in order to stabilize the initial basic construct. This silk has similar mechanical properties as MA silk but its composition differs from MA silk (see chapter 1.2.2).[65-67]

Another important component of an orb web is its capture spiral, which is based on prooteins of the flagelliform gland. Due to its high extensibility (up to 270 %), flagelliform silk is able to dissipate the high kinetic energy, which results from the impact of an insect in the web.[66,68-73] With its low stiffness of 0.003 GPa, this silk can be regarded as a rubber-like material. However, its strength of 500 MPa makes flagelliform silk 10 times stronger than other synthetic or natural rubbers. The combination of its high extensibility with a moderate strength gives flagelliform silk a toughness almost identical to that of MA silk.[11] In order to prevent prey from escaping the web, ecribellate spiders (e.g. black widow *Latrodectus hesperus*) use an aggregate silk, which consists of a mixture of small hygroscopic peptides and sticky glycoproteins to cover the capture spiral.[74-76] Cribellate spiders (e.g. from the *Uloborus* sp.) surround their capture spiral with 10 nm thick cribellar fibrils instead of a glue in order to prevent prey from escaping. These dry cribellar fibrils restrain the prey solely through a combination of hygroscopic and van der Waals forces.[77,78]

Whereas major and minor ampullate and flagelliform silks serve as web scaffold, aggregate, pyriform, tubuliform and aciniform silks are produced for accessory functions. Pyriform silk serves as an attachment cement of different fibers among themselves, as well as an attachment of the orb web on various surfaces, such as trees or walls.[79,80] The spider produces these attachment discs by embedding small diameter fibers in a glue-like cement, which build a network with large diameter fibers, such as dragline silk threads.[81] The viscous liquid solidifies rapidly, producing a strong, adhesive material.[82] In order to protect its offspring against predators and parasites, female orb web spiders use tubuliform (also referred to as cylindriform) silk to build a tough case around their eggs.[40,83-88]

Even though tubuliform and MI fibers show similar mechanical properties concerning their tensile strength and extensibility, this accessory silk differs significantly from other silks.[39] Apart from its low bending stiffness,[39] tubuliform silk is the only type, whose production is limited to a spider's reproductive season.[89] Tubuliform glands are only found in female spiders and the synthesis of tubuliform proteins is induced at sexual maturation.[54]

Aciniform silk is used for multiple purposes, such as prey wrapping and as reinforcement for pyriform silk, but also as a soft lining inside the egg case.[62,90-92] Strikingly, aciniform

silk fibers have the highest toughness out of all silk types. This high toughness, which is 50 % greater than the highest values measured for major ampullate fibers, is based on aciniform's great extensibility, which is increased fourfold, whereas its strength is only half of that of major ampullate fibers.[62]

1.2. Natural silk proteins

Despite the diversity of silk proteins from different organisms and silk types, these proteins contain common patterns. Generally, silkworm silk protein (fibroin) and spider silk protein (spidroin) comprise a highly repetitive core domain that contains alternating crystalline and amorphous regions strongly influencing the mechanical properties of the spun fibers.[11,93,94] Alanine-rich stretches, such as A_n or $(GA)_n$, build up β-sheets, which are stacked into crystallites and are responsible for the high strength of the silk fiber. In contrast, glycine-rich amino acid motifs, such as $(GGX)_n$ (X = tyrosine, glutamine, leucine), fold into 3_1-helices, β-turns and β-spirals (Figure 3).[95,96] These glycine-rich stretches serve as an amorphous matrix for the crystallites and thus provide elasticity and flexibility to the fiber. Non-repetitive and highly conserved amino- and carboxy-terminal domains flank the repetitive core domain.[22,28,97] and play an important role during protein storage at high concentrations and in triggering protein assembly (see chapter 1.4).[98-104]

1.2.1. Fibroin

As mentioned above, fibroin consist of 3 different components: heavy chain, light chain and a glycoprotein called P25. Whereas H- and L-chain are linked together by a disulfide bond at the carboxy-terminus of both proteins,[24,105,106] P25 is non-covalently linked through hydrophobic interactions.[107] P25 is assumed to act as a chaperone and aids during the transport and secretion of the highly insoluble fibroin H-chain,[24,107] which is considered to determine the mechanical properties of the silk fibers. H-chain mainly consists of non-polar and hydrophobic glycine (45.9 %) and alanine (30.3 %) residues.[108,109] The much smaller fibroin L-chain on the other hand exhibits a more hydrophilic nature, due to a lower content of alanine (14 %) and glycine (9 %) residues.[110] Two crystalline polymorphs are usually distinguished for fibroin: Silk I and Silk II.[111-114] Whereas Silk I refers to the dissolved, metastable form during storage in the silk glands, Silk II relates to the solid fibroin detected in spun silk fibers.[115] While the detailed structure of Silk I is not fully understood and was described as lacking secondary structure,

or being partially disordered,[115-117] Silk II closely resembles the structure of spider silk spidroins. Similar to spider silk, the crystalline domains of silkworm fibers are also based on antiparallel β-sheets and the amorphous regions are made up of β-turns and –loops. However, in contrast to spidroins, the anti-parallel β-sheets of fibroin do not consist of poly-alanine stretches, but of $(GX)_n$-repeats, where X predominately represents alanine, serine, tyrosine, valine or threonine residues.[108,118] Even though the crystalline domains constitute a higher total volume (40-50 %) of silkworm silk fibers compared to spider silk fibers (30-40 %), these domains are to a greater extent aligned in parallel to the fiber axis in spider silk fibers, emphasizing the influence of the alignment on the mechanical properties of the fiber.

1.2.2. Spidroin

One repeat of the repetitive core domain comprises 40-200 amino acids and theses amino acid motifs are repeated up to 100 times. Figure 3 shows an overview of structural motifs found in the different silk types of *A. diadematus* and *N. clavipes*.


spider species	silk protein	β-turn spiral GPGGX / GPGQQ elastic	β-sheet $(GA)_n$ / A_n crystalline	3_1-helix GGX amorphous	spacer ~ 30 aa spacer	non-repetitive terminal domains helical
Araneus diadematus	ADF3	✔	✔	✔		✔
	ADF4	✔	✔			✔
Nephila clavipes	MaSp1	✔ ✔		✔		✔
	MaSp2	✔ ✔	✔			✔
	MiSp1	✔ ✔		✔	✔	✔
	MiSp2	✔ ✔		✔	✔	✔
	Flag	✔		✔	✔	✔

Figure 3: Structural motifs of various spider silk proteins from *A. diadematus* and *N. clavipes*. X: predominantly tyrosine, leucine, glutamine, alanine, and serine. aa = amino acid (taken from [14] by courtesy of the publisher Elsevier).

These glycine-rich stretches serve as an amorphous matrix for the crystallites and thus provide elasticity and flexibility to the fiber. Contrary to the large repetitive core domain,

the terminal domains only consist of 100-150 amino acids and they are folded into α-helical secondary structures, which are arranged in five helix bundles.[83,119-121] Apart from enabling spidroin storage at high concentrations, the terminal domains play an important role in triggering spidroin assembly (see chapter 1.4.2).[98-104]

MI silk comprises two spidroins, MiSp1 and MiSp2, which have a molecular weight of approx. 250 kDa. Even though MI silk has similar mechanical properties as MA silk, their composition differs greatly. MI spidroins of *N. clavipes* contain almost no proline residues and their glutamic acid content is significantly reduced.[122] Similar to MA spidroins, the repetitive region of MI spidroins fold into crystalline and amorphous structures. Even though MI silk possesses a high tensile strength, NMR studies showed that only a small fraction of alanine residues take part in its β-sheet crystals. In contrast to MA silk, the crystallites in MI silk contain a significant amount of glycine, since the length of repeated alanine residues is as low as three and these regions are always flanked by GA-blocks. Whereas MiSp1 mainly consists of alternating GGXGGY (X = glutamine or alanine) and $(GA)_y(A)_z$ (y = 3-6 and z = 2-5) motifs, the repeat unit of MiSp2 comprises alternating $(GGX)_n$ (X = tyrosine, glutamine, alanine; n = 1-3) and GAGA motifs.[123] The repetitive regions of the spidroin, which include the glycine-alanine crystalline β-sheet stacks, separated by amorphous α-helical GGX domains, alternate with 137 amino acid-long non-repetitive serine-rich spacer regions. In MA silk, the additional hydrophobic interactions of the polyalanine-blocks (A_n) may account for the high tensile strength.[123] Due to its high glycine content, the strength of MI silk cannot solely be due to its β-sheet structures, and Dicko *et al.*[66] assumed that cross-linking combined with specific matrix properties different to those of MA spidroins have an impact on the high strength of MI silk.

FTIR-measurements during stretching of MA and MI silk fibers showed significant differences in the structural behavior of the two silks. While the β-sheets in MA silk remained mostly unchanged, the disordered regions decreased and coiled structures became visible.[123] Conversely, in MI silk no conformational changes of the amorphous structures were visible, and only the changes of the β-sheet crystals were observed prior to breaking of the fiber. It is assumed that the GGX and spacer regions in MI silk cannot reversibly withstand the same axial tension as the β-turns in MA silk can.[123] The minor ampullate spidroin from *A. diadematus* ADF1 is similar to the MiSps of *N. clavipes*. This 174 amino acid-long protein also comprises two repeating domains, namely $(GA)_y(A)_z$ and GGYGQGY. However, compared to MiSps, tyrosines and glutamines in ADF1 are not as highly conserved, and the length of each repeat varies.[123] The gene sequence of the

carboxy-terminal domain of ADF1 on the other hand has a high sequence conservation with the *N. clavipes* MiSp gene and it even consists of a possible non-repetitive spacer region at the 5' end of the gene, which is different to that of MiSps, but one stretch is identical coding for 13 amino acids.[123]

In contrast to MA and MI silk, flagelliform silk is mainly composed of one 500 kDa protein, which contains more proline and valine and less alanine residues than the other two silk types.[122] Contrary to other silk proteins, X-ray diffraction measurements showed no crystalline fraction in flagelliform silk, which is attributed to the lack of β-sheet-building structures such as polyalanine or $(GA)_n$-sequences.[124] Flagelliform proteins of *N. clavipes* mostly contain $(GGX)_n$ and $(GPGGX)_2$ motifs (X = serine or tyrosine), which build 3_1-helices and β-turn spirals, and are responsible for the high elasticity and flexibility of this silk.[68,73,125] More than 40 adjacent linked β-turns form spring-like spirals, presumably adding to the extraordinary extensibility (> 200 %) of the fiber.[126]

Major and minor ampullate spidroins, as well as flagelliform spidroin, all consist of one or more of four amino acid motifs, A_n, $(GA)_n$, $(GGX)_n$ and $GPGX_n$, in different compositions and arrangements.[127] Furthermore, these types of silks are all involved in prey capture, and their functions are dependent on their outstanding mechanical properties. At the same time, the accessory role of pyriform, tubuliform and aciniform silks is also reflected in the composition of the respective protein. Since they hardly contain any of the typical amino acid motifs found in MaSps, MiSps and flag,[40,89] these motifs appear not to be crucial for silks not involved in prey capture.[89] Nevertheless, pyriform, aciniform and tubuliform proteins all contain highly-conserved carboxy-terminal domains.

The protein component of the small diameter fibers found in attachment disc silk is called pyriform spidroin (PySp). PySp1 (pyriform spidroin of *L. hesperus*), apart from other spidroins, does not contain conventional subrepeat modules and it lacks glycine and proline residues within its repeat units.[81] Additionally, instead of long poly-alanine stretches, PySp1 only contains 3 consecutive alanine residues in a regular pattern.[81] Other aspects, setting pyriform spidroins apart from the spider silk protein family, are their high degree of polar and charged amino acid residues, as well as a high glutamine content.[81,82] These features are suspected to have evolved due to PySps distinctive feature of being spun into an aqueous matrix of the attachment discs.[81] Additionally, high glutamine content may aid protein aggregation which is necessary for a rapid solidification of the attachment discs.[82,128]

Tubuliform spidroin (TuSp) is the major component of tubuliform silk, which the spider uses to build the eggcase. Similar to PySps, the serine-rich and glycine-poor TuSps does not contain any of the typical amino acid motifs found in MaSps, MiSps and flag.[40,89]. Instead, TuSp comprises a series of new amino acid motifs such as S_n, $(SA)_n$, $(SQ)_n$ and GX (X = glutamine, asparagine, isoleucine, leucine, alanine, valine, tyrosine, phenylalanine and aspartic acid).[89] The high content of large-side-chain amino acid likely accounts for twisted crystalline structures found during transmission electron microscopy (TEM) studies,[129] which may explain the lower stiffness of tubuliform silk fibers compared to minor ampullate silk fibers.[89,130]

Similar to TuSps, poly-alanine and glycine-alanine stretches are also not present in AcSp1, the spidroin constituting aciniform silk fibers of the banded garden spider *Argiope trifasciata*.[62] In contrast to other spidroins, AcSp1 consists of over 200 amino acid long, complex repeats, which are virtually identical to each other.[62,131] Even the most common subrepeat, poly-serine, only accounts for 8.5 % of the repeat unit, and the amino acid motif TGPSG only occurs twice in one AcSp1 repeat unit.[62] Despite a similar alternation between hydrophobic and hydrophilic regions in AcSp1 compared to MaSps, the amino acid composition of AcSp1 is much more evenly distributed than in MaSps.[131]

1.3. Evolution of silk

As previously described araneoids produce different types of silk for distinguished purposes. Whereas MA silk excels in its toughness, the characteristics of MI silk are its high strength and flagelliform silk distinguishes itself due to its high elasticity. Sequencing of araneoid spidroin genes concluded that the repetitive regions of spider silk proteins can be reduced to variable arrangements and frequencies of four amino acid motifs: A_n, GA, GGX and $GPG(X)_n$.[126] DNA encoding the amino acid motifs A_n, GA and GGX were already found in the repetitive units of basal lineages of spiders, namely *Haplogynae* and *Mygalomorphae*. Strikingly, A_n motifs are present in each spidroin from these taxa and were found in all lineages of *Araneae* studied so far.[127] Since *Mygalomorphae* (tarantulas and close relatives) diverged from *Araneomorphae* at least 240 million years ago (Middle Triassic), A_n motifs have probably been maintained in spider silks since that time.[127] Whereas the motif $GPG(X)_n$ has only been found in silks produced by araneids, the motifs A_n, GA and GGX are also present in the silks and glues of *Lepidopteran* larvae, such as *B. mori*.[124] The fundamental differences of silk production between spiders (abdominal glands) and *lepidopteran* larvae (labial glands) indicate a convergent evolution of silks

from these taxa.[132] Additional distinctions, such as the number of silks, their gland morphology and the life stages in which silk is produced, suggest that different selective factors influenced the Lepidopteran and spider's silk organization and function.[124] Nevertheless, all silk fibrous proteins among the *Araneidae* and *Lepidoptera* have been proposed to belong to the same gene family.[126,133,134] Even though the proteins encoded by these genes vary greatly in their structural organization, they are generally composed of β-sheets (either tightly packed into crystallites or loosely attached), α-helices, β-turns and spacer-regions.[126,133,135-137] Due to their highly repetitive nature, all silk genes are susceptible to recombination errors and, additionally, they all show significant allelic variation, which is likely owed to unequal crossing over.[118,134,138,139] Regardless of all their differences, the organization of silk genes and proteins indicate that a dynamic evolutionary conflict between genetic processes and natural selection has played a role in silk evolution.[124,127,138]

1.4. Natural spinning processes

1.4.1. Natural silkworm spinning process

Natural silk spinning is a highly complex process involving several parameters in a highly regulated environment. Fibroin and sericin proteins are both produced by cells lining the long tubular silk gland, which comprises 3 successive parts: 1) the thin posterior part, 2) the wider middle, and 3) the anterior part. In the posterior part of the gland, the main fibroin components (H- and L-chain fibroins and P25) are produced.[140] Afterwards, fibroin is transported into the middle region of the gland, where sericin is produced and where the proteins are stored at high concentrations (20-30 %)[141] During storage, aggregation of the highly insoluble fibroin H-chain is likely prevented due to P25 stabilizing and enhancing hydration of the complex formed with fibroin L-chain. Association with P25, which is based on hydrophobic interactions,[18] likely allows an exposure of the hydrophilic parts to the surrounding aqueous environment.[24] The fiber assembly process starts by transfer of the fibroin and sericin through the gland with simultaneous changes in pH and ionic strength of the silk solution. The amino- and carboxy-terminal non-repetitive units of the fibroin H-chain may influence the general solubility of the protein, but they certainly play an important role in assembly of the proteins to a fiber. Due to the ionic changes occurring during passage through the gland, the hydrated fibroin complexes elongate, leading to an alignment and cross-linking of the proteins.[24] Removal of water and an increase in shear stress, inflicted by spinning, enable

the formation of a silk fiber. Silkworms increase the shear stress by moving their heads from side to side, which stretches the fiber and further aligns the molecules along the long fiber axis, increasing its strength. Sericin, covering both brins, dries more slowly, gluing the two threads together and aiding cocoon formation.

1.4.2. Natural spider silk spinning process

The natural *B. mori* and spider silk spinning processes are similar, however, there are some minor differences. The tail and ampulla of the major ampullate silk gland are covered with epithelial cells, which produce and secrete spidroins into the lumen of the gland (Figure 4).
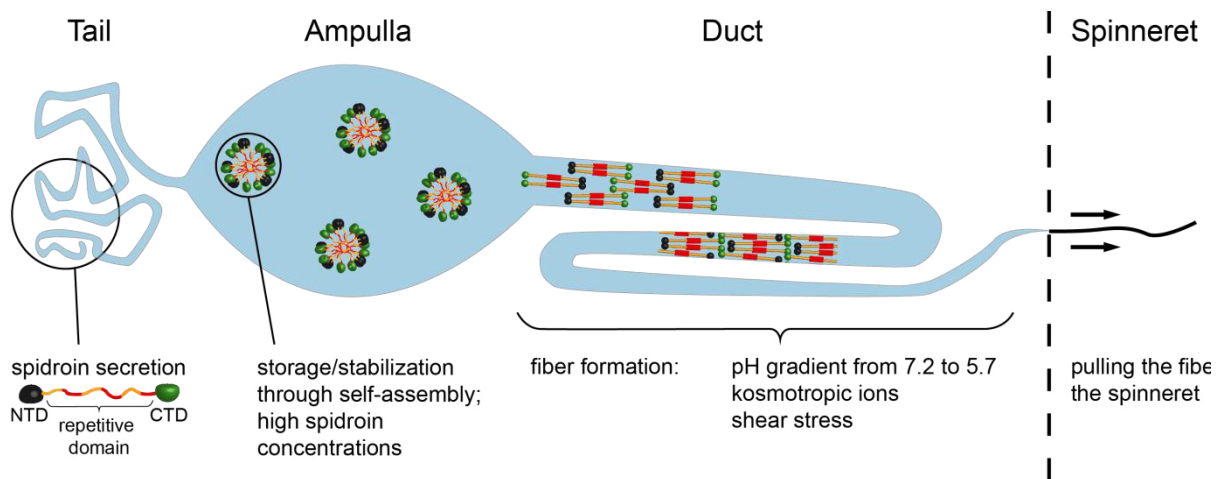

Figure 4: Overview of the natural spider silk spinning process (modified from [142] by courtesy of the publisher Springer Science and Business Media).

The presence of chaotropic sodium and chloride ions in the lumen in combination with spidroin pre-assembly enables a storage of the spidroins at very high concentrations (up to 50 % (w/v)).[143] From the ampulla, the spinning dope passes into an S-shaped tapered duct, where the transition from liquid to solid occurs. This process is explained by two theories, both of which are not mutually exclusive. The first theory regards the formation of micellar-like structures, which were detected during *in vitro* analysis of natural silk glands. The hydrophilic terminal domains of the spidroin form the interface of the micelles, shielding the hydrophobic areas from the surrounding aqueous environment.[15,100,144] However, *in vivo* analysis displayed a liquid crystal behavior of the spinning dope, providing the second theory.[45,55] In the spinning duct, the chaotropic sodium and chloride ions are replaced by the more kosmotropic potassium and phosphate ions, resulting in a salting-out of the spidroins.[145,146] Additionally, carbonic anhydrase[147]

causes an acidification from pH 7.2 to pH 5.7[148] along the duct, and this pH drop has contrary structural effects on the non-repetitive terminal domains of the spidroins. The glutamic acid residues of the amino-terminal domain are protonated sequentially, leading to a structural rearrangement resulting in the dimerization of this domain in an antiparallel manner.[149] Whereas the amino-terminal domain is stabilized by the acidification, the carboxy-terminal domain is destabilized. In combination with the addition of phosphate ions, this leads to an exposition of the hydrophobic areas within the carboxy-terminal domains enabling a parallel alignment of associated core domains.[100-102] The parallel (carboxy-terminal domain) and antiparallel (amino-terminal domain) orientation of the non-repetitive domains result in an endless spidroin network. The spinning duct is lined by the cuticular intima layer. Apart from supporting the spinning duct and protecting the epithelial cells, this layer is hypothesized to resemble a hollow fiber dialysis membrane and is responsible for the dehydration of the spinning dope.[150] Towards the end of the spinning process, excess water is resorbed by the cuticular intima layer and shear-stress is increased due to the tapering of the spinning duct and pulling of the fiber from the spider's abdomen. Recent molecular dynamics simulations[151] showed that shear stress induces the transition of a largely disordered structure into β-sheet structures in the poly-alanine region. Additionally, increasing shear stress and water removal results in a final alignment of the spidroins followed by solidification of the fiber.[152,153] The spider pulls the solid fiber from the spinneret, controlling the reeling speed either by using its hind legs or its body weight. By influencing the size and orientation of the β-sheet crystals, the reeling speed determines the mechanical properties of the silk fiber.[154] Compared to the quick formation of the liquid crystalline phase, the solid crystalline phase is formed slowly,[155] depending on the initial concentration and supersaturation of the spidroin solution. Shearing and post-stretching result in an extension of the protein chains, bringing them closer to each other, increasing the local protein concentration and thus triggering crystal nucleation between the protein chains. Applying a high reeling speed leads to a high β-sheet crystal nucleus density, resulting in fibers comprising smaller crystallites, but with an increased crystal proportion.[154] Additionally, a high reeling speed induces a stronger orientation of the β-sheet crystals along the fiber axis.[154,156]

1.5.   Structure vs. Function

As mentioned above, the crystalline and amorphous regions strongly influence the mechanical properties of the spun fibers. A fraction of the amorphous protein chains

connecting the nanocrystals is pre-stressed,[157] causing a microscopic non-equilibrium state in the mature fiber, which has been suggested to be the cause for the effect of supercontraction[158,159] in major ampullate (MA) spider silk. Supercontraction is the ability of spider silk to shrink up to 50 % when exposed to humidity.[61] Experiments using FTIR-spectroscopy in combination with mechanical forces (unidirectional stress or hydrostatic pressure) were used to demonstrate that this microscopic non-equilibrium state can be influenced through external stress. Stretching the fiber increases the stress on the protein chains, which results in a spectral red shift of the vibration peak corresponding to the β-sheet nanocrystals, whereas hydrostatic pressure on the fiber reduces the pre-stress which can be observed in a blue shift of the vibration peak.[160] It has been suggested that the load applied to a fiber is transported through the amorphous matrix to the nanocrystals, where it is transferred between chains, reinforcing the fiber similar to cross-linked polymer networks.[146,161]

The nanometer-size crystallites are made up of tightly stacked anti-parallel β-strands connected by hydrogen bonds, which contribute to the high strength of the nanocrystals.[57,162,163] Simulations revealed that under shear, these hydrogen bonds are considerably deformed in a small area of a few bonds. In this area, the hydrogen bonds act cooperatively, delocalizing the deformation and rupture of hydrogen bonds.[26,56,57,63] Through this cooperative deformation the weak, non-covalent hydrogen bonds resist to shear failure, essentially contributing to the strength of the nanocrystals. Keten *et al.*[162] performed pull-out and bending simulations to determine the size-dependent lateral stiffness of β-sheet nanocrystals during lateral loading, which represents the key loading condition of silk nanocrystals.[162,164-166] In order to examine the deformation and fracture behavior of the β-sheets at large forces, the middle β-strand of a crystal was pulled out while the outermost strands were fixed in simulations. During bending experiments, one end of the nanocrystal stayed fixed while a constant lateral force was applied to the other end. This set-up was used, because deformations of small β-sheet crystals are controlled by shear, whereas large crystals are dominated by bending. Additionally to the cooperative deformation, if a loaded β-sheet is pulled out of the nanocrystal, its hydrogen bonds can reform after an initial fracture, an ability referred to as stick-slip mechanism which considerably increases the strength of the crystals. Using computational experiments, the breaking and reforming of the nanocrystals hydrogen bonds was displayed by peaks in a force-displacement profile, leading to a considerable increase of the total dissipated energy.[161,162] While the hydrogen bonds in small crystals deform cooperatively in order to resist shear load, in large crystals, the hydrogen bonds are in tension, preventing this

cooperation. The bending to shear transition length was determined at about 2.5 nm.[161,162] Pull-out simulations of crystals with different sizes revealed that small crystals show a strong and stiff reaction, requiring greater pull-out forces and, therefore, implying a higher strength. The crystal size where strength, resilience and toughness were maximized was defined as the critical nanoconfinement size. The maximum initial stiffness, breaking strength and toughness was determined for crystals of about 3 nm in length. Resilience, meaning the elastic energy storage before initial failure, was shown to increase with a decrease in crystal size. The critical crystal width, resembling the size of one β-strand, was determined to be about 1-2 nm. Larger crystals were shown to be brittle and fail at a lower load. In these crystals, a crack-like flaw occurred due to local failure of hydrogen bonds under tension.

Even though the crystalline and amorphous areas were shown to be responsible for the strength and elasticity of the fiber, the spidroin secondary structure is not the only factor influencing the fibers mechanical properties. Based on MaSp2 of *Argiope aurantia* Brooks *et al.*[167] and Albertson *et al.*[168] designed three recombinant proteins with increasing elasticity (GPGXX) to strength (A$_n$) motif ratio, in order to determine the influence of these motifs on the mechanical properties of the spun fibers. It was hypothesized that fibers based on a spidroin with one motif each would be the strongest and least elastic of the fibers, while those containing a 3:1 ratio of elasticity to strength motif would yield the most elastic and least strong fibers. Surprisingly, the fibers containing the highest elasticity to strength ratio were shown to be the strongest (37.2 MPa), followed by fibers comprising the lowest elasticity to strength ratio (23.0 MPa). Since this behavior was not as expected, it was assumed that the mechanical properties are not only influenced by the primary and secondary structure of the proteins, but more importantly by the correct fiber assembly and alignment of the polyalanine motifs into β-sheets, in order to allow for the complex interaction of amorphous and crystalline areas (tertiary and quaternary structure).

Stress-strain curves, which are used to analyze material properties upon stretching, are commonly used to determine the mechanical properties of spider silk fibers. The characteristic stress-strain curve of spider silk fibers demonstrates their non-linear behavior and can be divided into four sections (Figure 5).
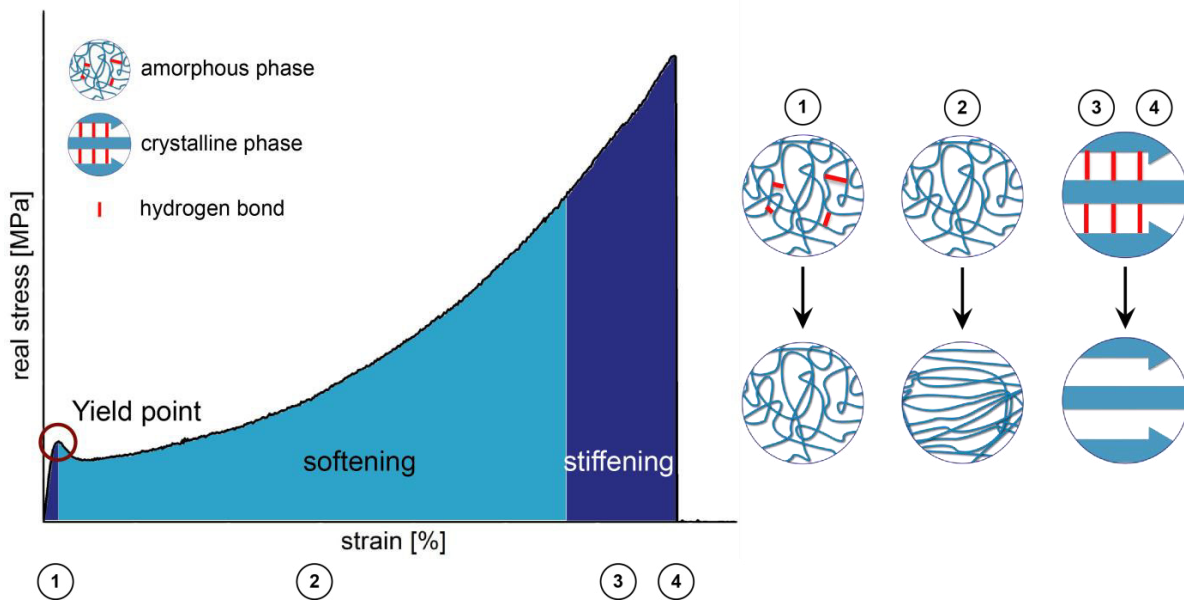
Figure 5: Characteristic stress-strain curve of spider silk fibers. 1) initial stiffening phase, 2) softening phase, 3) stiffening phase, 4) rupture of the fiber.

The first phase (1) is characterized by an initial stiff behavior of the fiber.[169] During this initial phase, the amorphous area of the composite is homogeneously stretched until a yield point is reached. At yield point, the hydrogen bonds of the 3_1-helices, β-turns and β-spirals forming the amorphous area break.[170,171] Next follows a softening phase (2), during which the amorphous phase unfolds along the stretching direction.[169] Due to the broken hydrogen bonds, the secondary structures unwind and reveal their hidden length.[170,171] During this phase, a decrease in β-turns along with an increase in β-strands was observed, meaning new hydrogen bonds were formed that build small β-sheet crystallites in the amorphous areas.[169,171] Raman analysis with simultaneously applied strain showed a perfect correlation between the wavenumber shift of hydrogen bonds under strain with the stress-strain behavior of the silk fibers.[172-174] This phase is followed by another stiffening phase (3) during which the load is transferred from the fully extended amorphous area to the β-sheet crystallites.[169,170] Additionally to the stick-slip (shear) failure, it was hypothesized that the stiffening behavior is caused by an unfolding of β-sheet crystals.[175] Using molecular dynamic calculations, the two mechanisms were compared and the following process was proposed: At first, failure of the β-sheet crystals occurs by the stick-slip mechanism, leading to the formation of smaller crystals or the separation of one β-sheet. If the failure strength of the newly build small crystal is greater than that of the original crystal, a stiffening behavior can be observed. Secondly, once the β-sheets are completely unfolded and stable, they function as a fiber reinforcing of the nanocomposite, leading to a secondary stiffening phase until the fiber ruptures (4).[162,170,176]

Summarizing, the nanoconfinement of β-sheet crystals plays an indispensable role in obtaining the great strength, extensibility and toughness of spider silk fibers. The cooperative deformation has been shown to be highly dependent on the size of the crystals and is absent once the crystals surpass a critical size. Given the plain amino acid sequence of β-sheet crystals, the mechanical properties do not arise from their chemical features (such as covalent bonds), but from the strict control over the structural arrangement. The combination of β-sheet crystals and an amorphous phase provides a great strength, extensibility and toughness to the silk fiber.

1.6.   Industrial demand for silk

Due to the above mentioned outstanding mechanical and biomedical properties of silk fibers, there is a high demand to use silk fibers industrially, and great efforts have been made to achieve this goal.

The process of farming the silkworm *B. mori* and harvesting its silk was well established and optimized to produce large amounts of silk with consistent quality. In the first stage of this process, a female silkworm lays 300-400 eggs and dies almost instantly afterwards.[6] These eggs are incubated for 10 days until the larvae hatch and begin their feeding period. For 6 weeks, a larva constantly eats mulberry leaves and molts 4 times until it reaches its fifth instar.[177] During this life stage, the larva spins silk fibers to build its cocoon, which protects it against microbial degradation and potential predators during its metamorphosis. Before the moth emerges from the cocoon, it's killed by immersing it in boiling water, thus the whole cocoon can be unraveled as a continuous fiber. A cocoon weighing several grams yields a fiber with a length between 600 to 1500 m.[10]

Because the mechanical properties of silkworm silk are inferior to that of spider silk fibers, an industrialization of spider silk production is highly desired. Farming of spiders is very time-consuming and cost-intensive, since spiders exhibit a territorial and cannibalistic behavior and cannot be kept in close quarters. Additionally, "forced silking", a process where spider silk fibers are pulled from the spinneret of the spider and reeled up onto a substrate (e.g. a motorized cylinder), only yields a few mg per spider in one silking session.[178] Further, the mechanical properties of fibers obtained by forced silking of spiders held in captivity, displayed varying mechanical properties, depending on the current climate and ambience, the applied parameters during silking as well as the spider's nutrition.[13,34,150,179-184] In general, mechanical properties of silk fibers vary, even for the same thread from the same spider.[185,186] In conclusion, to invest a great deal of time and

money in order to obtain low amounts of fibers with varying mechanical properties is not feasible for industrial application of spider silk fibers. One approach to avoid variations in quality was to dissolve natural spider silk fibers in varying solvents and to spin these reconstituted silks into fibers.

1.6.1. Reconstituted spider silk

Spinning dopes made from reconstituted insect and spider silk showed significant differences to natural silk dopes,[187] which is based on the harsh conditions needed to dissolve silk fibers. It has been shown that high temperatures and chaotropic agents caused severe degradation[188-190] and conformation changes[111,190] during dope preparation. Consequently, fibers spun from reconstituted silk dopes did neither have the structural integrity,[21] nor the mechanical properties[13,191-196] of natural silk fibers.

Seidel *et al.*[197,198] dissolved *N. clavipes* MA fibers in HFIP to a concentration of 2.5 % (w/w) and used wet-spinning to produce reconstituted spider silk fibers. The spinning dope was extruded into an acetone bath and the formed fibers were either directly post-stretched in air or immersed in water prior to poststretching. In comparison to natural MA silk fibers, these fibers showed a much higher extensibility of 100 %, but a lower strength of 320 MPa and a Young's modulus of 8 GPa.[197] In contrast, Shao *et al.*[194] hand-drew fibers from reconstituted *Nephila edulis* MA silk, which exhibited a MA-silk like extensibility of 10-27 % and a Young's modulus of 6 GPa, but a much inferior breaking strength of 100-140 MPa.[194] In this approach, the natural spider silk fibers were dissolved in buffered 8 M guanidinium chloride followed by removal of the solvent by gel filtration. From the obtained aqueous spinning dope, the group was able to hand-draw fibers.[194] Since reconstituted silk fibers are made from natural spider silk and access to the natural material is limited, producing artificial fibers from reconstituted silk dopes does not lead to the desired results. To get access to this outstanding material nevertheless, different approaches have been tested.

1.6.2. Transgenic silkworms producing silkworm/spider silk composite fibers

Another way to obtain large amounts of silk fibers with mechanical properties superior to that of the silkworm silk fibers, is to genetically modify silkworms to produce silkworm/spider silk composite fibers. Stable germline transformation of *B. mori* was achieved by using a *piggyBac*-derived vector, which is able to transpose chromosomes into *B. mori* and thus enables silkworm transformation with various genes.[199] Generally, to

create transgenic silkworms, genes are designed that encode synthetic spider silk-like sequences, as well as *B. mori* fibroin sequences and a *B. mori* promoter, which targets the protein production to the silk gland of the silkworm. These genes are then cloned into a *piggyBac*-vector, which is injected into *B. mori* eggs.

As mentioned above, the fibroin H-chain is considered to determine the mechanical properties of the silkworm silk fibers and therefore in several approaches, the fibroin H-chain genes were modified[200-202] to produce H-chain/spider silk protein, which dimerized with fibroin L-chain in the silk gland. Kuwana *et al.*[200] used the gene coding for a MA spidroin of *Araneus ventricosus* to generate transgenic silkworms that produced cocoon silk comprising the fusion protein of the fibroin H-chain and MA spidroin. The achieved spidroin content ranged from 0.37 to 0.61 % (w/w) of the fusion protein. The best performing composite fibers showed a slight increase in strength (590 MPa) and extensibility (28 %), resulting in an improved toughness (120 MJ/m^3) compared to the properties of the parental silkworm silk (520 MPa, 20 % and 80 MJ/m^3, respectively). In a similar approach, Zhu *et al.*[202] incorporated genes coding for MA silk of *N. clavipes* into the silkworms fibroin H-chain, achieving a fusion protein content in the composite fibers of 1-6 %. The best performing composite fiber showed a small increase in tensile strength (395 MPa), but no increase in extensibility (24 %) in comparison to the parental *B. mori* fiber (322 MPa, 22 %, respectively). [202] With a similar set-up, Teule *et al.*[201] achieved a fusion protein content in the composite fibers of 2-5 %. The best mechanical performance was obtained with a single composite silk fiber from one silkworm showing a toughness of 167.2 MJ/m^3, even surpassing that of natural *N. clavipes* MA silk (138.7 MJ/m^3).[201] In a different approach, Wen *et al.*[203] used a sericin promoter to target the spider silk protein component based on the MA silk of *N. clavata* to the sericin layer of the silk fiber.[203] On average, the composite fibers showed an increased strength (660 MPa) and extensibility (18.5 %) when compared to the parental silkworm silk (564 MPa and 15.3 %, respectively).[203]

In summary, the composite fibers showed an increase in breaking strain, breaking stress and toughness compared to the mechanical properties of natural silkworm silk. Despite reaching a breaking strain similar to that of MA silk fibers, the breaking stress and toughness of the composite fibers were still inferior (apart from a single outlier).[201] This performance lies in the nature of composite materials, which merge the properties of both employed materials and thus the mechanical properties of the composite fiber will always be inferior to those of natural spider MA silk fibers. Theoretically, a breaking stress of

cocoon silk equal to that of spider dragline silk could be obtained if a spidroin content of 5-8 %[200] was achieved. To this day, the maximum amount of modified H-chain/spider silk protein against total fibroin in a cocoon spun from a transgenic silkworm has been 2-5 %.[201]

1.6.3. Recombinant production of spider silk proteins

A third approach is to produce recombinant spider silk proteins biotechnologically followed by subsequent processing into fibers. Different host organisms, such as prokaryotes, eukaryotes, plants and even transgenic animals were used to produce recombinant spidroins, with varying success.

The expression of partial cDNAs in different host organisms has only led to limited success (protein yields: 4-150 mg/L[14,98,204]) because large differences in codon usages between spiders and the used host organisms cause inefficient translations. Additionally, the highly repetitive nature of spider silk genes hinders its gene manipulation and amplification.[12,69] In order to overcome these difficulties, synthetic genes were designed that encode proteins which differ from the natural spidroins but possess their key features. The expression of synthetic genes in different host organisms resulted in varying yields, which were ranging from 2 mg/L[205] to 300 mg/L[206] to 3 g/L[207] and was summarized by Heidebrecht & Scheibel (2013).[14] Regardless of the used host organisms, common problems using synthetic genes for spidroin production include inefficient transcription[208] because of secondary structure of mRNA and limitations of the cells' translational machinery, such as the depletion of tRNA pools[209] due to the highly repetitive nature of spider silk genes. With rising molecular weight of the proteins, heterologous proteins are produced due to truncations and gene instability.[191,210,211] Even though this problem is more pronounced using prokaryotes, it also occurs in eukaryotes. Compared to cytosolic production of spidroins, secretion of the spidroins to the extracellular environment simplifies the purification and results in higher spidroin yields. However, secretory production is more complex and thus more time-consuming and prone to errors.[212,213]

1.6.4. Artificial spider silk fiber spinning

1.6.4.1. *Spinning dope preparation*

For the first steps towards artificial spider silk fibers, the produced spidroins have to be dissolved. Organic solvents exhibiting strong hydrogen bonding properties are therefore

commonly used, as they assure strong solvent-protein interactions and allow production of highly concentrated spinning dopes.[214] One commonly used solvent is 1,1,1,3,3,3-hexafluoro-2-propanol (HFIP), whereby spinning dopes with spidroin concentrations of 10-30 % (w/v) can easily be achieved.[167,211,215-218] Additionally, formic acid (FA) has been employed as a solvent of spidroins.[219] The highest concentration (30 %) was achieved by dissolving lyophilized spidroin overnight in either a mixture containing NaNCS and acetate in water or in a 10 % solution of LiCl in 90 % formic acid.[220] Despite these harsh conditions a part of the spidroin did not dissolve and had to be removed by centrifugation.[220]

Despite high spidroin solubility, using organic solvents to produce spinning dopes has several disadvantages. Firstly, the putative toxicity of organic spinning dopes may cause adverse health effects, especially if the spun fibers are to be used for biomedical applications like as suture materials. Secondly, high spidroin solubility and, therefore, strong protein-solvent interactions may also prevent spidroin assembly. Thirdly, application of organic solvents for industrial-scale production is less favorable, due to high costs and strict regulations of organic waste disposal. For those reasons, employment of an aqueous spinning dope that allows spidroin self-assembly and does not inflict possible health risks of fibers spun for medical applications is desired.

Although the advantages of using aqueous spinning dopes are evident, these dopes are difficult to prepare. Often, spidroins are purified using a precipitation step such as lyophilization or salting-out. While these steps increase the spidroins purity and prevent degradation during storage, resolving a precipitated spidroin poses a great challenge. Concentrations achieved for spidroins in aqueous solutions range from 10 to 28 %, by far not reaching that of natural spinning dopes.[144,191,220-222]

Jones *et al.*[222] added a solution containing propionic acid and imidazole to the spidroin and used sonication and heating the suspension to 130 °C for more than 48 hours to dissolve the spidroin, achieving concentrations below 12 % (w/v).[222] This indicates the high energy input that is necessary to resolve spidroins directly at high concentrations. In a different approach, the purified spidroins were not precipitated, but dialyzed into a buffer containing 1 M urea, 10 mM NaH_2PO_4, 1 mM Tris and 20 mM NaCl after purification.[221] This solution was then concentrated by ultrafiltration till concentrations up to 25 % of spidroin were reached.[221] Several research groups reported a spontaneous self-assembly of spidroins in aqueous buffers into fibers or films after purification.[144,218,223,224] Although exploiting the spidroins intrinsic ability to self-assemble in aqueous buffers seems to be a

promising approach, this process has to be controlled and adjustable to be able to produce fibers with mechanical properties similar to those formed in nature.

1.6.4.2. *Spinning methods and post-treatment*

Commonly used artificial spinning methods differ significantly from natural silk spinning processes. Generally, methods used for spinning out of solution are wet spinning, dry spinning and electrospinning. During wet spinning, a polymer or protein solution is extruded into a coagulation bath, where the polymer precipitates and a fiber is formed. In dry spinning and electrospinning, polymers or proteins are solved in a high volatile organic solvent and extruded into air. While fiber formation depends solely on the fast evaporation of the solvent during the dry spinning process, during electrospinning, the dope is extruded into an electrostatic field, which triggers repulsive forces in the extruded solution. This leads to an eruption of a thin jet that is stretched towards the counter electrode (e.g. a collector), during which time the solvent evaporates and a solid fiber is formed.[225,226] Depending on the used collector, the spun fiber is deposited randomly or oriented in a certain direction, yielding a nonwoven mat or oriented fiber bundle.[227]

Theoretically, all three spinning methods are suitable for spider silk fiber spinning, because organic as well as aqueous spinning dopes can be used. Practically, however, attempts to dry-spin silk fibers have not been successful so far, since dry-spinning out of an organic solution results in mechanically unstable fibers.[15] Using an aqueous spinning dope for dry-spinning was not achieved so far, because this technique relies on a highly volatile solvent for fast fiber formation. Electrospinning and wet spinning, on the other hand, have successfully been used for producing artificial spider silk fibers. However, tensile testing of electrospun artificial fibers showed inferior mechanical properties compared to that of natural spider silk fibers.[220,228] Since electrospun fibers are commonly used as nonwoven meshes for filter[229] or biomedical applications[205,230-232] without the need of extraordinary mechanical properties, in this case, mechanical properties can be neglected. Therefore, of the commonly known spinning methods, only wet-spinning was employed successfully for producing artificial spider silk fibers with respectable mechanical properties.

Spinning dope extrusion into coagulation baths, containing monohydric alcohols, such as methanol, ethanol, or isopropanol initiates fiber formation through dehydration of the spidroins, yielding single spidroin fibers with a diameter in the micrometer range.

Compared to other spinning techniques, wet spinning has the advantage of a rather "slow" fiber formation that enables a high degree of alignment of the spidroins during the spinning process. An alignment of the spidroins is a prerequisite to produce fibers with outstanding mechanical properties, since it allows the formation of a structural hierarchy of the spidroins. Another advantage is the variability of the wet spinning process. By changing the spinning dope and/or the composition of the coagulation bath, fiber properties are influenced, allowing the production of fibers with tunable mechanical properties. Apart from pure alcohols,[168,202,215,216,222] mixtures with water are often used as coagulation baths.[191,211,218,220,221] The presence of water slows down the coagulation rate of the spidroins, and, at the same time, works as a plasticizer for the spun fiber, reducing its brittleness and preventing a clogging of the spinneret.[217] Post-treatment of the spun fibers, such as washing and/or stretching by drawing them in air or inside a bath, removes the solvent or coagulation bath residues after spinning and improves the mechanical properties of the fibers. Post-stretching has been shown to cause a higher content of β-sheets[216] and to align the β-sheet crystals along the long fiber axis.[15] Using baths consisting of primary alcohols (e.g. methanol, ethanol) for post-stretching was shown to induce a higher strength and stiffness in fibers, whereas secondary alcohols (e.g. isopropanol) added to the fibers extensibility.[168] Unlike coagulation baths, post-stretching baths containing pure alcohols are not feasible for post-treatment of the fibers, since the absence of water results in brittle fibers. Water adds plasticity to the fibers, enabling the proteins to rearrange and align along the fiber axis. Further, the post-stretching bath can be heated in order to increase plasticity of the fiber. Although a range of parameters have been shown to work for a lot of fibers spun from different protein solutions (see chapter 1.6.4.3), the optimal combination of the different parameters, such as the type of bath, water content and temperature have to be tuned for each protein and type of spinning dope.

1.6.4.3.   *Recombinant spider silk fibers produced by wet-spinning*

The majority of recombinant spider silk fibers were produced by wet-spinning from a HFIP-based spinning dope, and all of the recombinant proteins were produced by using *E. coli* as a host organism.

An *et al.*[216] used HFIP and recombinant spidroins based on MaSp1 of *N. clavipes* to produce a 30 % (w/v) spinning dope. After wet-spinning into 100 % isopropanol, the fibers were immersed in a bath containing a 75 % isopropanol/water mixture and were stretched to three times their initial length. Using these spinning and post-treatment parameters, the

recombinant fibers obtained a Young's modulus (6 GPa) and extensibility (31 %) similar to that of natural MA silk fibers (8 GPa and 24 %, respectively), but showed a strength (233 MPa) and toughness (47 MJ/m^3) far below that of the natural role model (1183 MPa and 167 MJ/m^3) (Table 3).

Table 3: Overview of wet-spinning conditions used for producing recombinant spider silk fibers from organic spinning dopes including the mechanical properties of fibers.

	Wet-spinning conditions			Mechanical Properties				
Spinning dope	Max. protein concentration [%]	Coagulation bath	Post-treatment	Stiffness [GPa]	Strength [MPa]	Extensibility [%]	Toughness [MJm^{-3}]	Source
HFIP	30	100 % IPA	75 % IPA	6.2± -	233.5± -	31.3± -	46.8± -	[216]
HFIP (addition of 15 % water prior to spinning)	30	90 % IPA	N/A	0.8±0.5	28.6±17.2	3.2±1.2	0.5±0.3	[218]
HFIP (5 % v/v added to dope prior to spinning)	15	100 % IPA	80 % IPA	-	150.6±31.3	84.5±37.8	89.1±23.9	[215]
HFIP (evaporation of HFIP prior to spinning)	60	100 % IPA	85 % IPA, 60 °C	1.8± -	34.4± -	302.7± -	35.4± -	[168]
HFIP	12	IPA	N/A	0.04±0.03	49.5±7.8	3.6±2.6	-	[167]
HFIP	20	90 % MeOH	90 % MeOH	21±4	508±108	15±5	-	[211]
HFIP	10	100 mM ZnCl$_2$, 1 mM FeCl$_3$ in H$_2$O	1st draw: air 2nd draw: 50-70 % EtOH	9.3±3	308±57	10.0± -	-	[217]
60 % NaNCS, 20 % acetate solution, mix ratio: 8:2 or 10 % LiCl in 90 % formic acid (FA)	30	96 % EtOH	1st draw: 92 % EtOH 2nd draw: 75 % EtOH	-	100-150	5-15	-	[220]
A. diadematus dragline	N/A	N/A	N/A	8±2	1183±334	24±8	167±65	[15]

MeOH: methanol; EtOH: ethanol; IPA: isopropyl alcohol; HFIP: 1,1,1,3,3,3-Hexafluoro-2-propanol; N/A:not applicable; -: values not reported

Teule *et al.*[218] used a spinning dope containing 25-30 % (w/v) of a recombinant spidroin based on the flagelliform protein of *N. clavipes* dissolved in HFIP to produce fibers. Prior to wet-spinning into a 90 % isopropanol coagulation bath, 15 % (v/v) water were added to the spinning dope. Since no post-treatment of the spun fibers was performed, the mechanical properties of the obtained fibers were far below that of natural spider silk fibers (Table 3).[218] In order to improve the mechanical properties of the spun fibers, prior to spinning, 5 % (v/v) toluene was added to the spinning dope containing 15 % recombinant flag-like proteins dissolved in HFIP.[215] Instead of spinning into a 90 % isopropanol bath, a coagulation bath containing 100 % isopropanol was chosen. Importantly, the as-spun fibers were post-stretched in a bath containing an 80 % isopropanol/water mixture, which led to improved mechanical properties compared to the fibers produced without post-stretching (Table 3).[215]

As mentioned above, one research group produced three different proteins with varying motif ratios.[167,168] Even though the mechanical properties of the spun fibers varied depending on the post-stretching conditions applied, the best performing fibers were obtained by extruding a spinning dope containing the protein with the highest amorphous to crystallinity ratio into a 100 % isopropanol bath. After post-stretching the spun fibers in a 75 % isopropanol/water mixture, the fibers showed a strength of 28 MPa, a stiffness of 1.8 GPa, an extensibility of 93 % and a toughness of 26 MJ/m^3.[168] Even though the extensibility of these fibers is almost 4-fold that of natural spider silk fibers, the overall mechanical properties are far below that of the natural silk.

By far the highest strength achieved for recombinant spider silk fibers was obtained by using a 285 kDa protein based on MaSp1 of *N. clavipes*.[211] This protein was solved in HFIP at a concentration of 20 % (w/v) and extruded into a coagulation bath containing a 90 % methanol/water mixture. After spinning, the fibers were post-stretched in the same bath to five times their original length. Even though this method yielded fibers with a high strength of 508 MPa and outstanding stiffness of 21 GPa, the fibers showed a lower extensibility (15 %) compared to natural silk, resulting in a medium toughness of approx. 70 MJ/m^3.[211]

Lin *et al.* [217] chose an inorganic aqueous coagulation bath containing 100 mM ZnCl$_2$ and 1 mM FeCl$_3$ for solidification of a recombinant spidroin based on TuSp1 from *N. antipodiana*. For wet-spinning, a 10 % (w/v) protein solution in HFIP was used, and the as-spun fibers were post-stretched in air followed by an additional post-stretching in 50-70 % (v/v) ethanol in water. The obtained fibers showed a higher strength (308 MPa) and

Young's modulus (9 GPa) than the natural eggcase silk (230 MPa and 6 GPa), but a lower extensibility (10 %) compared to the template (63 %).[217]

As mentioned above, a core issue of producing aqueous spinning dopes is the solubility of the recombinant spidroin. Purification of recombinant spidroins often includes a precipitation step such as lyophilization or salting-out and resolving a precipitated spidroin poses a great challenge.

In order to circumvent this obstacle, Arcidiacono *et al.* [221] chose a strategy based on column chromatography without a precipitation step to purifiy their recombinant spidroins derived from MaSp1/2 of *N. clavipes*. The obtained spidroin solution contained 160 mM to 1 M urea, 10 mM NaH_2PO_4, 1 mM Tris, 20 mM NaCl, and 10 to 100 mM glycine and was concentrated up to 25 % (w/v) protein by using ultrafiltration.[221] By extruding the spinning dope into a coagulation bath containing a methanol/water mixture, fibers were produced, but no post-treatment or characterization of the mechanical properties was performed (Table 4).

Table 4: Overview of wet-spinning conditions used for producing recombinant spider silk fibers from aqueous spinning dopes including the mechanical properties of fibers.

	Wet-spinning conditions			Mechanical Properties				
Spinning dope	Max. protein concentration [%]	Coagulation bath	Post-treatment	Stiffness [GPa]	Strength [MPa]	Extensibility [%]	Toughness [MJm^{-3}]	Source
160 mM or 1 M urea, 10 mM NaH$_2$PO$_4$, 1 mM Tris, 20 mM NaCl, 10 mM or 100 mM glycine, pH 5.0	25 (after ultrafiltration)	MeOH/H$_2$O mixture	N/A	-	-	-	-	[221]
0.1 % propionic acid, 10 mM imidazole, microwaved	12	100 % IPA	1st draw: 80 % IPA 2nd draw: 20 % IPA	-	192.2±51.5	28.1±26.0	33.8±33.5	[222]
PBS	28	MeOH/H$_2$O mixture	1st draw: MeOH 2nd draw: H$_2$O	4.9± -	219± -	59.6± -	103± -	[191]
A. diadematus dragline				8±2	1183±334	24±8	167±65	[15]

MeOH: methanol; EtOH: ethanol; IPA: isopropyl alcohol; PBS: phosphate buffered saline; N/A:not applicable; -: values not reported

Another approach to overcome the solubility issues was to use host organisms such as yeasts, plants, mammalian cells or transgenic goats to produce recombinant spidroins. Therefore, Bogush et al.[220] used the yeast *P. pastoris* for the production of recombinant spidroins derived from MaSp1 of *N. clavipes* and MaSp2 of *N. madagascariensis*. After a column chromatography-based purification, the lyophilized protein was dissolved in an 8:2 mixture of 60 % NaNCS in water with 20 % acetate solution or in a 10 % solution of LiCl in 90 % formic acid.[220] For wet-spinning, the targeted spidroin concentrations were 20-30 % (w/v), however, after overnight incubation insoluble remnants had be removed by centrifugation resulting in lower concentrated spinning dopes. Extrusion into a 96 % ethanol/water bath yielded fibers that were post-stretched firstly in a bath containing a 92 % ethanol/water mixture, followed by a 75 % ethanol/water mixture. Regarding the characterization of mechanical properties, only the strength (100-150 MPa) and extensibility (5-15 %) were reported.[220]

Solving a spidroin in an aqueous solution at high concentration requires a high energy input as shown by Jones et al. [222] Here, the spidroin, which was based on MaSp1/2 of *N. clavipes*, was produced in transgenic goats.[222] After purification, it was mixed with 0.1 % propionic acid and 10 mM imidazole in a glass vial and the mixture was sonicated and heated up to 130 °C for more than 48 h. This method yielded a spinning dope with a spidroin concentration of 12 % (w/v), and different ratios of recombinant MaSp1 and 2 were tested for fiber production. As a coagulation bath, 100 % isopropanol was used, followed by a first post-stretching step in an 80/20 mixture of isopropanol/water and a second stretching step in a 20/80 mixture of isopropanol/water. The best performing fibers showed a strength of 192 ± 51 MPa and an extensibility of 28±26 %, which results in a toughness of 34 ± 34 MJ/m^3.[222] The large variability of the fibers' mechanical properties indicates the necessity of refining the spinning and processing conditions in order to guarantee a fiber production with reproducible mechanical properties.

The highest toughness of wet-spun fibers from aqueous solutions was obtained by Lazaris et al.[191] This research group used mammalian cells to secrete soluble spidroins based on ADF3 of *A. diadematus* directly in the culture media. Even after a precipitation with 15 to 20 % ammonium sulfate, the spidroins were readily resolved in phosphate-buffered saline (PBS). This improved solubility was attributed to the presence of the carboxy-terminal domain. Extrusion of a spinning dope containing at least 23 % (w/v) of spidroin in PBS into an 80 % methanol/water mixture with subsequent post-stretching first in methanol and then in water, yielded fibers with the highest tensile properties. Spinning dopes with a

lower spidroin content and post-stretching with a lower draw ratio also yielded fibers but with inferior mechanical properties, emphasizing the strong influence of a highly concentrated spinning dope and optimal post-stretching conditions. The best performing fibers showed a strength of approx. 220 MPa, a stiffness of 5 GPa, an extensibility of 60 % and a toughness of 100 MJ/m^3 (these values were converted from the original unit gram per denier (gpd) assuming a density of 1.3 kg/m^3).[191]

1.6.4.4.   *Other recombinant spider silk fiber production methods*

Apart from wet- and electrospinning, microfluidic devices were used to produce recombinant spider silk fibers.[233] One advantage of this process is the ability to mimic aspects of the natural spinning process, such as pH drop, ion exchange and elongational flow conditions.

Exler *et al.*[144] showed that the addition of potassium phosphate to aqueous eADF3 solutions lead to spontaneous fiber formation. The recombinant spidroin eADF3 based on ADF3, a MaSp2 protein of *A. diadematus*, was produced using *E. coli* as a host organism. The feature of phosphate-induced self-assembly was used by Rammensee *et al.*[233] in order to produce fibers using a microfluidic device. The recombinant spidroin was dissolved in 6 M guanidinium thiocyanate, dialyzed against an aqueous buffer, and the obtained solution contained a spidroin concentration of 2 % (w/v). In the microfluidic device, a stream of this spidroin solution was mixed with two streams of varying potassium phosphate concentrations and pH values. Only upon applying a flow rate of 600 L/h, increasing the phosphate concentration to 500 mM and decreasing the pH to 6.0, eADF3 fibers were formed.[233] Apart from the shear forces affecting the formation of fibers, no additional post-stretching or characterization of the mechanical properties was performed. Even though this spinning method includes aspects from the natural spinning process, the gained fibers showed similar mechanical properties as fibers produced by wet-spinning. However, by fine-tuning parameters within the microfluidic channels, these devices have the potential to achieve a more sophisticated spinning process in the future.

Shear forces required for fiber formation can also be applied by hand-drawing fibers from aqueous, pre-assembled spidroin solutions.[144,218] Using the same process as Exler *et al.*[144] with subsequent ultrafiltration, Keerl & Scheibel[163] prepared aqueous spinning dopes with concentrations between 11 and 20 % (w/v). After mixing this solution with an equal volume of a phosphate-containing buffer, viscous gel-like aggregates formed, that

were separated from the solution. The best performing fibers that were hand-drawn from this solution exhibited a strength of 143.4 MPa and an extensibility of 32.2 %.[163]

After elution from a chromatography column, the recombinant spidroin purified by Teule *et al.*[218] spontaneously formed an oily looking film at the surface of the solution. Using forceps, this film was pulled to form single fibers. Due to the lack of post-stretching, the obtained fibers showed a low strength of 49.64 ± 19.35 MPa, a low Young's modulus of 1.08 ± 1.00 GPa, a nature-like extensibility of 34.06 ± 25.30 % and a low toughness of 10.6 ± 10.2 MJ/m^3.[218]

In a different approach, Stark *et al.* [223,224] used shear forces generated by gently shaking an aqueous solution for fiber formation. The recombinant spidroin based on a dragline protein of *Euprosthenops australis* was produced in a soluble form in *E. coli* using thioredoxin as fusion partner. Proteolytic release of the fusion partner after purification resulted in spontaneous fiber formation, and fibers were post-stretched two times in air. The obtained fibers appeared to be very stiff with a Young's modulus of 7 GPa, a tensile strength of approx. 150 MPa and a low extensibility of 1 %.[223,224]

2. AIM

The high toughness of natural spider silk fibers distinguishes them from other natural or man-made fibrous materials and designates spider silk fibers as an interesting material for various industrial applications in textile, automotive and biomedical fields. The large amount and consistent quality needed for industrial applications cannot be obtained by harvesting spider silk webs or by farming and forcible spider silking. Therefore, the production of artificial spider silk fibers is a prerequisite in order to make spider silk fibers industrially available.

Even though spider silk fibers and especially their outstanding mechanical properties have been in the focus of research for decades, the production of artificial fibers mimicking the mechanical properties of natural spider silk fibers is still unsuccessful. The simple looking fiber spinning of spiders actually comprises highly complex processes, which cannot be easily mimicked by technological processes. Therefore, the main objective of this work was to develop the processing and spinning of recombinant spider silk proteins to produce fibers possessing the same toughness as that of natural spider silk fibers.

For this work, eight recombinant spidroins based on ADF3, one of the spidroins found in the dragline silk of the European garden spider *A. diadematus*, were investigated. Even though the tripartite structure of spidroins, comprising a highly repetitive core and non-repetitive amino- and carboxy-terminal domains, is well known, the function of the terminal-domains is not fully understood. In order to get an insight into their function, the contribution of individual spidroin domains to assembly and their influence on the mechanical properties of the spun fibers should be analyzed. For this purpose, proteins comprising either the repetitive domain in varying lengths ($(AQ)_{12}$ and $(AQ)_{24}$), or additional terminal domains ($N1L(AQ)_{12}$, $N1L(AQ)_{24}$, $(AQ)_{12}NR3$ and $(AQ)_{24}NR3$) or both ($N1L(AQ)_{12}NR3$ and $N1L(AQ)_{24}NR3$) were chosen. Using biotechnological processes, the recombinant spidroins were produced in large amounts and with consistent quality. The parameters during fermentation of the host organism *E. coli* and purification had to be adjusted to each of the eight spidroins.

The next step towards fiber production is the preparation of spinning dopes. Organic solvents are often used for spidroin solving, due to their strong hydrogen bonding properties, which promote solvent-protein interactions and allow the production of highly

concentrated spinning dopes. However, high protein solubility and, therefore, good solvent-protein interactions may prevent protein assembly. Additionally, if the artificial fibers are supposed to be used for biomedical applications, health risks caused by toxic solvents have to be avoided. Therefore, in this work, highly concentrated biomimetic spinning dopes based on aqueous solutions should be developed. Since the recombinant spidroins eADF3 are only moderately soluble in aqueous solutions, the greatest challenge was to achieve a high spidroin concentration in aqueous solution while preventing aggregation of the protein. After developing a suitable spinning dope, it should be processed into fibers, using a wet-spinning process. During this process, the dope is extruded into a coagulation bath, where the spidroin precipitates and the solid fiber is formed. Advantages of wet-spinning over other spinning techniques are the ability to spin from different spinning dopes, allowing the use of any biopolymer, and the rather "slow" fiber formation, allowing a high degree of alignment of the spidroins during spinning, enabling the formation of fibers with superior mechanical properties.

Following their production, the recombinant spidroin fibers should be analyzed concerning their mechanical properties, as well as the influence of post-stretching thereon, and the structure of the underlying proteins in the fiber, compared to the dragline silk of *A. diadematus*. The analysis of fibers spun from dopes made of eight different proteins under different spinning and post-stretching conditions should give information about the influence of the natural spidroin structure and its spinning process on the fibers mechanical and structural properties.

3. SYNOPSIS

The present dissertation consists of four publications (shown in chapter 5), which each address development of one or more processes towards the production of artificial spider silk fibers. An overview of the whole processing steps including the corresponding publications is shown in Figure 6.
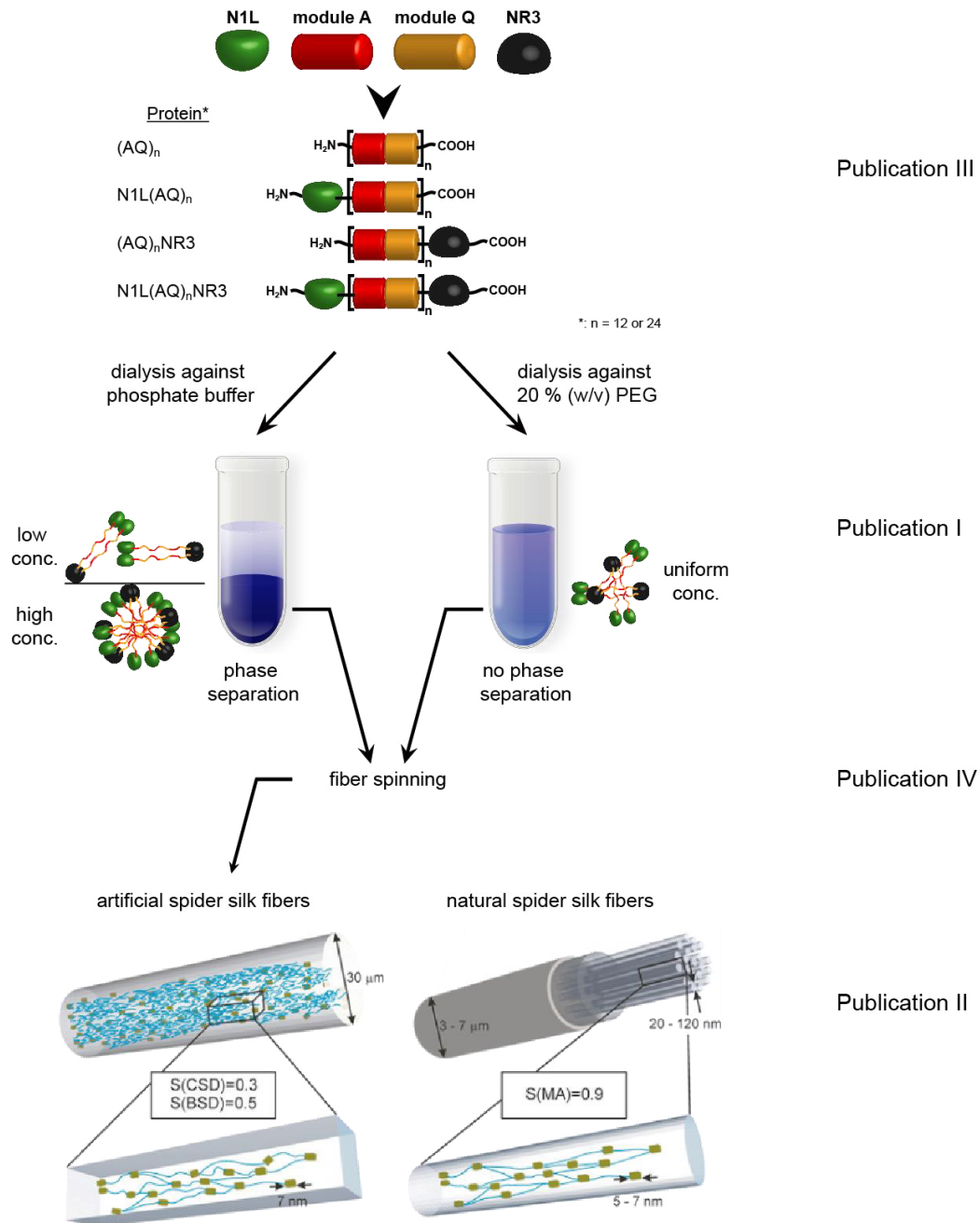

Figure 6: Overview over the steps towards the production of artificial spider silk fibers.

Initially, an overview of different attempts to produce spidroins recombinantly is given (Publication III), covering the first step towards spinning artificial spider silk fibers. Here, the advantages and disadvantages of two approaches for recombinant spidroin production, namely the expression of partial cDNAs and the expression of synthetic genes in different host organisms, were reviewed and discussed. Using the gram-negative bacteria *E. coli* for cytosolic production of recombinant spidroins is the most promising approach, because *E. coli* can easily be modified genetically and has short generation times, enabling a fast adjustment of the production system and the produced spidroins. Based hereon, the expression of synthetic genes in the host organism *E. coli* was the system of choice for recombinant spidroin production. The production and purification of eADF3((AQ)$_{12}$), -(AQ)$_{24}$, -(AQ)$_{12}$NR3, -(AQ)$_{24}$NR3 and -N1L(AQ)$_{12}$NR3 were already established before the beginning of this work, while the constructs eADF3(N1L(AQ)$_{12}$), -N1L(AQ)$_{24}$ and -N1L(AQ)$_{24}$NR3 were not available at this point. After cloning of plasmid DNA encoding these constructs, their production and purification were developed and optimized. Following the production and purification of large amounts (several grams) of each spidroin, the next aim was to develop a suitable aqueous spinning dope for wet-spinning of recombinant spidroin fibers. To achieve this aim, two approaches towards aqueous spinning dopes were realized, one conservative approach by increasing the spidroin concentration manually and one approach based on the properties of the natural spinning dope (Publication I). All eight spidroins were used to produce both spinning dope types, revealing a high impact of the carboxy-terminal domain on the assembly and storage behavior of the recombinant spidroins (Publication I).

After wet-spinning and post-stretching, if applicable, tensile testing of the fibers provided information about the influence of the terminal domains, the size of the repetitive domain and the impact of post-stretching on the mechanical properties of the spun fibers. The combination of eADF3 N1L(AQ)$_{12}$NR3 used for the production of a "biomimetic" spinning dope (BSD) and post-stretching the spun fibers at 600 % resulted in recombinant spidroin fibers with the same toughness (189.0 ± 33.4 MJ/m^3) as its natural counterpart (167.0 ± 65.3 MJ/m^3). Analysis of (AQ)$_{12}$NR3-fibers revealed a structure of the artificial fibers similar to that of natural spider silk fibers on a molecular level (Publication II), concerning the size of the β-sheet crystallites, as well as the orientation of the crystalline and amorphous phases.

3.1. Production of nature-like spider silk proteins

Since the yields of recombinant proteins decreases dramatically with increasing molecular weight, we abstained from the production of recombinant proteins with the same molecular weight as the natural spidroins (200-350 kDa), but instead focused on including all functional domains into the recombinant spidroins, namely a repetitive domain flanked by two different non-repetitive terminal domains (Figure 7).
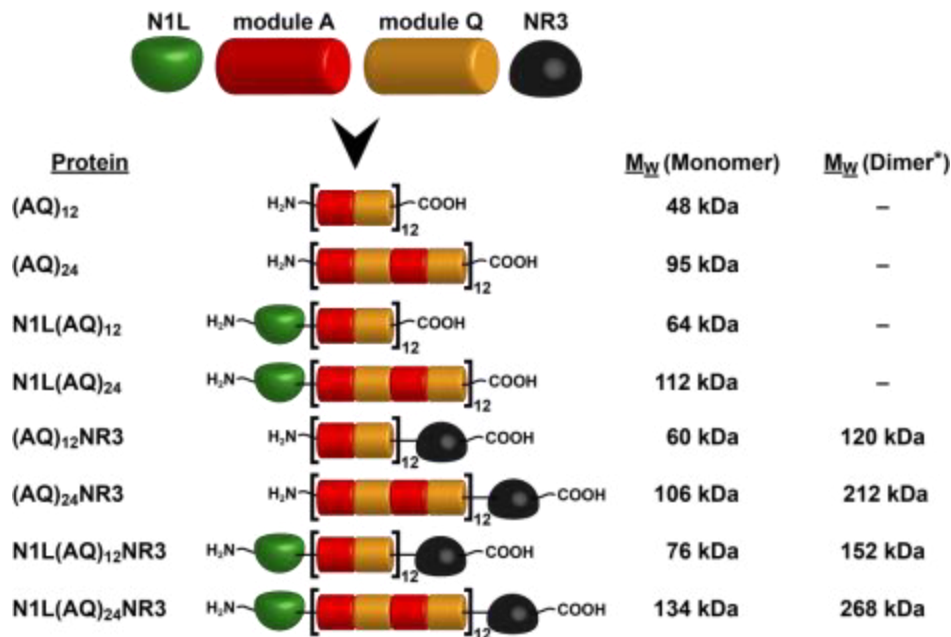

Figure 7: Scheme of the employed recombinant proteins, the sequences of the individual domains are derived from ADF3 (see the Supporting Information of Publication III), one of the two identified MaSp2 components of *A. diadematus* dragline silk. The theoretical molecular weight is shown (MW, calculated using the ProtParam tool: http://web.expasy.org/protparam/) of the respective recombinant proteins. *: Disulfide linked.[15] By courtesy of the publisher John Wiley and sons.

One of the spidroins found in the dragline of the European garden spider *A. diadematus*, namely ADF3, was used a blueprint for the recombinant spidroins. As mentioned in chapter 1.2.2, the core domain of ADF3 contains several repetitive amino acid motifs, where poly-alanine blocks fold into antiparallel β-sheets, which form crystals upon assembly of natural spider silk fibers. These crystals are responsible for the strength of the fiber and they are embedded in an extensible amorphous matrix, which comprises glycine- and proline-rich amino acid motifs.

Based on these motifs, consensus modules were developed containing a poly-alanine block (module A) and 4 repeats of the GPGQQ-sequence (module Q).[121] For the repetitive domain of the recombinant spidroins, a 12- and 24-mer of this AQ-module was used in

order to determine the influence of the molecular weight on the protein production, fiber spinning and mechanical properties. The amino- and carboxy-terminal domains, namely N1L and NR3, were added to the spidroins in order to determine their influence on handling, assembly and spinning of the spidroins into fibers. The carboxy-terminal domain NR3 corresponds to the native sequence in ADF3. Since the amino-terminal domains of natural spider silk proteins are highly conserved between spidroins and even between spider species, the amino acid sequence of the well-described amino-terminal domain NRN1 of *Latrodectus hesperus* including a linker-sequence was chosen.[98,102]

3.2. Development of aqueous spinning dopes

Apart from the used spidroins, the spinning dope has been shown to be a highly important factor for spinning.[221] As mentioned in chapter 1.4.2, natural spider silk spinning dopes are highly concentrated (up to 50 % (w/v)). In order to achieve a high spidroin concentration in an aqueous solution, different approaches have been used by scientists, and these can be assigned to three classes (as reviewed in publication IV):

1) Spidroin self-assembly in aqueous buffers[15,144,218,223,224]
2) Concentration of a diluted aqueous spidroin solution[15,221]
3) Direct solvation at high spidroin concentrations[220,222]

The aqueous spinning dopes developed in this work can be categorized to approach 1 and 2 (Figure 8).[15] For both dope types, the strong denaturant guanidinium thiocyanate was initially used for spidroin solvation, followed by its removal using dialysis against a 50 mM Tris/HCl buffer (pH 8.0). During the dialysis, 100 mM NaCl was added to the dialysis buffer in order to stabilize the spidroins in solution. Using this method, relatively low spidroin concentrations of 2-3 % (w/v) were achieved. By removal of excess water from the solution using a dialysis against a polyethylene glycol (PEG) solution, a step-wise concentration of the diluted spidroin solution was achieved. The resulting dope called "classical" spinning dope (CSD), yielded spidroin concentrations between 10-17 % (w/v). In order to achieve a self-assembled spinning dope, diluted spidroin solutions of eADF3-variants comprising the carboxy-terminal domain NR3 were dialyzed against a phosphate-containing buffer. The addition of phosphate ions to the spidroins causes a partial refolding of the carboxy-terminal domain NR3, which leads to spidroin assembly into micelles. This

self-assembly leads to a liquid-liquid phase separation of the spidroins into a low-density and a self-assembled high-density phase. Previous dynamic light scattering experiments showed that the low density phase only obtained dimeric spidroins, while in the high density phase, non-covalently associated spidroin oligomers were present (MW > 30 MDa).[144] The high-density phase yielded concentrations between 10-15 % (w/v) and was named BSD, due to the self-assembly of the spidroins. In contrast to CSD, which gelled within a few hours due to nucleated fertilization of the spidroins,[234,235] BSD was stable for 3-5 days. Even though both types of spinning dopes were suitable to wet-spin recombinant fibers from all proteins (if applicable), the mechanical properties of the spun fibers differed depending on the type of dope used for wet-spinning (see chapter 3.3).


Figure 8: Processing of recombinant spider silk proteins into (a) biomimetically and (b) classically concentrated spinning dopes. (a) Dialysis against a phosphate-containing buffer enables the formation of micellar-like structures[15,100,144] yielding a spinning dope with pre-oriented silk proteins. (b) Without pre-assembly of the proteins in the dope the formed network is weak yielding less stable fibers upon post-stretching (modified from [15] by courtesy of the publisher John Wiley and sons).

3.3. Mechanical properties of spun fibers

During wet-spinning the spinning dope is extruded into a coagulation bath containing a mixture of isopropanol and water in which the spidroin precipitates and a fiber is formed. After wet-spinning from both BSD and CSD, the spun fibers were post-stretched in order to improve their mechanical properties. In nature, spiders use their hind legs to post-stretch the fiber directly when it leaves the spinneret. The size and orientation of the β-sheet crystals in the fiber change with the reeling speed and, thus, directly influence the mechanical properties of the fiber. Du *et al.*[154] showed that a high reeling speed leads to a high β-sheet crystal nucleus density in natural silk, resulting in fibers containing smaller crystals but with an increased crystal proportion. In this work, the recombinant fibers were stretched up to 600 % of their initial length after spinning in order to align the spidroins. Tensile testing of all recombinant fibers showed that the post-stretching significantly improved the mechanical properties of the fibers (see table 1 in publication I). While recombinant fibers spun from CSD, resulted in mostly inhomogeneous and brittle fibers (Figure 9), especially when spun from dopes containing spidroins without the carboxy-terminal domain NR3, wet-spinning of BSD led to very homogeneous and long fibers. Tensile testing revealed that a) the molecular set-up of the spidroins and b) the type of dope used for spinning had a great impact on the mechanical properties of the recombinant fibers.
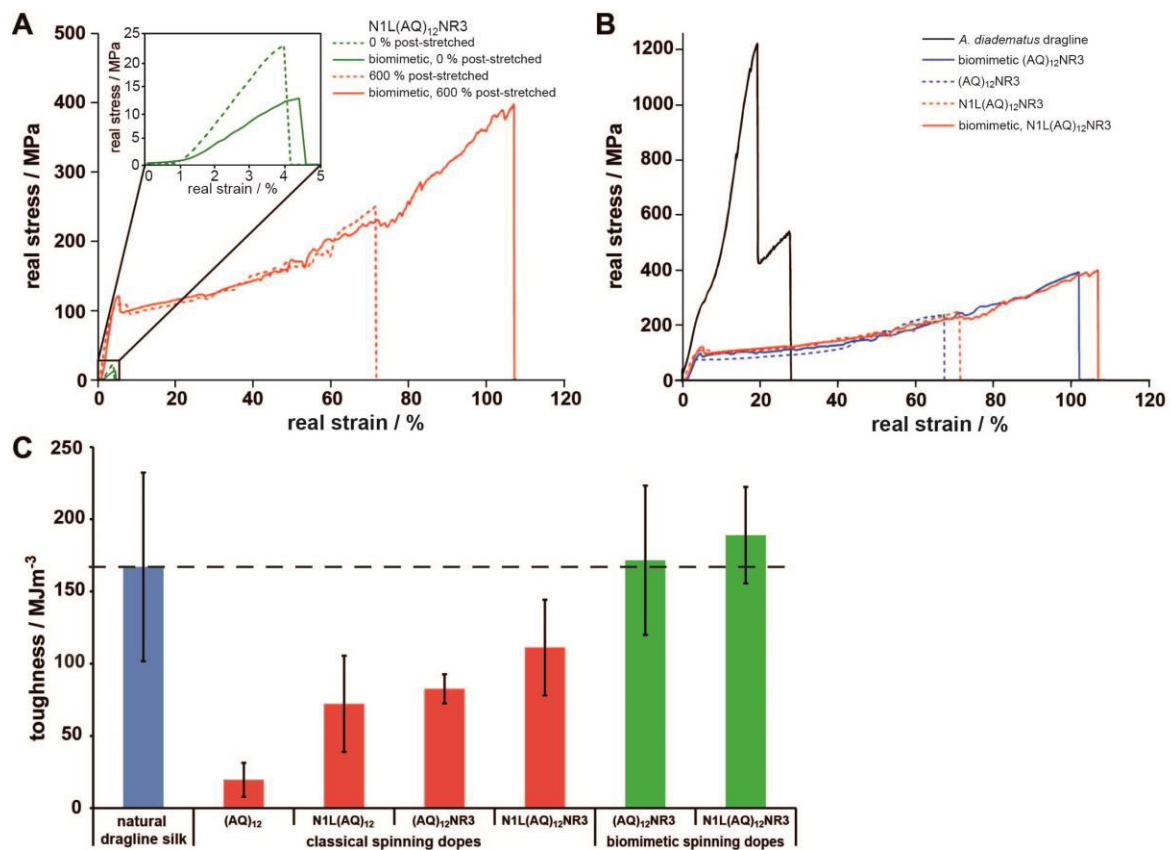
Figure 9: A,B) Real stress–real strain curves of recombinant and natural spider silk fibers. **A)** As-spun (inset) and 600% post-stretched N1L(AQ)$_{12}$ NR3-fibers, spun from "classical" (CSD) as well as "biomimetic" (BSD) spinning dopes (both 10% (w/v)) and **B)** 600% post-stretched (AQ)$_{12}$NR3- and N1L(AQ)$_{12}$NR3-fibers from CSD as well as BSD in comparison to natural *A. diadematus* dragline silk fibers. **C)** Average toughness of natural dragline silk fibers (blue), fibers spun from CSD (red) and BSD (green).[15] By courtesy of the publisher John Wiley and sons.

Post-stretching of (AQ)$_{12}$-fibers spun from CSD was only possible up to 400 % of their initial length, and the fibers appeared very brittle. In comparison, fibers spun from CSD of N1L(AQ)$_{12}$ and (AQ)$_{12}$NR3, showed a higher extensibility and strength reaching a higher overall toughness than (AQ)$_{12}$ fibers. For fibers wet-spun from CSD, the highest toughness (111 ± 33 MJ/m^3) was achieved with N1L(AQ)$_{12}$NR3 fibers that were post-stretched to 600 % of their initial length. While post-stretched (AQ)$_{12}$NR3 and N1L(AQ)$_{12}$NR3 fibers had the same strength, N1L(AQ)$_{12}$NR3 fibers showed an increase in extensibility and a lower stiffness than the (AQ)$_{12}$NR3 fibers. Determining the mechanical properties of post-stretched (AQ)$_{12}$NR3 and N1L(AQ)$_{12}$NR3 fibers spun from BSD revealed a significant increase in extensibility and toughness compared to the corresponding fibers spun from CSD. The toughness was equal to ((AQ)$_{12}$NR3, 171.6 ± 52.7 MJ/m^3) or even slightly exceeding (N1L(AQ)$_{12}$NR3, 189.0 ± 33.4 MJ/m^3) that of natural spider silk fibers (167.0 ± 65.3 MJ/m^3) (Figure 9).

Since the mechanical properties of polymer fibers are strongly influenced by the molecular weight of the polymer,[236,237] the mechanical properties of fibers spun from $(AQ)_{24}$-variants were also determined, possessing almost twice the molecular weight of the corresponding $(AQ)_{12}$-variants. As anticipated, $(AQ)_{24}$-fibers spun from CSD showed improved mechanical properties compared to $(AQ)_{12}$-fibers. Surprisingly, during the presence of one or both terminal domains N1L/NR3, the mechanical properties were no longer solely influenced by the molecular weight of the underlying core domain, but by their assembly process. N1L$(AQ)_{24}$, $(AQ)_{24}$NR3 and N1L$(AQ)_{24}$NR3 fibers spun from CSD all revealed inferior mechanical properties in comparison to $(AQ)_{24}$ fibers (see table 1 in publication I). This indicates that spider silk proteins cannot solely be treated like polymers, but that their "protein" features have a considerable influence on fiber mechanics. Since the amino-terminal domain only dimerizes upon a pH drop in the spinning duct, it is still in its monomeric form in the spinning dope, preventing a correct alignment of the repetitive parts of the spidroins. This effect is even amplified during the absence of the carboxy-terminal domain, yielding brittle fibers (see table 2 in publication I). Corresponding to the discoveries with $(AQ)_{12}$-variants, the mechanical properties of $(AQ)_{24}$NR3 and N1L$(AQ)_{24}$NR3 fibers spun from BSD showed a significant increase in strength and toughness when compared to those spun from CSD. Overall, fibers spun from both CSD and BSD of $(AQ)_{24}$-variants comprising either one or both non-repetitive terminal domains showed inferior mechanical properties in comparison to that spun from the corresponding $(AQ)_{12}$-variants. This indicates an entanglement of the large spidroin molecules once the assembly-controlling terminal domains are present, which cannot be straightened out when using the limited and non-biomimetic wet-spinning process.

The highest mean toughness $(189.0 \pm 33.4\,MJ/m^3)$ was obtained with post-stretched N1L$(AQ)_{12}$NR3-fibers spun from BSD. Even though the toughness of the recombinant fibers lies in the same range as that of natural spider silk fibers, it has to be noted that strength, extensibility and stiffness of the recombinant fibers differ significantly. The recombinant fibers are not as strong as the natural fibers, but are far more extensible. This may be due to two major discrepancies between the used set-up for this work and the natural role-model, namely 1) the application of only one spidroin and 2) the applied wet-spinning process. As mentioned in chapter 1.2.2, natural spider dragline fibers contain at least two spidroins, which likely are both crucial in order to obtain outstanding mechanical properties. Accordingly, the highly complex natural spinning process (chapter 1.4.2) cannot possibly be mimicked by a simple wet-spinning process. The development of a biomimetic spinning technology, as well as the application of more than one recombinant

spidroin will likely achieve the production of recombinant fibers with mechanical properties superior to that of the natural role-model, opening up new possibilities for fibrous materials.

3.4. Molecular structure of artificial spider silk fibers compared to natural ones

In order to determine the molecular structure of the artificial fibers, especially similarities and differences to natural spider silk fibers, FTIR and SAXS measurements were performed. Using SAXS measurements, the size of the β-sheet crystallites of the artificial fibers was determined with 7.1 ± 0.1 nm (data not shown), which corresponds to the reported size of these crystallites in natural spider silk fibers (5.5-7.3 nm).[238-240]

FTIR measurements of both, natural major ampullate spider silk of the gray cross spider *Araneus sclopetarius* and artificial $(AQ)_{12}NR3$ fibers, revealed a similar orientation of the structural elements in both silks and enabled a refined assignment of absorption peaks to amino acid motifs (Figure 10). The fingerprint region of FTIR spectra of natural major ampullate spider silk fibers shows five distinct absorption peaks (Figure 10). The most dominant absorption peak when measuring in parallel to the long fiber axis, was identified as a combined stretching vibration within β-sheet crystallites formed by A_n motifs ($\overline{v} = 965 \ cm^{-1}$).[146,157,160,241] When measuring perpendicular to the fiber axis, another peak at $\overline{v} = 1055 \ cm^{-1}$ is more pronounced, which also arises from the A_n motif. These two peaks indicate an alignment of the β-sheet crystallites in parallel to the long fiber axis. The absorption peak at $\overline{v} = 1000 \ cm^{-1}$ has been assigned to $(GA)_n$ motifs,[146] which surround the A_n regions, whereas the peaks at $\overline{v} = 1015 \ cm^{-1}$ and $\overline{v} = 1025 \ cm^{-1}$ were together assigned to skeletal stretching vibrations of glycine—rich parts, which form β-turns, β-spirals, 3_1 helices, or amorphous structures.[146,242,243]
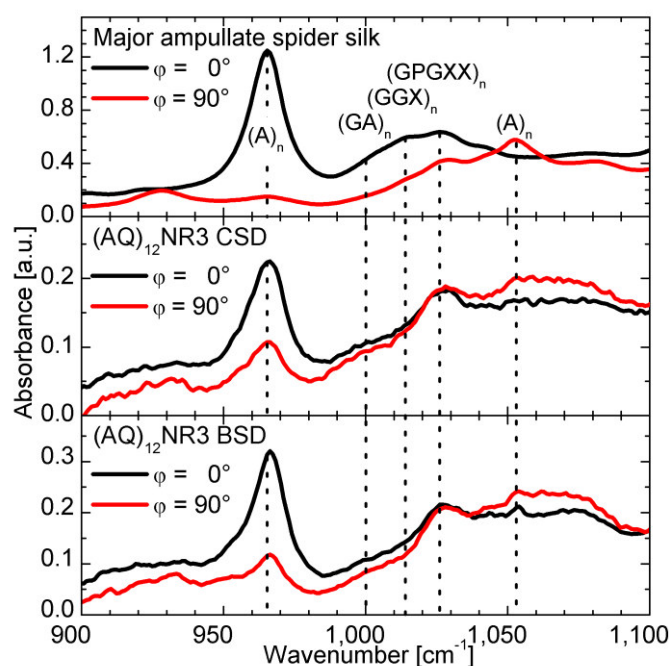
Figure 10: FTIR spectra of (top) natural major ampullate spider silk, (middle) non-biomimetic $(AQ)_{12}NR3$ CSD fibers 600% post-stretched, and (bottom) biomimetic $(AQ)_{12}NR3$ BSD fibers 600% post-stretched with the electric field of the incoming IR light in parallel ($\varphi = 0°$, black) and perpendicular to the fiber axis ($\varphi = 90°$, red). As evident from the amino acid sequence (Figure 1) vibrations at 965 cm^{-1}, 1025 cm^{-1}, and 1055 cm^{-1} arise from the polyalanine ($(A)_n$) and the glycine-rich ($(GPGXX)_n$) motifs.

Concerning the artificial fibers, on the other hand, not all absorption peaks identified for the natural spider silk fibers are present. The recombinant spidroins do not contain any $(GA)_n$ motif and thus the absorption peak at $\overline{\nu} = 1000\ cm^{-1}$ is not visible in the spectra of artificial fibers.[15] Additionally, $(AQ)_{12}NR3$ only contains one GGX sequence (X = tyrosine), in next proximity to the A_n motif and, therefore, cannot take part in any other secondary structure. Due to the lack of GGX repeats in the recombinant spidroin, the two peaks assigned to glycine-rich parts in the natural spidroins can now be separated and the peaks at $\overline{\nu} = 1015\ cm^{-1}$ and $\overline{\nu} = 1025\ cm^{-1}$ can clearly be assigned to the GGX and GPGXX motifs, respectively.

Another characteristic attribute of natural spider silk fibers is the orientation of the crystals and glycine-rich arrangements along the fiber axis, which gives rise to anisotropic absorption on a macroscopic scale (Figure 11a and b). In order to determine the degree of orientation of those assemblies in the artificial fibers, polar plots were created, and the order parameters were determined of molecular moieties located within the nanocrystals and the amorphous matrix.
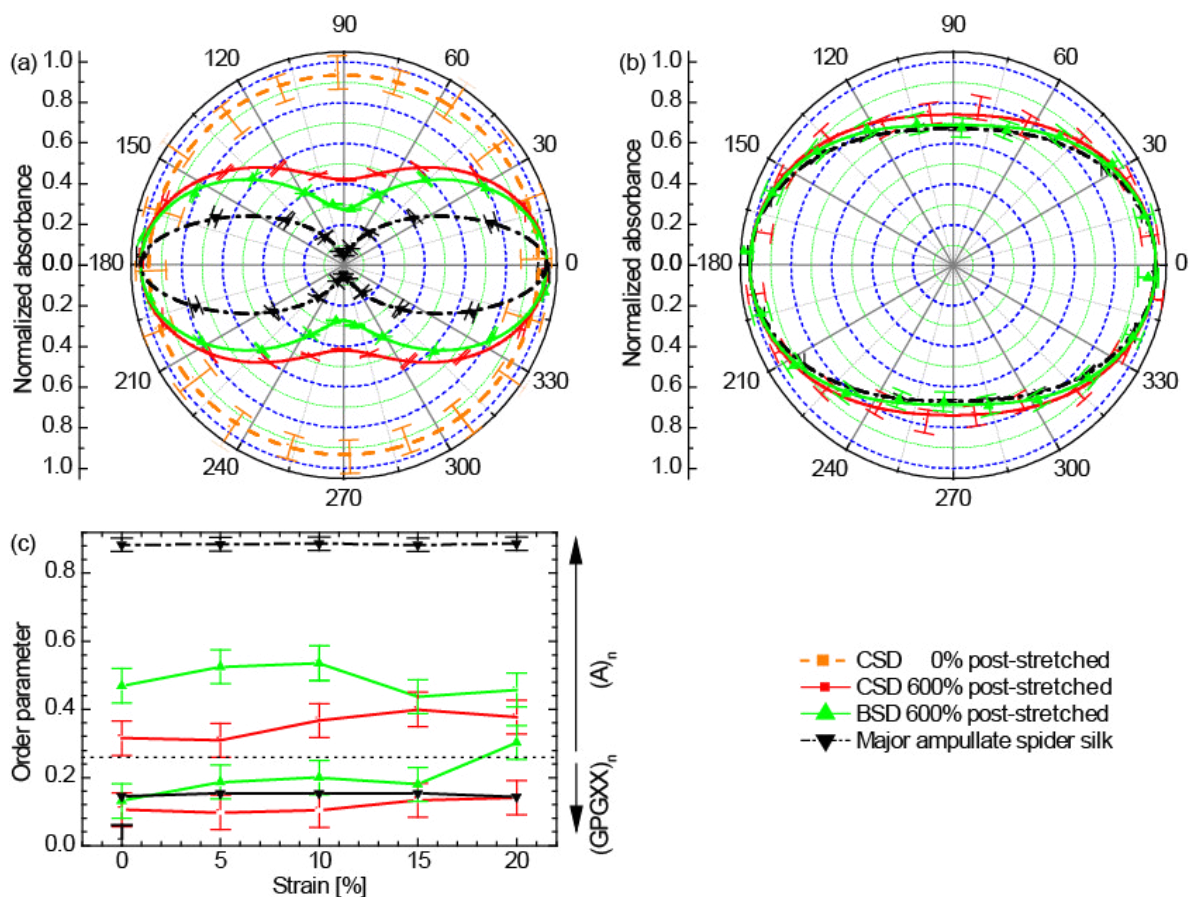
Figure 11: Polar plots and order parameters of molecular moieties. (a) Polar plot of the integrated absorbance (area under the curve) of the $(A)_n$ vibration of $((AQ)_{12}NR3$ CSD 0% post-stretched: orange squares; $(AQ)_{12}NR3$ CSD 600% post-stretched: red squares; $(AQ)_{12}NR3$ BSD 600% post-stretched: green triangles) fibers, as well as the natural major ampullate spider silk (black triangles). The solid lines represent fits of Equation 1 in publication II. The data points are normalized upon dividing them by the corresponding maximum value. (b) Polar plot of the $(GPGXX)_n$ vibration. (c) Change of the molecular order parameter with rising strain. While the molecular orientation in the natural fiber is hardly affected, the crystallites in the engineered fibers further align until the yield point is reached (CSD 600% post-stretched: $S = 0.32$ to 0.40; BSD 600% post-stretched: $S = 0.47$ to 0.54). At strains higher than the yield point the orientation of the amorphous matrix is significantly higher.

For the IR transition moments (TMs) of the specific vibrations within the β-sheet A_n- and the helical/amorphous GPGXX motifs of the natural spider silk fibers, the molecular order parameter (Equation 3, chapter 6, part II) was determined at $S = 0.89 \pm 0.02$ and $S = 0.17 \pm 0.02$, respectively (Figure 11a and b). Assuming that the individual TMs are distributed along the fiber axis obeying a rotational symmetric Gaussian function the order parameter would result in a distribution width (Equation 4 in publication II) of $\omega = 11.3°\pm1.0°$ and $\omega = 46.7°\pm1.7$.[244,245]

After wet-spinning, the artificial fibers already contained the characteristic secondary structure elements, but without post-stretching, these elements did not show any

orientational order beyond the local coordination necessary to develop the protein secondary structure ($S = 0.01 \pm 0.02$; Figure 11a and b).

However, post-stretching of the wet fibers results in a macroscopic alignment of the nanocrystals and glycine-rich parts, which enhances their mechanical properties (Figure 11c). For fibers spun from CSD that were post-stretched for 600 % a molecular order parameter of the nanocrystals of $S = 0.32 \pm 0.03$ ($\omega = 36.6° \pm 1.6°$) was determined, which increased further to $S = 0.40 \pm 0.03$ ($\omega = 32.6° \pm 1.4°$) upon further straining the fibers. The order of the glycine-rich parts slightly increased from $S = 0.10 \pm 0.03$ ($\omega = 54.1° \pm 4.1°$) to $S = 0.14 \pm 0.03$ ($\omega = 49.5° \pm 4.1°$). Compared to fibers spun from CSD, post-stretched fibers spun from BSD showed an increased order of the crystallites with a molecular order parameter of $S = 0.47 \pm 0.03$ ($\omega = 29.4° \pm 1.3°$), which increased to $S = 0.54 \pm 0.03$ ($\omega = 26.5° \pm 1.4°$) under further strain. The glycine-rich parts of these fibers were also more ordered compared to fibers spun from CSD ($S = 0.13 \pm 0.03$, $\omega = 50.5° \pm 3.3°$) and additionally aligned more quickly under strain reaching the value of natural dragline silk ($S = 0.20 \pm 0.03$, $\omega = 44.2° \pm 2.3°$).

Post-stretched fibers spun from the "biomimetic" spinning dope (BSD) showed the best performance in absorbing load, while they exhibited the biggest molecular order of the artificial threads. The previously determined superior mechanical properties of fibers spun from BSD compared to that spun from CSD can clearly be ascribed to the increased alignment of the nanocrystals and amorphous structures in the BSD fibers (Figure 9).[15]

The mechanical response of the artificial fibers to load is significantly influenced by the post-spinning treatment: fibers as-spun (CSD 0% and BSD 0%) appeared to be very brittle, while post-spinning elongation enhanced the elastic modulus and extensibility.[15] Moreover, the threads' stress-strain characteristic was sustainably changed. As evident in Figure 2 of Heidebrecht *et al.* (2015)[15] as-spun fibers showed no yield point in stress-strain experiments, whereas post-stretched samples did show a distinct yield point.[15] It is highly interesting that the presence or absence of a yield point for semi-crystalline polymers indicates an energy dissipation through oriented and ordered or unordered structures, respectively.[246,247] Accordingly, the applied load in case of the as-spun samples was applied predominantly to amorphous structures, whereas when the samples were post-stretched the stress-strain curves indicate the involvement of ordered parts. The highest toughness (172 MPa), was achieved for $(AQ)_{12}NR3$ fibers spun from BSD with 600% post-strain, which was therefore used for the detailed further analysis.

A refined assessment on the interplay between nanocrystals and amorphous parts was provided by stress-dependent IR spectroscopy experiments. In the past, one exceptional characteristic of major (and minor) ampullate spider silk has been found, namely the load-dependent and reversible shift of the alanine-specific IR absorption band at $\bar{\nu} = 965\ cm^{-1}$.[146,157,160,241] Although the nanometer-sized alanine-rich crystals are embedded within a less ordered glycine-rich matrix, macroscopically applied stress affects vibrations on the molecular length scale inside those rigid crystallites. Consequently, a mechanism responsible for the stress transfer has to exist. It is believed that amorphous parts interconnecting the nanocrystals experienced shear forces during spinning that orient and elongate pre-aggregates.[34,248] This strain, and hence, stress is preserved while the thread is formed; the tendency to contract is counterbalanced by the surrounding layers of the fiber. Thus, the arising inherent non-equilibrium state of the pre-stressed morphology causes the transduction of the applied load from the macroscopic scale down to the molecular level, where the emerging energy affects the crystallites and is dissipated.[146,157,160,241] Exposing BSD 600% fibers to macroscopic stress induced a shift of the A_n-specific peak ($\bar{\nu} = 965\ cm^{-1}$) (Figure 12).
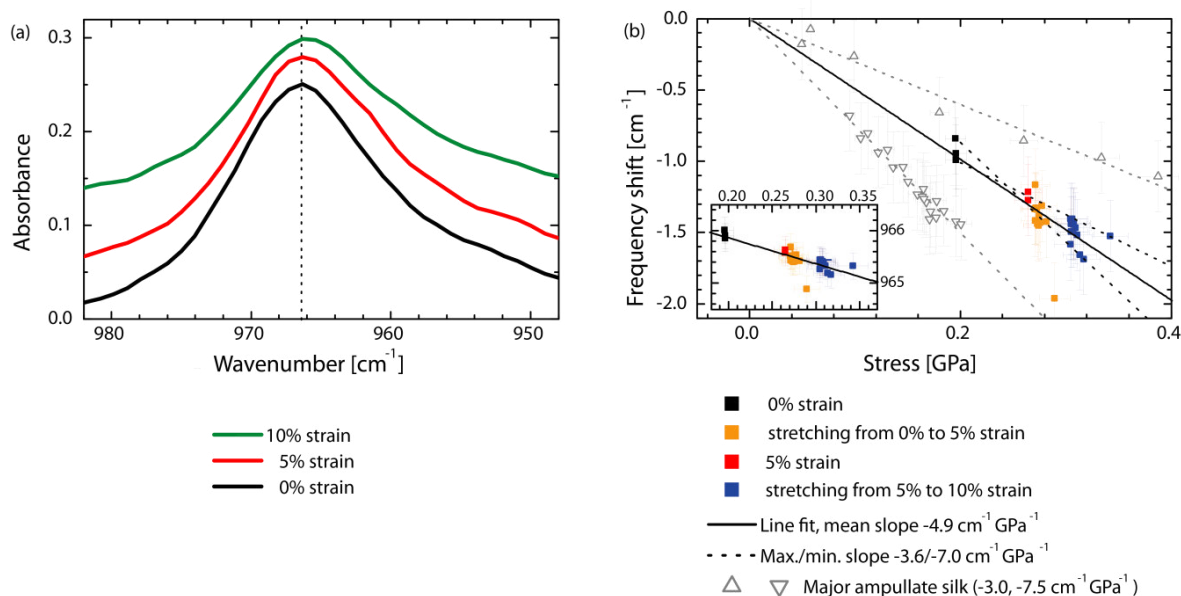

Figure 12: Microscopic response of a biotech fiber (BSD, 600 % post-stretched) to macroscopic load. (a) The frequency position of the $(A)_n$ peak is shifted to lower wavenumbers as a consequence of the applied force (and hence stress). (b) Similar to that of natural spider silk this frequency shift is linear with the applied stress (inset) with a slope of -4.9 cm⁻¹GPa⁻¹ being in full agreement with the literature.[146,157,160,241] The black squares correspond to the black curve in (a), the orange squares result from stretching the sample from 0% to 5% strain. The red squares correspond to the red curve in (a) and the blue squares represent the sample stretched to 10% strain. Since the $(A)_n$ vibration is exclusively located within in the crystallites,[146] it is demonstrated that the macroscopic load affects the crystalline parts of the protein chains, even though the nanocrystals are embedded in an amorphous matrix.

Furthermore, after the sample had been stressed and relaxed subsequently, the spectral displacement decreased in accordance to the lowered apparent force. This spectral shift was linearly dependent on the applied stress, as for natural dragline silk, and the slope of $-4.9\,\mathrm{cm^{-1}GPa^{-1}}$ corresponded to frequently derived values of spider silk,[146,241,249] it even fitted to the slope under hydrostatic pressure.[160] These results explicitly demonstrated that macroscopically applied stress is transferred through a less-ordered matrix and affects the crystalline parts of the biomimetic fibers. This mechanism is identical to that in natural major ampullate spider silk and is responsible for the exceptional ability of dissipating impinging energy.

The results obtained in this work reveal that the approach of developing a biomimetic spinning dope points in the right direction of producing nature-like spider silk fibers. On a molecular level, artificial fibers already closely resemble natural spider silk fibers (Figure 13).
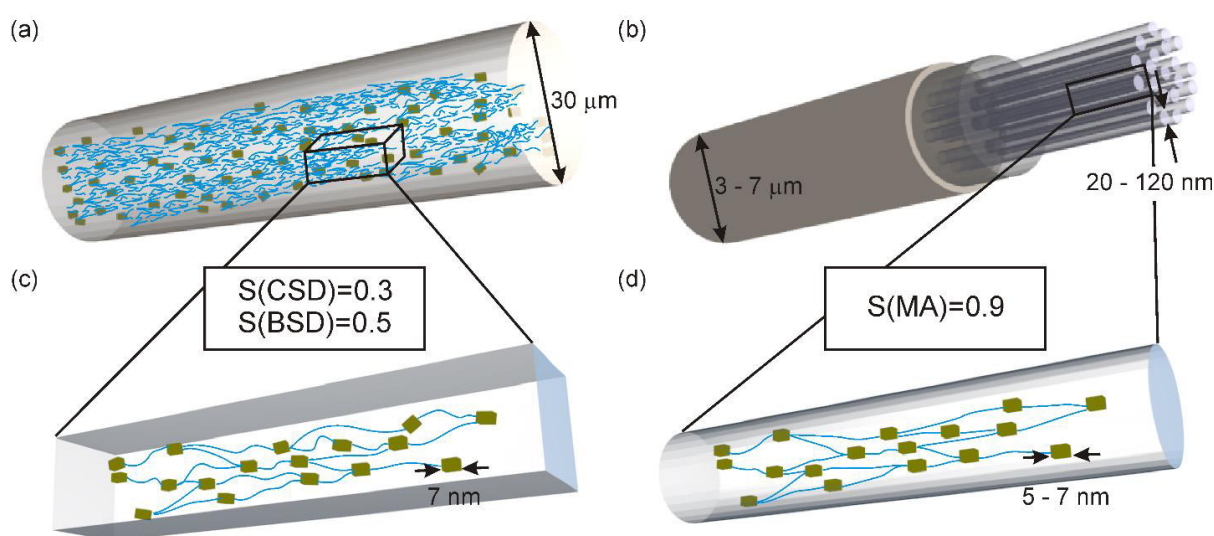

Figure 13: Schematic view of (a) a biotech fiber $(AQ)_{12}NR3$ (CSD or BSD) and (b) a natural major ampullate spider silk thread. The former comprises a homogeneous distribution of polyalanine β-sheet crystallites embedded in a glycine rich, amorphous matrix, whereas the latter, in addition, exhibits a refined hierarchical structure composed of fibrils and a surrounding layered structure. In both samples the nanocrystals show a length of 7 nm. Post-stretching aligns the crystallites resulting in a significant increase in the molecular order parameter (CSD: $S = 0.32$; BSD: $S = 0.47$), and in enhanced mechanical properties.[15] The natural blueprint shows a molecular order parameter of $S = 0.90$.

Both fibers contain 7 nm long crystals comprised of poly-alanine β-sheets, which are embedded in an amorphous matrix. Whereas the amorphous and crystalline areas of natural major ampullate silk fibers show a high order directly after spinning, this is not the case for

biotech fibers, which are only exposed to shear forces upon post-stretching, triggering an orientation of the structural areas in the fiber. Interestingly, the effect of post-stretching on the molecular order in the fibers was higher in fibers spun from BSD than CSD, meaning the foundation for a high structural order is already laid in the spinning dope. By further stretching these already post-stretched fibers, the molecular order parameter of the crystalline and amorphous areas is further increased, the latter (of fibers spun from BSD) even reaches the same order as found in natural spider silk fibers. These results indicate that the production of artificial fibers with the same mechanical properties as natural silk fibers requires a spinning process that integrates shear forces during formation of the fiber in order to obtain a high order as found in natural silk fibers.

4. REFERENCES

1   Sutherland, T. D., Young, J. H., Weisman, S., Hayashi, C. Y. & Merritt, D. J. Insect silk: one name, many materials. *Annu Rev Entomol* **55**, 171-188 (2010).

2   Neuenfeldt, M. & Scheibel, T. in *Insect Molecular Biology and Ecology*, 376-400 (CRC Press, 2014).

3   Craig, C. L. Evolution of arthropod silks. *Annu Rev Entomol* **42**, 231-267 (1997).

4   Porter, D. & Vollrath, F. Silk as a Biomimetic Ideal for Structural Polymers. *Adv Mater* **21**, 487-492 (2009).

5   Greving, I., Cai, M. Z., Vollrath, F. & Schniepp, H. C. Shear-Induced Self-Assembly of Native Silk Proteins into Fibrils Studied by Atomic Force Microscopy. *Biomacromolecules* **13**, 676-682 (2012).

6   Pereira, R. F. P., Silva, M. M. & de Zea Bermudez, V. *Bombyx mori* Silk Fibers: An Outstanding Family of Materials. *Macromol Mater Eng* **300**, 1171-1198 (2015).

7   Vainker, S. J. *Chinese silk: a cultural history*. (British Museum, 2004).

8   Arunkumar, K. P., Metta, M. & Nagaraju, J. Molecular phylogeny of silkmoths reveals the origin of domesticated silkmoth, *Bombyx mori* from Chinese *Bombyx mandarina* and paternal inheritance of *Antheraea proylei* mitochondrial DNA. *Mol Phylogenet Evol* **40**, 419-427 (2006).

9   Maekawa, H., Takada, N., Mikitani, K., Ogura, T., Miyajima, N., Fujiwara, H., Kobayashi, M. & Ninaki, O. Nucleolus Organizers in the Wild Silkworm *Bombyx Mandarina* and the Domesticated Silkworm *B. Mori*. *Chromosoma* **96**, 263-269 (1988).

10   Kundu, B., Rajkhowa, R., Kundu, S. C. & Wang, X. Silk fibroin biomaterials for tissue regenerations. *Adv Drug Deliv Rev* **65**, 457-470 (2013).

11   Gosline, J. M., Guerette, P. A., Ortlepp, C. S. & Savage, K. N. The mechanical design of spider silks: from fibroin sequence to mechanical function. *J Exp Biol* **202**, 3295-3303 (1999).

12   Heim, M., Keerl, D. & Scheibel, T. Spider silk: from soluble protein to extraordinary fiber. *Angew Chem, Int Ed* **48**, 3584-3596 (2009).

13   Madsen, B., Shao, Z. Z. & Vollrath, F. Variability in the mechanical properties of spider silks on three levels: interspecific, intraspecific and intraindividual. *Int J Biol Macromol* **24**, 301-306 (1999).

14   Heidebrecht, A. & Scheibel, T. Recombinant production of spider silk proteins. *Adv Appl Microbiol* **82**, 115-153 (2013).

15   Heidebrecht, A., Eisoldt, L., Diehl, J., Schmidt, A., Geffers, M., Lang, G. & Scheibel, T. Biomimetic Fibers Made of Recombinant Spidroins with the Same Toughness as Natural Spider Silk. *Adv Mater* **27**, 2189-2194 (2015).

16   Zhao, H. P., Feng, X. Q. & Shi, H. J. Variability in mechanical properties of *Bombyx mori* silk. *Mat Sci Eng C* **27**, 675-683 (2007).

17   He, Y. X., Zhang, N. N., Li, W. F., Jia, N., Chen, B. Y., Zhou, K., Zhang, J., Chen, Y. & Zhou, C. Z. N-Terminal domain of *Bombyx mori* fibroin mediates the assembly of silk in response to pH decrease. *J Mol Biol* **418**, 197-207 (2012).

18   Tanaka, K., Mori, K. & Mizuno, S. Immunological Identification of the Major Disulfide-Linked Light Component of Silk Fibroin. *J Biochem* **114**, 1-4 (1993).

19   Inoue, S., Tanaka, K., Arisaka, F., Kimura, S., Ohtomo, K. & Mizuno, S. Silk fibroin of *Bombyx mori* is secreted, assembling a high molecular mass elementary unit consisting of H-chain, L-chain, and P25, with a 6:6:1 molar ratio. *J Biol Chem* **275**, 40517-40528 (2000).

20   Miller, L. D., Putthanarat, S., Eby, R. K. & Adams, W. W. Investigation of the nanofibrillar morphology in silk fibers by small angle X-ray scattering and atomic force microscopy. *Int J Biol Macromol* **24**, 159-165 (1999).

21   Putthanarat, S., Stribeck, N., Fossey, S. A., Eby, R. K. & Adams, W. W. Investigation of the nanofibrils of silk fibers. *Polymer* **41**, 7735-7747 (2000).

22   Altman, G. H., Diaz, F., Jakuba, C., Calabro, T., Horan, R. L., Chen, J., Lu, H., Richmond, J. & Kaplan, D. L. Silk-based biomaterials. *Biomaterials* **24**, 401-416 (2003).

23   Fedic, R., Zurovec, M. & Sehnal, F. Correlation between fibroin amino acid sequence and physical silk properties. *J Biol Chem* **278**, 35255-35264 (2003).

24   Sehnal, F. & Zurovec, M. Construction of silk fiber core in lepidoptera. *Biomacromolecules* **5**, 666-674 (2004).

25   Gamo, T., Inokuchi, T. & Laufer, H. Polypeptides of Fibroin and Sericin Secreted from Different Sections of Silk Gland in *Bombyx Mori*. *Insect Biochem* **7**, 285-295 (1977).

26   Fournier, A. Quantitative data on the *Bombyx mori* L. silkworm: A review. *Biochimie* **61**, 283-320 (1979).

27   Zhang, Y. Q. Applications of natural silk protein sericin in biomaterials. *Biotechnol Adv* **20**, 91-100 (2002).

28   Vepari, C. & Kaplan, D. L. Silk as a Biomaterial. *Prog Polym Sci* **32**, 991-1007 (2007).

29   Gerritsen, V. B. The tiptoe of an airbus. *Protein Spotlight, Swiss Prot* **24**, 1-2 (2002).

30   Lewis, R. Unraveling the weave of spider silk. *Bioscience* **46**, 636-638 (1996).

31   Bon, M. A Discourse upon the Usefulness of the Silk of Spiders. *Phil Trans* **27**, 2-16 (1710).

32   Vollrath, F., Barth, P., Basedow, A., Engstrom, W. & List, H. Local tolerance to spider silks and protein polymers in vivo. *In Vivo* **16**, 229-234 (2002).

33   Kiliani, O. G. II. On Traumatic Keloid of the Median Nerve, with Observations upon the Absorption of Silk Sutures. *Ann Surg* **33**, 13-22 (1901).

34   Vollrath, F. & Knight, D. P. Liquid crystalline spinning of spider silk. *Nature* **410**, 541-548 (2001).

35   Rising, A. Controlled assembly: A prerequisite for the use of recombinant spider silk in regenerative medicine? *Acta Biomater* **10**, 1627-1631 (2014).

36   Allmeling, C., Jokuszies, A., Reimers, K., Kall, S., Choi, C. Y., Brandes, G., Kasper, C., Scheper, T., Guggenheim, M. & Vogt, P. M. Spider silk fibres in artificial nerve constructs promote peripheral nerve regeneration. *Cell Prolif* **41**, 408-420 (2008).

37   Radtke, C., Allmeling, C., Waldmann, K.-H., Reimers, K., Thies, K., Schenk, H. C., Hillmer, A., Guggenheim, M., Brandes, G. & Vogt, P. M. Spider silk constructs enhance axonal regeneration and remyelination in long nerve defects in sheep. *PLoS One* **6**, e16990 (2011).

38   Wendt, H., Hillmer, A., Reimers, K., Kuhbier, J. W., Schafer-Nolte, F., Allmeling, C., Kasper, C. & Vogt, P. M. Artificial skin--culturing of different skin cell lines for generating an artificial skin substitute on cross-weaved spider silk fibres. *PLoS One* **6**, e21833 (2011).

39   Stauffer, S. L., Coguill, S. L. & Lewis, R. V. Comparison of physical properties of 3 silks from *Nephila clavipes* and *Araneus gemmoides*. *J Arachnol* **22**, 5-11 (1994).

40   Garb, J. E. & Hayashi, C. Y. Modular evolution of egg case silk genes across orb-weaving spider superfamilies. *Proc Natl Acad Sci U S A* **102**, 11379-11384 (2005).

41   Gosline, J., Lillie, M., Carrington, E., Guerette, P., Ortlepp, C. & Savage, K. Elastic proteins: biological roles and mechanical properties. *Philos Trans R Soc, B* **357**, 121-132 (2002).

42   Gosline, J. M., Denny, M. W. & Demont, M. E. Spider Silk as Rubber. *Nature* **309**, 551-552 (1984).

43   Gosline, J. M., Pollak, C. C., Guerette, P. A., Cheng, A., Demont, M. E. & Denny, M. W. Elastomeric network models for the frame and viscid silks from the orb web of the spider *Araneus diadematus*. *Acs Sym Ser* **544**, 328-341 (1994).

44   Thiel, B. L. & Viney, C. Beta sheets and spider silk. *Science* **273**, 1480-1481 (1996).

45   Viney, C. Natural silks: archetypal supramolecular assembly of polymer fibres. *Supramol Sci* **4**, 75-81 (1997).

46   Blackledge, T. A., Summers, A. P. & Hayashi, C. Y. Gumfooted lines in black widow cobwebs and the mechanical properties of spider capture silk. *Zoology* **108**, 41-46 (2005).

47   Vollrath, F. & Porter, D. Spider silk as archetypal protein elastomer. *Soft Matter* **2**, 377-385 (2006).

48   Ap Rhisiart, A. & Vollrath, F. Design features of the orb web of the spider, *Araneus diadematus*. *Behav Ecol* **5**, 280-287 (1994).

49   Hinman, M. B. & Lewis, R. V. Isolation of a clone encoding a second dragline silk fibroin. *Nephila clavipes* dragline silk is a two-protein fiber. *J Biol Chem* **267**, 19320-19324 (1992).

50   Sponner, A., Vater, W., Monajembashi, S., Unger, E., Grosse, F. & Weisshart, K. Composition and hierarchical organisation of a spider silk. *PLoS One* **2**, e998 (2007).

51   Augsten, K., Weisshart, K., Sponner, A. & Unger, E. Glycoproteins and skin-core structure in *Nephila clavipes* spider silk observed by light- and electron microscopy. *Scanning* **21**, 77 (2000).

52   Schulz, S. Composition of the silk lipids of the spider *Nephila clavipes*. *Lipids* **36**, 637-647 (2001).

53   Liu, Y., Shao, Z. & Vollrath, F. Relationships between supercontraction and mechanical properties of spider silk. *Nat Mater* **4**, 901-905 (2005).

54   Candelas, G. C., Ortiz, A. & Molina, C. The cylindrical or tubiliform glands of *Nephila clavipes*. *J Exp Zool* **237**, 281-285 (1986).

55   Knight, D. P. & Vollrath, F. Liquid crystals and flow elongation in a spider's silk production line. *Proc R Soc London, Ser B* **266**, 519-523 (1999).

56   Kohler, T. & Vollrath, F. Thread Biomechanics in the 2 Orb-Weaving Spiders *Araneus Diadematus* (*Araneae*, *Araneidae*) and *Uloborus Walckenaerius* (*Araneae*, *Uloboridae*). *J Exp Zool* **271**, 1-17 (1995).

57   Denny, M. Physical-Properties of Spiders Silk and Their Role in Design of Orb-Webs. *J Exp Biol* **65**, 483-506 (1976).

58   Perez-Rigueiro, J., Elices, M., Guinea, G. V., Plaza, G. R., Karatzas, C., Riekel, C., Agullo-Rueda, F. & Daza, R. Bioinspired fibers follow the track of natural spider silk. *Macromolecules* **44**, 1166-1176 (2011).

59   Agnarsson, I., Kuntner, M. & Blackledge, T. A. Bioprospecting finds the toughest biological material: extraordinary silk from a giant riverine orb spider. *Plos One* **5**, e11234 (2010).

60   Swanson, B. O., Blackledge, T. A., Beltran, J. & Hayashi, C. Y. Variation in the material properties of spider dragline silk across species. *Appl Phys A: Mater Sci Process* **82**, 213-218 (2006).

61   Work, R. W. Dimensions, Birefringences, and Force-Elongation Behavior of Major and Minor Ampullate Silk Fibers from Orb-Web-Spinning Spiders - Effects of Wetting on These Properties. *Text Res J* **47**, 650-662 (1977).

62   Hayashi, C. Y., Blackledge, T. A. & Lewis, R. V. Molecular and mechanical characterization of aciniform silk: Uniformity of iterated sequence modules in a novel member of the spider silk fibroin gene family. *Mol Biol Evol* **21**, 1950-1959 (2004).

63   Van Nimmen, E., Gellynck, K., Gheysens, T., Van Langenhove, L. & Mertens, J. Modeling of the stress-strain behavior of egg sac silk of the spider *Araneus diadematus*. *J Arachnol* **33**, 629-639 (2005).

64   Zhao, A. C., Zhao, T. F., Nakagaki, K., Zhang, Y. S., SiMa, Y. H., Miao, Y. G., Shiomi, K., Kajiura, Z., Nagata, Y., Takadera, M. & Nakagaki, M. Novel molecular and mechanical properties of egg case silk from wasp spider, *Argiope bruennichi*. *Biochemistry* **45**, 3348-3356 (2006).

65   Riekel, C. & Vollrath, F. Spider silk fibre extrusion: combined wide- and small-angle X-ray microdiffraction experiments. *Int J Biol Macromol* **29**, 203-210 (2001).

66   Dicko, C., Knight, D., Kenney, J. M. & Vollrath, F. Secondary structures and conformational changes in flagelliform, cylindrical, major, and minor ampullate silk proteins. Temperature and concentration effects. *Biomacromolecules* **5**, 2105-2115 (2004).

67   Tillinghast, E. K. & Townley, M. A. Silk glands of araneid spiders - selected morphological and physiological aspects. *Acs Sym Ser* **544**, 29-44 (1994).

68   Brooks, A. E., Steinkraus, H. B., Nelson, S. R. & Lewis, R. V. An investigation of the divergence of major ampullate silk fibers from *Nephila clavipes* and *Argiope aurantia*. *Biomacromolecules* **6**, 3095-3099 (2005).

69   Scheibel, T. Spider silks: recombinant synthesis, assembly, spinning, and engineering of synthetic proteins. *Microb Cell Fact* **3**, 14 (2004).

70   Winkler, S. & Kaplan, D. L. Molecular biology of spider silk. *J Biotechnol* **74**, 85-93 (2000).

71   Becker, N., Oroudjev, E., Mutz, S., Cleveland, J. P., Hansma, P. K., Hayashi, C. Y., Makarov, D. E. & Hansma, H. G. Molecular nanosprings in spider capture-silk threads. *Nat Mater* **2**, 278-283 (2003).

72   Bini, E., Knight, D. P. & Kaplan, D. L. Mapping domain structures in silks from insects and spiders related to protein assembly. *J Mol Biol* **335**, 27-40 (2004).

73   Ohgo, K., Kawase, T., Ashida, J. & Asakura, T. Solid-state NMR analysis of a peptide (Gly-Pro-Gly-Gly-Ala)(6)-Gly derived from a flagelliform silk sequence of *Nephila clavipes*. *Biomacromolecules* **7**, 1210-1214 (2006).

74   Vollrath, F. & Tillinghast, E. K. Glycoprotein glue beneath a spider webs aqueous coat. *Naturwissenschaften* **78**, 557-559 (1991).

75   Vollrath, F. Spider silk: Thousands of nano-filaments and dollops of sticky glue. *Curr Biol* **16**, R925-R927 (2006).

76   Hu, X. Y., Yuan, J., Wang, X. D., Vasanthavada, K., Falick, A. M., Jones, P. R., La Mattina, C. & Vierra, C. A. Analysis of aqueous glue coating proteins on the silk fibers of the cob weaver, *Latrodectus hesperus*. *Biochemistry* **46**, 3294-3303 (2007).

77   Hawthorn, A. C. & Opell, B. D. Evolution of adhesive mechanisms in cribellar spider prey capture thread: evidence for van der Waals and hygroscopic forces. *Biol J Linn Soc* **77**, 1-8 (2002).

78   Hawthorn, A. C. & Opell, B. D. Van-der-Waals and hygroscopic forces of adhesion generated by spider capture threads. *J Exp Biol* **206**, 3905-3911 (2003).

79   Hajer, J. & Rehakova, D. Spinning activity of the spider *Trogloneta granulum* (Araneae, Mysmenidae): web, cocoon, cocoon handling behaviour, draglines and attachment discs. *Zoology* **106**, 223-231 (2003).

80   Kovoor, J. & Zylberberg, L. Fine structural aspects of silk secretion in a spider (*Araneus diadematus*). I. Elaboration in the pyriform glands. *Tissue Cell* **12**, 547-556 (1980).

81   Blasingame, E., Tuton-Blasingame, T., Larkin, L., Falick, A. M., Zhao, L., Fong, J., Vaidyanathan, V., Visperas, A., Geurts, P., Hu, X., La Mattina, C. & Vierra, C. Pyriform Spidroin 1, a Novel Member of the Silk Gene Family That Anchors Dragline Silk Fibers in Attachment Discs of the Black Widow Spider, *Latrodectus hesperus*. *J Biol Chem* **284**, 29097-29108 (2009).

82   Geurts, P., Zhao, L., Hsia, Y., Gnesa, E., Tang, S., Jeffery, F., La Mattina, C., Franz, A., Larkin, L. & Vierra, C. Synthetic spider silk fibers spun from pyriform spidroin 2, a glue silk protein discovered in orb-weaving spider attachment discs. *Biomacromolecules* **11**, 3495-3503 (2010).

83   Rising, A., Hjalm, G., Engstrom, W. & Johansson, J. N-terminal nonrepetitive domain common to dragline, flagelliform, and cylindriform spider silk proteins. *Biomacromolecules* **7**, 3120-3124 (2006).

84   Bittencourt, D., Souto, B. M., Verza, N. C., Vineck, F., Dittmar, K., Silva, P. I., Andrade, A. C., da Silva, F. R., Lewis, R. V. & Rech, E. L. Spidroins from the Brazilian spider *Nephilengys cruentata* (*Araneae: Nephilidae*). *Comp Biochem Physiol, Part B: Biochem Mol Biol* **147**, 597-606 (2007).

85   Hu, X. Y., Kohler, K., Falick, A. M., Moore, A. M. F., Jones, P. R., Sparkman, O. D. & Vierra, C. Egg case protein-1 - A new class of silk proteins with fibroin-like properties from the spider *Latrodectus hesperus*. *J Biol Chem* **280**, 21220-21230 (2005).

86   Hu, X. Y., Kohler, K., Falick, A. M., Moore, A. M. F., Jones, P. R. & Vierra, C. Spider egg case core fibers: Trimeric complexes assembled from TuSp1, ECP-1, and ECP-2. *Biochemistry* **45**, 3506-3516 (2006).

87   Hu, X. Y., Lawrence, B., Kohler, K., Falick, A. M., Moore, A. M. F., McMullen, E., Jones, P. R. & Vierra, C. Araneoid egg case silk: A fibroin with novel ensemble repeat units from the black widow spider, *Latrodectus hesperus*. *Biochemistry* **44**, 10020-10027 (2005).

88   Huang, W., Lin, Z., Sin, Y. M., Li, D., Gong, Z. & Yang, D. Characterization and expression of a cDNA encoding a tubuliform silk protein of the golden web spider *Nephila antipodiana*. *Biochimie* **88**, 849-858 (2006).

89   Tian, M. & Lewis, R. V. Molecular Characterization and Evolutionary Study of Spider Tubuliform (Eggcase) Silk Protein. *Biochemistry* **44**, 8006-8012 (2005).

90   Blackledge, T. A. & Hayashi, C. Y. Silken toolkits: biomechanics of silk fibers spun by the orb web spider *Argiope argentata* (Fabricius 1775). *J Exp Biol* **209**, 2452-2461 (2006).

91   Vasanthavada, K., Hu, X., Falick, A. M., La Mattina, C., Moore, A. M. F., Jones, P. R., Yee, R., Reza, R., Tuton, T. & Vierra, C. Aciniform spidroin, a constituent of

egg case sacs and wrapping silk fibers from the black widow spider *Latrodectus hesperus*. *J Biol Chem* **282**, 35088-35097 (2007).

92   La Mattina, C., Reza, R., Hu, X., Falick, A. M., Vasanthavada, K., McNary, S., Yee, R. & Vierra, C. A. Spider minor ampullate silk proteins are constituents of prey wrapping silk in the cob weaver *Latrodectus hesperus*. *Biochemistry* **47**, 4692-4700 (2008).

93   Zhang, K., Si, F. W., Duan, H. L. & Wang, J. Microstructures and mechanical properties of silks of silkworm and honeybee. *Acta Biomater* **6**, 2165-2171 (2010).

94   Perez-Rigueiro, J., Elices, M., Plaza, G. R. & Guinea, G. V. Similarities and differences in the supramolecular organization of silkworm and spider silk. *Macromolecules* **40**, 5360-5365 (2007).

95   Lefevre, T., Rousseau, M. E. & Pezolet, M. Protein secondary structure and orientation in silk as revealed by Raman spectromicroscopy. *Biophys J* **92**, 2885-2895 (2007).

96   van Beek, J. D., Hess, S., Vollrath, F. & Meier, B. H. The molecular structure of spider dragline silk: folding and orientation of the protein backbone. *Proc Natl Acad Sci U S A* **99**, 10266-10271 (2002).

97   Omenetto, F. G. & Kaplan, D. L. New opportunities for an ancient material. *Science* **329**, 528-531 (2010).

98   Askarieh, G., Hedhammar, M., Nordling, K., Saenz, A., Casals, C., Rising, A., Johansson, J. & Knight, S. D. Self-assembly of spider silk proteins is controlled by a pH-sensitive relay. *Nature* **465**, 236-238 (2010).

99   Eisoldt, L., Scheibel, T. & Smith, A. Decoding the secrets of spider silk. *Mater Today* **14**, 80-86 (2011).

100   Eisoldt, L., Hardy, J. G., Heim, M. & Scheibel, T. R. The role of salt and shear on the storage and assembly of spider silk proteins. *J Struct Biol* **170**, 413-419 (2010).

101   Eisoldt, L., Thamm, C. & Scheibel, T. The role of terminal domains during storage and assembly of spider silk proteins. *Biopolymers* **97**, 355-361 (2012).

102   Hagn, F., Eisoldt, L., Hardy, J. G., Vendrely, C., Coles, M., Scheibel, T. & Kessler, H. A conserved spider silk domain acts as a molecular switch that controls fibre assembly. *Nature* **465**, 239-242 (2010).

103   Knight, D. P. & Vollrath, F. Spinning an elastic ribbon of spider silk. *Philos Trans R Soc Lond B Biol Sci* **357**, 219-227 (2002).

104   Braun, F. N. & Viney, C. Modelling self assembly of natural silk solutions. *Int J Biol Macromol* **32**, 59-65 (2003).

105   Shimura, K., Kikuchi, A., Ohtomo, K., Katagata, Y. & Hyodo, A. Studies on silk fibroin of *Bombyx mori*. I. Fractionation of fibroin prepared from the posterior silk gland. *J Biochem* **80**, 693-702 (1976).

106   Tanaka, K., Kajiyama, N., Ishikura, K., Waga, S., Kikuchi, A., Ohtomo, K., Takagi, T. & Mizuno, S. Determination of the site of disulfide linkage between

heavy and light chains of silk fibroin produced by *Bombyx mori*. *Biochim Biophys Acta* **1432**, 92-103 (1999).

107   Tanaka, K., Inoue, S. & Mizuno, S. Hydrophobic interaction of P25, containing Asn-linked oligosaccharide chains, with the H-L complex of silk fibroin produced by *Bombyx mori*. *Insect Biochem Mol Biol* **29**, 269-276 (1999).

108   Zhou, C. Z., Confalonieri, F., Jacquet, M., Perasso, R., Li, Z. G. & Janin, J. Silk fibroin: structural implications of a remarkable amino acid sequence. *Proteins* **44**, 119-122 (2001).

109   Murphy, A. R. & Kaplan, D. L. Biomedical applications of chemically-modified silk fibroin. *J Mater Chem* **19**, 6443-6450 (2009).

110   Yamaguchi, K., Kikuchi, Y., Takagi, T., Kikuchi, A., Oyama, F., Shimura, K. & Mizuno, S. Primary structure of the silk fibroin light chain determined by cDNA sequencing and peptide analysis. *J Mol Biol* **210**, 127-139 (1989).

111   Asakura, T., Kuzuhara, A., Tabeta, R. & Saito, H. Conformation Characterization of *Bombyx Mori* Silk Fibroin in the Solid State by High-Frequency C-13 Cross Polarization-Magic Angle Spinning NMR, X-Ray Diffraction, and Infrared Spectroscopy. *Macromolecules* **18**, 1841-1845 (1985).

112   Hakimi, O., Knight, D. P., Vollrath, F. & Vadgama, P. Spider and mulberry silkworm silks as compatible biomaterials. *Composites, Part B* **38**, 324-337 (2007).

113   Marsh, R. E., Corey, R. B. & Pauling, L. An investigation of the structure of silk fibroin. *Biochim Biophys Acta* **16**, 1-34 (1955).

114   Lotz, B. & Colonna Cesari, F. The chemical structure and the crystalline structures of *Bombyx mori* silk fibroin. *Biochimie* **61**, 205-214 (1979).

115   Valluzzi, R., He, S. J., Gido, S. P. & Kaplan, D. *Bombyx mori* silk fibroin liquid crystallinity and crystallization at aqueous fibroin-organic solvent interfaces. *Int J Biol Macromol* **24**, 227-236 (1999).

116   Inoue, S. I., Magoshi, J., Tanaka, T., Magoshi, Y. & Becker, M. Atomic force microscopy: *Bombyx mori* silk fibroin molecules and their higher order structure. *J Polym Sci, Part B: Polym Phys* **38**, 1436-1439 (2000).

117   Asakura, T., Suzuki, Y., Nakazawa, Y., Yazawa, K., Holland, G. P. & Yarger, J. L. Silk structure studied with nuclear magnetic resonance. *Prog Nucl Magn Reson Spectrosc* **69**, 23-68 (2013).

118   Gage, L. P. & Manning, R. F. Internal structure of the silk fibroin gene of *Bombyx mori*. I The fibroin gene consists of a homogeneous alternating array of repetitious crystalline and amorphous coding sequences. *J Biol Chem* **255**, 9444-9450 (1980).

119   Challis, R. J., Goodacre, S. L. & Hewitt, G. M. Evolution of spider silks: conservation and diversification of the C-terminus. *Insect Mol Biol* **15**, 45-56 (2006).

120   Hedhammar, M., Rising, A., Grip, S., Martinez, A. S., Nordling, K., Casals, C., Stark, M. & Johansson, J. Structural properties of recombinant nonrepetitive and repetitive parts of major ampullate spidroin 1 from *Euprosthenops australis*: Implications for fiber formation. *Biochemistry* **47**, 3407-3417 (2008).

121 Huemmerich, D., Helsen, C. W., Quedzuweit, S., Oschmann, J., Rudolph, R. & Scheibel, T. Primary structure elements of spider dragline silks and their contribution to protein solubility. *Biochemistry* **43**, 13604-13612 (2004).

122 Andersen, S. O. Amino acid composition of spider silks. *Comp Biochem Physiol* **35**, 705-711 (1970).

123 Colgin, M. A. & Lewis, R. V. Spider minor ampullate silk proteins contain new repetitive sequences and highly conserved non-silk-like "spacer regions". *Protein Sci* **7**, 667-672 (1998).

124 Craig, C. L. & Riekel, C. Comparative architecture of silks, fibrous proteins and their encoding genes in insects and spiders. *Comp Biochem Physiol B Biochem Mol Biol* **133**, 493-507 (2002).

125 Liu, Y., Sponner, A., Porter, D. & Vollrath, F. Proline and processing of spider silks. *Biomacromolecules* **9**, 116-121 (2008).

126 Hayashi, C. Y. & Lewis, R. V. Evidence from flagelliform silk cDNA for the structural basis of elasticity and modular nature of spider silks. *J Mol Biol* **275**, 773-784 (1998).

127 Gatesy, J., Hayashi, C., Motriuk, D., Woods, J. & Lewis, R. Extreme diversity, conservation, and convergence of spider silk fibroin sequences. *Science* **291**, 2603-2605 (2001).

128 Kim, S., Nollen, E. A. A., Kitagawa, K., Bindokas, V. P. & Morimoto, R. I. Polyglutamine protein aggregates are dynamic. *Nat Cell Biol* **4**, 826-831 (2002).

129 Barghout, J. Y. J., Thiel, B. L. & Viney, C. Spider (*Araneus diadematus*) cocoon silk: a case of non-periodic lattice crystals with a twist? *Int J Biol Macromol* **24**, 211-217 (1999).

130 Parkhe, A. D., Seeley, S. K., Gardner, K., Thompson, L. & Lewis, R. V. Structural studies of spider silk proteins in the fiber. *J Mol Recognit* **10**, 1-6 (1997).

131 Ayoub, N. A., Garb, J. E., Kuelbs, A. & Hayashi, C. Y. Ancient Properties of Spider Silks Revealed by the Complete Gene Sequence of the Prey-Wrapping Silk Protein (AcSp1). *Mol Biol Evol* **30**, 589-601 (2013).

132 Shultz, J. W. THE ORIGIN OF THE SPINNING APPARATUS IN SPIDERS. *Biological Reviews* **62**, 89-113 (1987).

133 Guerette, P. A., Ginzinger, D. G., Weber, B. H. & Gosline, J. M. Silk properties determined by gland-specific expression of a spider fibroin gene family. *Science* **272**, 112-115 (1996).

134 Mita, K., Ichimura, S. & James, T. C. Highly Repetitive Structure and Its Organization of the Silk Fibroin Gene. *J Mol Evol* **38**, 583-592 (1994).

135 Simmons, A. H., Michal, C. A. & Jelinski, L. W. Molecular orientation and two-component nature of the crystalline fraction of spider dragline silk. *Science* **271**, 84-87 (1996).

136   Beckwitt, R. & Arcidiacono, S. Sequence Conservation in the C-Terminal Region of Spider Silk Proteins (Spidroin) from *Nephila Clavipes* (*Tetragnathidae*) and *Araneus Bicentenarius* (*Araneidae*). *J Biol Chem* **269**, 6661-6663 (1994).

137   Xu, M. & Lewis, R. V. Structure of a Protein Superfiber - Spider Dragline Silk. *Proc Natl Acad Sci U S A* **87**, 7120-7124 (1990).

138   Hayashi, C. Y. & Lewis, R. V. Molecular architecture and evolution of a modular spider silk protein gene. *Science* **287**, 1477-1479 (2000).

139   Sezutsu, H. & Yukuhiro, K. Dynamic rearrangement within the *Antheraea pernyi* silk fibroin gene is associated with four types of repetitive units. *J Mol Evol* **51**, 329-338 (2000).

140   Asakura, T., Umemura, K., Nakazawa, Y., Hirose, H., Higham, J. & Knight, D. Some observations on the structure and function of the spinning apparatus in the silkworm *Bombyx mori*. *Biomacromolecules* **8**, 175-181 (2007).

141   Matsumoto, K., Uejima, H., Iwasaki, T., Sano, Y. & Sumino, H. Studies on regenerated protein fibers .3. Production of regenerated silk fibroin fiber by the self-dialyzing wet spinning method. *J Appl Polym Sci* **60**, 503-511 (1996).

142   Doblhofer, E., Heidebrecht, A. & Scheibel, T. To spin or not to spin: spider silk fibers and more. *Appl Microbiol Biotechnol* **99**, 9361-9380 (2015).

143   Hijirida, D. H., Do, K. G., Michal, C., Wong, S., Zax, D. & Jelinski, L. W. 13C NMR of *Nephila clavipes* major ampullate silk gland. *Biophys J* **71**, 3442-3447 (1996).

144   Exler, J. H., Hummerich, D. & Scheibel, T. The amphiphilic properties of spider silks are important for spinning. *Angew Chem, Int Ed* **46**, 3559-3562 (2007).

145   Knight, D. P. & Vollrath, F. Changes in element composition along the spinning duct in a *Nephila* spider. *Naturwissenschaften* **88**, 179-182 (2001).

146   Papadopoulos, P., Solter, J. & Kremer, F. Structure-property relationships in major ampullate spider silk as deduced from polarized FTIR spectroscopy. *Eur Phys J E: Soft Matter Biol Phys* **24**, 193-199 (2007).

147   Andersson, M., Chen, G., Otikovs, M., Landreh, M., Nordling, K., Kronqvist, N., Westermark, P., Jornvall, H., Knight, S., Ridderstrale, Y., Holm, L., Meng, Q., Jaudzems, K., Chesler, M., Johansson, J. & Rising, A. Carbonic anhydrase generates CO2 and H+ that drive spider silk formation via opposite effects on the terminal domains. *PLoS Biol* **12**, e1001921 (2014).

148   Kronqvist, N., Otikovs, M., Chmyrov, V., Chen, G., Andersson, M., Nordling, K., Landreh, M., Sarr, M., Jornvall, H., Wennmalm, S., Widengren, J., Meng, Q., Rising, A., Otzen, D., Knight, S. D., Jaudzems, K. & Johansson, J. Sequential pH-driven dimerization and stabilization of the N-terminal domain enables rapid spider silk formation. *Nat. Commun.* **5**, 3254 (2014).

149   Rising, A. & Johansson, J. Toward spinning artificial spider silk. *Nat Chem Biol* **11**, 309-315 (2015).

150   Vollrath, F. & Knight, D. P. Structure and function of the silk production pathway in the spider *Nephila edulis*. *Int J Biol Macromol* **24**, 243-249 (1999).

151 Giesa, T., Perry, C. C. & Buehler, M. J. Secondary Structure Transition and Critical Stress for a Model of Spider Silk Assembly. *Biomacromolecules* **17**, 427-436 (2016).

152 Hagn, F., Thamm, C., Scheibel, T. & Kessler, H. pH-dependent dimerization and salt-dependent stabilization of the N-terminal domain of spider dragline silk – implications for fiber formation. *Angew Chem, Int Ed* **50**, 310-313 (2011).

153 Hardy, J. G., Romer, L. M. & Scheibel, T. R. Polymeric materials based on silk proteins. *Polymer* **49**, 4309-4327 (2008).

154 Du, N., Liu, X. Y., Narayanan, J., Li, L. A., Lim, M. L. M. & Li, D. Q. Design of superior spider silk: From nanostructure to mechanical properties. *Biophys J* **91**, 4528-4535 (2006).

155 Viney, C., Huber, A. E., Dunaway, D. L., Kerkam, K. & Case, S. T. in *Silk Polymers. Materials Science and Biotechnology* (eds D. L. Kaplan, W.W. Adams, B. Farmer, & C. Viney) 120-136 (American Chemical Society, 1994).

156 Riekel, C., Madsen, B., Knight, D. & Vollrath, F. X-ray diffraction on spider silk during controlled extrusion under a synchrotron radiation X-ray beam. *Biomacromolecules* **1**, 622-626 (2000).

157 Papadopoulos, P., Sölter, J. & Kremer, F. Hierarchies in the structural organization of spider silk—a quantitative model. *Colloid Polym Sci* **287**, 231-236 (2009).

158 Ene, R., Papadopoulos, P. & Kremer, F. Quantitative analysis of infrared absorption coefficient of spider silk fibers. *Vib Spectrosc* **57**, 207-212 (2011).

159 Ene, R., Papadopoulos, P. & Kremer, F. Partial deuteration probing structural changes in supercontracted spider silk. *Polymer* **51**, 4784-4789 (2010).

160 Anton, A. M., Kossack, W., Gutsche, C., Figuli, R., Papadopoulos, P., Ebad-Allah, J., Kuntscher, C. & Kremer, F. Pressure-Dependent FTIR-Spectroscopy on the Counterbalance between External and Internal Constraints in Spider Silk of *Nephila pilipes*. *Macromolecules* **46**, 4919-4923 (2013).

161 Mita, K., Ichimura, S., Zama, M. & James, T. C. Specific Codon Usage Pattern and Its Implications on the Secondary Structure of Silk Fibroin Messenger-RNA. *J Mol Biol* **203**, 917-925 (1988).

162 Keten, S., Xu, Z., Ihle, B. & Buehler, M. J. Nanoconfinement controls stiffness, strength and mechanical toughness of beta-sheet crystals in silk. *Nat Mater* **9**, 359-367 (2010).

163 Keerl, D. & Scheibel, T. Characterization of natural and biomimetic spider silk fibers. *Bioinspired, Biomimetic Nanobiomater* **1**, 83-94 (2012).

164 Shao, Z., Vollrath, F., Sirichaisit, J. & Young, R. J. Analysis of spider silk in native and supercontracted states using Raman spectroscopy. *Polymer* **40**, 2493-2500 (1999).

165 Oroudjev, E., Soares, J., Arcdiacono, S., Thompson, J. B., Fossey, S. A. & Hansma, H. G. Segmented nanofibers of spider dragline silk: atomic force microscopy and single-molecule force spectroscopy. *Proc Natl Acad Sci U S A* **99**, 6460-6465 (2002).

166   Sirichaisit, J., Brookes, V. L., Young, R. J. & Vollrath, F. Analysis of structure/property relationships in silkworm (*Bombyx mori*) and spider dragline (*Nephila edulis*) silks using Raman Spectroscopy. *Biomacromolecules* **4**, 387-394 (2003).

167   Brooks, A. E., Stricker, S. M., Joshi, S. B., Kamerzell, T. J., Middaugh, C. R. & Lewis, R. V. Properties of synthetic spider silk fibers based on *Argiope aurantia* MaSp2. *Biomacromolecules* **9**, 1506-1510 (2008).

168   Albertson, A. E., Teule, F., Weber, W., Yarger, J. L. & Lewis, R. V. Effects of different post-spin stretching conditions on the mechanical properties of synthetic spider silk fibers. *J Mech Behav Biomed Mater* **29**, 225-234 (2014).

169   Keten, S. & Buehler, M. J. Nanostructure and molecular mechanics of spider dragline silk protein assemblies. *J R Soc Interface* **7**, 1709-1721 (2010).

170   Nova, A., Keten, S., Pugno, N. M., Redaelli, A. & Buehler, M. J. Molecular and nanostructural mechanisms of deformation, strength and toughness of spider silk fibrils. *Nano Lett* **10**, 2626-2634 (2010).

171   Qin, Z. & Buehler, M. J. Cooperativity governs the size and structure of biological interfaces. *J Biomech* **45**, 2778-2783 (2012).

172   Alam, P. Protein unfolding versus beta-sheet separation in spider silk nanocrystals. *Adv Nat Sci: Nanosci Nanotechnol* **5** (2014).

173   Tsujimoto, Y. & Suzuki, Y. Structural-Analysis of the Fibroin Gene at the 5' End and Its Surrounding Regions. *Cell* **16**, 425-436 (1979).

174   Colomban, P., Dinh, H. M., Riand, J., Prinsloo, L. C. & Mauchamp, B. Nanomechanics of single silkworm and spider fibres: a Raman and micro-mechanical in situ study of the conformation change with stress. *J Raman Spectrosc* **39**, 1749-1764 (2008).

175   Du, N., Yang, Z., Liu, X. Y., Li, Y. & Xu, H. Y. Structural Origin of the Strain-Hardening of Spider Silk. *Adv Funct Mater* **21**, 772-778 (2011).

176   Qin, Z., Dimas, L., Adler, D., Bratzel, G. & Buehler, M. J. Biological materials by design. *J Phys Condens Matter* **26**, 073101 (2014).

177   Zhao, H.-P., Feng, X.-Q., Yu, S.-W., Cui, W.-Z. & Zou, F.-Z. Mechanical properties of silkworm cocoons. *Polymer* **46**, 9192-9201 (2005).

178   Work, R. W. & Emerson, P. D. An Apparatus and Technique for the Forcible Silking of Spiders. *J Arachnol* **10**, 1-10 (1982).

179   Riekel, C., Muller, M. & Vollrath, F. In situ X-ray diffraction during forced silking of spider silk. *Macromolecules* **32**, 4464-4466 (1999).

180   Ortlepp, C. S. & Gosline, J. M. Consequences of forced silking. *Biomacromolecules* **5**, 727-731 (2004).

181   Knight, D. P., Knight, M. M. & Vollrath, F. Beta transition and stress-induced phase separation in the spinning of spider dragline silk. *Int J Biol Macromol* **27**, 205-210 (2000).

182   Vollrath, F., Madsen, B. & Shao, Z. Z. The effect of spinning conditions on the mechanics of a spider's dragline silk. *Proc R Soc London, Ser B* **268**, 2339-2346 (2001).

183   Craig, C. L., Riekel, C., Herberstein, M. E., Weber, R. S., Kaplan, D. & Pierce, N. E. Evidence for diet effects on the composition of silk proteins produced by spiders. *Mol Biol Evol* **17**, 1904-1913 (2000).

184   Fox, L. R. Cannibalism in natural populations. *Annu Rev Ecology and Systematics* **6**, 87-106 (1975).

185   Perez-Rigueiro, J., Viney, C., Llorca, J. & Elices, M. Silkworm silk as an engineering material. *J Appl Polym Sci* **70**, 2439-2447 (1998).

186   Vollrath, F. Strength and structure of spiders' silks. *J Biotechnol* **74**, 67-83 (2000).

187   Holland, C., Terry, A. E., Porter, D. & Vollrath, F. Natural and unnatural silks. *Polymer* **48**, 3388-3392 (2007).

188   Iridag, Y. & Kazanci, M. Preparation and characterization of *Bombyx mori* silk fibroin and wool keratin. *J Appl Polym Sci* **100**, 4260-4264 (2006).

189   Yamada, H., Nakao, H., Takasu, Y. & Tsubouchi, K. Preparation of undegraded native molecular fibroin solution from silkworm cocoons. *Mater Sci Eng C* **14**, 41-46 (2001).

190   Zuo, B., Dai, L. & Wu, Z. Analysis of structure and properties of biodegradable regenerated silk fibroin fibers. *J Mater Sci* **41**, 3357-3361 (2006).

191   Lazaris, A., Arcidiacono, S., Huang, Y., Zhou, J. F., Duguay, F., Chretien, N., Welsh, E. A., Soares, J. W. & Karatzas, C. N. Spider silk fibers spun from soluble recombinant silk produced in mammalian cells. *Science* **295**, 472-476 (2002).

192   Liivak, O., Blye, A., Shah, N. & Jelinski, L. W. A microfabricated wet-spinning apparatus to spin fibers of silk proteins. Structure-property correlations. *Macromolecules* **31**, 2947-2951 (1998).

193   Marsano, E., Corsini, P., Arosio, C., Boschi, A., Mormino, M. & Freddi, G. Wet spinning of *Bombyx mori* silk fibroin dissolved in N-methyl morpholine N-oxide and properties of regenerated fibres. *Int J Biol Macromol* **37**, 179-188 (2005).

194   Shao, Z. Z., Vollrath, F., Yang, Y. & Thogersen, H. C. Structure and behavior of regenerated spider silk. *Macromolecules* **36**, 1157-1161 (2003).

195   Xie, F., Zhang, H. H., Shao, H. L. & Hu, X. C. Effect of shearing on formation of silk fibers from regenerated *Bombyx mori* silk fibroin aqueous solution. *Int J Biol Macromol* **38**, 284-288 (2006).

196   Yao, J. M., Masuda, H., Zhao, C. H. & Asakura, T. Artificial spinning and characterization of silk fiber from *Bombyx mori* silk fibroin in hexafluoroacetone hydrate. *Macromolecules* **35**, 6-9 (2002).

197   Seidel, A., Liivak, O., Calve, S., Adaska, J., Ji, G. D., Yang, Z. T., Grubb, D., Zax, D. B. & Jelinski, L. W. Regenerated spider silk: Processing, properties, and structure. *Macromolecules* **33**, 775-780 (2000).

198   Seidel, A., Liivak, O. & Jelinski, L. W. Artificial spinning of spider silk. *Macromolecules* **31**, 6733-6736 (1998).

199   Tamura, T., Thibert, C., Royer, C., Kanda, T., Abraham, E., Kamba, M., Komoto, N., Thomas, J. L., Mauchamp, B., Chavancy, G., Shirk, P., Fraser, M., Prudhomme, J. C. & Couble, P. Germline transformation of the silkworm *Bombyx mori* L. using a piggyBac transposon-derived vector. *Nat Biotechnol* **18**, 81-84 (2000).

200   Kuwana, Y., Sezutsu, H., Nakajima, K., Tamada, Y. & Kojima, K. High-toughness silk produced by a transgenic silkworm expressing spider (*Araneus ventricosus*) dragline silk protein. *PLoS One* **9**, e105325 (2014).

201   Teule, F., Miao, Y. G., Sohn, B. H., Kim, Y. S., Hull, J. J., Fraser, M. J., Jr., Lewis, R. V. & Jarvis, D. L. Silkworms transformed with chimeric silkworm/spider silk genes spin composite silk fibers with improved mechanical properties. *Proc Natl Acad Sci U S A* **109**, 923-928 (2012).

202   Zhu, Z. H., Kikuchi, Y., Kojima, K., Tamura, T., Kuwabara, N., Nakamura, T. & Asakura, T. Mechanical properties of regenerated *Bombyx mori* silk fibers and recombinant silk fibers produced by transgenic silkworms. *J Biomater Sci, Polym Ed* **21**, 395-412 (2010).

203   Wen, H. X., Lan, X. Q., Zhang, Y. S., Zhao, T. F., Wang, Y. J., Kajiura, Z. & Nakagaki, M. Transgenic silkworms (*Bombyx mori*) produce recombinant spider dragline silk in cocoons. *Mol Biol Rep* **37**, 1815-1821 (2010).

204   Arcidiacono, S., Mello, C., Kaplan, D., Cheley, S. & Bayley, H. Purification and characterization of recombinant spider silk expressed in *Escherichia coli*. *Appl Microbiol Biotechnol* **49**, 31-38 (1998).

205   Bini, E., Foo, C. W., Huang, J., Karageorgiou, V., Kitchel, B. & Kaplan, D. L. RGD-functionalized bioengineered spider dragline silk biomaterial. *Biomacromolecules* **7**, 3139-3145 (2006).

206   Fahnestock, S. R. & Bedzyk, L. A. Production of synthetic spider dragline silk protein in *Pichia pastoris*. *Appl Microbiol Biotechnol* **47**, 33-39 (1997).

207   Werten, M. W. T., Moers, A. P. H. A., Vong, T., Zuilhof, H., van Hest, J. C. M. & de Wolf, F. A. Biosynthesis of an Amphiphilic Silk-Like Polymer. *Biomacromolecules* (2008).

208   Grip, S., Rising, A., Nimmervoll, H., Storckenfeldt, E., McQueen-Mason, S. J., Pouchkina-Stantcheva, N., Vollrath, F., Engström, W. & Fernandez-Arias, A. Transient expression of a major ampullate spidroin 1 gene fragment from *Euprosthenops* sp. in mammalian cells. *Cancer Genomics Proteomics* **3**, 83-87 (2006).

209   Rosenberg, A. H., Goldman, E., Dunn, J. J., Studier, F. W. & Zubay, G. Effects of consecutive AGG codons on translation in *Escherichia coli*, demonstrated with a versatile codon test system. *J Bacteriol* **175**, 716-722 (1993).

210   Fahnestock, S. R. & Irwin, S. L. Synthetic spider dragline silk proteins and their production in *Escherichia coli*. *Appl Microbiol Biotechnol* **47**, 23-32 (1997).

211   Xia, X.-X., Qian, Z.-G., Ki, C. S., Park, Y. H., Kaplan, D. L. & Lee, S. Y. Native-sized recombinant spider silk protein produced in metabolically engineered

Escherichia coli results in a strong fiber. *Proc Natl Acad Sci U S A* **107**, 14059-14063 (2010).

212   Harvey, B. R., Georgiou, G., Hayhurst, A., Jeong, K. J., Iverson, B. L. & Rogers, G. K. Anchored periplasmic expression, a versatile technology for the isolation of high-affinity antibodies from *Escherichia coli*-expressed libraries. *Proc Natl Acad Sci U S A* **101**, 9193-9198 (2004).

213   Lee, P. A., Tullman-Ercek, D. & Georgiou, G. The bacterial twin-arginine translocation pathway. *Ann Rev Microbiol* **60**, 373-395 (2006).

214   Um, I. C., Ki, C. S., Kweon, H., Lee, K. G., Ihm, D. W. & Park, Y. H. Wet spinning of silk polymer. II. Effect of drawing on the structural characteristics and properties of filament. *Int J Biol Macromol* **34**, 107-119 (2004).

215   Adrianos, S. L., Teule, F., Hinman, M. B., Jones, J. A., Weber, W. S., Yarger, J. L. & Lewis, R. V. *Nephila clavipes* Flagelliform silk-like GGX motifs contribute to extensibility and spacer motifs contribute to strength in synthetic spider silk fibers. *Biomacromolecules* **14**, 1751-1760 (2013).

216   An, B., Hinman, M. B., Holland, G. P., Yarger, J. L. & Lewis, R. V. Inducing beta-sheets formation in synthetic spider silk fibers by aqueous post-spin stretching. *Biomacromolecules* **12**, 2375-2381 (2011).

217   Lin, Z., Deng, Q., Liu, X. Y. & Yang, D. Engineered large spider eggcase silk protein for strong artificial fibers. *Adv Mater* **25**, 1216-1220 (2013).

218   Teule, F., Furin, W. A., Cooper, A. R., Duncan, J. R. & Lewis, R. V. Modifications of spider silk sequences in an attempt to control the mechanical properties of the synthetic fibers. *J Mater Sci* **42**, 8974-8985 (2007).

219   Peng, H., Zhou, S., Jiang, J., Guo, T., Zheng, X. & Yu, X. Pressure-induced crystal memory effect of spider silk proteins. *J Phys Chem B* **113**, 4636-4641 (2009).

220   Bogush, V. G., Sokolova, O. S., Davydova, L. I., Klinov, D. V., Sidoruk, K. V., Esipova, N. G., Neretina, T. V., Orchanskyi, I. A., Makeev, V. Y., Tumanyan, V. G., Shaitan, K. V., Debabov, V. G. & Kirpichnikov, M. P. A novel model system for design of biomaterials based on recombinant analogs of spider silk proteins. *J Neuroimmune Pharmacol* **4**, 17-27 (2009).

221   Arcidiacono, S., Mello, C. M., Butler, M., Welsh, E., Soares, J. W., Allen, A., Ziegler, D., Laue, T. & Chase, S. Aqueous processing and fiber spinning of recombinant spider silks. *Macromolecules* **35**, 1262-1266 (2002).

222   Jones, J. A., Harris, T. I., Tucker, C. L., Berg, K. R., Christy, S. Y., Day, B. A., Gaztambide, D. A., Needham, N. J., Ruben, A. L., Oliveira, P. F., Decker, R. E. & Lewis, R. V. More Than Just Fibers: An Aqueous Method for the Production of Innovative Recombinant Spider Silk Protein Materials. *Biomacromolecules* (2015).

223   Grip, S., Johansson, J. & Hedhammar, M. Engineered disulfides improve mechanical properties of recombinant spider silk. *Protein Sci* **18**, 1012-1022 (2009).

224   Stark, M., Grip, S., Rising, A., Hedhammar, M., Engstrom, W., Hjalm, G. & Johansson, J. Macroscopic fibers self-assembled from recombinant miniature spider silk proteins. *Biomacromolecules* **8**, 1695-1701 (2007).

225   Greiner, A. & Wendorff, J. H. Electrospinning: A fascinating method for the preparation of ultrathin fibres. *Angew Chem, Int Ed* **46**, 5670-5703 (2007).

226   Smit, E., Buttner, U. & Sanderson, R. D. Continuous yarns from electrospun fibers. *Polymer* **46**, 2419-2423 (2005).

227   Teo, W. E. & Ramakrishna, S. A review on electrospinning design and nanofibre assemblies. *Nanotechnology* **17**, R89-R106 (2006).

228   Zhu, B., Li, W., Lewis, R. V., Segre, C. U. & Wang, R. E-spun composite fibers of collagen and dragline silk protein: fiber mechanics, biocompatibility, and application in stem cell differentiation. *Biomacromolecules* **16**, 202-213 (2015).

229   Lang, G., Jokisch, S. & Scheibel, T. Air filter devices including nonwoven meshes of electrospun recombinant spider silk proteins. *J Vis Exp*, e50492 (2013).

230   Yu, Q., Xu, S., Zhang, H., Gu, L., Xu, Y. & Ko, F. Structure-property relationship of regenerated spider silk protein nano/microfibrous scaffold fabricated by electrospinning. *J Biomed Mater Res A* **102**, 3828-3837 (2014).

231   Leal-Egana, A., Lang, G., Mauerer, C., Wickinghoff, J., Weber, M., Geimer, S. & Scheibel, T. Interactions of Fibroblasts with Different Morphologies Made of an Engineered Spider Silk Protein. *Adv Eng Mater* **14**, B67-B75 (2012).

232   Fredriksson, C., Hedhammar, M., Feinstein, R., Nordling, K., Kratz, G., Johansson, J., Huss, F. & Rising, A. Tissue Response to Subcutaneously Implanted Recombinant Spider Silk: An in Vivo Study. *Materials* **2**, 1908-1922 (2009).

233   Rammensee, S., Slotta, U., Scheibel, T. & Bausch, A. R. Assembly mechanism of recombinant spider silk proteins. *Proc Natl Acad Sci U S A* **105**, 6590-6595 (2008).

234   Schacht, K. & Scheibel, T. Controlled hydrogel formation of a recombinant spider silk protein. *Biomacromolecules* **12**, 2488-2495 (2011).

235   Humenik, M., Magdeburg, M. & Scheibel, T. Influence of repeat numbers on self-assembly rates of repetitive recombinant spider silk proteins. *J Struct Biol* **186**, 431-437 (2014).

236   Hancock, T. A., Spruiell, J. E. & White, J. L. Wet spinning of aliphatic and aromatic polyamides. *J Appl Polym Sci* **21**, 1227-1247 (1977).

237   Gupta, P., Elkins, C., Long, T. E. & Wilkes, G. L. Electrospinning of linear homopolymers of poly(methyl methacrylate): exploring relationships between fiber formation, viscosity, molecular weight and concentration in a good solvent. *Polymer* **46**, 4799-4810 (2005).

238   Grubb, D. T. & Jelinski, L. W. Fiber morphology of spider silk: The effects of tensile deformation. *Macromolecules* **30**, 2860-2867 (1997).

239   Sampath, S., Isdebski, T., Jenkins, J. E., Ayon, J. V., Henning, R. W., Orgel, J. P. R. O., Antipoa, O. & Yarger, J. L. X-ray diffraction study of nanocrystalline and amorphous structure within major and minor ampullate dragline spider silks. *Soft Matter* **8**, 6713-6722 (2012).

240   Glisovic, A., Vehoff, T., Davies, R. J. & Salditt, T. Strain dependent structural changes of spider dragline silk. *Macromolecules* **41**, 390-398 (2008).

241   Ene, R., Papadopoulos, P. & Kremer, F. Combined structural model of spider dragline silk. *Soft Matter* **5**, 4568-4574 (2009).

242   Fu, C. J., Shao, Z. Z. & Vollrath, F. Animal silks: their structures, properties and artificial production. *Chem Commun*, 6515-6529 (2009).

243   Hayashi, C. Y., Shipley, N. H. & Lewis, R. V. Hypotheses that correlate the sequence, structure, and mechanical properties of spider silk proteins. *Int J Biol Macromol* **24**, 271-275 (1999).

244   Anton, A. M., Gutsche, C., Kossack, W. & Kremer, F. Methods to determine the pressure dependence of the molecular order parameter in (bio) macromolecular fibres. *Soft Matter* **11**, 1158-1164 (2015).

245   Pulay, P. Vibrational Spectroscopy of Polymers: Principles and Practice *J Am Chem Soc* **130**, 5000 (2008).

246   Adhikari, R., Huy, T. A., Buschnakowski, M., Michler, G. H. & Knoll, K. Asymmetric PS-block-(PS-co-PB)-block-PS block copolymers: morphology formation and deformation behaviour. *New J Phys* **6** (2004).

247   Mahmood, N., Anton, A. M., Gupta, G., Babur, T., Knoll, K., Thurn-Albrecht, T., Kremer, F., Beiner, M. & Weidisch, R. Influence of shear processing on morphology orientation and mechanical properties of styrene butadiene triblock copolymers. *Polymer* **55**, 3782-3791 (2014).

248   Boulet-Audet, M., Terry, A. E., Vollrath, F. & Holland, C. Silk protein aggregation kinetics revealed by Rheo-IR. *Acta Biomater* **10**, 776-784 (2014).

249   Papadopoulos, P., Ene, R., Weidner, I. & Kremer, F. Similarities in the Structural Organization of Major and Minor Ampullate Spider Silk. *Macromol Rapid Comm* **30**, 851-857 (2009).

5. PUBLICATION LIST

I. **Heidebrecht, A.**, Eisoldt, L., Diehl, J., Schmidt, A., Geffers, M., Lang, G., and Scheibel, T. (2015) Biomimetic Fibers Made of Recombinant Spidroins with the Same Toughness as Natural Spider Silk. *Advanced Materials*. 27, pp. 2189-2194

II. Anton, M. A.*, **Heidebrecht, A.***, Mahmood, N., Beiner, M., Scheibel, T.[§], and Kremer, F.[§] (2016) Foundation of the outstanding toughness in biomimetic & natural spider silk. *Manuscript*.

III. **Heidebrecht, A.** & Scheibel, T. (2013) Recombinant Production of Spider Silk Proteins. *Advances in Applied Microbiology*. 82, pp. 115-153

IV. Doblhofer, E.*, **Heidebrecht, A.*** & Scheibel, T. (2015) To Spin or Not to Spin: Spider Silk Fibers and More. *Applied Microbiology & Biotechnology*. 99, pp. 9361-9380

* These authors contributed equally to the work.

[§] These authors contributed equally to the work.

6. INDIVIDUAL CONTRIBUTION TO JOINED PUBLICATIONS AND MANUSCRIPTS

The results presented in this dissertation were achieved in joint work with cooperation partners and were published in the specified scientific journals. Following the individual contributions of all authors to the publications are indicated.

I. **Heidebrecht, A.**, Eisoldt, L., Diehl, J., Schmidt, A., Geffers, M., Lang, G., and Scheibel, T. (2015) Biomimetic Fibers Made of Recombinant Spidroins with the Same Toughness as Natural Spider Silk. *Advanced Materials.* 27, pp. 2189-2194

Research for this publication was designed by T. Scheibel and me. Cloning work and establishment of purification strategies was performed by L. Eisoldt and me. Production and purification of proteins was performed by J. Diehl, A. Schmidt and me. M. Geffers and G. Lang performed preliminary spinning dope preparation (classical) and wet-spinning tests. Optimization of the classical spinning dope, the wet-spinning and post-stretching processes was done by me. The biomimetic spinning dope was developed by me and I performed all wet-spinning and post-stretching experiments. Characterization of the fibers using optical microscope and FTIR-measurements, as well as performing tensile tests, statistical analysis and writing of the manuscript was done by me. J. Diehl provided SEM-images and T. Scheibel engaged in finalizing the manuscript.

II. Anton, M. A.*, **Heidebrecht, A.***, Mahmood, N., Beiner, M., Scheibel, T.[§], and Kremer, F.[§] (2016) Foundation of the outstanding toughness in biomimetic & natural spider silk. *Manuscript.*

Research for this publication was designed by A. M. Anton, F. Kremer, T. Scheibel and me. Production and purification of proteins, as well as producing classical and biomimetic spinning dopes and performing wet spinning and post-stretching was done by me. A. M. Anton performed FTIR measurements and N. Mahmood and M. Beiner executed the X-ray scattering. All authors contributed to analyzing the results and writing the manuscript.

* These authors contributed equally to the work.

§ These authors contributed equally to the work.

III.   **Heidebrecht, A.** and Scheibel, T. (2013) Recombinant Production of Spider Silk Proteins. Advances in Applied Microbiology. 82, pp. 115-153

The concept of this publication was prepared by T. Scheibel and me. I wrote the manuscript and it was finalized by T. Scheibel and me.

IV.   Doblhofer, E.*, **Heidebrecht, A.***, and Scheibel, T. (2015) To Spin or Not to Spin: Spider Silk Fibers and More. Applied Microbiology & Biotechnology. 99, pp. 9361-9380

The concept of this publication was prepared by T. Scheibel and me. All authors contributed in writing and finalizing the manuscript.

* These authors contributed equally to the work.

Part 1

Biomimetic Fibers Made of Recombinant Spidroins with the Same Toughness as Natural Spider Silk

Heidebrecht, A., Eisoldt, L., Diehl, J., Schmidt, A., Geffers, M., Lang, G., and Scheibel, T.

Biomimetic Fibers Made of Recombinant Spidroins with the Same Toughness as Natural Spider Silk

Aniela Heidebrecht, Lukas Eisoldt, Johannes Diehl, Andreas Schmidt, Martha Geffers, Gregor Lang, and Thomas Scheibel*

Spider dragline silk exhibits extraordinary mechanical properties combining a moderate strength with good extensibility resulting in a toughness exceeding that of all other natural or synthetic fibers. Although spider silk has been in the focus of research since decades, the mechanical properties, especially the toughness, of reconstituted man-made fibers have never reached those of natural spider silk. The properties are based on the underlying spider silk proteins (spidroins), their self-assembly and their explicit processing. Here, two out of three pre-requisites for tough fibers are tackled; the contribution of individual spidroin domains to assembly is analyzed, and processing of recombinant spidroins into fibers is shown. Fiber toughness upon processing equals and even slightly exceeds that of natural ones dependent on both the underlying proteins and preparation (biomimetic self-assembly) of the silk dope, although the overall strength is lower based on the used and simplified single-protein set-up.

Spider dragline silk has for long been in the focus of materials' research mainly due to a toughness no other fiber can accomplish. Spider major ampullate (MA) silk fibers, aka dragline silk, show a core-shell-structure, with the core comprising proteinaceous fibrils covered by a three-layered shell of minor ampullate (MI) silk, glycoproteins and lipids, with only a minor role for the mechanical properties of the fibers.[1] The mechanics are mainly based on the protein fibrils comprising at least two proteins classified as MaSp1 and MaSp2 (MaSp, spidroin = spider fibroin), both of which are generally distinguished by their proline content, which is significantly higher in MaSp2.[2–4] MA spidroins have a molecular weight of 200–350 kDa[5,6] and are composed of a highly repetitive core domain flanked by amino- and carboxy-terminal domains with a distinct sequence. The core domain contains repeated (up to 100 times)[4,5] amino acid modules of 40–200 amino acids[3–5] composed of polyalanine stretches and glycine/proline-rich motifs. The strength of natural spider silk fibers is based on the polyalanine stretches stacked into β-sheets[7] resembling nanocrystallites which are embedded in an amorphous matrix,[1,8] based on the glycine/proline-rich areas and being responsible for the fiber's elasticity and flexibility.[9]

The number of tandemly arrayed glycine/proline-rich motifs (GPGXX, X = predominantly tyrosine, leucine, glutamine)[4] is directly connected to the extensibility of silks. MaSp2 has nine consecutive GPGXX-motifs in a single repeat unit,[4] whereas flagelliform silk has at least 43 of these motifs in one unit[10] and is the most extensible spider silk with 200% of elongation.[2] Strikingly, the terminal domains are highly conserved between different spider species and even between silk types of individual spiders; they are composed of 100–150 amino acids and are folded into five-helix bundles.[11,12] The terminal domains are assembly triggers enabling the spidroin storage at high concentrations (up to 50% (w/v)) in the ampulla of the spinning gland (resembling the so-called spinning dope) and play an important role during initiation of fiber assembly.[13–16]

It has been hypothesized that pre-assembly of spidroins in the gland is the cause for lyotropic liquid crystal behavior in vivo.[17,18] Upon passage of the spinning dope through the tapered S-shaped spinning duct, sodium and chloride ions are replaced by potassium and more kosmotropic phosphate ions (inducing salting-out of the spidroins).[19,20] In combination with shear-stress, emerging from pulling the fibers from the spider's abdomen, the spidroins assemble into a nematic phase,[17] enabling formation and correct alignment of β-sheet-rich structures.[16] In vitro, during storage of the spidroins at pH 8.0 micellar-like structures can be detected, strictly depending on the presence of the carboxy-terminal domain[14] based on the fact that carboxy-terminal domains form disulfide-linked parallel dimers,[16] while the amino-terminal domains are monomeric at neutral pH.[21] Adding phosphate ions causes the nonrepetitive carboxy-terminal domain to partially refold and subsequently expose hydrophobic areas,[16] necessary to initiate fiber assembly. Further, upon decreasing the pH to ≈5.7, as found at the end of the spinning duct in vivo,[22] dimerization of the amino-terminal domain in an antiparallel manner is triggered in vitro,[22] yielding head-to-tail dimers enabling the formation of an endless network connecting the nanocrytalline β-sheet structures.[14–16,21]

Even though plenty of artificial spider silk fibers have been produced in the past using different recombinant or reconstituted spidroins and spinning-techniques, so far no fibers have been obtained with mechanical properties, i.e., toughness, even getting close to that of natural spider silk fibers.[23]

Here, we made use of previously established technologies to recombinantly produce spider silk-like proteins based on the sequence of garden spider (*A. diadematus*) MA spidroins. *A. diadematus* MA silk contains, in contrast to other investigated spider species, at least two MaSp2 proteins which are called *A. diadematus* fibroin 3 and 4 (ADF3 and ADF4). Here, based on

A. Heidebrecht, L. Eisoldt, J. Diehl, A. Schmidt,
M. Geffers, G. Lang, Prof. T. Scheibel
Lehrstuhl Biomaterialien
Fakultät für Ingenieurwissenschaften
Universität Bayreuth
95440, Bayreuth, Germany
E-mail: thomas.scheibel@bm.uni-bayreuth.de
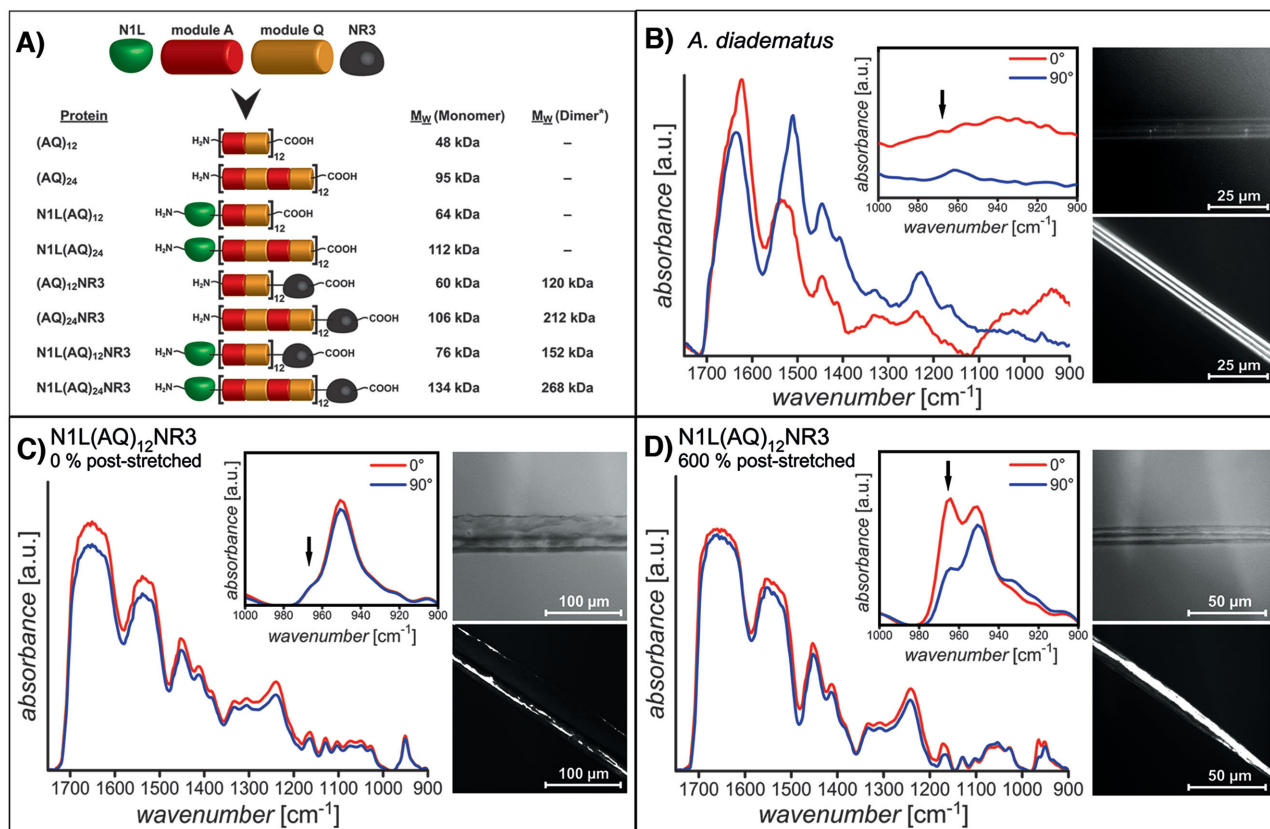
Figure 1. A) Scheme of the employed recombinant proteins, the sequences of the individual domains are derived from ADF3 (see the Supporting Information), one of the two identified MaSp2 components of *A. diadematus* dragline silk. The theoretical molecular weight (M_W, calculated using the ProtParam tool: http://web.expasy.org/protparam/) of the respective recombinant proteins is shown. *: Disulfide linked. B–D) Polarized FTIR spectra taken in parallel (0°, red) and perpendicular (90°, blue) to the fiber axis. (Inset) Enlargement of the absorption between 1000 and 900 cm^{-1}. The arrows in the insets mark the specific $(Ala)_n$ absorbance at ≈963 cm^{-1}; B) *A. diadematus* dragline silk, C) eADF3 $(N1L(AQ)_{12}NR3)$-fibers, 0% poststretched, D) eADF3 $(N1L(AQ)_{12}NR3)$-fibers, 600% poststretched.

consensus sequences of ADF3 (sequence accession number: AAC47010) eight engineered variants (eADF3) were designed for recombinant production in *E. coli*, varying in length/number of core repeats and presence/absence of the amino- and/or carboxy-terminal domains (**Figure 1**A), in order to investigate the impact of individual domains on storage, spinning dope conditions, assembly, and mechanical properties of fibers upon spinning.

Previously, the spinning dope has been identified as one highly important factor for spinning.[24] In nature, spider silk spinning dopes are highly concentrated (up to 50% (w/v)). Technically, such high concentrations can be achieved by step-wise concentrating solutions. "Classical" spinning dopes (CSD) were produced by simply removing excess water from the protein solution using dialysis against polyethylene glycol (PEG) yielding concentrations between 10% (w/v) to 17% (w/v). In order to prevent unspecific aggregation, 100×10^{-3} M NaCl was added to the buffered (50×10^{-3} M Tris/HCl, pH 8.0) solution prior to dialysis against PEG. Electrolytic conductivity measurements (Table S1, Supporting Information) showed no detectable amounts of salt after PEG-dialysis. Further, structural analysis of recombinant spider silk solutions before and after dialysis against PEG showed no change in protein structure.[25]

Dialysis of a solution with low protein concentration against a phosphate-containing buffer induced a liquid–liquid phase separation of eADF3 variants comprising the carboxy-terminal domain NR3 into a low density phase and a "self-concentrated" high density micellar phase[14] yielding a dope named "bio-mimetic" from now on. The addition of the phosphate ions induces a partial refolding of the carboxy-terminal domain, leading to initiation of protein assembly into micelles. Further, the presence of the carboxy-terminal domain is an important prerequisite for fiber self-assembly. Dynamic light scattering experiments on eADF3 high and low density phases revealed that the high density phase contains protein oligomers ($M_W > 30$ MDa), which were noncovalently associated, whereas the low density phase only showed dimeric proteins.[26]

While the phase-separated "biomimetic" spinning dopes (BSD) were stable for 3–5 days, the CSD gelled within a few hours due to nucleated fertilization of the proteins.[27,28]

Wet-spinning of CSD (before gelation started) by precipitation of the spidroins in a coagulation bath containing a mixture of water and isopropanol, as used previously,[29] typically yielded inhomogeneous fibers (Figure S1, Supporting Information) and sometimes short fiber fragments. The least homogeneous fibers were obtained from dopes comprising spidroins without

the carboxy-terminal domain ((AQ)$_{12}$, (AQ)$_{24}$, N1L(AQ)$_{12}$, N1L(AQ)$_{24}$). In contrast, spinning from BSD generally resulted in very homogeneous and long fibers. However, it was necessary to improve the performance of the fibers by poststretching. Du et al.[30] detected that the protein network structure (predominantly size and orientation of β-sheet crystals) changes substantially with the silk reeling speed and thus determines the mechanical properties of the silk fiber. In the natural spinning process the spider can control the reeling speed with its hind legs, poststretching the fiber as soon as it leaves the spinneret. While the formation of the liquid crystalline phase occurs quickly, the crystalline phase is formed slowly,[31] and this phase transition depends on the initial concentration and supersaturation of the silk protein solution. Upon shearing as well as poststretching, the protein chains are extended and thus getting closer to each other. As the local protein concentration is increased, crystal nucleation between the protein chains is triggered. A high reeling speed results in a high β-sheet crystal nucleus density, leading to fibers containing smaller crystallites, but with an increased crystal proportion.[30] Concerning the orientation of the β-sheet crystals, it was observed that a high reeling speed induces a better orientation of the β-sheet crystals along the thread axis.[30,32] Therefore, reeling and poststretching of the spider's silk fiber defines its mechanical properties. Similar observations were made with fibers from flexible polymers, where drawing and postdraw stretching led to better mechanical properties (e.g., higher tenacity) due to better strain alignment.[33] In our set-up, the recombinant fibers were stretched up to 600% of their initial length directly after

spinning to align the spidroins. The diameter of poststretched fibers spun from BSD was uniform throughout each individual fiber with a mean diameter variation <5%. Approximately 5% of fibers spun from BSD were disposed due to defects or inhomogeneity, while poststretched fibers which were spun from CSD contained approximately 15% inhomogeneous or defective fibers. Polarized Fourier transformation infrared (FTIR) spectroscopy was used in parallel (0°) and perpendicular (90°) to the fiber axis to determine the alignment of the β-sheet stacks in the fibers (Figure 1, B–D). The absorption peak at ≈963 cm^{-1} corresponds to a highly specific coupled main- and side chain stretching (CH$_3$ rock, N–Cα stretch)[20] of the β-sheet forming (Ala)$_n$ sequences.

The intensity of the (Ala)$_n$ peak at 963 cm^{-1} in *A. diadematus* dragline fibers is significantly higher in parallel than perpendicular to the fiber axis, demonstrating the alignment of the (Ala)$_n$ β-sheet stacks along the fiber axis. The polarized FTIR spectra of the recombinant spider silk fibers showed a similar result, but only in poststretched ones, confirming the impact of shear stress on structure alignment. Tensile testing of all recombinant spidroin fibers showed that poststretching also significantly improved the mechanical properties, while as-spun fibers without structural alignment (0% poststretching) appeared to be very brittle (**Figure 2**).

The differences in mechanics upon stretching depended on a) the molecular set-up of the recombinant spidroins and, even more importantly, b) the dope preparation. (AQ)$_{12}$-fibers spun from CSD were very brittle and poststretching was only possible up to 400% of the initial length without breaking
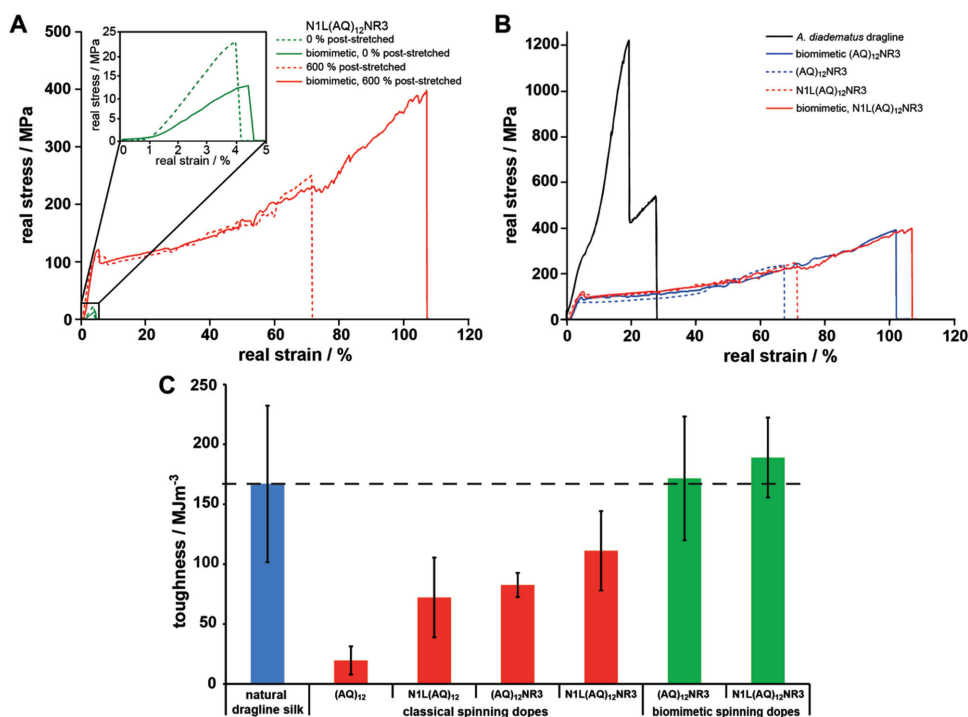
**Figure 2.** A,B) Real stress–real strain curves of recombinant and natural spider silk fibers. A) As-spun (inset) and 600% poststretched N1L(AQ)$_{12}$NR3-fibers, spun from "classical" (CSD) as well as "biomimetic" (BSD) spinning dopes (both 10% (w/v)) and B) 600% poststretched (AQ)$_{12}$NR3- and N1L(AQ)$_{12}$NR3-fibers from CSD as well as BSD in comparison to natural *A. diadematus* dragline silk fibers. C) Average toughness of natural dragline silk fibers (blue), fibers spun from CSD (red) and BSD (green).

Table 1. Mechanical properties of natural and recombinant spider silk fibers. (A, B) CSD (all variants) and (C) BSD (variants with carboxy-terminal domain only). Tensile testing was performed at 30% rH.

A

Protein	$(AQ)_{12}$		$(AQ)_{24}$		$N1L(AQ)_{12}$		$N1L(AQ)_{24}$	
Stretching [%]	0	400	0	600	0	400	0	300
Diameter [µm]	35 ± 7	15 ± 5	70 ± 7	22 ± 2	42 ± 6	15 ± 2	78 ± 21	55 ± 9
Extensibility [%]	17 ± 9	38 ± 16	22 ± 3	65 ± 6	8 ± 1	51 ± 17	6 ± 2	10 ± 6
Strength [MPa]	10 ± 2	66 ± 22	22 ± 4	280 ± 48	19 ± 3	212 ± 53	15 ± 3	24 ± 7
Toughness [MJ m^{-3}]	0.9 ± 0.4	20 ± 12	4 ± 1	110 ± 24	1 ± 0.4	72 ± 33	0.4 ± 0.2	2 ± 1
Young's modulus [GPa]	0.9 ± 0.4	2 ± 0.9	0.4 ± 0.1	4 ± 0.6	0.5 ± 0.1	4 ± 0.9	0.7 ± 0.2	1 ± 0.3

B

Protein	$(AQ)_{12}NR3$		$(AQ)_{24}NR3$		$N1L(AQ)_{12}NR3$		$N1L(AQ)_{24}NR3$	
Stretching [%]	0	600	0	600	0	600	0	600
Diameter [µm]	59 ± 8	23 ± 3	57 ± 0	30 ± 5	57 ± 3	24 ± 7	62 ± 8	27 ± 4
Extensibility [%]	10 ± 3	64 ± 11	5 ± 1	50 ± 12	4 ± 2	82 ± 13	8 ± 2	47 ± 14
Strength [MPa]	32 ± 12	244 ± 23	29 ± 2	161 ± 65	21 ± 8	251 ± 57	22 ± 3	180 ± 50
Toughness [MJ m^{-3}]	2 ± 1.5	83 ± 10	0.6 ± 0.1	49 ± 26	0.4 ± 0.1	111 ± 33	0.8 ± 0.4	50 ± 13
Young's modulus [GPa]	2 ± 0.5	4 ± 0.4	1 ± 0.2	3 ± 0.7	0.9 ± 0.4	3 ± 0.5	0.8 ± 0.2	4 ± 0.5

C

Protein	$(AQ)_{12}NR3$		$(AQ)_{24}NR3$		$N1L(AQ)_{12}NR3$		$N1L(AQ)_{24}NR3$		Natural dragline silk
Stretching [%]	0	600	0	600	0	600	0	600	N/A[a]
Diameter [µm]	39 ± 6	26 ± 6	56 ± 1	21 ± 5	155 ± 8	27 ± 10	75 ± 14	20 ± 6	4 ± 0.4[b]
Extensibility [%]	7 ± 2	95 ± 24	7 ± 3	44 ± 13	6 ± 1	110 ± 25	7 ± 2	54 ± 15	24 ± 8[b]
Strength [MPa]	54 ± 16	383 ± 113	23 ± 4	355 ± 92	13 ± 2	370 ± 59	25 ± 5	308 ± 131	1183 ± 334[b]
Toughness [MJ m^{-3}]	2 ± 0.8	172 ± 52	0.7 ± 0.6	83 ± 18	0.3 ± 0.1	189 ± 33	0.8 ± 0.4	90 ± 29	167 ± 65
Young's modulus [GPa]	2 ± 0.9	3 ± 2	0.8 ± 0.3	5 ± 2	0.5 ± 0.1	4 ± 1	0.9 ± 0.2	5 ± 2	8 ± 2

[a]Not applicable; [b]Values correspond to rupture of a single filament (not to the naturally occurring brin).

of the fibers. In contrast, N1L(AQ)$_{12}$- and (AQ)$_{12}$NR3-fibers spun from CSD showed a higher extensibility and strength resulting in a higher toughness than the corresponding (AQ)$_{12}$-fibers (**Table 1**). Like with (AQ)$_{12}$-fibers, poststretching of N1L(AQ)$_{12}$-fibers spun from CSD was only possible up to 400% of the initial length, whereas (AQ)$_{12}$NR3-fibers spun from CSD could be poststretched up to 600% (Table 1A). The strength and toughness of the poststretched N1L(AQ)$_{12}$-fibers increased more than 3-fold, and that of (AQ)$_{12}$NR3-fibers increased 4-fold in comparison to the poststretched (AQ)$_{12}$-fibers (Figure 2C). In that set of experiments, the highest toughness (111 MJ m^{-3}) was obtained with poststretched N1L(AQ)$_{12}$NR3-fibers. While showing the same strength, N1L(AQ)$_{12}$NR3-fibers were significantly more extensible ($p = 0.0030$) and less stiff (lower young's modulus ($p = 0.0009$)) than (AQ)$_{12}$NR3-fibers.

Next, fibers were spun using self-assembled, phase-separated (biomimetic) spinning dopes (BSD). In this set-up, self-assembly determined the final concentration of the spinning dopes in a regime between 10%–15% (w/v). Poststretched "biomimetic" (AQ)$_{12}$NR3-, and N1L(AQ)$_{12}$NR3-fibers showed a significant increase in extensibility and toughness in comparison to the poststretched fibers spun from CSD (Figure 2C), yielding a toughness equal ((AQ)$_{12}$NR3, 171.6 ± 51.7 MJ m^{-3}) or

even slightly superior (N1L(AQ)$_{12}$NR3, 189.0 ± 33.4 MJ m^{-3}) to natural spider silk fibers (167.0 ± 65.3 MJ m^{-3}).

Since typically the molecular weight influences the mechanical properties of polymer fibers,[34] fibers were also spun using (AQ)$_{24}$-derivatives with a doubled molecular weight in comparison to (AQ)$_{12}$-derivatives. As expected for a "plain" polymer, (AQ)$_{24}$-fibers spun from CSD showed improved mechanical properties in comparison to (AQ)$_{12}$-fibers, such as a 1.5-fold increase in extensibility and a 4-fold increase in strength, resulting in a 5-fold increase in toughness. However, in presence of the folded amino- or carboxy-terminal domains N1L/NR3 the effects were no longer dominated by molecular weight of the underlying proteins but obviously by their assembly features. All fibers spun from N1L(AQ)$_{24}$, (AQ)$_{24}$NR3, and N1L(AQ)$_{24}$NR3 (CSD) revealed substantially inferior mechanical properties to the corresponding (AQ)$_{24}$-fibers (Table 1A,B), indicating a substantial "protein"-influence on the silk polymer. N1L(AQ)$_{24}$-fibers were very brittle, and poststretching was only possible up to 300% of the initial length. As the aminoterminal domain of the spidroins only dimerizes upon a pH change during the spinning process, it is still in its monomeric form in the spinning dope, thus preventing a correct alignment of the repetitive part of the protein molecules, especially in the absence of the dimerized carboxy-terminal domain, resulting

Table 2. Roles of spidroins terminal domains.

	Non-repetitive amino-terminal domain	Non-repetitive carboxy-terminal domain
Spinning dope	High impact: monomeric during storage, folded domain inhibits protein aggregation; crucial in order to obtain an intermolecular protein network	High impact: dimerized/assembled domain renders protein less prone to unspecific aggregation; crucial for protein assembly into micellar structures and self-assembly to BSD
Assembly	High impact: dimerization occurs upon acidification, step-wise initiation of fiber assembly	High impact: initiation of fiber assembly
Mechanical properties of fibers	No direct impact: indirect influence due to impact on assembly and spinning dope	No direct impact: only indirect influence due to high impact on assembly

in brittle fibers (**Table 2**). In comparison to N1L(AQ)$_{24}$ fibers, (AQ)$_{24}$NR3 and N1L(AQ)$_{24}$NR3 fibers had a 5-fold increased extensibility and strength and a 30-fold increased toughness (Table 1A,B).

Again, similar to the findings with (AQ)$_{12}$-derivatives, the mechanical properties of (AQ)$_{24}$NR3-fibers spun from BSD showed a significant increase in strength and toughness compared to (AQ)$_{24}$NR3-fibers spun from CSD. Likewise, N1L(AQ)$_{24}$NR3-fibers spun from BSD showed a significantly higher strength (307.5 MPa) and toughness (89.6 MJ m^{-3}) than fibers spun from the corresponding CSD (180.0 MPa, 50.3 MJ m^{-3}). Unexpectedly, the overall mechanical properties of the (AQ)$_{24}$-derivatives containing either one or both terminal domains were much lower than that of the (AQ)$_{12}$-derivatives from both CSD and BSD, likely due to incorrect higher order assembly of the individual chains in the spinning dope. It is likely that once the assembly-controlling terminal domains are present, the large repetitive unit of the (AQ)$_{24}$-derivatives causes entanglement of the molecules. Additionally, intermolecular interactions of the nonrepetitive terminal domains in the micellar structures prevent a perfect alignment as it is known for classical polymers. These entanglements cannot be straightened out during the used limited and nonbiomimetic wet-spinning process. In the natural spinning process, the preassembled proteins are gradually exposed to the pH drop as well as the shear forces, supporting their correct assembly into fibers. Clearly, to overcome the entanglement of the repetitive unit, a biomimetic spinning process will have to be developed for future experiments, tackling the third of three prerequisites: i) underlying spidroins, ii) their self-assembly, and iii) their explicit processing for natural spider silk formation.

The obtained results underline that the domain-set-up as well as prestructuring/preassembly of spidroins in the spinning dope (both resembling a "protein feature") have a highly significant impact on the mechanical properties of the spun fibers. During wet-spinning their impact even supersedes that of the molecular weight of the protein (resembling a "polymer feature"). Phosphate-induced self-assembly/pre-structuring of recombinant spidroins in spinning dopes initiates the formation of an extended intermolecular protein network necessary for the extraordinary mechanical properties of the fibers.

Strikingly, the toughness of recombinant silk fibers spun from (AQ)$_{12}$NR3 and N1L(AQ)$_{12}$NR3 BSD equals that of the so far unmatched natural spider silk fibers. The highest mean toughness (189 MJ m^{-3}) was obtained with poststretched fibers wet-spun from biomimetic N1L(AQ)$_{12}$NR3 spinning dopes, even slightly exceeding the toughness (on average) of natural spider silk fibers. This toughness is based on the fact that the engineered fibers are not as strong as natural fibers, but far more extensible, which relies on the properties of the employed proline-rich MaSp2-analogue. Important differences between the used set-up and the natural blueprint are: i) the simple one-protein system (in nature the fibers are composed of at least two different major ampullate spidroins with different sequences and protein features), and ii) the simple wet-spinning process (in comparison to the complex natural spinning process). Combination of more than one recombinant spidroin, as well as the development of a biomimetic spinning technology will likely allow to achieve fibers with mechanical properties superior to that of spiders in the future, opening routes to so far none achievable fibrous materials.

Experimental Section

Protein Production: The genes encoding recombinant spider silk proteins eADF3 (AQ)$_{12}$, (AQ)$_{24}$, (AQ)$_{12}$NR3, (AQ)$_{24}$NR3, N1L(AQ)$_{12}$, and N1L(AQ)$_{24}$ were cloned, expressed, and the proteins were purified as previously described.[12] N1L(AQ)$_{12}$NR3 and N1L(AQ)$_{24}$NR3 were produced using the SUMO system[35] and purified using nickel affinity chromatography, followed by cleavage of the SUMO-TAG and ammonium sulfate precipitation.

Spinning Dope Preparation: The lyophilized proteins were dissolved in 6 M GdmSCN and dialyzed against 50 × 10^{-3} M Tris/HCl, pH 8.0, 100 × 10^{-3} M NaCl, using dialysis membranes with a molecular weight cut-off of 6000–8000 Da. CSD were prepared by dialysis against a 20% (w/v) PEG (35 kDa) solution, and BSD were prepared by dialysis against 30 × 10^{-3}–50 × 10^{-3} M sodium phosphate buffer, pH 7.2.

Fiber Production: Spinning dopes were extruded through a syringe into a large beaker filled with a coagulation bath. After fiber formation the fibers were taken out of the bath and manually poststretched in an additional bath. For wet-spinning and poststretching (if applicable) coagulation baths were used containing a mixture of water and isopropanol, as described previously.[29] *A. diadematus* (body weight: 300–600 mg) were fed with blowflies, and fibers were obtained by forcibly silking an adult *A. diadematus* at 160 mm s^{-1}.

Fiber Analysis: The fibers were analyzed with an optical microscope (Leica DMI3000B), and fibers showing defects were disposed. Fiber diameters were determined using 20×, 40×, and 100× object lenses and the software Leica V4.3. Birefringence was detected using polarizers at 0°, 45°, and 90° and pictures were obtained with the camera Leica DMC2900. For scanning electron microscopy (SEM, Zeiss LEO 1530, 3 kV), fiber samples and fiber breaking edges were sputtered with a 2 nm platinum coating (Cressington 208HR high-resolution sputter coater) before imaging. Fourier transformation infrared (FTIR) spectroscopy measurements of the fibers were performed using a Bruker Tensor 27 (Bruker Optics, Ettlingen, Germany) with a Hyperion 1000 FTIR microscope. Alignment of the β-sheet crystals was analyzed using a 15× object lens with polarizing filters at 0° and 90° in transmission mode (IR polarizers supplied by Optometrics Corporation). Spectra were plotted using Origin 8.1G (OriginLab Corporation, Northampton, MA, USA).

Tensile Testing: For tensile testing fiber pieces were mounted onto plastic sample holders with a 2 mm gap using superglue (UHU GmbH & Co. KG). Tensile testing was performed using a BOSE Electroforce 3220 with a 0.49 N load cell and a pulling rate of 0.04 mm s^{-1} at 30%

relative humidity. Mechanical data were calculated considering real stress and real strain data and using Microsoft Excel 2010 (Microsoft Corporation, Redmond, WA, USA). For statistical analysis an unpaired two-sided *t*-test was performed for groups with similar variances and sample numbers were $\geq$10, except for poststretched N1L(AQ)$_{12}$NR3 fibers spun from CSD ($n = 7$).

Supporting Information

Supporting Information is available from the Wiley Online Library or from the author.

Acknowledgements

[1] A. Sponner, W. Vater, S. Monajembashi, E. Unger, F. Grosse, K. Weisshart, *PLoS One* **2007**, *2*, e998.

[2] C. Y. Hayashi, N. H. Shipley, R. V. Lewis, *Int. J. Biol. Macromol.* **1999**, *24*, 271.

[3] a) P. A. Guerette, D. G. Ginzinger, B. H. Weber, J. M. Gosline, *Science* **1996**, *272*, 112; b) K. W. Sanggaard, J. S. Bechsgaard, X. Fang, J. Duan, T. F. Dyrlund, V. Gupta, X. Jiang, L. Cheng, D. Fan, Y. Feng, L. Han, Z. Huang, Z. Wu, L. Liao, V. Settepani, I. B. Thøgersen, B. Vanthournout, T. Wang, Y. Zhu, P. Funch, J. J. Enghild, L. Schauser, S. U. Andersen, P. Villesen, M. H. Schierup, T. Bilde, J. Wang, *Nat. Commun.* **2014**, *5*, 1.

[4] M. B. Hinman, R. V. Lewis, *J. Biol. Chem.* **1992**, *267*, 19320.

[5] N. A. Ayoub, J. E. Garb, R. M. Tinghitella, M. A. Collin, C. Y. Hayashi, *PLoS One* **2007**, *2*, e514.

[6] a) G. C. Candelas, J. Cintron, *J. Exp. Zool.* **1981**, *216*, 1; b) C. Jackson, J. P. O'Brien, *Macromolecules* **1995**, *28*, 5975.

[7] B. L. Thiel, C. Viney, *Science* **1996**, *273*, 1480.

[8] a) J. Perez-Rigueiro, M. Elices, G. R. Plaza, G. V. Guinea, *Macromolecules* **2007**, *40*, 5360; b) A. Sponner, E. Unger, F. Grosse, K. Weisshart, *Nat. Mater.* **2005**, *4*, 772.

[9] a) A. E. Brooks, H. B. Steinkraus, S. R. Nelson, R. V. Lewis, *Biomacromolecules* **2005**, *6*, 3095; b) Y. Liu, A. Sponner, D. Porter, F. Vollrath, *Biomacromolecules* **2008**, *9*, 116; c) K. Ohgo, T. Kawase, J. Ashida, T. Asakura, *Biomacromolecules* **2006**, *7*, 1210.

[10] C. Y. Hayashi, R. V. Lewis, *J. Mol. Biol.* **1998**, *275*, 773.

[11] a) R. J. Challis, S. L. Goodacre, G. M. Hewitt, *Insect Mol. Biol.* **2006**, *15*, 45; b) M. Hedhammar, A. Rising, S. Grip, A. S. Martinez, K. Nordling, C. Casals, M. Stark, J. Johansson, *Biochemistry* **2008**, *47*, 3407; c) A. Rising, G. Hjalm, W. Engstrom, J. Johansson, *Biomacromolecules* **2006**, *7*, 3120.

[12] D. Huemmerich, C. W. Helsen, S. Quedzuweit, J. Oschmann, R. Rudolph, T. Scheibel, *Biochemistry* **2004**, *43*, 13604.

[13] a) G. Askarieh, M. Hedhammar, K. Nordling, A. Saenz, C. Casals, A. Rising, J. Johansson, S. D. Knight, *Nature* **2010**, *465*, 236; b) L. Eisoldt, A. Smith, T. Scheibel, *Mater. Today* **2011**, *14*, 80.

[14] L. Eisoldt, J. G. Hardy, M. Heim, T. R. Scheibel, *J. Struct. Biol.* **2010**, *170*, 413.

[15] L. Eisoldt, C. Thamm, T. Scheibel, *Biopolymers* **2012**, *97*, 355.

[16] F. Hagn, L. Eisoldt, J. G. Hardy, C. Vendrely, M. Coles, T. Scheibel, H. Kessler, *Nature* **2010**, *465*, 239.

[17] a) D. P. Knight, F. Vollrath, *Philos. Trans. R. Soc. London, Ser. B* **2002**, *357*, 219; b) F. N. Braun, C. Viney, *Int. J. Biol. Macromol.* **2003**, *32*, 59.

[18] L. Onsager, *Ann. Ny. Acad. Sci.* **1949**, *51*, 627.

[19] D. P. Knight, F. Vollrath, *Naturwissenschaften* **2001**, *88*, 179.

[20] P. Papadopoulos, J. Sölter, F. Kremer, *Eur. Phys. J. E: Soft Matter Biol. Phys.* **2007**, *24*, 193.

[21] a) F. Hagn, C. Thamm, T. Scheibel, H. Kessler, *Angew. Chem. Int. Ed.* **2011**, *50*, 310; b) F. Hagn, C. Thamm, T. Scheibel, H. Kessler, *Angew. Chem.* **2011**, *123*, 324.

[22] N. Kronqvist, M. Otikovs, V. Chmyrov, G. Chen, M. Andersson, K. Nordling, M. Landreh, M. Sarr, H. Jornvall, S. Wennmalm, J. Widengren, Q. Meng, A. Rising, D. Otzen, S. D. Knight, K. Jaudzems, J. Johansson, *Nat. Commun.* **2014**, *5*, 3254.

[23] A. Heidebrecht, T. Scheibel, *Adv. Appl. Microbiol.* **2013**, *82*, 115.

[24] S. Arcidiacono, C. M. Mello, M. Butler, E. Welsh, J. W. Soares, A. Allen, D. Ziegler, T. Laue, S. Chase, *Macromolecules* **2002**, *35*, 1262.

[25] a) M. Humenik, T. Scheibel, *ACS Nano* **2014**, *8*, 1342; b) K. Schacht, T. Jüngst, M. Schweinlin, A. Ewald, J. Groll, T. Scheibel, *Angew. Chem. Int. Ed.* **2015**, *54*, DOI: 10.1002/ange.201409846.

[26] a) J. H. Exler, D. Hummerich, T. Scheibel, *Angew. Chem. Int. Ed.* **2007**, *46*, 3559; b) J. H. Exler, D. Hummerich, T. Scheibel, *Angew. Chem.* **2007**, *119*, 3629.

[27] K. Schacht, T. Scheibel, *Biomacromolecules* **2011**, *12*, 2488.

[28] M. Humenik, M. Magdeburg, T. Scheibel, *J. Struct. Biol.* **2014**, *186*, 431.

[29] F. Teule, W. A. Furin, A. R. Cooper, J. R. Duncan, R. V. Lewis, *J. Mater. Sci.* **2007**, *42*, 8974.

[30] N. Du, X. Y. Liu, J. Narayanan, L. Li, M. L. M. Lim, D. Li, *Biophys. J.* **2006**, *91*, 4528.

[31] C. Viney, A. E. Huber, D. L. Dunaway, K. Kerkam, S. T. Case, in *Silk Polymers. Materials Science and Biotechnology*, (Eds: D. L. Kaplan, W. W. Adams, B. Farmer, C. Viney) American Chemical Society, Washington D.C. **1994**, pp. 120–136.

[32] C. Riekel, B. Madsen, D. Knight, F. Vollrath, *Biomacromolecules* **2000**, *1*, 622.

[33] T. Ohta, *Polym. Eng. Sci.* **1983**, *23*, 697.

[34] a) T. A. Hancock, J. E. Spruiell, J. L. White, *J. Appl. Polym. Sci.* **1977**, *21*, 1227; b) P. Gupta, C. Elkins, T. E. Long, G. L. Wilkes, *Polymer* **2005**, *46*, 4799.

[35] a) T. R. Butt, S. C. Edavettal, J. P. Hall, M. R. Mattern, *Protein Expression Purif.* **2005**, *43*, 1; b) J. G. Marblestone, S. C. Edavettal, Y. Lim, P. Lim, X. Zuo, T. R. Butt, *Protein Sci.* **2006**, *15*, 182.

ADVANCED MATERIALS

Supporting Information

Biomimetic Fibers Made of Recombinant Spidroins with the Same Toughness as Natural Spider Silk

Aniela Heidebrecht, Lukas Eisoldt, Johannes Diehl, Andreas Schmidt, Martha Geffers, Gregor Lang, and Thomas Scheibel*

WILEY-VCH

Supporting Information

Biomimetic Fibers Made of Recombinant Spidroins with the Same Toughness as Natural Spider Silk

Aniela Heidebrecht, Lukas Eisoldt, Johannes Diehl, Andreas Schmidt, Martha Geffers, Gregor Lang, Thomas Scheibel*

Amino acid sequences:

<u>**N1L**</u>

```
        10         20         30         40         50
 GQANTPWSSK ANADAFINSF ISAASNTGSF SQDQMEDMSL IGNTLMAAMD
        60         70         80         90        100
 NMGGRITPSK LQALDMAFAS SVAEIAASEG GDLGVTTNAI ADALTSAFYQ
       110        120        130        140        150
 TTGVVNSRFI SEIRSLIGMF AQASANDVYA SAGSGSGGGG YGASSASAAS
       160        170        180
 ASAAAPSGVA YQAPAQAQIS FTLRGQQPVS
```

<u>**Module A**</u>

```
        10         20
 GPYGPGASAA AAAAGGYGPG  SGQQ
```

<u>**Module Q**</u>

```
        10         20
 GPGQQGPGQQ GPGQQGPGQQ
```

<u>**NR3**</u>

```
        10         20         30         40         50
 GAASAAVSVG GYGPQSSSAP VASAAASRLS SPAASSRVSS AVSSLVSSGP
        60         70         80         90        100
 TNQAALSNTI SSVVSQVSAS NPGLSGCDVL VQALLEVVSA LVSILGSSSI
       110        120
 GQINYGASAQ YTQMVGQSVA  QALAG
```

Extended experimental section

Protein production:

The genes encoding recombinant spider silk proteins eADF3 $(AQ)_{12}$, $(AQ)_{24}$, $(AQ)_{12}NR3$, $(AQ)_{24}NR3$, $N1L(AQ)_{12}$ and $N1L(AQ)_{24}$ were cloned, expressed and the proteins were purified as previously described.[12] $N1L(AQ)_{12}NR3$ and $N1L(AQ)_{24}NR3$ were produced

using the SUMO system[35] and purified using nickel affinity chromatography, followed by cleavage of the SUMO-TAG and ammonium sulfate precipitation. Identity of proteins was confirmed by discontinuous sodium dodecyl sulfate-polyacrylamide gel electrophoresis (SDS-PAGE, 12.5 % Tris-Glycine gels) followed by silver staining (**Figure S3**) and/or western blotting (not shown) as previously published.[12]

Spinning dope preparation:

The lyophilized proteins were dissolved in 6 M GdmSCN (at a calculated protein concentration of 20-25 mg/mL) and dialyzed over night at room temperature against 5 L of 50 mM Tris/HCl, pH 8.0, 100 mM NaCl, using dialysis membranes with a molecular weight cut-off of 6,000-8,000 Da. During the first dialysis, 10-40 % of the dissolved protein precipitated in the dialysis membrane. The precipitated protein was separated from the supernatant by centrifugation (8,500 rpm, 30 min, 20 °C), and subsequently the supernatant was again dialyzed against 50 mM Tris/HCl, pH 8.0, 100 mM NaCl. Buffers were changed after 5-6 hours and a protein solution was dialyzed against 3 X 5 L of buffer prior to further processing.

Preparation of "classical" spinning dopes (CSD)

In order to obtain highly concentrated CSD, the protein solutions with a concentration of 15-20 mg/mL were dialyzed against a 20 % (w/v) polyethylenglycol (PEG, 35 kDa) solution. Dialysis against a PEG solution removes water from the protein solution by osmotic stress and allows an accurate adjustment of protein concentration.[27] Electrolytic conductivity measurements were performed using a FG3 conductivity meter (Mettler Toledo) with a 1 point calibration using a conductivity standard with a conductivity of 12.88 mS/cm (Mettler Toledo). After reaching the desired concentration of the CSD (ranging between 100-150 mg/mL, depending on the used protein) dialysis was stopped and the CSD (pH 7.8) was transferred into a syringe without drawing any air, and fiber production was started.

Preparation of "biomimetic" spinning dopes (BSD)

BSD were prepared by dialysis over night at room temperature against 30-50 mM sodium phosphate buffer, pH 7.2. During the dialysis, phase separation occurs in the dialysis membrane, and the BSD sediments at the bottom of the dialysis membrane. In order to separate the BSD from the rest of the protein solution, the dialysis is stopped and the content of the dialysis membrane is centrifuged in a 50 mL reaction tube at 6,000 rpm, 20 °C for 5 minutes. The upper phase (protein concentration: 10-15 mg/mL) was transferred into a separate 50 mL reaction tube. The protein concentrations in BSD were 90-110 mg/mL and after BSD were transferred into a syringe without drawing any air, the fiber production was started.

Fiber production

Spinning dopes were extruded through a syringe with an inner needle diameter of 0.8 mm at a spinning rate of 5 µL/min into a 3 L beaker filled with a coagulation bath. After fiber formation the fibers were taken out of the bath and manually post-stretched with a drawing rate of 5 mm/sec in an additional bath. For wet-spinning and post-stretching (if applicable) coagulation baths were used containing a mixture of water and isopropanol, as used previously,[29] at pH 7.7. *A. diadematus* spiders (body weight: 300-600 mg) were fed with blowflies, and fibers were obtained by forcibly silking adult spiders at 160 mms^{-1}. After spinning or post-stretching, the obtained fibers were stored in plastic petri dishes until they were mounted onto plastic sample holders. Variations in storage time (2 hours to 4 weeks) did not show an impact on the mechanical properties of the fibers. The fibers were not actively dried, but they were stored for at least 2 hours at room temperature (21-25 °C) and 30 % relative humidity before mounting on sample holders.

Fiber analysis

The fibers were analyzed with an optical microscope (Leica DMI3000B), and fibers showing defects were disposed (approx. 5 % of post-stretched fibers spun from BSD, approx. 15 % of post-stretched fibers spun from CSD).

Fiber diameters were determined using 20x, 40x and 100x object lenses and the software

Leica V4.3. Birefringence was detected using polarizers at 0°, 45° and 90° and pictures were

obtained with the camera Leica DMC2900. For scanning electron microscopy (SEM, Zeiss

LEO 1530, 3 kV), fiber samples and fiber breaking edges were sputtered with a 2 nm

platinum coating (Cressington 208HR high-resolution sputter coater) before imaging. Fourier

transformation infrared (FTIR) spectroscopy measurements of the fibers were performed

using a Bruker Tensor 27 (Bruker Optics) with a Hyperion 1000 FTIR microscope. Alignment

of the β-sheet crystals was analyzed using a 15x object lens with polarizing filters at 0° and

90° in transmission mode (IR polarizers supplied by Optometrics Corporation). Spectra were

plotted using Origin 8.1G (OriginLab Corporation, Northampton, MA, USA).

Tensile testing

For tensile testing fiber pieces were mounted onto plastic sample holders with a 2 mm gap

using superglue (UHU GmbH & Co. KG). Tensile testing was performed using a BOSE

Electroforce 3220 with a 0.49 N load cell and a pulling rate of 0.04 mm/s at 30 % relative

humidity. Mechanical data were calculated considering real stress and real strain data and

using Microsoft Excel 2010 (Microsoft Corporation, Redmond, WA, USA). For statistical

analysis an unpaired two-sided t-test was performed for groups with similar variances and

sample numbers were ≥ 10, except for post-stretched $N1L(AQ)_{12}NR3$ fibers spun from CSD

(n = 7).

Figure S1. (a, b) CSD (all variants) and **(c)** BSD (variants with carboxy-terminal domain

only). SEM images show 600 % post-stretched fibers **(I)** and breaking edges thereof **(II)**. **(III)**

Natural spider silk fiber obtained by forced silking of *A. diadematus*

Figure S2. Processing of recombinant spider silk proteins into **(a)** biomimetically and **(b)**

classically concentrated spinning dopes. **(a)** Dialysis against a phosphate-containing buffer

enables the formation of micellar-like structures[14] yielding a spinning dope with pre-oriented silk proteins. Importantly, this orientation/pre-structure formation is fully reversible. Upon fiber spinning β-sheet crystals are formed, and the non-repetitive amino-terminal domains are dimerized (upon shifting the pH from ~ 7.2 to ~ 5.7) leading to an intermolecular network responsible for extraordinary mechanical properties after post-stretching the fibers. **(b)** Without pre-assembly of the proteins in the dope the formed network is weak yielding less stable fibers upon post-stretching with properties similar to other polymer fibers, such as nylon, or previously reported wet-spun spider silks.

Figure S3. Analysis of the purified proteins **(a)** N1L(AQ)$_{12}$NR3 and **(b)** (AQ)$_{12}$NR3 using discontinuous SDS-PAGE with subsequent silver staining (exemplary for all used proteins). Under reducing conditions the disulfide bonds of the carboxyterminal domains are "reduced" to thiol groups (monomeric state), in contrast to "not reduced" samples, whose carboxyterminal domains dimerize.[16]

Table S1. Electrolytic conductivity measurements of solutions and buffers during PEG-dialysis of a (AQ)$_{12}$ solution.

Solution or buffer	Electrolytic conductivity / mScm^{-1}
25 mM Tris/HCl, pH 8.0	1.49
50 mM Tris/HCl, pH 8.0	2.98
50 mM Tris/HCl, pH 8.0, 25 mM NaCl	5.52
50 mM Tris/HCl, pH 8.0, 50 mM NaCl	8.02
50 mM Tris/HCl, pH 8.0, 75 mM NaCl	10.28
50 mM Tris/HCl, pH 8.0, 100 mM NaCl	12.68
50 mM Tris/HCl, pH 8.0, 125 mM NaCl	15.10
(AQ)$_{12}$ solution before PEG-dialysis	12.20
(AQ)$_{12}$ solution after PEG-dialysis	1.53

Part 2

Foundation of the outstanding toughness in biomimetic & natural spider silk

Anton, A. M.*, Heidebrecht, A.*, Mahmood, N., Beiner, M., Scheibel, T.§ and Kremer, F.§

* The authors contributed equally

§ The authors contributed equally

To be submitted

Foundation of the outstanding toughness in biomimetic & natural spider silk

Arthur Markus Anton[1‡], Aniela Heidebrecht[2,3‡], Nasir Mahmood[4], Mario Beiner[4,5],

Thomas Scheibel[2,6,7,8,9§], Friedrich Kremer[1§]

[1] Institut für Experimentelle Physik I, Universität Leipzig,

   Linnéstr. 5, D-04103 Leipzig, Germany

[2] Fakultät für Ingenieurswissenschaften, Universität Bayreuth,

   D-95440 Bayreuth, Germany

3 present address: R&D IT, Bayer Business Services GmbH, D-51368 Leverkusen, Germany

[4] Institut für Chemie, Martin-Luther-Universität Halle-Wittenberg,

   Heinrich-Damerow-Str. 4, D-06120 Halle (Saale), Germany

[5] Fraunhofer-Institut für Mikrostruktur von Werkstoffen und Systemen IMWS,

   Walter-Hülse-Straße 1, D-06120 Halle (Saale), Germany

[6] Institut für Bio-Makromoleküle (bio-mac), Universität Bayreuth,

   Universitätsstraße 30, D-95440 Bayreuth, Germany

[7] Bayreuther Zentrum für Kolloide und Grenzflächen (BZKG), Universität Bayreuth,

   Universitätsstraße 30, D-95440 Bayreuth, Germany

[8] Bayreuther Zentrum für Molekulare Biowissenschaften (BZMB), Universität Bayreuth,

   Universitätsstraße 30, D-95440 Bayreuth, Germany

[9] Bayreuther Materialzentrum (BayMAT), Universität Bayreuth,

   Universitätsstraße 30, D-95440 Bayreuth, Germany

[‡] both authors contributed equally to this work

[§] both authors contributed equally to this work

Abstract

Spider dragline silk is distinguished through the highest toughness of all fibre materials. In order to unravel its molecular foundation and to progress in manufacturing biomimetic analogues, the morphological and functional structure of recombinant fibres, that exhibit toughness similar to the natural template, is investigated: on the molecular scale by means of vibrational spectroscopy and on the mesoscale by small angle X-ray scattering. While the former ensures similar protein secondary structures in the natural as well as artificial silks, the latter reveals nanometre-sized crystallites. Thus, on the basis of a similar block-like peptide the same assembly –namely alanine-rich nanocrystals embedded in a glycine-rich matrix– is formed. Furthermore, a spectral red shift of a crystal-specific absorption band demonstrates that macroscopically applied stress is transferred without any threshold to the molecular scale, where it is finally dissipated. This mechanism works analogously to natural silk giving rise to the toughness of both materials.

Introduction

Major ampullate spider silk (or synonymously dragline silk) combines high tensile strength and great elasticity, which renders this fibre to be tougher than even modern synthetic materials and has brought it into the focus of research for decades[1-3]. Because the spiders' territorial behaviour and cannibalism restricts the production of natural silk and especially of non-processed spider silk proteins (i.e. spidroins), the question for manufacturing recombinant silk in order to enable industrial scales arises. Even though the molecular structure of major ampullate fibres has been thoroughly studied and concepts for applications such as in drug delivery and as cell scaffold systems as well as optical and biosensor systems have been successfully established, artificial fibres have not achieved all the properties of the natural blueprint, yet[4-6].

The mechanical properties of major ampullate spider silk are based on the molecular structure of the constituent spider silk proteins (spidroins) but as well on their refined mesoscale architecture. A major ampullate thread consists mainly of two protein classes, major ampullate spidroin 1 and 2 (MaSp1, MaSp2), which can be considered as block copolymers with a core of alternating alanine- and glycine-rich motifs surrounded by non-repetitive amino- and carboxy-terminal domains[7,8]. During spinning the highly concentrated protein solution (the spinning dope) experiences pH and ion exchange, water segregation, and shear forces[9,10] in order to control the structural transition from the spidroins' storage form into the assembly form, whilst those globules are elongated and aligned to establish fibrillary assemblies[11-14]. The resulting filaments (with a diameter of 20-150 nm[15]) build up the core of the mature spider silk thread (Figure 1a). Recently, the delicate interplay between protein-protein interactions and structural water in filaments comprising the core domain of MaSp2 has been proposed as origin of the filaments'

1   extensibility and as prerequisite for the toughness of natural silk fibers (Lang et al, manuscript

2   submitted).

3   In natural dragline silk, the core is coated with layers of spridroin-like proteins, glycoproteins,

4   and lipids, which gives rise to a final diameter of 2-7 mm[4,17-19].

5   On the basis of the spidroins' primary structures the alanine-rich motifs (polyalanine A_n) form

6   nanometre-sized crystals from β-sheet stacks (white space) already present at the exit of the

7   spigot[20-22], whereas the glycine-rich motifs (GGX, GPGXX) form presumably β-turns, β-spirals,

8   3_1-helices, and random structures[23,24] representing the less-ordered (hereafter amorphous) matrix

9   in which the crystallites are embedded (Figure 1b,d)[3]. The crystal volume fraction amounts to

10   between 30 and 40% depending on the employed measurement technique and spider silk

11   species[25-27] . By means of X-ray scattering a crystal size in the direction along the fibre axis of

12   5.5-7.3 nm and an orientational order of 0.97-0.99 (Herman's orientation function)[28,29] has been

13   determined, whereas the order may drop significantly to 0.68 for low reeling speed[30]. Simulations

14   on the size and the orientation of nanocrystals with similar composition revealed that there is an

15   optimal size of the confinement and an optimal orientation of the nanocrystals in regard to the

16   toughness of silk[15,31,32].

17   Besides X-ray scattering[25,28-30] and nuclear magnetic resonance[13,20,24,27], the structure of spider

18   dragline silk has been studied by other techniques as Raman[11,23,34] or infrared (IR)

19   spectroscopy[18,19,26,33,35-38]. Especially the latter in combination with mechanical fields provides

20   detailed information on the functional organisation of spider silk and the proteins therein. On the

21   basis of the *load-dependent* spectral shift of an IR-active molecular vibration ($\bar{\nu} = 965 \text{ cm}^{-1}$)

22   located exclusively within the nanocrystals, it has been concluded that a mechanism is

23   mandatory, which transports the macroscopically applied load through the amorphous, and hence,

soft matrix so that it affects the much harder crystallites on the microscopic scale[36-38]. This mechanism can be explained solely by stretched amorphous protein chains, which are elongated during spinning and give rise to a microscopic non-equilibrium state in the mature fibre. Those *pre-stressed* chains have been successfully employed to resolve the macroscopic stress-strain-curve solely based on microscopic properties[36,38] as well as to reveal the origin of supercontraction and its impact on the microscopic quantities in major ampullate (MA) spider silk[35]. It has been demonstrated that the microscopic non-equilibrium state can be influenced through macroscopic stress that increases the microscopic pre-stress and gives rise to a spectral red shift, whereas vice versa hydrostatic pressure reduces the pre-stress evident in a blue shift[19]. Furthermore, the thread's mechanical properties can be reversibly tailored via supercontraction and subsequent stretching, which resets this non-equilibrium and establishes a customized state conditioned through the post-strain[39,40]. Apart from the stress-strain behaviour, a hypersonic phononic bandgap and negative dispersion relation due to the pre-stressed protein chains have recently been publish, which is the first report of a negative group velocity, negative refraction and potential focusing of hypersonic phonons in a *natural* material[41].

Concerning artificial silk fibres, the highest tenacity (508 MPa) and elastic modulus (21 GPa) has been achieved by wet-spinning of high molecular weight proteins (285 kDa) containing only amino acid motifs from the core domain of the natural spidroins[42]. However, these fibres reached only 48% of the natural tenacity (of 1.1 GPa[3]) and approximately 44% of the natural toughness (of 160 MPa[3]; toughness is calculated using the mean values: elongation 15%, tenacity 508 MPa and elastic modulus 21 GPa, whilst assuming a linear increase in stress due to strain up to the value of tenacity followed by a constant course up to 15% strain as indicated by the stress-strain curve in Figure 3 in Reference [42]). Other artificial silk fibres showed 69% of the natural toughness with greater elongation but at the expense of lower tenacity[43]. On the basis of the

engineered MaSp2-derivative $(AQ)_{12}NR3$ inspired from the sequence of ADF3 (araneus diadematus fibroin3) of the European garden spider *Araneus diadematus*, recently two different spinning dopes have been produced: a classical (CSD) and a biomimetic spinning dope (BSD, Figure 1c)[44]. To prepare CSD excess water has been removed by dialysis in order to achieve a high protein concentration (10-17% w/v). In the case of BSD, instead, spidroin self-assembly and phase separation (resulting in a concentration of 10-15% w/v) have been triggered in the presence of phosphate ions by the non-repetitive carboxy-terminal domain NR3[44]. Interestingly, wet spun fibres spun out of BSD have shown superior mechanical properties to that from CSD. Moreover, to the best of our knowledge as *first artificial spider silk* threads those BSD fibres have proven to accomplish a toughness (172 MPa[44], Figure 1e) which is able to compete with that of natural spider silk fibres (160 MPa[3] or 167 MPa[44]).

In order to investigate the origin of the high toughness of the artificial fibres, small and wide angle X-ray scattering (SAXS and WAXS) and polarised Fourier-transform infrared spectroscopy (FTIR) experiments have been carried out. The former is suitable to obtain information about the size of the crystallites, whereas the latter provides detailed insight into the material's organization; on the one hand concerning the protein secondary structure and on the other hand acting as molecular sensor of relative force variations within the β-sheet nanocrystals[19,36-38]. Thus, one is able to reveal how the morphology *and* the functional structure have to cooperate in order to realise energy dissipation.

1 Results and discussion

2 Small angle X-ray scattering

3 The diffraction patterns of the artificial fibres (CSD 0%, CSD 600%, BSD 0% and BSD 600%)

4 appear isotropic in case the threads are macroscopically not-oriented (Figure 2a). In contrast,

5 when they are macroscopically oriented, the scattering signal is biased (Figure 2b). This

6 demonstrates the durable presence of ordered structures on the mesoscale, which have already

7 been formed during the course of wet spinning. Furthermore, the magnitude of the q_{100}-signal is

8 deduced from the azimuthal integration of the scattering pattern and results in $|q_{100}| =$

9 (0.89 ± 0.01) nm^{-1} (Figure 2c). This value corresponds to a *periodic length* of the scattering-

10 causative structures of $d = (7.1 \pm 0.1)$ nm $(d = 2\pi/|q_{100}|)$. Because the persistence of the

11 crystal size as well as its integrity throughout stretching of wet fibres is well known for major

12 ampullate silk,[45] an effect of the post-spinning treatment on the crystallites apart from alignment

13 is not reasonable. Furthermore, the determined periodic length is in full agreement with

14 previously derived values for major ampullate spider silk (5.5-7.3 nm)[28,29]. Since the primary

15 structure of the underlying recombinant silk-like protein $(AQ)_{12}NR3$ consists of similar amino

16 acid motifs as the natural ADF3 (Figure 1c)[44] and is identical for all four kinds of artificial fibres

17 Since the primary structure of the recombinant silk-like protein $(AQ)_{12}NR3$ consists of similar

18 amino acid motifs as the natural blueprint ADF3 (Figure 1c)[44] and its fibre structure shows the

19 same periodic length in SAXS experiments as major ampullate spider silk, we suspect that the

20 molecular morphology of the biomimetic samples is highly similar to that of the natural template.

21 This assumption is further consolidated by the findings from FTIR spectroscopy experiments.

FTIR Spectroscopy

For all recombinant spider silk fibres absorption peaks are evident at $\bar{\nu} = 965\ \text{cm}^{-1}$ and $\bar{\nu} = 1025\ \text{cm}^{-1}$ (Figure 3), which can be found as well in the fingerprint region of IR spectra of natural major ampullate spider silk[19,36-38]. The former frequency represents a combined stretching vibration within the β-sheet crystallites formed by the A_n-motifs; the latter corresponds to GPGQQ in β-turn, β-spiral, 3_1-helix, or amorphous structures[37]. When comparing the spectra from the recombinant samples with that derived from natural silk, peaks at $\bar{\nu} = 1000\ \text{cm}^{-1}$ and $\bar{\nu} = 1015\ \text{cm}^{-1}$are absent (Figure 3). The first missing peak arises from the $(GA)_n$-motif[37], which is part of certain natural spidroins and surrounds the A_n regions[8], but it is not included in the recombinant protein[44]. In the case of the second peak, so far it was solely possible to assign this band together with that at $\bar{\nu} = 1025\ \text{cm}^{-1}$ to skeletal stretching vibrations of glycine—rich parts. ~~Now,~~ With the information from the recombinant protein we are now able to separate those two peaks and address the peak at $\bar{\nu} = 1015\ \text{cm}^{-1}$ to the GGX-motif, which is not present in $(AQ)_{12}$NR3 but in other major ampullate spidroins[8].

Another characteristic attribute of natural major ampullate spider silk fibres is the orientation of the crystallites and glycine-rich arrangements along the fibre axis, which gives rise to anisotropic absorption on macroscopic scale (Figure 3a and 4a and b).The molecular order parameter (Equation 3) was $S = 0.89 \pm 0.02$ and $S = 0.17 \pm 0.02$, respectively, for the IR transition moments (TMs) of the specific vibrations within the aggregated β-sheet A_n-motif and the helical/amorphous GPGXX-motif (Figure 4a and b). Assuming that the individual TMs are distributed along the fibre axis obeying a rotational symmetric Gaussian function the order parameter would result in a distribution width (Equation 4) of $\omega = 11.3° \pm 1.0°$ and $\omega = 46.7° \pm 1.7°$, respectively[46].

In the case of the biotech fibres, the characteristic secondary structure elements are present after wet-spinning, whereas they do not show any orientational order beyond that local coordination necessary to develop the protein secondary structure ($S = 0.01 \pm 0.02$; Figure 4a and b). However, post-spinning elongation of the wet threads, gives rise to a macroscopic alignment of the nanocrystals and glycine-rich parts. For fibres spun from from the CSD that have been post-stretched to 600% of its initial length a molecular order parameter of the nanocrystals of $S = 0.32 \pm 0.03$ ($\omega = 36.6° \pm 1.6°$) is determined, which increases further to $S = 0.40 \pm 0.03$ ($\omega = 32.6° \pm 1.4°$) when the threads are strained. The order of the glycine-rich parts slightly increases from $S = 0.10 \pm 0.03$ ($\omega = 54.1° \pm 4.1°$) to $S = 0.14 \pm 0.03$ ($\omega = 49.5° \pm 4.1°$). Compared to fibres spun from CSD, post-stretched fibres spun from BSD show an increased order of the crystallites with a molecular order parameter of $S = 0.47 \pm 0.03$ ($\omega = 29.4° \pm 1.3°$), which rises to $S = 0.54 \pm 0.03$ ($\omega = 26.5° \pm 1.4°$) under further strain. The glycine-rich parts are also more ordered compared to that of samples spun from CSD ($S = 0.13 \pm 0.03$, $\omega = 50.5° \pm 3.3°$) and additionally align more quickly under strain reaching the value of natural dragline silk ($S = 0.20 \pm 0.03$, $\omega = 44.2° \pm 2.3°$).

Interestingly, the increase in alignment order is accompanied by a significant enhancement of the fibres' mechanical properties (Figure 1)[44]. Previously, post-stretched fibres spun from the BSD have shown the best performance in absorbing load, and here they exhibited the biggest molecular order. Thus, the superior mechanical properties of the BSD-fibres over CSD ones can be ascribed to the increased alignment of the nanocrystals and amorphous structures.

Response to External Load

The mechanical response to load of the biotech fibres is significantly influenced by the post-spinning treatment: fibres as-spun (CSD 0% and BSD 0%) appear to be brittle, whereas post-

spinning elongation enhances the elastic modulus and extensibility[44]. Moreover, the threads'

stress-strain characteristic is sustainably changed. As evident in Figure 2 of Reference [44] fibres

as-spun have shown no yield point in stress-strain experiments, whereas post-stretched samples,

have evinced a distinct yield point[44]. In this context it is highly interesting that the presence or

absence of a yield point for semi-crystalline polymers, to which spider silk can be assigned,

indicates the energy dissipation through oriented and ordered or unordered structures,

respectively[47,48]. Accordingly, the applied load in the case of the as-spun samples is applied

predominantly to amorphous structures, whereas when the samples are post-streched the stress-

strain curves indicate the involvement of ordered parts. The highest toughness (172 MPa), which

is able to compete with that of natural major ampullate spider silk (160 MPa[3] or 167 MPa[44], has

been achieved for $(AQ)_{12}NR3$ fibres spun from BSD with 600% post-strain. Therefore, we focus

on sample BSD 600% hereafter.

Orientational order of the TMs for both vibrations, A_n in the crystallites and GPGQQ in the

amorphous matrix, is induced through elongation. Between 10 and 15% strain (for BSD 600%,

for CSD 600% between 15 and 20%) the yield point is reached, at which the deformation changes

from elastic to plastic. As a consequence, the molecular order parameter drops but recovers

afterward. Its decrease is stronger for the crystallites than for the amorphous parts, but the

increase after the yield point is pronounced for the latter. Thus, up to the yield point the

nanocrystals are highly incorporated in dissipating the stress, whereas for greater strain the

amorphous matrix is stronger involved. This finding is in accordance to a recent simulation study,

in which the relative contribution of the crystals to the macroscopic deformation has dropped at

the yield point, whereas that of the amorphous part has increased[49].

A more refined assessment of the interplay between nanocrystals and amorphous parts is provided by stress-dependent IR spectroscopy experiments. In the past, one exceptional characteristic of major (and minor) ampullate spider silk has been found: the *load-dependent* and *reversible* spectral shift of the alanine-specific IR absorption band at $\overline{\nu} = 965\ \mathrm{cm}^{-1}$ [19,36-38]. Although the nanometre-sized alanine-rich crystals are embedded within a less ordered glycine-rich matrix, macroscopically applied stress affects vibrations on the molecular length scale inside those rigid crystallites. Consequently, a mechanism responsible for the stress transfer has to exist. It is believed that amorphous parts interconnecting the nanocrystals experienced shear forces during spinning inducing orientation and elongation of pre-aggregates [10]. This strain, and hence, stress is preserved while the thread is formed; the tendency to contract is counterbalanced by the surrounding layers of the fibre. Thus, the arising inherent non-equilibrium state of the *pre-stressed* morphology causes the transduction of the applied load from the macroscopic scale down to the molecular level, where the emerging energy affects the crystallites and is dissipated [19,36-38].

In case sample BSD 600% is exposed to macroscopic stress a shift of this A_n-specific peak ($\overline{\nu} = 695\ \mathrm{cm}^{-1}$) becomes evident (Figure 5a). Furthermore, after the sample has been stressed and relaxed, the spectral displacement decreases in accordance to the lowered apparent force. This spectral shift is linearly dependent on the applied stress, as for natural dragline silk. The slope of $-4.9\ \mathrm{cm}^{-1}\mathrm{GPa}^{-1}$ corresponds to frequently derived values for spider silk [18,36,37]; it even fits to the slope under hydrostatic pressure [19]. These results explicitly demonstrate that macroscopically applied stress is transferred through the less-ordered matrix and affects the crystalline parts of the biomimetic fibres. This mechanism in the biotech fibres is identical to that

1   in natural major ampullate spider silk and responsible for the exceptional ability of dissipating

2   impinging energy.

3

1 Conclusion

On the basis of the recombinant protein $(AQ)_{12}NR3$ four different types of biotech spider silk fibres (resulting from two distinct preparation techniques and post-treatment) have been investigated; on the mesoscale by small angle X-ray scattering and on the molecular scale by polarized and stress-dependent FTIR spectroscopy. It is demonstrated that alanine-rich nanometre-sized crystallites (7.1 nm) with comparable dimensions (5.5-7.3 nm) as found in natural major ampullate spider silk are formed in the course of wet spinning, whilst glycine-rich parts establish an amorphous matrix embedding those crystals. Thus, on a molecular level, biotech fibres already closely resemble natural fibres.

Opposed to natural silk, in which crystalline and amorphous parts show a (high) order directly after spinning ($S = 0.89$ and $S = 0.17$), no orientational order is evident on the macroscopic scale in the biotech fibres (due to the different spinning technique, $S = 0.01$). Post-spinning elongation of the fibres aligns the crystalline parts as well as the glycine-rich structures and enhances their mechanical properties. This post-stretching effect on the molecular order is more pronounced in fibres spun from BSD than from CSD. Fibres, that are spun from the "biomimetic" spinning dope (BSD) and elongated afterward to 600 % of their initial length, show the best performance in absorbing load, while they exhibit at the same time the biggest molecular order of the artificial threads ($S = 0.47$ and $S = 0.13$). When those fibres are exposed to stress, the molecular order parameters of the crystalline and amorphous regions are further increased reaching for the latter the same order as in natural spider silk fibres.

In addition, under external stress an IR absorption peak specific for molecular vibrations within those crystallites is shifted linearly, which explicitly reveals that macroscopic stress is transferred through a less-ordered matrix and affects the crystalline parts of this composite. This mechanism

is identical to that in natural major ampullate spider silk and responsible for the exceptional ability of dissipating impinging energy present in both materials.

Our results indicate that the production of biotech fibres having the same toughness as natural silk requires a well-defined dope preparation in combination with a spinning process which integrates shear forces during fibre formation in order to obtain the naturally high orientational order.
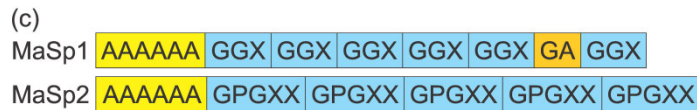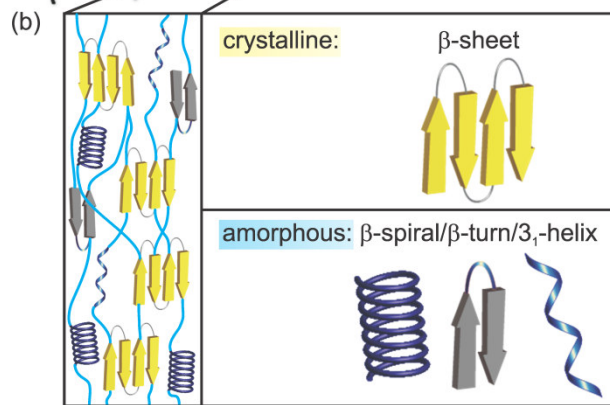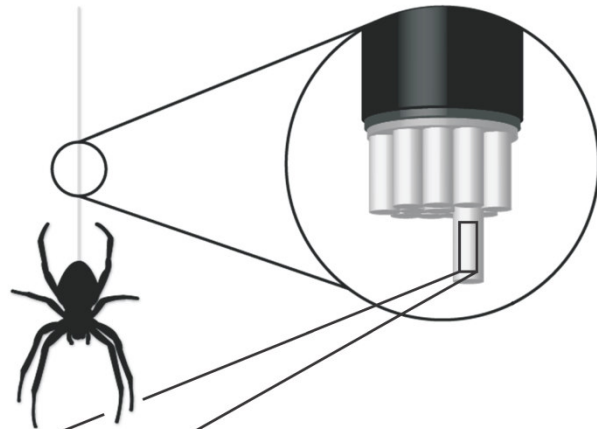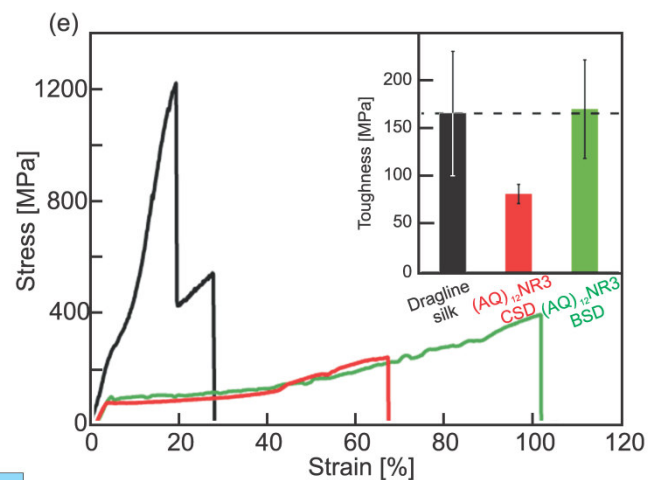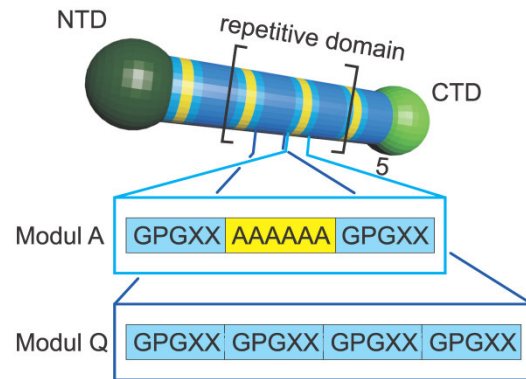
Figure 1: Principle morphology of major ampullate and recombinant spider silk along with the stress-strain dependence and resulting toughness. (a) One thread of the natural major ampullate silk is composed of fibrils which itself (b) comprise nanometre-sized crystallites (yellow) embedded in an amorphous matrix (blue). (c) The major ampullate spidroins (MaSp1 and 2) may be considered as block-copolymers with alanine- and glycine-rich motifs, which give rise to the crystalline and amorphous parts. (d) The natural amino acid sequences are partially employed as template for the repetitive core of the recombinant protein $(AQ)_{12}NR3$, in order to obtain the distinct secondary structures. (e) In comparison, the elastic modulus of major ampullate silk is greater than that of the recombinant samples, whereas on the other hand, the artificial materials are more elastic. As a result the natural draglines as well as the recombinant $(AQ)_{12}NR3$ silk absorb the same amount of energy per unit volume (toughness) (taken from Ref. [44] with permission) A: alanine, G: glycine, P: proline, Q: glutamine X: predominantly tyrosine, leucine, glutamine, alanine and serine residues, NTD: N-terminal domain, CTD: C-terminal domain.

1
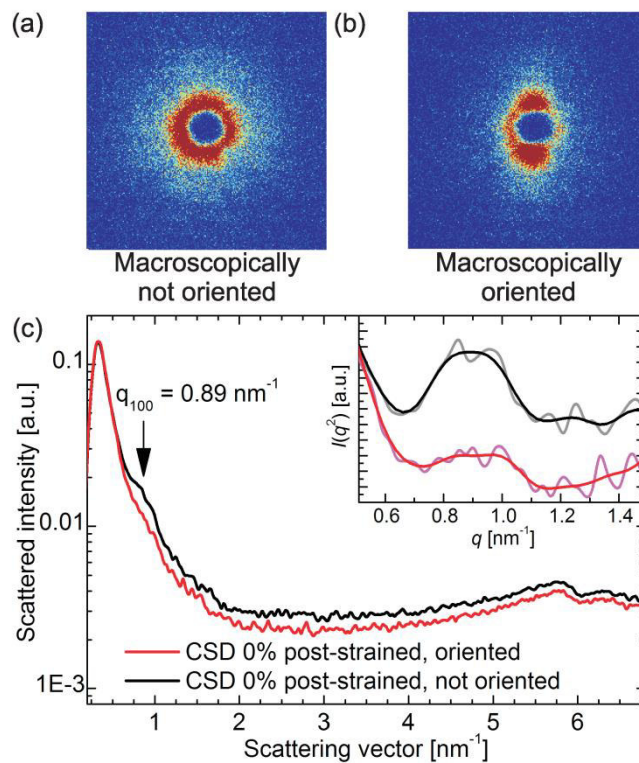
Figure 2: Small angle X-ray scattering (SAXS) pattern of the recombinant $(AQ)_{12}NR3$ fibres. When comparing the diffraction characteristics of (a) macroscopically not-oriented and (b) oriented fibres (CSD 0% post-strained) an anisotropic scattering emerges as a result of aligned structures on the mesoscale. (c) Azimuthally integrated scattering signal. The shoulder at 0.89 nm^{-1} ($2\pi/0.89$ $nm^{-1} = 7.1$ nm) reflects the reduced/enhanced intensity as a result of the fibres' orientation, and hence, the lack/excess of scattering structures at the particular azimuthal angle. The inset depicts an enlargement of the shoulder at 0.89 nm^{-1} along with the Fourier-filtered curves.

16
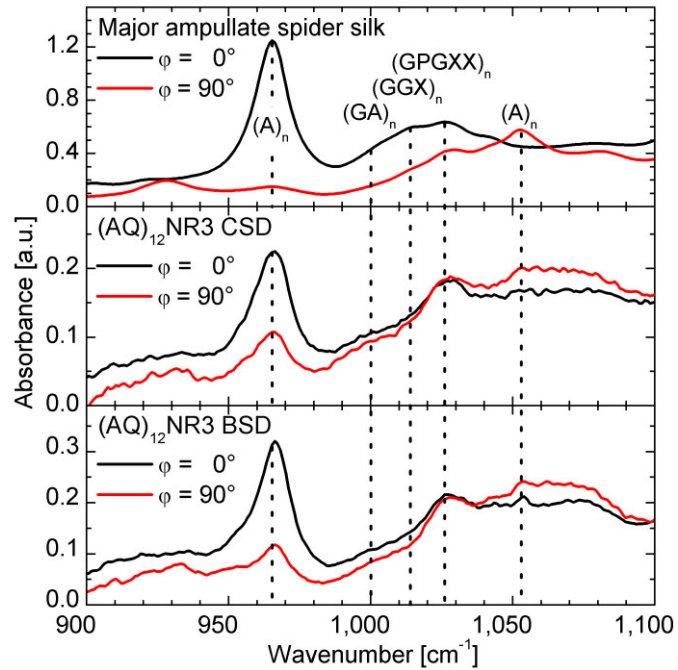
Figure 3: FTIR spectra of (top) major ampullate spider silk, (middle) recombinant (AQ)12NR3 CSD fibres 600% post-strained, and (bottom) (AQ)$_{12}$NR3 BSD fibres 600% post-strained with the electric field of the incoming IR light in parallel to the fibre axis ($\varphi = 0°$, black) and perpendicular to it ($\varphi = 90°$, red). As evident from the amino acid sequence (Figure 1) vibrations at 965 cm^{-1}, 1025 cm^{-1}, and 1055 cm^{-1} arise from the polyalanine ((A)$_n$) and the glycine-rich ((GPGXX)$_n$) motifs. Peaks at 1000 cm^{-1} (GA) and 1015 cm^{-1} ((GGX)$_n$) are absent, due to a lack of those motifs in the primary structure of (AQ)$_{12}$NR3.
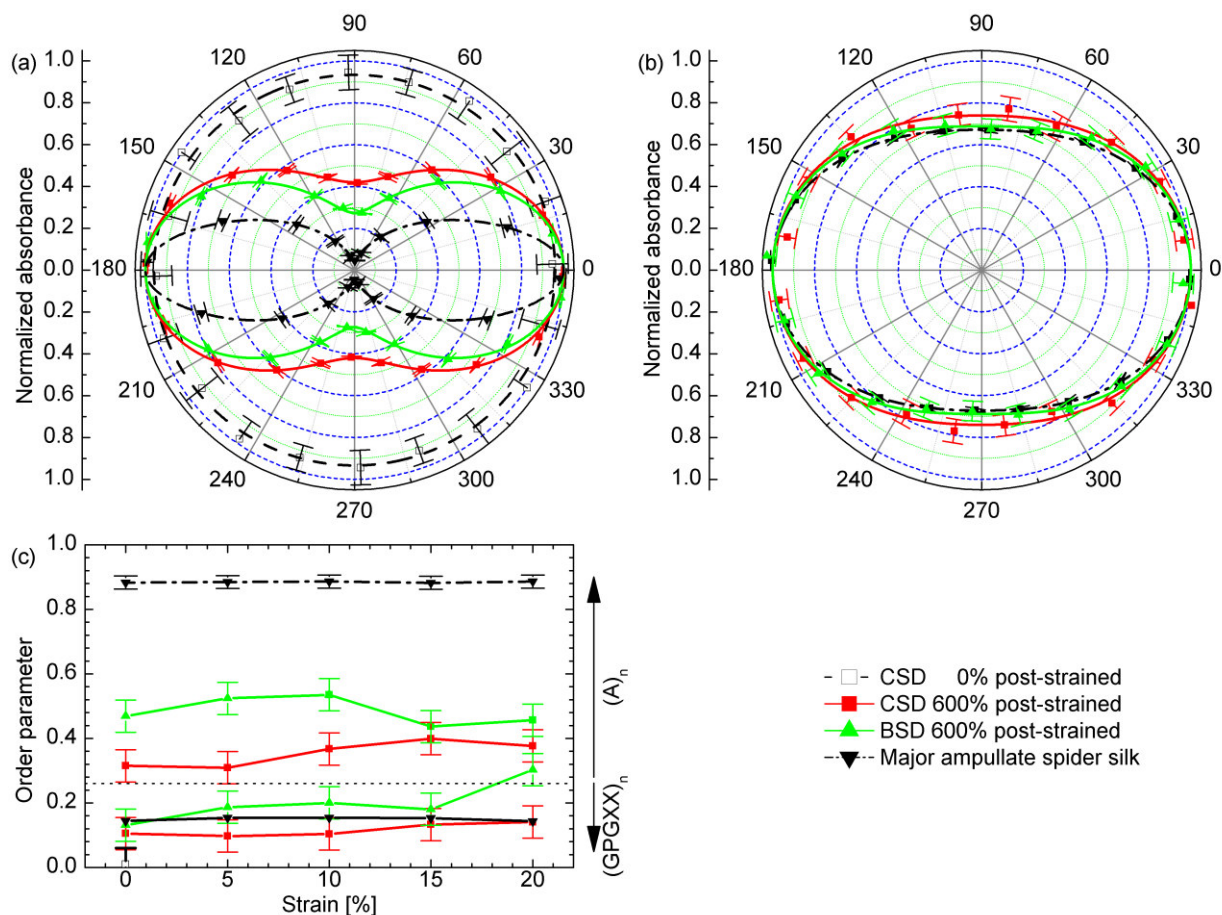
Figure 4: Polar plots and order parameters of molecular moieties located within the nanocrystals or the amorphous matrix. (a) Polar plot of the integrated absorbance (area under the curve) of the $(A)_n$ vibration of the recombinant fibres $((AQ)_{12}NR3$ CSD 0% post-strained: open black squares; $(AQ)12NR3$ CSD 600% post-strained: solid red squares; $(AQ)_{12}NR3$ BSD 600% post-strained: solid green triangles) as well as the natural major ampullate spider silk threads (solid black triangles). The dashed, dashed-dotted, and solid lines represent fits of Equation 1. The data points are normalized through dividing by the corresponding maximum value. (b) Polar plot of the $(GPGXX)_n$ vibration. The decoding is identical to that of panel a. (c) Change of the molecular order parameter with rising strain. While the orientation in the natural sample is hardly affected, the crystallites in the recombinant fibres align further up to the yield point (CSD 600% post strain: S = 0.32 to 0.40; BSD 600% post strained: S = 0.47 to 0.54). For greater strain than the yield point the amorphous matrix orient significantly better. The dotted line separates the curves of the $(A)_n$ and the $(GPGXX)n$ motifs.
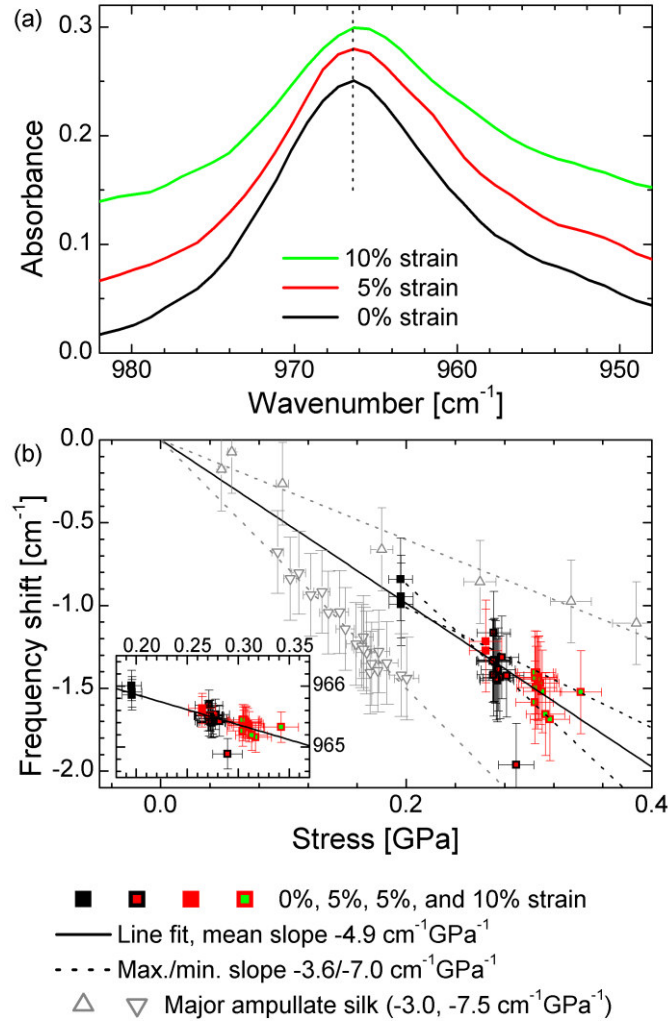
Figure 5: Microscopic response of the recombinant sample to macroscopic load. (a) The frequency position of the $(A)_n$ peak is shifted to lower wavenumbers as a consequence of the applied force (and hence stress). (b) Similar to that of natural spider silk this frequency shift is linear with the applied stress (inset) with a slope of -4.9 cm^{-1}GPa^{-1} being in full agreement with the literature[19,36-38]. The black spares correspond to the black curve in panel a, the red squares with black frame result from stretching the sample from 0% to 5% strain. The red squares correspond to the red curve in a and the green squares with red frame represent the sample stretched to 10% strain. Since the $(A)_n$ vibration is exclusively located within in the crystallites[37], it is demonstrated that the macroscopic load is transferred down the molecular scale, where it affects the crystalline parts of the peptide chains, even though the nanocrystals are embedded in an amorphous matrix.
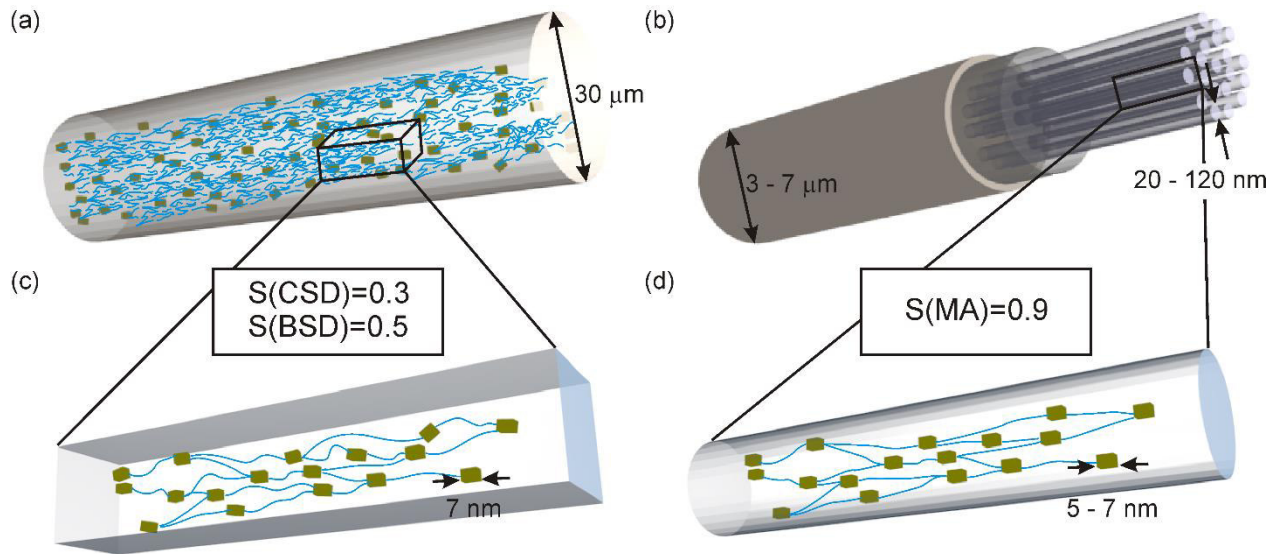
Figure 6: Schematic of (a) a recombinant $(AQ)_{12}NR3$ (CSD or BSD) and (b) a natural major ampullate spider silk thread. The former comprises a homogeneous compound of polyalanine β-sheet crystallites embedded in a glycine rich, amorphous matrix, whereas the latter, in addition, exhibits a refined mesoscopic architecture composed of fibrils and a surrounding layered structure. In both samples the nanocrystals show a periodic length of about 7 nm. Stretching as post-spinning treatment aligns the crystallites resulting in a significant increase of the molecular order parameter (CSD: S = 0.32; BSD: S = 0.47), which gives rise to enhanced mechanical properties[44], but does not reach the performance of the natural counterpart (S = 0.90).

Methods

Fibre formation

The recombinant spider silk proteins are produced and purified as reported previously[44]. The "classical" spinning dope (CSD) is obtained through removing excess water from the diluted spider silk protein solutions during dialysis against polyethylene glycol[50]. Dialysis of the protein solution against a phosphate-containing buffer, instead, yields the phase-separated, "biomimetic" spinning dope (BSD)[14]. Afterward, the fibres are formed by wet spinning from the CSD or BSD and are used either as such or after subsequent post-straining to 600% of their initial length (denoted as 0% and 600% post-strained, respectively)[44].

The natural major ampullate fibres are obtained by forced silking from adult female spiders of the species *Nephila edulis*. The spiders are fed with crickets and are not exposed to low temperature or CO_2 atmosphere prior to silking.

Infrared spectroscopy

Polarized vibrational spectra are recorded by means of a mercury-cadmium-telluride detector (MCT, Kolmar Technologies, Germany) with a spectral resolution of 2 cm^{-1} in transmission mode on a Bio-Rad FTS 6000 FTIR spectrometer equipped with a UMA500 IR microscope. In order to perform stress-dependent measurements one natural silk thread is wound around two parallel rods and glued onto them as described previously[19,36,37]. After the glue has set, one side of the so formed double-sided grating is removed. In case of the recombinant samples, pieces of fibres were glued in parallel onto those rods. Afterward, all fibres were wetted with paraffin oil (Fluka, Switzerland) to reduce light scattering. Former studies showed that this procedure does not alter the mechanical properties or spectral signature in the fingerprint region[37]. The samples were stretched by micrometre screws whilst the emerging force was recorded by a force sensor

1 (8411–50 or 8411–2,5, Burster GmbH, Germany). The data points depicted in Figure 5b resulted

2 from tracing the apparent force and spectral position of the polyalanine peak during stretching

3 and subsequent relaxation while the IR light is polarised parallel to the fibre axis. After the force

4 has had decayed (it does not change during the time needed for the measurement) spectra were

5 measured at different polarisations from $0°$ to $180°$ relative to the fibre axis in steps of $18°$. The

6 latter gives the polar dependence of the absorbance and the order parameters as provided in

7 Figures 3 and 4.

8 The integrated absorbance was determined through fitting a Gaussian function to the measured

9 spectra after a straight baseline was subtracted (for A_n) or the adjacent band was modelled

10 through an additional Gaussian (for GPGXX) as background. The polar-dependent absorbance is

11 given by

12 $$A(\overline{v}, \varphi) = -\log_{10}\left[10^{-A_{max}(\overline{v})}\cos^2(\varphi - \varphi_0) + 10^{-A_{min}(\overline{v})}\sin^2(\varphi - \varphi_0)\right], \quad (1)$$

13 where $A(\overline{v}, \varphi)$ is the integrated absorbance depending on the wavenumber $\overline{v}$ and the polarisation

14 of the light's electric field φ, φ_0 is the polar angle at which the absorbance reaches its maximum,

15 and $A_{max}(\overline{v})$ and $A_{min}(\overline{v})$ are the according maximum and minimum absorbance values.

16 Afterward, the molecular order parameter S_x was calculated with respect to the principle axis x

17 (out of the set of principles axes $\{x, y, z\}$) as follows

18 $$S_x = \frac{1}{2}\left(3\frac{A_x(\overline{v})}{A_x(\overline{v}) + A_y(\overline{v}) + A_z(\overline{v})} - 1\right), \qquad (2a)$$

19 which is in case of a rotational symmetric distribution of the TMs as given for a fibre along the

20 x-axis ($A_{max}(\overline{v}) = A_x(\overline{v})$ and $A_{min}(\overline{v}) = A_y(\overline{v}) = A_z(\overline{v})$) identical with

21 $$S = \frac{A_{max}(\overline{v}) - A_{min}(\overline{v})}{A_{max}(\overline{v}) + 2A_{min}(\overline{v})}. \qquad (2b)$$

22 Furthermore, under the assumptions that all TMs are distributed obeying a Gaussian function

23 $G(\varphi, \varphi_0, \omega, B)$ and the maximum absorbance is centred at the fibre axis ($\varphi_0 = 0°$),

$$G(\varphi, \varphi_0, \omega, B) = B \exp\left(-\frac{(\varphi - \varphi_0)^2}{2\omega^2}\right), \tag{3}$$

the molecular order parameter can be expressed via the width ω of the Gaussian distribution,

$$S(\omega) = \frac{1}{2}\left(3\frac{\int_0^{180°} G(\varphi, \omega, B)\cos^2(\varphi)\sin(\varphi)\mathrm{d}\varphi}{\int_0^{180°} G(\varphi, \omega, B)\sin(\varphi)\mathrm{d}\varphi} - 1\right). \tag{4}$$

The parameter B, that represents measurement-dependent values as the strength of the electric field and of the dipole moment, is canceled out by calculating the ratio in Equation 4.

Small-angle X-ray scattering

Small-angle X-ray scattering (SAXS) experiments were accomplished at room temperature using a micro-focus source (AXO Nova, Germany; CuK_α $\lambda = 0.1542$ nm), multilayer optics (Osmic, USA), and a Hi-Star 2D detector (Bruker, Germany) with a sample-to-detector distance of 1580 mm. The threads were either rolled to a ball and place into the pinhole of the sample holder (denoted as macroscopically not oriented) or glued in parallel onto the holder's surface covering the bore (macroscopically oriented).

References

[1]   Gosline, J. M., Denny, M. W. & DeMont, M. E. Spider silk as rubber. *Nature* **309**, 551–552 (1984).

[2]   Vollrath, F., Holtet, T., Thogersen, H. C. & Frische, S. Structural Organization of Spider Silk. *Proc. Roy. Soc. B* **263,** 147–151 (1996).

[3]   Kubik, S. High-Performance Fibers from Spider Silk. *Angew. Chem., Int. Ed.* **41,** 2721–2723 (2002).

[4]   Hardy, J. G., Römer, L. M. & Scheibel, T. R. Polymeric materials based on silk proteins. *Polymer* **49,** 4309–4327 (2008).

[5]   Doblhofer, E., Heidebrecht, A. & Scheibel, T. To spin or not to spin: spider silk fibers and more. *Appl. Microbiol. Biotechnol.* **99,** 936–9380 (2015).

[6]   Borkner, C. B., Elsner, M. B. & Scheibel, T. Coatings and Films Made of Silk Proteins. *ACS Appl. Mater. Interfaces* **6,** 15611–15625 (2014).

[7]   Gatesy, J., Hayashi, C., Motriuk, D., Woods, J. & Lewis, R. Extreme Diversity, Conservation, and Convergence of Spider Silk Fibroin Sequences. *Science* **291,** 2603–2605 (2001).

[8]   Fu, C., Shao, Z. & Vollrath, F. Animal silks: their structures, properties and artificial production. *Chem. Commun.* , 6515–6529 (2009).

[9]   Knight, D. P. & Vollrath, F. Changes in element composition along the spinning duct in a Nephila spider. *Naturwissenschaften* **88,** 179–182 (2001).

[10]   Vollrath, F. & Knight, D. P. Liquid crystalline spinning of spider silk. *Nature* **400**, 541–548 (2001).

[11]   Lefèvre, T., Boudreault, S., Cloutier, C. & Pézolet, M. Conformational and Orientational Transformation of Silk Proteins in the Major Ampullate Gland of Nephila clavipes Spiders. *Biomacromolecules* **9,** 2399–2407 (2008).

[12]   Jin, H.-J. & Kaplan, D. L. Mechanism of silk processing in insects and spiders. *Nature* **424,** 1057–1061 (2003).

[13]   Hagn, F. *et al.* A conserved spider silk domain acts as a molecular switch that controls fibre assembly. *Nature* **465,** 239–242 (2010).

[14]   Eisoldt, L., Hardy, J. G., Heim, M. & Scheibel, T. R. The role of salt and shear on the storage and assembly of spider silk proteins. *J. Struct. Biol.* **170,** 413 – 419 (2010).

[15]   Giesa, T., Arslan, M., Pugno, N. M. & Buehler, M. J. Nanoconfinement of Spider Silk Fibrils Begets Superior Strength, Extensibility, and Toughness. *Nano Lett.* **11,** 5038–5046 (2011).

[16]   Sponner, A., Unger, E., Grosse, F. & Weisshart, K. Impact of initial solvent on thermal stability and mechanical properties of recombinant spider silk films. *Nat. Mater.* **4,** 772–775 (2005).

[17]   Sponner, A. *et al.* Composition and Hierarchical Organisation of a Spider Silk. *PLoS ONE* **2,** 1–8 (2007).

[18]   Papadopoulos, P., Ene, R., Weidner, I. & Kremer, F. Similarities in the Structural Organization of Major and Minor Ampullate Spider Silk. *Macromol. Rapid Commun.* **30,** 851–857 (2009).

[19]   Anton, A. M. *et al.* Pressure-Dependent FTIR-Spectroscopy on the Counterbalance between External and Internal Constraints in Spider Silk of *Nephila pilipes*. *Macromolecules* **46,** 4919–4923 (2013).

[20]   Simmons, A., Ray, E. & Jelinski, L. W. Solid-State 13C NMR of *Nephila clavipes* Dragline Silk Establishes Structure and Identity of Crystalline Regions. *Macromolecules* **27,** 5235–5237 (1994).

[21]   Riekel, C. & Vollrath, F. Spider silk fibre extrusion: combined wide- and small-angle X-ray microdiffraction experiments. *Int. J. Biol. Macromol.* **29,** 203–210 (2001).

[22]   Rabotyagova, O. S., Cebe, P. & Kaplan, D. L. Role of Polyalanine Domains in β-Sheet Formation in Spider Silk Block Copolymers. *Macromol. Biosci.* **10,** 49–59 (2010).

[23]   Lefèvre, T., Rousseau, M.-E. & Pézolet, M. Protein Secondary Structure and Orientation in Silk as Revealed by Raman Spectromicroscopy. *Biophys. J.* **92,** 2885–2895 (2007).

[24]   van Beek, J. D., Hess, S., Vollrath, F. & Meier, B. H. The molecular structure of spider dragline silk: Folding and orientation of the protein backbone. *Proc. Natl. Acad. Sci. USA* **99,** 10266–10271 (2002).

[25]   Riekel, C., Craig, C., Burghammer, M. & Müller, M. Microstructural homogeneity of support silk spun by *Eriophora fuliginea* (C.L. Koch) determined by scanning X-ray microdiffraction. *Naturwissenschaften* **88,** 67–72 (2001).

[26] Ene, R., Papadopoulos, P. & Kremer, F. Quantitative analysis of infrared absorption coefficient of spider silk fibers. *Vib. Spectros.* **57,** 207–212 (2011).

[27] Simmons, A. H., Michal, C. A. & Jelinski, L. W. Molecular Orientation and Two-Component Nature of the Crystalline Fraction of Spider Dragline Silk. *Science* **271,** 84–87 (1996).

[28] Sampath, S. *et al.* X-ray diffraction study of nanocrystalline and amorphous structure within major and minor ampullate dragline spider silks. *Soft matter* **8,** 6713–6722 (2012).

[29] Glišović, A., Vehoff, T., Davies, R. J. & Salditt, T. Strain Dependent Structural Changes of Spider Dragline Silk. *Macromolecules* **41,** 390–398 (2008).

[30] Du, N. *et al.* Design of Superior Spider Silk: From Nanostructure to Mechanical Properties. *Biophys. J.* **91,** 4528–4535 (2006).

[31] Knowles, T. P. *et al.* Role of Intermolecular Forces in Defining Material Properties of Protein Nanofibrils. *Science* **318,** 1900–1903 (2007).

[32] Keten, S. & Buehler, M. J. Nanostructure and molecular mechanics of spider dragline silk protein assemblies. *J. R. Soc. Interface* **7,** 1709–1721 (2010).

[33] Paquet-Mercier, F., Lefèvre, T., Auger, M. & Pézolet, M. Evidence by infrared spectroscopy of the presence of two types of β-sheets in major ampullate spider silk and silkworm silk. *Soft Matter* **9,** 208–215 (2013).

[34] Rousseau, M.-E., Lefèvre, T., Beaulieu, L., Asakura, T. & Pézolet, M. Study of Protein Conformation and Orientation in Silkworm and Spider Silk Fibers Using Raman Microspectroscopy. *Biomacromolecules* **5,** 2247–2257 (2004).

1   [35]   Ene, R., Papadopoulos, P. & Kremer, F. Supercontraction in Nephila spider dragline silk

2   – Relaxation into equilibrium state. *Polymer* **52,** 6056–6060 (2011).

3   [36]   Ene, R., Papadopoulos, P. & Kremer, F. Combined structural model of spider dragline

4   silk. *Soft Matter* **5,** 4568–4574 (2009).

5   [37]   Papadopoulos, P., Sölter, J. & Kremer, F. Structure-property relationships in major

6   ampullate spider silk as deduced from polarized FTIR spectroscopy. *Eur. Phys. J. E* **24,** 193–199

7   (2007).

8   [38]   Papadopoulos, P., Sölter, J. & Kremer, F. Hierarchies in the structural organization of

9   spider silk – quantitative model. *Colloid. Polym. Sci.* **287,** 231–236 (2009).

10   [39]   Elices, M., Pérez-Rigueiro, J., Plaza, G. R. & Guinea, G. V. Recovery in spider silk

11   fibers. *J. Appl. Polym. Sci.* **92,** 3537–3541 (2004).

12   [40]   Elices, M., Plaza, G. R., Pérez-Rigueiro, J. & Guinea, G. V. The hidden link between

13   supercontraction and mechanical behavior of spider silks. *J. Mech. Behav. Biomed.* **4,** 658–669

14   (2011).

15   [41]   Schneider, D. *et al.* Nonlinear control of high-frequency phonons in spider silk. *Nat.*

16   *Mater.* (2016), DOI: 10.1038/nmat4697.

17   [42]   Xia, X.-X. *et al.* Native-sized recombinant spider silk protein produced in metabolically

18   engineered Escherichia coli results in a strong fiber. *Proc. Natl. Acad. Sci. USA* **107,** 14059–

19   14063 (2010).

20   [43]   Lazaris, A. et al. Spider Silk Fibers Spun from Soluble Recombinant Silk Produced in

21   Mammalian Cells. *Science* **295,** 472–476 (2002).

[44]   Heidebrecht, A. *et al.* Biomimetic Fibers Made of Recombinant Spidroins with the Same Toughness as Natural Spider Silk. *Adv. Mater.* **27,** 2189–2194 (2015).

[45]   Plaza, G. R. *et al.* Relationship between microstructure and mechanical properties in spider silk fibers: identification of two regimes in the microstructural changes. *Soft Matter* **8,** 6015–6026 (2012).

[46]   Anton, A. M., Gutsche, C., Kossack, W. & Kremer, F. Methods to determine the pressure dependence of the molecular order parameter in (bio)macromolecular fibres. *Soft Matter* **11,** 1158–1164 (2015).

[47]   Adhikari, R., Huy, T. A., Buschnakowski, M., Michler, G. H. & Knoll, K. Asymmetric PS-block-(PS-co-PB)-block-PS block copolymers: morphology formation and deformation behavior. *New J. Phys.* **6,** 28 (2004).

[48]   Mahmood, N. *et al.* Influence of shear processing on morphology orientation and mechanical properties of styrene butadiene triblock copolymers. *Polymer* **55,** 3782–3791 (2014).

[49]   Nova, A., Keten, S., Pugno, N. M., Redaelli, A. & Buehler, M. J. Molecular and Nanostructural Mechanisms of Deformation, Strength and Toughness of Spider Silk Fibrils. *Nano Lett.* **10,** 2626–2634 (2010).

[50]   Kim, U.-J. *et al.* Structure and Properties of Silk Hydrogels. *Biomacromolecules* **5,** 786–792 (2004),

Acknowledgements

Author contributions

A.M.A. and F.K. initiated the spectroscopic, A.H. and T.S. the biochemistry research. A.H. and T.S. performed the recombinant spider silk protein production and fibre formation, A.M.A. and F.K. accomplished the FTIR measurements, and N.M. and M.B. executed the X-ray scattering. All authors contributed to analysing the results and writing the paper.

Author information

Reprints and permissions information is available at www.nature.com/reprints. The authors declare no competing financial interests. Both scientist A.M.A. and A.H. (‡) contributed equally and both professors F.K. and T.S. (§) contributed equally to this work. Correspondence concerning the measurements and discussion should be addressed to A.M.A. (anton@physik.uni leipzig.de); requests concerning the discussion and for sample materials should be addressed to T.S. (thomas.scheibel@bm.uni bayreuth.de).

Part 3

Recombinant Production of Spider Silk Proteins

Heidebrecht, A., and Scheibel, T.

Recombinant Production of Spider Silk Proteins

Aniela Heidebrecht*, Thomas Scheibel*,1
*Department of Biomaterials, University of Bayreuth, Universitätsstr. 30, 95440 Bayreuth, Germany
[1]Corresponding author: E-mail: thomas.scheibel@bm.uni-bayreuth.de

Contents

Abstract

Natural spider silk fibers combine extraordinary properties such as stability and flexibility which results in a toughness superseding that of all other fiber materials. As the spider's aggressive territorial behavior renders their farming not feasible, the

biotechnological production of spider silk proteins (spidroins) is essential in order to investigate and employ them for applications. In order to accomplish this task, two approaches have been tested: firstly, the expression of partial cDNAs, and secondly, the expression of synthetic genes in several host organisms, including bacteria, yeast, plants, insect cells, mammalian cells, and transgenic animals. The experienced problems include genetic instability, limitations of the translational and transcriptional machinery, and low solubility of the produced proteins. Here, an overview of attempts to recombinantly produce spidroins will be given, and advantages and disadvantages of the different approaches and host organisms will be discussed.

1. INTRODUCTION

The outstanding mechanical properties of spider silk fibers have impressed mankind since ancient times (Gerritsen, 2002). Its combination of stability and flexibility gives natural spider silk fibers a toughness no other natural or synthetic fiber can achieve (Gosline, Guerette, Ortlepp, & Savage, 1999). Even compared to Kevlar, one of the strongest known synthetic fibrous materials (Table 4.1), spider silk fibers are superior, because they can absorb three times more energy before breaking (Römer & Scheibel, 2007). In addition, spider silk comprises antimicrobial and hypoallergenic properties suitable in applications, such as in wound dressings. A spider's web has been reported to be able to stop bleeding and to support the healing process by isolating the wound from the surrounding air (Bon, 1710).

The outstanding mechanical properties of spider silk fibers are based on their hierarchical setup and the proteins involved. A spider silk fiber mainly consists of proteins, the so–called spidroins ("spidroin" = spider fibroin)

Table 4.1 The mechanical properties of *A. diadematus* dragline silk compared with other materials

Material	Young's modulus [GPa]	Strength [MPa]	Extensibility [%]	Toughness [MJ/m³]
A. diadematus dragline	6	700	30	150
B. mori cocoon	7	600	18	70
Elastin	0.001	2	15	2
Nylon 6.6	5	950	18	80
Kevlar 49	130	3600	2.7	50
Steel	200	1500	0.8	6
Carbon fiber	300	4000	1.3	25

Adapted from Gosline et al., (1999); Heim et al., (2009); Madsen et al., (1999).

(Hinman & Lewis, 1992). The spidroin's secondary structure elements provide a combination of stability and flexibility that results in the outstanding toughness of the fiber.

However, in order to both investigate and employ spider silk for applications, a large-scale silk production is necessary. In contrast to farming of the silkworm *Bombyx mori*, farming of spiders is not feasible, because spiders are territorial and show a cannibalistic behavior (Fox, 1975). Additionally, it has been discovered that spiders held in captivity produce less silk and with a lower quality, as its amino acid content directly reflects the spider's diet (Craig et al., 2000). In order to obtain silk proteins on a large scale, the main approach is the recombinant production of natural spidroins or of designed proteins which comprise essential features of natural spidroins. The tested host organisms include bacteria, yeast, as well as insect cells, plants, mammalian cells, and even transgenic mammals. In this review, an overview of recombinantly produced spidroins will be given, and advantages and disadvantages of the different approaches and host organisms will be discussed.

2. SPIDERS AND SPIDER SILK

Web spiders (*Aranea*), the best known order of the *Arachnida*, benefit from their silk every day. Some spiders, such as female orb-weavers, produce up to seven different types of silk and use them for a range of different applications, such as in a complex web for catching prey, for wrapping prey, and for protecting their offsprings. Each silk has unique mechanical properties, depending on their intended use (Stauffer, Coguill, & Lewis, 1994) and is named after the gland in which its proteins are produced (see below).

2.1. The Different Types of Spider Silk and Their Properties

The different types of silk of a female orb web spider have mechanical properties (Table 4.2) adapted to their tasks (Fig. 4.1).

2.1.1. Major Ampullate (MA)/Dragline Silk

Spiders use MA silk with a very high tensile strength (Blackledge, Summers, & Hayashi, 2005; Gosline, Denny, & Demont, 1984; Gosline et al., 1994, 1999, 2002; Thiel & Viney, 1996; Viney, 1997; Vollrath & Porter, 2006) for the outer frame as well as the radii of their web. MA silk also functions as a lifeline for the spider in case it has to escape from a predator (Aprhisiart & Vollrath, 1994).

Table 4.2 Mechanical properties of the different types of spider silk from different spiders

| Silk	Young's modulus [GPa]	Strength [MPa]	Extensibility [%]	Toughness [MJ/m³]	Reference
MA					
Argiope trifasciata	9.3	1290	22	145	(Hayashi et al., 2004)
MI					
Argiope trifasciata	8.5	342	54	148	(Hayashi et al., 2004)
Flagelliform					
Araneus diadematus	0.003	500	270	150	(Gosline et al., 1999)
Cylindriform					
Argiope bruennichi	9.1	390	40	128	(Zhao et al., 2006)
Aciniform					
Argiope trifasciata	9.6	687	86	367	(Hayashi et al., 2004)
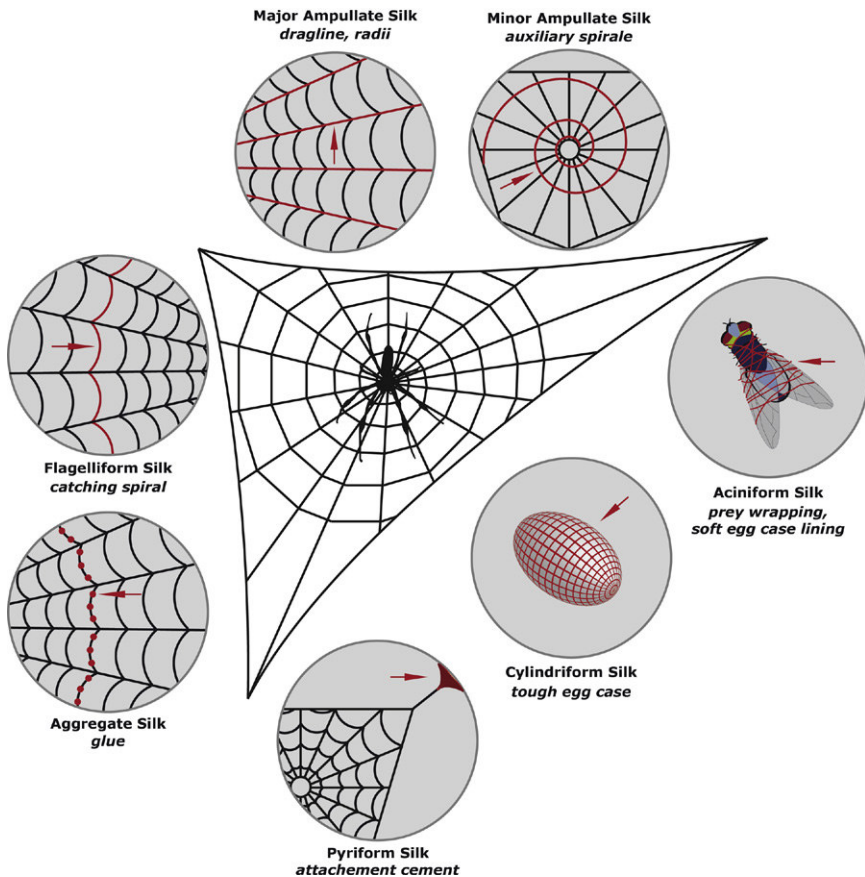
Figure 4.1 Schematic presentation of the seven different types of spider silk. (For color version of this figure, the reader is referred to the online version of this book.)

The core of the MA silk fiber consists of fibrils comprising at least two MA spidroins, with a molecular weight of 200–350 kDa (Ayoub, Garb, Tinghitella, Collin, & Hayashi, 2007; Candelas & Cintron, 1981; Jackson & O'Brien, 1995; O'Brien, Fahnestock, Termonia, & Gardner, 1998). In principle, MA spidroins can be divided into two classes, one poor in proline residues (MaSp1) and one proline-rich (MaSp2). All MA spidroins consist of repetitive core sequences that are flanked by nonrepetitive, folded amino- and carboxy-terminal domains. Individual amino acid motifs of the core sequences (see below) are repeated up to 100 times (Ayoub et al., 2007; Hinman & Lewis, 1992), and generally a motif contains 40–200 amino acids (Ayoub et al., 2007; Guerette, Ginzinger, Weber, & Gosline, 1996; Hayashi, Blackledge, & Lewis, 2004).

Strikingly, the proline content varies greatly between spider species, indicating a different ratio of MaSp1 and MaSp2 (Andersen, 1970; Lombardi & Kaplan, 1990; Mello, Senecal, Yeung, Vouros, & Kaplan, 1994). Due to its molecular structure, a pyrrolidine ring, a proline residue inflicts steric constraints on the protein backbone, since it doesn't supply an amide proton that can take part in hydrogen bonds (Hurley, Mason, & Matthews, 1992; Vollrath & Porter, 2006). Thus, proline residues favor the formation of β-turn and γ-turn structures over α-helix and β-sheet structures (Hayashi, Shipley, & Lewis, 1999; Thiel, Guess, & Viney, 1997; Zhou, Wu, & Conticello, 2001). The proline-containing structured motifs, such as GPGXX, are not capable of forming crystalline structures, which result in a higher elasticity of the fiber (Hayashi et al., 1999; Thiel et al., 1997). The supercontraction of a fiber, which is closely linked to its mechanical properties, is also based on its proline content (Liu, Shao, & Vollrath, 2005; Liu, Shao, et al., 2008). Silkworm and spider MI silk both contain only a small amount of proline and show almost no supercontraction (Colgin & Lewis, 1998; Ito et al., 1995; Jelinski et al., 1999; Vollrath, 1994), whereas the supercontraction of MA silks differs from species to species, since their proline content differs as well (Vollrath & Porter, 2006). An intrinsic disorder in combination with hydration, as it is caused by proline- and glycine residues, is fundamental for an elastomeric function of silk fibers (Rauscher, Baud, Miao, Keeley, & Pomes, 2006).

Strikingly, in the inner core of the MA silk fiber of *Nephila clavipes*, both MaSp1 and MaSp2 were found (Sponner et al., 2007), while the surrounding area contains only MaSp1, whose proline content is low.

The repetitive domains of MA spidroins of *Araneus diadematus* and *N. clavipes* contain stretches of polyalanine, as well as motifs containing $(GGX)_n$ or GPGXX (X = tyrosine, leucine, glutamine) (Winkler & Kaplan, 2000). The alanine-rich areas form crystalline β-sheets (Thiel & Viney, 1996) and grant the high tensile strength of the spider silk fibers (Simmons, Michal, & Jelinski, 1996). In contrast, the $(GGX)_n$ and GPGQQ (ADF3) or GPGXX (ADF4) sequences fold into 3_1-helices (Hijirida et al., 1996) and β-turn spirals, respectively. These glycine-rich areas provide an amorphous matrix for the crystalline β-sheets (Perez-Rigueiro, Elices, Plaza, & Guinea, 2007; Sponner et al., 2007; Sponner, Unger, et al., 2005), and thus generate the elasticity and flexibility of the spider silk fiber as mentioned above (Brooks, Steinkraus, Nelson, & Lewis, 2005; Liu, Sponner, et al., 2008; Ohgo, Kawase, Ashida, & Asakura, 2006). The structural motifs of MA spidroins, as well as Minor ampullate (MI) spidroins and Flagelliform silk are shown in Fig. 4.2.

The nonrepetitive terminal domains comprise 100–150 amino acids and have α-helical secondary structures arranged in a five-helix bundle (Challis, Goodacre, & Hewitt, 2006; Hedhammar et al., 2008; Huemmerich, Helsen, et al., 2004; Rising, Hjalm, Engstrom, & Johansson, 2006). These terminal

spider species	silk protein	β-turn spiral GPGGX / GPGQQ elastic	β-sheet $(GA)_n$ / A_n crystalline	3_1-helix GGX amorphous	spacer ~ 30 aa spacer	non-repetitive terminal domains helical
Araneus diadematus	ADF3	✔	✔	✔		✔
	ADF4	✔	✔			✔
Nephila clavipes	MaSp1		✔ ✔	✔		✔
	MaSp2	✔ ✔	✔			✔
	MiSp1		✔ ✔	✔	✔	✔
	MiSp2		✔ ✔	✔	✔	✔
	Flag	✔		✔	✔	✔

Figure 4.2 Structural motifs of various spider silk proteins from *A. diadematus* and *N. clavipes*. X: predominantly tyrosine, leucine, glutamine, alanine, and serine. aa = amino acid. (For color version of this figure, the reader is referred to the online version of this book.)

domains enable the storage of spidroins at high concentrations in the spinning duct and play an important role during the initiation of fiber assembly (Askarieh et al., 2010; Eisoldt, Hardy, Heim, & Scheibel, 2010; Eisoldt, Scheibel, & Smith, 2011; Eisoldt, Thamm, & Scheibel, 2012; Hagn, Thamm, et al., 2010).

2.1.2. MI Silk

MI silk, which has similar properties as MA silk, is used by the spider as an auxiliary spiral to stabilize the scaffold during web construction (Dicko, Knight, Kenney, & Vollrath, 2004; Riekel & Vollrath, 2001; Tillinghast & Townley, 1994). MI silks are mainly composed of two proteins, MiSp1 and MiSp2, which have molecular weights of approx. 250 kDa (Candelas & Cintron, 1981), and strikingly differ considerably from MA silk in their composition, as they contain almost no proline residues (Fig. 4.2). Further, their glutamic acid content is significantly reduced (Andersen, 1970). MiSp1 and MiSp2 of *N. clavipes* contain repetitive sequences that are composed of 10 repeat units. In the case of MiSp1, one repeat unit contains two motifs, GGXGGY (X = glutamine or alanine) alternating with $(GA)_y(A)_z$ (y = 3–6, z = 2–5) (Colgin & Lewis, 1998). MiSp2 of *N. clavipes* comprises $(GGX)_n$ (X = tyrosine, glutamine or alanine, n = 1–3) blocks, alternating with GAGA. In contrast to MA spidroins, the repetitive regions of MI spidroins are disrupted by 137 amino acid-long nonrepetitive serine-rich spacer regions being almost identical in MiSp1 and MiSp2. Comparable to MA spidroins, crystalline structures are embedded in an amorphous matrix (Colgin & Lewis, 1998). However, NMR studies showed that in contrast to MA silk, only a small fraction of alanine residues contribute to crystalline β-sheets in MI silk. Thus, the high tensile strength of MI silk cannot solely be due to β-sheet structures, but must also be based on other structural features, and in this content it is assumed that cross-linking as well as specific matrix properties of MI proteins, different to those of MA proteins, have some impact thereon (Dicko et al., 2004).

2.1.3. Flagelliform Silk

Flagelliform silk is highly elastic and is used as the capture spiral of an orb web, because it can absorb the high kinetic energy that results from the impact of an insect (Becker et al., 2003; Bini, Knight, & Kaplan, 2004; Brooks et al., 2005; Dicko et al., 2004; Ohgo et al., 2006; Scheibel, 2004; Winkler & Kaplan, 2000). Flagelliform silk, which is also called "viscid"

silk, mainly consists of one protein that has a molecular weight of approx. 500 kDa and contains more proline and valine residues, whereas its alanine content is reduced in comparison to MA and MI silks (Andersen, 1970). The *N. clavipes* flagelliform protein comprises blocks of $(GGX)_n$ and GPGXX, which build 3_1-helices and β-turn spirals, respectively. These secondary structural motifs are responsible for the high elasticity and flexibility of this type of silk (Brooks et al., 2005; Liu, Sponner, et al., 2008; Ohgo et al., 2006). $(GPGGX)_2$ motifs (X = serine or tyrosine) form β-turns, and assemble a structure similar to a spring (Hayashi et al., 1999). Since flagelliform silk has more than 40 adjacent linked β-turns in spring-like spirals, it is likely that this structure adds to the extraordinary elasticity (200%) of the fiber (Hayashi & Lewis, 1998).

2.1.4. Pyriform Silk

Pyriform silk is used by the spider to securely attach individual MA, MI, and Flagelliform silk fibers to each other as well as to a substrate, such as a tree branch or a wall (Hajer & Rehakova, 2003; Kovoor & Zylberberg, 1980). Pyriform silk proteins of *A. diadematus* have a randomly coiled structure as they contain a low amount of small nonpolar amino acids as well as significant quantities of polar and charged amino acids, which are important for physical cross-linking (Andersen, 1970).

2.1.5. Aggregate Silk

In order to prevent prey to escape the spider's web, ecribellate spiders, such as *Latrodectus hesperus*, cover their capture spiral with an aggregate silk, which is a mixture of sticky glycoproteins and small highly hygroscopic peptides (Hu et al., 2007; Vollrath, 2006; Vollrath & Tillinghast, 1991). The aggregate silk proteins of *L. hesperus* (Hu et al., 2007) contain a low amount of small nonpolar amino acids, as well as significant amounts of proline residues, polar and charged amino acids (Andersen, 1970). In contrast to that, cribellate spiders, e.g. from the *Uloborus* sp., surround their capture spiral not with an aqueous sticky glue but with thin cribellar fibrils, which are 10 nm in diameter. The stickiness of these dry cribellar fibrils is accomplished through a combination of van der Waals and hygroscopic forces (Hawthorn & Opell, 2002, 2003).

2.1.6. Cylindriform/Tubiliform Silk

Araneus diadematus cylindriform silk proteins are composed of polyalanine blocks in combination with $(GGX)_n$ (X = alanine, leucine, glutamine, or

tyrosine) motifs, which form β-sheet stacks (similar to *N. clavipes* MA silk) (Barghout, Thiel, & Viney, 1999), giving the cylindriform fibers a high strength. They are suitable to be used by the spider as a tough egg case in order to protect its offspring (Bittencourt et al., 2007; Garb & Hayashi, 2005; Huang et al., 2006; Hu, Kohler, et al., 2005, 2006; Hu, Lawrence, et al., 2005; Hu, Vasanthavada, et al., 2006; Kohler et al., 2005; Rising et al., 2006).

2.1.7. Aciniform Silk

Female orb web spiders use aciniform silk for multiple purposes, such as a soft lining inside the egg case, as well as in order to reinforce the prey wrapping and the pyriform silk attachment cement (Blackledge & Hayashi, 2006; Hayashi et al., 2004; La Mattina et al., 2008; Vasanthavada et al., 2007). Even though the 300 kDa AcSp (*L. hesperus* (Vasanthavada et al., 2007)) contains $(GGX)_n$ domains, they differ greatly from other types of silk proteins (Andersen, 1970).

2.2. Hierarchical Structure of MA Silk Fibers

MA threads of the orb-weaver *N. clavipes* show a core–shell structure (Fig. 4.3). Its proteinaceous core is composed of MA spidroin fibrils, which are oriented in direction of the fiber axis, and which itself can be divided into an inner and outer region, based on the protein content. The core is covered by a 150–250 nm-thick three-layer shell (Augsten, Muhlig, & Herrmann, 2000; Augsten, Weisshart, Sponner, & Unger, 1999), consisting of MI silk, glycoproteins, and lipids (Sponner et al., 2007).
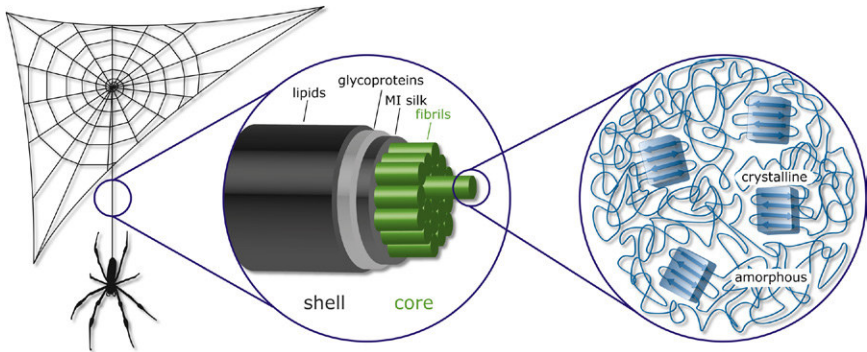
Figure 4.3 *Core–shell structure of the dragline silk of N. clavipes.* The core of the fiber comprises fibrils that are oriented along the fiber axis. On a molecular level, these fibrils consist of crystalline areas that are embedded in an amorphous matrix, depending on the amino acid composition. The core is covered by a three-layer shell containing MI silk, glycoproteins, and lipids. (For color version of this figure, the reader is referred to the online version of this book.)

A 10–20 nm-thick lipid layer builds the outer coat of the fiber (Sponner et al., 2007), and it fulfills a number of tasks, as it serves as a carrier for pheromones that play an important role in the sex and species recognition (Schulz, 2001). As this coat is just loosely attached, it offers only limited protection from the surrounding environment and does not contribute to the mechanical properties of the fiber (Sponner et al., 2007). The underlying layer is about 40–100 nm thick and composed of glycoproteins (Augsten et al., 2000). This layer offers a more profound protection from microorganisms, since it is tighter attached than the lipid layer. Additionally, the glycoprotein coat indirectly influences the mechanical strength of the fiber, as it is able to regulate the water balance, which has an impact on the contraction state of the fiber (Liu et al., 2005). Even though the proteins in the glycoprotein layer differ from those in the skin and the core of the fiber, their molecular weights are comparable (Sponner et al., 2007). The inner layer of the fiber's shell is 50–100 nm thick and comprises MI silk proteins. This layer plays a dual role: firstly, it protects the fiber from environmental damage inflicted by chemical agents and microbial activity, and, secondly, it mechanically supports the fiber as it adds plasticity (Sponner et al., 2007).

2.3. Natural MA Spidroin Processing

The spider's silk glands contain a highly concentrated protein solution (up to 50% (w/v) (Hijirida et al., 1996)), the so-called spinning dope. In the spinning gland, the protein solution is stored at a neutral pH and high salt concentration that prevents aggregation of the proteins. It is assumed that the proteins form supramolecular micelle-like structures (Eisoldt et al., 2010; Exler, Hummerich, & Scheibel, 2007; Hagn, Eisoldt, et al., 2010; Lin, Huang, Zhang, Fan, & Yang, 2009), with the unfolded repeated sequences being inside of the micelle and the folded polar ends on its surface (Hagn, Thamm, et al., 2010). At the beginning of the assembly process, the spinning dope is transferred to the spinning duct, where acidification, ion exchange, and extraction of water take place. Additionally, the proteins are arranged in the direction of strain and exposed to shear forces, due to the accelerating flow of the spinning dope (Hardy & Scheibel, 2009; Heim, Keerl, & Scheibel, 2009; Knight & Vollrath, 1999). The pH drop from 7.2 in the gland to 6.3 in the spinning duct causes dimerization of the amino-terminal domains of the proteins into antiparallel dimers (head-to-tail) (Askarieh et al., 2010; Eisoldt et al., 2010; Hagn, Thamm, et al., 2010). The lowering of the sodium chloride concentration (Knight & Vollrath, 2001; Tillinghast, Chase, & Townley, 1984) in combination with shear forces results in the

alignment of the protein chains parallel to the fiber axis (Eisoldt et al., 2010; van Beek, Hess, Vollrath, & Meier, 2002). During this assembly step, the carboxy-terminal domains control the correct orientation of the repetitive regions, and thus support the formation of β–sheet stacks, which strongly influence the mechanical properties of the spider silk fiber (Hagn, Eisoldt, et al., 2010). After being pulled from the spinneret, the excess water of the fibers evaporates, and fiber formation is completed.

2.4. Artificial Fiber Formation

In order to use the outstanding mechanical properties of spider silk fibers for industrial purposes, many attempts have been made to spin reconstituted silk into fibers. For this purpose, natural silk fibers were dissolved in different solvents, and the artificial silk dopes were spun with several techniques, ranging from wet-spinning into alcohol baths (Matsumoto, Uejima, Iwasaki, Sano, & Sumino, 1996) (fiber formation by protein precipitation in a coagulation bath) to electrospinning (Zarkoob et al., 2004) (solvent evaporation by accelerating the spinning solution in an electrical field). The reconstituted silk fibers did neither have the mechanical properties (Lazaris et al., 2002; Liivak, Blye, Shah, & Jelinski, 1998; Madsen, Shao, & Vollrath, 1999; Marsano et al., 2005; Shao, Vollrath, Yang, & Thogersen, 2003; Xie, Zhang, Shao, & Hu, 2006; Yao, Masuda, Zhao, & Asakura, 2002) nor the structural integrity (Putthanarat, Stribeck, Fossey, Eby, & Adams, 2000) of natural silk fibers.

Further, the properties of natural and reconstituted silk dopes showed significant differences (Holland, Terry, Porter, & Vollrath, 2007). Due to the harsh conditions that are necessary to dissolve the silk fibers for dope preparation, high temperatures and chaotropic agents cause severe degradation of the silk proteins. It has been shown that the molecular weight of the proteins (Iridag & Kazanci, 2006; Yamada, Nakao, Takasu, & Tsubouchi, 2001; Zuo, Dai, & Wu, 2006) as well as their conformation (Asakura, Kuzuhara, Tabeta, & Saito, 1985; Zuo et al., 2006) is significantly altered during the silk dope preparation.
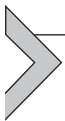
3. RECOMBINANT PRODUCTION OF SPIDER SILK PROTEINS

As mentioned above, the livestock breeding and harvesting the silk fibers, like it is done with the mulberry silkworm *B. mori* (Yamada et al., 2001), is not possible with spiders. In contrast to *B. mori*, the spider's aggressive

territorial behavior and its cannibalism render farming not feasible in large scale, hampering the accessibility to the raw material. Furthermore, spiders that are held in captivity produce silk with lower qualities, likely depending on their nutrition (Madsen et al., 1999;Vollrath, 1999). In order to overcome these difficulties, different approaches have been tested to produce recombinant spider silk proteins in large quantities, followed by artificial processing similar to the attempts with regenerated silk proteins.

One tested route is the expression of natural spider silk genes in different host organisms. Apart from prokaryotes and eukaryotes, even transgenic animals have been used as host organisms with varying results. An overview of the recombinantly produced proteins based on native silk genes in different host organisms is given in Table 4.3.

Limited success has been achieved by expressing partial cDNAs in different host organisms, as differences in codon usage cause inefficient translations. Additionally, the highly repetitive nature of spider silk genes impedes their manipulation and amplification using polymerase chain reaction (Heim et al., 2009; Scheibel, 2004).

In order to overcome these problems, synthetic genes were produced encoding proteins that differ from the natural spider silk proteins, but possess their key features. These synthetic mimics of spider silk genes were created by identifying relevant amino-acid sequence motifs of natural spidroins (see above) and subsequently back-translating these into DNA sequences considering the codon usage of the corresponding host organism (Huemmerich, Helsen, et al., 2004; Lewis, Hinman, Kothakota, & Fournier, 1996; Prince, Mcgrath, Digirolamo, & Kaplan, 1995). An overview of recombinantly produced spider silk proteins in bacterial host organisms using synthetic genes is given in Table 4.4, and in eukaryotic hosts in Table 4.5.

3.1. Bacterial Expression Hosts Used for Spider Silk Production

3.1.1. *Escherichia coli*

Escherichia coli is a gram-negative enterobacterium, which is often used as a host organism for recombinant protein production. Its relative simplicity, its well-known genetics, and the capability of fast high-density cultivation render it a suitable host organism for the fast and inexpensive large-scale production of recombinant proteins. The availability of different plasmids, fusion protein partners, and mutated strains are additional advantages (Sorensen & Mortensen, 2005).

Table 4.3 Overview of natural spider silk genes expressed in different host organisms

Type of silk protein	Terminal domains*	M$_W$** [kDa]	Yield** [mg/L]	Spider	Host organism	References
MA silk						
MaSp1	−	22, 25	N/A	*Euprosthenops* sp.	Mammalian cells (COS-1)	(Grip et al., 2006)
	±NTD, ±CTD	10–28	25–150	*Euprosthenops australis*	Bacteria (*Escherichia coli*)	(Askarieh et al., 2010; Hedhammar et al., 2008; Stark et al., 2007)
	+CTD	43	4	*Nephila clavipes*	Bacteria (*Escherichia coli*)	(Arcidiacono et al., 1998)
MaSp1 (fibroin chimera)	−	83	N/A	*Nephila clavata*	Transgenic animals (*Bombyx mori*)	(Wen et al., 2010)
MaSp1 & MaSp2	±CTD	12	N/A	*Nephila clavipes*	Bacteria (*Escherichia coli*)	(Sponner, Vater, et al., 2005)
	+CTD	60–140	N/A	*Nephila clavipes*	Mammalian cells (MAC-T & BHK)[†]	(Lazaris et al., 2002)
	−	31–66	8–12	*Nephila clavipes*	Transgenic animals (mice)	(Xu et al., 2007)
	−	33–39	N/A	*Nephila clavipes*	Yeast (*Pichia pastoris*)	(Teule, Aube, Ellison, & Abbott, 2003)
MaSp1- & MaSp2- collagen fusion protein	−	57–61	N/A	*Nephila clavipes*	Yeast (*Pichia pastoris*)	(Teule et al., 2003)

Table 4.3 Overview of natural spider silk genes expressed in different host organisms—cont'd

Type of silk protein	Terminal domains*	M$_W$** [kDa]	Yield** [mg/L]	Spider	Host organism	References
ADF3	+CTD	60–140	25–50	*Araneus diadematus*	Mammalian cells (MAC-T & BHK[†])	(Lazaris et al., 2002)
	−	60	N/A	*Araneus diadematus*	Transgenic animals (goats)	(Karatzas et al., 1999)
ADF3 & ADF4	±CTD	50–105	50	*Araneus diadematus*	Insect cells (*Spodoptera frugiperda*)	(Ittah et al., 2006)
	+CTD	35–56	N/A	*Araneus diadematus*	Insect cells (*Spodoptera frugiperda*)	(Huemmerich, Scheibel, et al., 2004)
Flagelliform						
Flag	+CTD	28	N/A	*Araneus ventricosus*	Insect cells (*Spodoptera frugiperda*)	(Lee et al., 2007)
Polyhedron-Flag fusion protein	+CTD	61	N/A	*Araneus ventricosus*	Insect cells (*Spodoptera frugiperda*)	(Lee et al., 2007)
Tubiliform						
TuSp1	±NTD, ±CTD	12–15	N/A	*Nephila antipodiana*	Bacteria (*Escherichia coli*)	(Lin et al., 2009)
TuSp1	±CTD	33, 45	4.8–7.2	*Latrodectus hesperus*	Bacteria (*Escherichia coli*)	(Gnesa et al., 2012)
Pyriform						
PySp2	±CTD	N/A	N/A	*Latrodectus hesperus*	Bacteria (*Escherichia coli*)	(Geurts et al., 2010)

*NTD: amino-terminal domain, CTD: carboxy-terminal domain.
**N/A: not applicable.
[†]MAC-T: bovine mammary epithelial alveolar cells, BHK: baby hamster kidney cells.

Even though several work groups succeeded in producing recombinant spider silk-like proteins using *E. coli* as a host organism (Arcidiacono, Mello, Kaplan, Cheley, & Bayley, 1998, 2002; Bini et al., 2006; Brooks, Stricker, et al., 2008; Cappello & Crissman, 1990; Fukushima, 1998; Huang, Wong, George, & Kaplan, 2007; Huemmerich, Slotta, & Scheibel, 2006; Slotta, Rammensee, Gorb, Scheibel, 2008; Slotta, Tammer, Kremer, Koelsch, & Scheibel, 2006; Stephens et al., 2005; Winkler, Wilson, & Kaplan, 2000; Zhou et al., 2001), limitations such as low protein yields (Arcidiacono et al., 1998; Prince et al., 1995), heterologous proteins (Fahnestock & Irwin, 1997; Lazaris et al., 2002; Xia et al., 2010), and low protein solubility (Bini et al., 2006; Fukushima, 1998; Mello, Soares, Arcidiacono, & Butlers, 2004; Szela et al., 2000; Winkler et al., 2000; Wong Po Foo et al., 2006) have been encountered. Translation limitations are caused by unwanted recombination events shortening the repetitive genes (Arcidiacono et al., 1998; Fahnestock & Irwin, 1997; Rising, Widhe, Johansson, & Hedhammar, 2011) and depletion of tRNA pools due to the guanine- and cytosine-rich genes (Rosenberg, Goldman, Dunn, Studier, & Zubay, 1993). Moreover, an overproduction of recombinant spider silk proteins in *E. coli* can lead to the formation of inclusion bodies (Liebmann, Huemmerich, Scheibel, & Fehr, 2008), which comprise incorrect or incompletely folded proteins and which retard cell growth (Sorensen & Mortensen, 2005). Fairly good protein yields have been obtained for recombinant spider silk proteins with a molecular weight up to approx. 100 kDa. With an increasing molecular weight of the recombinant spider silk proteins, the impact of these limitations increases greatly.

Escherichia coli is incapable of performing most eukaryotic posttranslational modifications (PTMs), such as glycosylation and phosphorylation of proteins. The dragline silk of *N. clavipes* contains phosphorylated tyrosine and serine residues (Michal, Simmons, Chew, Zax, & Jelinski, 1996). Since the biological function and the correct folding of proteins are dependent on PTMs (Gellissen et al., 1992; Kukuruzinska & Lennon, 1998), it is suspected that the phosphorylated residues influence the processing of the spidroins into fibers, even though the impact on the physical properties has not yet been determined (Michal et al., 1996). However, as nowadays recombinant spidroins have successfully been produced in *E. coli*, the PTMs do not seem crucial at least for the protein production.

A native-sized recombinant spider silk protein (285 kDa) was produced using metabolically engineered *E. coli* (Xia et al., 2010). By analyzing the influence of the silk gene expression on the host protein synthesis, it was found that the silk gene expression causes stress to the host cells, since

Table 4.4 Overview of synthetic spider silk genes expressed in bacterial host organisms

Type of silk protein**	Terminal domains*	M$_W$** [kDa]	Yield** [mg/L]	Spider**	Host organism	References
MA silk						
MaSp1	–	N/A	N/A	*Latrodectus hesperus*	*Salmonella typhimurium*	(Widmaier & Voigt, 2010; Widmaier et al., 2009)
	–	100–285	1.2 g/L	*Nephila clavipes*	*Escherichia coli*[†]	(Xia et al., 2010)
	–	15–26	16–95	*Nephila clavipes*	*Escherichia coli*	(Szela et al., 2000; Winkler et al., 1999, 2000)
	–	45–60	2.5–150	*Nephila clavipes*	*Escherichia coli*	(Bini et al., 2006; Huang et al., 2007; Wong Po Foo et al., 2006)
MaSp1 (Gly-rich repeats)	–	10–20	1.2–5.2	*Nephila clavipes*	*Escherichia coli*	(Fukushima, 1998)
MaSp2	–	63–71	N/A	*Argiope aurantia*	*Escherichia coli*	(Brooks, Stricker, et al., 2008; Teule et al., 2009)
	–	31–112	N/A	N/A	*Escherichia coli*	(Lewis et al., 1996)
MaSp2/Flag	–	58, 62	7–10	*Nephila clavipes*	*Escherichia coli*	(Teule, Furin, Cooper, Duncan, & Lewis, 2007)
MaSp1 & MaSp2	NTD	14	N/A	*Latrodectus hesperus*	*Escherichia coli*	(Hagn, Thamm, et al., 2010)
	±CTD	20–56	15–35	*Nephila clavipes*	*Escherichia coli*	(Arcidiacono et al., 2002; Mello et al., 2004)
	–	N/A	N/A	*Nephila clavipes*	*Bacillus subtilis*	(Fahnestock, 1994)
	–	55, 67	N/A	*Nephila clavipes*	*Escherichia coli*	(Brooks, Nelson, et al., 2008)
	–	15–41	2–15	*Nephila clavipes*	*Escherichia coli*	(Prince et al., 1995)
	–	65–163	N/A	*Nephila clavipes*	*Escherichia coli*	(Fahnestock & Irwin, 1997)

ADF3, ADF4	±CTD	34–106	N/A	*Araneus diadematus*	*Escherichia coli*	(Huemmerich, Helsen, et al., 2004; Schmidt, Romer, Strehle, & Scheibel, 2007)
ADF1, ADF2, ADF3, ADF4	−	25–56	N/A	*Araneus diadematus*	*Salmonella typhimurium*	(Widmaier & Voigt, 2010; Widmaier et al., 2009)
Flagelliform silk						
Flag	−	N/A	N/A	*Nephila clavipes*	*Salmonella typhimurium*	(Widmaier & Voigt, 2010; Widmaier et al., 2009)
Flag	±CTD	14–94	N/A	*Nephila clavipes*	*Escherichia coli*	(Heim, Ackerschott, & Scheibel, 2010)
Flag (Gly-rich repeats)	−	25	11.6	*Nephila clavipes*	*Escherichia coli*	(Zhou et al., 2001)
N/A						
N/A	−	76–89	N/A	N/A	*Escherichia coli*	(Cappello et al., 1990)
Gly-rich repeats & Ala-blocks	−	18–36	21–41	N/A	*Escherichia coli*	(Yang & Asakura, 2005)

*NTD: amino-terminal domain, CTD: carboxy-terminal domain.
**N/A: not applicable.
†Metabolically engineered.

Table 4.5 Overview of synthetic spider silk genes expressed in different eukaryotic host organisms

Type of silk protein**	Terminal* domains	M_W** [kDa]	Yield** [mg/L]	Spider**	Host organism	References
MA silk						
MaSp1	–	N/A	~300	*Nephila clavipes*	Yeast (*Pichia pastoris*)	(Fahnestock & Bedzyk, 1997)
	–	94	N/A	*Nephila clavipes*	Yeast (*Pichia pastoris*)	(Agapov et al., 2009; Bogush et al., 2009)
	–	64, 127	N/A	*Nephila clavipes*	Plants (*Arabidopsis thaliana*)	(Barr et al., 2004; Yang et al., 2005)
	–	13–100	80	*Nephila clavipes*	Plants (Tobacco: *Nicotiana tabacum*)	(Scheller & Conrad, 2005; Scheller et al., 2001, 2004)
	–	13–100	80	*Nephila clavipes*	Plants (Potato: *Solanum tuberosum*)	(Scheller & Conrad, 2005; Scheller et al., 2001, 2004)
	–	70	N/A	*Nephila clavata*	Insect cells (*Bombyx mori*)	(Zhang et al., 2008)
	–	70	6[†]	*Nephila clavata*	Transgenic animals (*Bombyx mori*)	(Zhang et al., 2008)
MaSp2	–	113	N/A	*Nephila madagascariensis*	Yeast (*Pichia pastoris*)	(Bogush et al., 2009)
	+CTD	65	N/A	*Nephila clavipes*	Plants (Tobacco: *Nicotiana tabacum*)	(Patel et al., 2007)

MaSp1 & MaSp2	+CTD	60	0.3–3[‡]	*Nephila clavipes*	Plants (Tobacco: *Nicotiana tabacum*)	(Menassa et al., 2004)
	–	50	N/A	*Nephila clavipes*	Transgenic animals (goat)	(Perez–Rigueiro et al., 2011)

Flagelliform

Flag	–	37	13.3	*Nephila clavipes*	Insect cells (*Bombyx mori*)	(Miao et al., 2006)

N/A

Amphiphilic silk-like protein	–	28–32	1–3 g/L	N/A	Yeast (*Pichia pastoris*)	(Werten et al., 2008)

*NTD: amino-terminal domain, CTD: carboxy-terminal domain.
**N/A: not applicable.
†6 mg/larva.
‡0.3–3 mg/kg of tissue.

many stress–response proteins were upregulated. In order to increase the yield of large recombinant glycine-rich proteins (100–285 kDa), the over-expression of glycyl-tRNA synthetase, as well as the elevation of meta-bolic pools of tRNA^{Gly} and glycine, was tested. By elevating the tRNA^{Gly} pool, an increased production of the 147–285 kDa proteins as well as an enhanced cell growth by 30–50% was observed (Xia et al., 2010). Addi-tionally, amongst addition of glycine to the expression medium, the inac-tivation of the glycine cleavage system and a glyA overexpression only the latter increased the yield of the largest proteins 10- to 35-fold (Xia et al., 2010). The produced proteins were purified by acidic precipitation of the cell lysate, followed by a fractional ammonium sulfate precipitation. After solubilizing the precipitated protein, dialysis and freeze drying, 1.2 g protein with a purity of ∼90% was obtained from 1 L of cell suspension from a high cell–density cultivation (Xia et al., 2010). The purified proteins were dissolved in hexafluoroisopropanol (HFIP), and a 20% (w/v) solution was spun into fibers. The obtained fibers showed a tenacity (508 ± 108 MPa), elongation (15 ± 5%) and Young's modulus (21 ± 4 GPa) similar to those of *N. clavipes* dragline silk fibers (740–1200 MPa; 18–27% and 11–14 GPa, respectively) (Xia et al., 2010). The attempt to spin fibers from a recombi-nant 377 kDa protein using the stated process failed, because not only the target protein but also several truncated forms were obtained after purification. It is assumed that this is caused by a limitation of the *E. coli* translational machinery (Xia et al., 2010).

3.1.2. *Salmonella typhimurium*

Apart from *E. coli*, other bacterial hosts have been tested for the recombinant silk production, as codon usage of different host organisms can be compared with increasing genomic's knowledge (Terpe, 2006). Other bacterial hosts, such as the gram-negative bacteria *S. typhimurium*, have some advantages over *E. coli*, since *S. typhimurium* has the capability to secrete proteins, which simplifies the isolation of the target silk protein from foreign proteins. For the large-scale production of recombinant spider silk proteins, secretion of the target proteins into the extracellular environment seems to be the feasible way, as no production limitations will be reached due to the lack of intracel-lular space of the host cells. In general, the secretion of recombinant proteins into the extracellular environment of gram-negative bacteria is difficult, as the proteins have to transfer through an inner and outer membrane. Further-more, due to its complexity, the underlying mechanism has not yet been fully understood (Harvey et al., 2004; Lee, Tullman–Ercek, & Georgiou, 2006).

Using *Salmonella* SPI-1 T3SS (Type III secretion system encoded on *Salmonella* Pathogenicity Island I), the secretion of recombinant proteins into the extracellular environment of the cells has been shown. SPI-1 T3SS forms needle-like structures that cross both the inner and outer membrane and allow secretion (Marlovits et al., 2006). The mechanism of the protein secretion through the needle into the extracellular environment is highly complex. It requires the co-expression of an amino-terminal peptide TAG, which is not cleaved after secretion, as well as a corresponding chaperone that targets the proteins to the SPI-1 T3SS and a chaperone-binding domain (CBD) (Galan & Collmer, 1999). In order to be able to cleave the amino-terminal TAG after the protein production, an additional cleavage site has to be included within the protein. In order to be able to transfer through the needle, the proteins must at least be partially unfolded due to the dimensions of the needle and have to refold outside of the cells (Widmaier et al., 2009). The amino-terminal TAG, the co-expression of the chaperones and CBD and the partial folding of the target proteins, complicates subsequent purification processes.

Based on the *A. diadematus* proteins ADF1, ADF2, and ADF3, synthetic genes were created that encode proteins (25–56 kDa), which were secreted to the extracellular environment (Widmaier et al., 2009). A tobacco etch virus (TEV) protease site was included following the amino-terminal TAG. Using different TAG/chaperone pairs in combination with the different recombinant proteins, the amount of totally secreted protein ranged between 0.7 and 14 mg/L after 8 h (Widmaier et al., 2009). A secretion efficiency of 7–14%, defined as the ratio of the secreted to the expressed protein, was obtained (Widmaier et al., 2009).

In an additional work, synthetic spider silk genes coding for fragments of *B. mori* cocoon silk proteins, *N. clavipes* flagelliform silk protein, *A. diadematus* ADF1, ADF2, ADF3 and ADF4 and *L. hesperus* MaSp1 were expressed using SPI-1 T3SS (Widmaier & Voigt, 2010). Whereas many of the tested proteins were produced, only a few were secreted into the extracellular environment. The degree of protein secretion was found to be dependent on the length of the recombinant silk protein. All proteins with less than 628 amino acids (including amino-terminal TAG and TEV-recognition site) were secreted, whereas only a fraction of proteins with up to 863 amino acids and no proteins over 863 amino acids were secreted. (Widmaier & Voigt, 2010).

3.1.3. Bacillus subtilis

The gram-positive bacteria *B. subtilis* was used for the recombinant production of spidroins, as it is able to secrete large quantities of the target protein

into the medium, but its secretion system is much simpler than those of yeasts and filamentous fungi (Fahnestock, Yao, & Bedzyk, 2000).

The production of consensus sequences of the repeating units from MaSp1 and MaSp2 of *N. clavipes* in this host organism has been published in a patent (Fahnestock, 1994), but information concerning the produced proteins such as the molecular weight, the obtained yield, and purity has not been published so far.

3.2. Yeast

The yeast *Pichia pastoris* is a promising alternative host organism to *E. coli*, because it is able to correctly process high molecular–weight proteins (Cregg, 2007). Proteins that could not be produced efficiently in bacteria, *Saccharomyces cerevisiae*, or other host organisms, have been successfully produced in *P. pastoris* (Cereghino, Cereghino, Ilgen, & Cregg, 2002). *Pichia pastoris* is a methylotrophic yeast that can use methanol as the sole carbon and energy source. Additionally, this organism is able to grow to high cell densities (>100 g/L dry cell mass) (Cereghino et al., 2002). Importantly, *P. pastoris* allows cytosolic as well as secretory protein production (Macauley-Patrick, Fazenda, McNeil, & Harvey, 2005).

Even upon the production of silk proteins in *P. pastoris*, a variety of protein sizes were obtained (Fahnestock & Bedzyk, 1997). This is due to *P. pastoris*' ability to integrate multiple gene copies into its genome. Because of the highly repetitive sequence of the recombinant spider silk genes, it is likely that the second insertion of a gene occurs at the repetitive region of the first inserted gene (Clare, Rayment, Ballantine, Sreekrishna, & Romanos, 1991; Fahnestock & Bedzyk, 1997), which leads to genes and subsequently to proteins with varying sizes.

An amphiphilic silk–like polymer named EL28 ($[(GA)_3GE(GA)_3GL]_{28}$; 32.4 kDa) and a nonamphiphilic silk–like polymer named EE24 ($[(GA)_3GE(GA)_3GE]_{24}$; 28.2 kDa) have been secreted using *P. pastoris*. These silk–like polymers were used to determine the usefulness of producing a pH–responsive surface active polymer in this host organism (Werten et al., 2008). The produced EE24 was purified by isoelectric precipitation, and remaining host proteins were removed by ethanol precipitation. Using this purification strategy, 3 g/L of 98% pure protein was obtained. The amphiphilic protein EL28 was purified by dissolving the protein precipitate in formic acid and a subsequent dilution with water, which resulted in a precipitation of the host proteins, whereas the target protein remained soluble for a while. This purification strategy yielded 1 g/L of a 98% pure protein

(Werten et al., 2008). The obtained 1–3 g/L of pure protein reflect high yields for *P. pastoris* (Cregg, Cereghino, Shi, & Higgins, 2000) as well as host organisms in general (Schmidt, 2004).

Further, two synthetic genes were created, based on nucleotide sequences of cDNA of *N. clavipes* (MaSp1) and *Nephila madagascariensis* (MaSp2). Both genes, which encode a 94 kDa and a 113 kDa protein, respectively, were subcloned and expressed in *P. pastoris* (Agapov et al., 2009; Bogush et al., 2009). The proteins were purified using cation exchange chromatography followed by dialysis and lyophylization. The purified proteins were processed into meshes by electrospinning, cast into thin films, and spun into fibers using wet-spinning. The fibers obtained by wet-spinning showed an elasticity of 5–15% and a tensile strength of 0.1–0.15 GPa (Bogush et al., 2009). Possible applications of the recombinant proteins include biomedical ones, such as drug delivery and tissue engineering (Bogush et al., 2009).

Fahnestock and Bedzyk (1997) created synthetic genes encoding mimicking sequences of the two dragline proteins MaSp1 and MaSp2 of *N. clavipes*. The proteins were purified from the cell lysate by acid and heat precipitation, followed by a step-wise $(NH_4)_2SO_4$ precipitation. Of the totally produced target protein (663 mg/L), 45% was obtained after purification (with 5% impurities). Immunoblotting revealed a protein ladder, probably due to internal deletions within the gene. The obtained proteins were spun into fibers under varying conditions, but the tensile strength of natural spider silk fibers could not be gained (Fahnestock et al., 2000). Using *P. pastoris* as a host organism for the recombinant spider silk protein production was included in the above mentioned patent (Fahnestock, 1994), but no further publications were made.

3.3. Plants

Introducing and expressing synthetic spider silk genes in transgenic plants is another promising approach in order to obtain large amounts of spider silk proteins, as plants are capable of producing foreign proteins on a large scale with lower costs than most other host organisms (Barr, Fahnestock, & Yang, 2004). Additionally, the production of recombinant spidroins in plants is easily scalable. By targeting recombinant proteins to cellular compartments, such as the endoplasmic reticulum (ER), vacuole, and apoplast (Conrad & Fiedler, 1998; Moloney & Holbrook, 1997), protein degradation can be prevented, and consequently higher yields can be achieved. Besides *Arabidopsis*, tobacco (*Nicotiana tabacum*) and potato (*Solanum tuberosum*) plants have been used as hosts for the production of spider silk proteins.

Disadvantages of this system are a more complicated genetic manipulation than for bacteria and longer generation intervals (Heim et al., 2009). Furthermore, only the production of recombinant spidroins with a molecular weight up to 100 kDa is reliable, as the underlying genes of larger proteins are prone to genetic rearrangements and multiple insertions of the target gene (Barr et al., 2004).

Synthetic genes that encode silk proteins based on sequences of MaSp1 of *N. clavipes* were expressed in the leaves and seeds of *Arabidopsis thaliana*, as well as somatic soybean embryos (Barr et al., 2004). A 64 kDa silk-like protein was produced successfully, whereas the production of a 127 kDa protein yielded not only the target protein but many smaller by-products as well, being caused by genetic rearrangements and multiple insertions of the target genes (Barr et al., 2004). Further, in contrast to the 64 kDa silk-like protein, the 127 kDa protein was not detectable in the somatic soybean embryos (Barr et al., 2004).

Targeting of these proteins to special cellular compartments, such as the ER and apoplasts in *Arabidopsis* leaves, increased protein yields 5-fold and 13-fold, respectively, as degradation is prevented. In *Arabidopsis* seeds, targeting the recombinant spidroins to the ER and vacuole increased the yield 7.8-fold and 5.4-fold, respectively (Yang, Barr, Fahnestock, & Liu, 2005).

Recombinant *N. clavipes* dragline proteins with a molecular weight of up to 100 kDa have been accumulated in the ER of tobacco (*N. tabacum*) and potato leaves (*S. tuberosum*), as well as in potato tubers (Menassa et al., 2004; Scheller, Guhrs, Grosse, & Conrad, 2001). The extraction of the pure recombinant protein yielded up to 3 mg protein per kg of tissue (Menassa et al., 2004). In order to simplify purification, hybrid systems of silk and another structural protein, namely elastin, have been developed. Synthetic elastin-like polypeptides, which comprise repeats of Val-Pro-Gly-Xaa-Gly (where Xaa can be any amino acid but proline), can undergo inverse temperature transition. Such synthetic polypeptide is soluble in water below 25 °C, but when the temperature is raised above 25 °C, the polypeptide aggregates, and phase separation occurs (Meyer & Chilkoti, 1999; Urry, Haynes, Zhang, Harris, & Prasad, 1988). By fusing such elastin-like domains to the target silk protein, selective precipitation can be achieved. The extraction of a spider silk–elastin fusion protein out of 1 kg of tobacco leaves yielded 80 mg of pure recombinant protein (Scheller & Conrad, 2005; Scheller, Henggeler, Viviani, & Conrad, 2004).

3.4. Insect Cells

Introducing foreign genes into higher organisms can be achieved through different procedures, such as the integration of the synthetic genes into

the chromosomal DNA or by transporting the target DNA into the cell, resulting in transient expression (Maeda, 1989). Since the transformation efficiency is low with both approaches, viruses are much more promising as a transporter, as they are extraordinarily efficient in transferring their own genome into foreign cells. Using the baculovirus as a vector has been widely used in the successful expression of target genes at high levels (Maeda, 1989). For this purpose, both *Autographa californica* nuclear polyhedrosis virus (AcNPV) (Pennock, Shoemaker, & Miller, 1984) and *B. mori* NPV (BmNPV)(Maeda et al., 1985) have been established. The use of BmNPV has several advantages, since the natural host of BmNPV is the silkworm *B. mori* (Maeda, 1989). Using the insect cells for the recombinant production of spider silk proteins has several advantages, one being that insects are phylogenetically closest related to spiders compared to other commonly used expression systems (Huemmerich, Scheibel, et al., 2004). In addition, translational stops or pauses, which result in truncated proteins, were not observed using insect cells as host organisms. Other advantages include high-expression efficiencies, low feeding costs, the capability to secrete proteins simplifying the purification, as well as the ability to posttranslationally modify the proteins (Heim et al., 2009; Miao et al., 2006).

Disadvantages include more complex cloning procedures and longer generation times compared to bacteria. In addition, some spider silk proteins formed aggregates in the cytosol of the cells, which complicates the purification and subsequently lowers the protein yield (Heim et al., 2009; Huemmerich, Scheibel, et al., 2004).

Using the baculovirus in combination with the insect cell line Sf9, derived from the fall armyworm *Spodoptera frugiperda* (Huemmerich, Scheibel, et al., 2004), partial cDNAs encoding 35–105 kDa MA spidroins from *A. diadematus* (ADF3 and/or ADF4 ± carboxy-terminal domains) have been expressed (Huemmerich, Scheibel, et al., 2004; Ittah, Barak, & Gat, 2010; Ittah, Cohen, Garty, Cohn, & Gat, 2006; Ittah, Michaeli, Goldblum, & Gat, 2007). In contrast to ADF3, which was soluble in the cytosol of the insect cell, ADF4 was insoluble and self-assembled into filaments. This difference is assumed to be based on different properties of the proteins, such as hydropathicity (Huemmerich, Scheibel, et al., 2004). Contrary to other expression systems, only few degradation products or smaller protein fragments were detected, which confirms that no translational pauses or stops take place.

The baculovirus expression system using AcNPV and the insect cell line Sf9 was employed to produce a 28 kDa *Araneus ventricosus* Flagelliform

protein (AvFlag), as well as a 61 kDa polyhedron–AvFlag fusion protein (Lee et al., 2007), but no information was given concerning the yield of the proteins.

The BmNPV expression system was used to produce a 37 kDa-recombinant spidroin based on the silk of *N. clavipes* in BmN cells (Miao et al., 2006). The target protein was purified from the BmN cell lysate by using Ni–NTA spin columns under denaturing conditions. Analysis of the eluted fractions showed the 37 kDa protein, as well as a 74 kDa protein, which is assumed to result from dimerization of the 37 kDa protein. The 37 kDa protein was obtained with yields of 13.3 mg/L (Miao et al., 2006). Information about chemical and structural characteristics of the produced protein has not been published so far.

3.5. Mammalian Cells

When producing recombinant spider silk proteins in different host organisms, truncated synthesis especially of high molecular weight proteins is the limiting factor. In order to overcome this limitation, mammalian cells were used (Grip et al., 2006; Lazaris et al., 2002). Additionally, mammalian cells are capable of secreting the produced proteins, which simplifies purification and enables higher protein yields.

Even though mammalian cells are able to produce larger proteins than bacteria, problems with the transcription and translation of the highly repetitive spider silk genes have been reported (Grip et al., 2006). Inefficient transcription due to the secondary structure of the mRNA, low copy number transfection of the target constructs and limitations of the cell's translational machinery were listed as possible reasons for the low expression levels. Aggregation of the produced proteins and insufficient secretion of large proteins were stated as reasons for the low protein yield (Grip et al., 2006; Lazaris et al., 2002).

Bovine mammary epithelial alveolar (MAC-T) and baby hamster kidney (BHK) cells have been tested for the expression of spider dragline silk cDNAs from two spider species, ADF3 from *A. diadematus* and MaSp1 and MaSp2 from *N. clavipes*, (molecular weights ranging from 60 kDa to 140 kDa)(Lazaris et al., 2002). Even though 110 and 140 kDa proteins were secreted to the extracellular environment, their yields in BHK cells were much lower than that of the 60 kDa protein.

Different constructs of a partial cDNA fragment of MaSp1 of *Euprosthenops* sp. were expressed in mammalian cells (COS-1) in order to provide recombinant spider silk proteins as a biomaterial for bone

replacement after tumor surgery. With this approach, low expression levels were obtained caused by the above stated reasons (Grip et al., 2006).

3.6. Transgenic Animals

Transgenic animals have also been tested for the production of recombinant spider silk proteins. Advantages are possible PTMs and secretion into the milk or urine of transgenic goats and mice, which enables protein production for long time intervals, thus gaining a higher protein yield (Heim et al., 2009; Karatzas, Turner, & Karatzas, 1999). Additionally, the produced proteins can be directly spun as fibers as in the case of transgenic silkworms (Wen et al., 2010).

The process of using transgenic mammals for recombinant spider silk production has been patented (Karatzas et al., 1999). Importantly, there are a lot of disadvantages of such system that have to be considered. Firstly, the creation of transgenic mammals is very time-consuming and complex. Secondly, obtaining the spider silk proteins that were secreted into the milk of goats and mice is challenging, as the spider silk proteins have to be separated from milk caseins, and especially mice only produce a small amount of milk (Heim et al., 2009; Xu et al., 2007).

3.6.1. Transgenic Silkworms

Using a Bac-to-Bac/BmNPV Baculovirus expression system, a 70 kDa-fusion protein consisting of a recombinant spidroin (MaSp1) from *Nephila clavata*, fused to EGFP, was co-produced with silk fibroin in BmN cells as well as in the transgenic silkworm larva (Zhang et al., 2008). As 60% of the produced fusion protein was found to be insoluble, and the silkworm was not able to assemble the spider silk proteins into fibers, this approach is not feasible to obtain large amount of spider silk proteins. In order to overcome these difficulties, transgenic silkworms were created that produce a chimeric silkworm and spider silk protein (Chung, Kim, & Lee, 2012). Using this approach, composite silk fibers can be obtained, which are tougher than the parental silkworm silk fibers, and that are mechanically comparable to natural MA spider silk fibers (Teule et al., 2012).

In another approach, a vector was created that carries a partial cDNA encoding MaSp1 (83 kDa) of *N. clavata* under the sericin promoter (Ser1) (Wen et al., 2010). Transgenic silkworms grown from eggs that were injected with the altered vector spun a cocoon that contained recombinant spider silk that was located in the sericin layer of the original silkworm silk. A comparison of the mechanical properties of wild-type silkworm

silk with transgenic silkworm silk and natural spider silk showed that the silk from the transgenic silkworm (18.5% elasticity, 660 MPa tensile strength) was superior to natural silkworm silk (15.3% elasticity, 564 MPa tensile strength) but did not reach the extraordinary properties of natural spider silk fibers (30% elasticity, 1300 MPa tensile strength)(Wen et al., 2010).

3.6.2. Transgenic Mice and Goats

Transgenic mice have been used to express synthetic genes based on the partial cDNA of the MaSp1/MaSp2 dragline proteins from *N. clavipes*. It was found that some mice produced a 55 kDa target protein, whereas other mice produced inhomogenous proteins with molecular weights of 31, 45, and 66 kDa. The different molecular weights are assumed to be caused by an error during protein synthesis. Yields of up to 11.7 mg/L were obtained, and the synthetic genes were stably transmitted to the mice's offspring (Xu et al., 2007).

Two recombinant 50 kDa proteins, whose encoding DNA is based on the genes of MaSp1 and MaSp2 of *N. clavipes*, were produced in the milk of transgenic goats. These proteins were purified by tangential flow filtration and chromatography, followed by alcohol precipitation. The purity of the obtained proteins was >95%. Four different w/w–ratios of the two proteins (100:0, 70:30, 30:70, 0:100 (% MaSp1 analog − % MaSp2 analog)) were solved in hexafluoroisopropanol (HFIP) to prepare individual spinning dopes. By extruding the spinning dope into a 2-propanol coagulation bath followed by post-spin drawing, recombinant fibers were produced. It was shown that the tensile strength of the artificial fibers made from all dopes (280–350 MPa) were considerably lower than that of the natural spider silk fibers (1800 MPa), whereas their elasticities were in the same range (30–40% for artificial and 26% for natural spider silk fibers) (Perez-Rigueiro et al., 2011).

4. CONCLUSION AND OUTLOOK

Natural spider silk fibers have outstanding mechanical properties with a combination of stability and extensibility resulting in a toughness accomplished by no other fibrous material. Due to its extraordinary properties, spider silk is eligible to be used in various textile, automotive, and medical engineering applications.

The biotechnological production of spider silk proteins is essential in order to investigate and to employ them for applications, because in contrast

to the silkworm *B. mori*, the spider's aggressive territorial behavior and its cannibalism render their farming not feasible. The expression of partial cDNAs in different host organisms (Table 4.3) has only led to limited success (protein yields: 4–50 mg/L), as differences in the codon usages cause inefficient translations, and the highly repetitive nature of spider silk genes impedes its gene manipulation and amplification (Heim et al., 2009; Scheibel, 2004).

In order to overcome these problems, synthetic genes were produced encoding proteins differing from the natural spider silk proteins but possessing their key features. The expression of synthetic spider silk genes in different host organisms resulted in protein yields ranging from 2 mg/L (Bini et al., 2006) to 300 mg/L (Fahnestock & Bedzyk, 1997), with one exception of 3 g/L (Werten et al., 2008). Common problems are inefficient transcription due to the secondary structure of the mRNA and limitations of the cells' translational machinery, such as depletion of tRNA pools due to the highly repetitive nature of the spider silk genes. Heterologous proteins caused by truncations and gene instability are more pronounced in prokaryotes, but occur in eukaryotes as well, a problem rising with increasing molecular weights of the proteins. Secretion of the produced proteins into the extracellular environment simplifies the purification and results in higher yields, but as the underlying mechanism is more complex than that of cytosolic production, this system is more time-consuming and more prone to errors.

For many applications, using *E. coli* as a host organism for the recombinant spider silk protein production seems most promising, as the simple genetic manipulation and the short generation times enable fast adjustments. For biomedical applications such as tissue engineering and drug delivery, the engineered spider silk proteins are processed mostly into films (Slotta et al., 2006; Wohlrab et al., 2012), nonwovens (Leal-Egana et al., 2012), hydrogels (Schacht & Scheibel, 2011), and particles (Lammel, Hu, Park, Kaplan, & Scheibel, 2010). In contrast to fibers, where the molecular weight has a decisive influence on the properties concerning both the processing of the proteins and the fabricated fiber, the molecular weight contributes little to the properties of these morphologies.

Until today, recombinant spider silk proteins produced by metabolically engineered *E. coli* or transgenic goats were spun into fibers with mechanical properties, that were similar but still lower than those of natural spider silk fibers. Therefore, gaining artificial silk fibers with mechanical properties as found as in nature still remains the holy grail of silk research.

ACKNOWLEDGMENTS

REFERENCES

Agapov, II, Pustovalova, O. L., Moisenovich, M. M., Bogush, V. G., Sokolova, O. S., Sevastyanov, V. I., et al. (2009). Three-dimensional scaffold made from recombinant spider silk protein for tissue engineering. *Doklady Biochemistry and Biophysics*, *426*, 127–130.

Andersen, S. O. (1970). Amino acid composition of spider silks. *Comparative Biochemistry and Physiology*, *35*, 705–711.

Ap Rhisiart, A., & Vollrath, F. (1994). Design features of the orb web of the spider, *Araneus diadematus*. *Behavioral Ecology*, *5*, 280–287.

Arcidiacono, S., Mello, C. M., Butler, M., Welsh, E., Soares, J. W., Allen, A., et al. (2002). Aqueous processing and fiber spinning of recombinant spider silks. *Macromolecules*, *35*, 1262–1266.

Arcidiacono, S., Mello, C., Kaplan, D., Cheley, S., & Bayley, H. (1998). Purification and characterization of recombinant spider silk expressed in *Escherichia coli*. *Applied Microbiology and Biotechnology*, *49*, 31–38.

Asakura, T., Kuzuhara, A., Tabeta, R., & Saito, H. (1985). Conformation characterization of *Bombyx mori* silk fibroin in the solid state by high-frequency C-13 cross polarization-magic angle spinning NMR, X-ray diffraction, and infrared spectroscopy. *Macromolecules*, *18*, 1841–1845.

Askarieh, G., Hedhammar, M., Nordling, K., Saenz, A., Casals, C., Rising, A., et al. (2010). Self-assembly of spider silk proteins is controlled by a pH-sensitive relay. *Nature*, *465*, 236–238.

Augsten, K., Muhlig, P., & Herrmann, C. (2000). Glycoproteins and skin-core structure in *Nephila clavipes* spider silk observed by light and electron microscopy. *Scanning*, *22*, 12–15.

Augsten, K., Weisshart, K., Sponner, A., & Unger, E. (1999). Glycoproteins and skin-core structure in *Nephila clavipes* spider silk observed by light- and electron microscopy. *Scanning*, *21*, 77.

Ayoub, N. A., Garb, J. E., Tinghitella, R. M., Collin, M. A., & Hayashi, C. Y. (2007). Blueprint for a high-performance biomaterial: full-length spider dragline silk genes. *PLoS ONE*, *2*, e514.

Barghout, J. Y. J., Thiel, B. L., & Viney, C. (1999). Spider (*Araneus diadematus*) cocoon silk: a case of non-periodic lattice crystals with a twist? *International Journal of Biological Macromolecules*, *24*, 211–217.

Barr, L. A., Fahnestock, S. R., & Yang, J. J. (2004). Production and purification of recombinant DP1B silk-like protein in plants. *Molecular Breeding*, *13*, 345–356.

Becker, N., Oroudjev, E., Mutz, S., Cleveland, J. P., Hansma, P. K., Hayashi, C. Y., et al. (2003). Molecular nanosprings in spider capture-silk threads. *Nature Materials*, *2*, 278–283.

Bini, E., Foo, C. W., Huang, J., Karageorgiou, V., Kitchel, B., & Kaplan, D. L. (2006). RGD-functionalized bioengineered spider dragline silk biomaterial. *Biomacromolecules*, *7*, 3139–3145.

Bini, E., Knight, D. P., & Kaplan, D. L. (2004). Mapping domain structures in silks from insects and spiders related to protein assembly. *Journal of Molecular Biology*, *335*, 27–40.

Bittencourt, D., Souto, B. M., Verza, N. C., Vineck, F., Dittmar, K., Silva, P. I., et al. (2007). Spidroins from the Brazilian spider *Nephilengys cruentata* (Araneae: nephilidae). *Comparative Biochemistry and Physiology. Part B, Biochemistry & Molecular Biology*, *147*, 597–606.

Blackledge, T. A., & Hayashi, C. Y. (2006). Silken toolkits: biomechanics of silk fibers spun by the orb web spider *Argiope argentata* (Fabricius 1775). *Journal of Experimental Biology*, *209*, 2452–2461.

Blackledge, T. A., Summers, A. P., & Hayashi, C. Y. (2005). Gumfooted lines in black widow cobwebs and the mechanical properties of spider capture silk. *Zoology*, *108*, 41–46.

Bogush, V. G., Sokolova, O. S., Davydova, L. I., Klinov, D. V., Sidoruk, K. V., Esipova, N. G., et al. (2009). A novel model system for design of biomaterials based on recombinant analogs of spider silk proteins. *Journal of Neuroimmune Pharmacology*, *4*, 17–27.

Bon, M. (1710). A discourse upon the usefulness of the silk of spiders. *Philosophical Transactions*, *27*, 2–16.

Brooks, A. E., Nelson, S. R., Jones, J. A., Koenig, C., Hinman, M., Stricker, S., et al. (2008). Distinct contributions of model MaSp1 and MaSp2 like peptides to the mechanical properties of synthetic major ampullate silk fibers as revealed in silico. *Nanotechnology, Science and Applications*, *1*, 9–16.

Brooks, A. E., Steinkraus, H. B., Nelson, S. R., & Lewis, R. V. (2005). An investigation of the divergence of major ampullate silk fibers from *Nephila clavipes* and *Argiope aurantia*. *Biomacromolecules*, *6*, 3095–3099.

Brooks, A. E., Stricker, S. M., Joshi, S. B., Kamerzell, T. J., Middaugh, C. R., & Lewis, R. V. (2008). Properties of synthetic spider silk fibers based on *Argiope aurantia* MaSp2. *Biomacromolecules*, *9*, 1506–1510.

Candelas, G. C., & Cintron, J. (1981). A spider fibroin and its synthesis. *Journal of Experimental Zoology*, *216*, 1–6.

Cappello, J., & Crissman, J. W. (1990). The design and production of bioactive protein polymers for biomedical applications. *Abstracts of Papers of the American Chemical Society*, *199*, 66.

Cappello, J., Crissman, J., Dorman, M., Mikolajczak, M., Textor, G., Marquet, M., et al. (1990). Genetic engineering of structural protein polymers. *Biotechnology Progress*, *6*, 198–202.

Cereghino, G. P., Cereghino, J. L., Ilgen, C., & Cregg, J. M. (2002). Production of recombinant proteins in fermenter cultures of the yeast *Pichia pastoris*. *Current Opinion in Biotechnology*, *13*, 329–332.

Challis, R. J., Goodacre, S. L., & Hewitt, G. M. (2006). Evolution of spider silks: conservation and diversification of the C-terminus. *Insect Molecular Biology*, *15*, 45–56.

Chung, H., Kim, T. Y., & Lee, S. Y. (2012). Recent advances in production of recombinant spider silk proteins. *Current Opinion in Biotechnology*, *23*, 1–8.

Clare, J. J., Rayment, F. B., Ballantine, S. P., Sreekrishna, K., & Romanos, M. A. (1991). High-level expression of tetanus toxin fragment C in *Pichia pastoris* strains containing multiple tandem integrations of the gene. *Biotechnology*, *9*, 455–460.

Colgin, M. A., & Lewis, R. V. (1998). Spider minor ampullate silk proteins contain new repetitive sequences and highly conserved non-silk-like "spacer regions". *Protein Science*, *7*, 667–672.

Conrad, U., & Fiedler, U. (1998). Compartment-specific accumulation of recombinant immunoglobulins in plant cells: an essential tool for antibody production and immunomodulation of physiological functions and pathogen activity. *Plant Molecular Biology*, *38*, 101–109.

Craig, C. L., Riekel, C., Herberstein, M. E., Weber, R. S., Kaplan, D., & Pierce, N. E. (2000). Evidence for diet effects on the composition of silk proteins produced by spiders. *Molecular Biology and Evolution*, *17*, 1904–1913.

Cregg, J. M. (Ed.), (2007). *Pichia protocols*. Totowa, New Jersey: Humana Press Inc.

Cregg, J. M., Cereghino, J. L., Shi, J. Y., & Higgins, D. R. (2000). Recombinant protein expression in *Pichia pastoris*. *Molecular Biotechnology*, *16*, 23–52.

Dicko, C., Knight, D., Kenney, J. M., & Vollrath, F. (2004). Secondary structures and conformational changes in flagelliform, cylindrical, major, and minor ampullate silk proteins. Temperature and concentration effects. *Biomacromolecules*, *5*, 2105–2115.

Eisoldt, L., Hardy, J. G., Heim, M., & Scheibel, T. R. (2010). The role of salt and shear on the storage and assembly of spider silk proteins. *Journal of Structural Biology*, *170*, 413–419.

Eisoldt, L., Smith, A. & Scheibel, T. (2011). Decoding the secrets of spider silk. *Materials Today*, *14*, 80–86.

Eisoldt, L., Thamm, C., & Scheibel, T. (2011). The role of terminal domains during storage and assembly of spider silk proteins. *Biopolymers*, *97*, 355–361.

Exler, J. H., Hummerich, D., & Scheibel, T. (2007). The amphiphilic properties of spider silks are important for spinning. *Angewandte Chemie International Edition*, *46*, 3559–3562.

Fahnestock, S. (1994). In W. E. I. DuPont (Ed.), *Novel, recombinantly produced spider silk analogs*. USA, int. patent number: WO 94/29450.

Fahnestock, S. R., & Bedzyk, L. A. (1997). Production of synthetic spider dragline silk protein in *Pichia pastoris*. *Applied Microbiology and Biotechnology*, *47*, 33–39.

Fahnestock, S. R., & Irwin, S. L. (1997). Synthetic spider dragline silk proteins and their production in *Escherichia coli*. *Applied Microbiology and Biotechnology*, *47*, 23–32.

Fahnestock, S. R., Yao, Z., & Bedzyk, L. A. (2000). Microbial production of spider silk proteins. *Journal of Biotechnology*, *74*, 105–119.

Fox, L. R. (1975). Cannibalism in natural populations. *Annual Review of Ecology and Systematics*, *6*, 87–106.

Fukushima, Y. (1998). Genetically engineered syntheses of tandem repetitive polypeptides consisting of glycine-rich sequence of spider dragline silk. *Biopolymers*, *45*, 269–279.

Galan, J. E., & Collmer, A. (1999). Type III secretion machines: bacterial devices for protein delivery into host cells. *Science*, *284*, 1322–1328.

Garb, J. E., & Hayashi, C. Y. (2005). Modular evolution of egg case silk genes across orb-weaving spider superfamilies. *Proceedings of the National Academy of Sciences of the United States of America*, *102*, 11379–11384.

Gellissen, G., Melber, K., Janowicz, Z. A., Dahlems, U. M., Weydemann, U., Piontek, M., et al. (1992). Heterologous protein production in yeast. *Antonie Van Leeuwenhoek International Journal of General and Molecular Microbiology*, *62*, 79–93.

Gerritsen, V. B. (2002). The tiptoe of an airbus. *Protein Spotlight, Swiss Prot*, *24*, 1–2.

Geurts, P., Zhao, L., Hsia, Y., Gnesa, E., Tang, S., Jeffery, F., et al. (2010). Synthetic spider silk fibers spun from pyriform spidroin 2, a glue silk protein discovered in orb-weaving spider attachment discs. *Biomacromolecules*, *11*, 3495–3503.

Gnesa, E., Hsia, Y., Yarger, J. L., Weber, W., Lin-Cereghino, J., Lin-Cereghino, G., et al. (2012). Conserved C-terminal domain of spider tubuliform spidroin 1 contributes to extensibility in synthetic fibers. *Biomacromolecules*, *13*, 304–312.

Gosline, J. M., Denny, M. W., & DeMont, M. E. (1984). Spider silk as rubber. *Nature*, *309*, 551–552.

Gosline, J. M., Guerette, P. A., Ortlepp, C. S., & Savage, K. N. (1999). The mechanical design of spider silks: from fibroin sequence to mechanical function. *Journal of Experimental Biology*, *202*, 3295–3303.

Gosline, J., Lillie, M., Carrington, E., Guerette, P., Ortlepp, C., & Savage, K. (2002). Elastic proteins: biological roles and mechanical properties. *Philosophical Transactions of the Royal Society of London. Series B, Biological Sciences*, *357*, 121–132.

Gosline, J. M., Pollak, C. C., Guerette, P. A., Cheng, A., DeMont, M. E., & Denny, M. W. (1993). Elastomeric network models for the frame and viscid silks from the orb web of the spider *Araneus diadematus*. *Silk Polymers*, *544*, 328–341.

Grip, S., Rising, A., Nimmervoll, H., Storckenfeldt, E., Mcqueen-Mason, S. J., Pouchkina-Stantcheva, N., et al. (2006). Transient expression of a major ampullate spidroin 1 gene fragment from *Euprosthenops* sp. in mammalian cells. *Cancer Genomics & Proteomics*, *3*, 83–87.

Guerette, P. A., Ginzinger, D. G., Weber, B. H., & Gosline, J. M. (1996). Silk properties determined by gland-specific expression of a spider fibroin gene family. *Science*, *272*, 112–115.

Hagn, F., Eisoldt, L., Hardy, J. G., Vendrely, C., Coles, M., Scheibel, T., et al. (2010). A conserved spider silk domain acts as a molecular switch that controls fibre assembly. *Nature*, *465*, 239–242.

Hagn, F., Thamm, C., Scheibel, T., & Kessler, H. (2010). pH-dependent dimerization and salt-dependent stabilization of the N-terminal domain of spider dragline silk – implications for fiber formation. *Angewandte Chemie International Edition*, *49*, 1–5.

Hajer, J., & Rehakova, D. (2003). Spinning activity of the spider *Trogloneta granulum* (Araneae, Mysmenidae): web, cocoon, cocoon handling behaviour, draglines and attachment discs. *Zoology*, *106*, 223–231.

Hardy, J. G., & Scheibel, T. R. (2009). Silk-inspired polymers and proteins. *Biochemical Society Transactions*, *37*, 677–681.

Harvey, B. R., Georgiou, G., Hayhurst, A., Jeong, K. J., Iverson, B. L., & Rogers, G. K. (2004). Anchored periplasmic expression, a versatile technology for the isolation of high-affinity antibodies from *Escherichia coli*-expressed libraries. *Proceedings of the National Academy of Sciences of the United States of America*, *101*, 9193–9198.

Hawthorn, A. C., & Opell, B. D. (2002). Evolution of adhesive mechanisms in cribellar spider prey capture thread: evidence for van der Waals and hygroscopic forces. *Biological Journal of the Linnean Society*, 77, 1–8.

Hawthorn, A. C., & Opell, B. D. (2003). Van der Waals and hygroscopic forces of adhesion generated by spider capture threads. *Journal of Experimental Biology*, *206*, 3905–3911.

Hayashi, C. Y., Blackledge, T. A., & Lewis, R. V. (2004). Molecular and mechanical characterization of aciniform silk: uniformity of iterated sequence modules in a novel member of the spider silk fibroin gene family. *Molecular Biology and Evolution*, *21*, 1950–1959.

Hayashi, C. Y., & Lewis, R. V. (1998). Evidence from flagelliform silk cDNA for the structural basis of elasticity and modular nature of spider silks. *Journal of Molecular Biology*, *275*, 773–784.

Hayashi, C. Y., Shipley, N. H., & Lewis, R. V. (1999). Hypotheses that correlate the sequence, structure, and mechanical properties of spider silk proteins. *International Journal of Biological Macromolecules*, *24*, 271–275.

Hedhammar, M., Rising, A., Grip, S., Martinez, A. S., Nordling, K., Casals, C., et al. (2008). Structural properties of recombinant nonrepetitive and repetitive parts of major ampullate spidroin 1 from *Euprosthenops australis*: implications for fiber formation. *Biochemistry*, *47*, 3407–3417.

Heim, M., Ackerschott, C. B., & Scheibel, T. (2010). Characterization of recombinantly produced spider flagelliform silk domains. *Journal of Structural Biology*, *170*, 420–425.

Heim, M., Keerl, D., & Scheibel, T. (2009). Spider silk: from soluble protein to extraordinary fiber. *Angewandte Chemie International Edition*, *48*, 3584–3596.

Hijirida, D. H., Do, K. G., Michal, C., Wong, S., Zax, D., & Jelinski, L. W. (1996). 13C NMR of *Nephila clavipes* major ampullate silk gland. *Biophysical Journal*, *71*, 3442–3447.

Hinman, M. B., & Lewis, R. V. (1992). Isolation of a clone encoding a second dragline silk fibroin. *Nephila clavipes* dragline silk is a two-protein fiber. *Journal of Biological Chemistry*, *267*, 19320–19324.

Holland, C., Terry, A. E., Porter, D., & Vollrath, F. (2007). Natural and unnatural silks. *Polymer*, *48*, 3388–3392.

Huang, W., Lin, Z., Sin, Y. M., Li, D., Gong, Z., & Yang, D. (2006). Characterization and expression of a cDNA encoding a tubuliform silk protein of the golden web spider *Nephila antipodiana*. *Biochimie*, *88*, 849–858.

Huang, J., Wong, C., George, A., & Kaplan, D. L. (2007). The effect of genetically engineered spider silk-dentin matrix protein 1 chimeric protein on hydroxyapatite nucleation. *Biomaterials*, *28*, 2358–2367.

Huemmerich, D., Helsen, C. W., Quedzuweit, S., Oschmann, J., Rudolph, R., & Scheibel, T. (2004). Primary structure elements of spider dragline silks and their contribution to protein solubility. *Biochemistry*, *43*, 13604–13612.

Huemmerich, D., Scheibel, T., Vollrath, F., Cohen, S., Gat, U., & Ittah, S. (2004). Novel assembly properties of recombinant spider dragline silk proteins. *Current Biology*, *14*, 2070–2074.

Huemmerich, D., Slotta, U., & Scheibel, T. (2006). Processing and modification of films made from recombinant spider silk proteins. *Applied Physics. A, -Materials Science & Processing*, *82*, 219–222.

Hu, X. Y., Kohler, K., Falick, A. M., Moore, A. M.F., Jones, P. R., Sparkman, O. D., et al. (2005). Egg case protein-1-A new class of silk proteins with fibroin-like properties from the spider *Latrodectus hesperus*. *Journal of Biological Chemistry*, *280*, 21220–21230.

Hu, X., Kohler, K., Falick, A. M., Moore, A. M., Jones, P. R., & Vierra, C. (2006). Spider egg case core fibers: trimeric complexes assembled from TuSp1, ECP-1, and ECP-2. *Biochemistry*, *45*, 3506–3516.

Hu, X. Y., Lawrence, B., Kohler, K., Falick, A. M., Moore, A. M.F., McMullen, E., et al. (2005). Araneoid egg case silk: a fibroin with novel ensemble repeat units from the black widow spider, *Latrodectus hesperus*. *Biochemistry*, *44*, 10020–10027.

Hurley, J. H., Mason, D. A., & Matthews, B. W. (1992). Flexible-geometry conformational energy maps for the amino acid residue preceding a proline. *Biopolymers*, *32*, 1443–1446.

Hu, X., Vasanthavada, K., Kohler, K., McNary, S., Moore, A. M., & Vierra, C. A. (2006). Molecular mechanisms of spider silk. *Cellular and Molecular Life Sciences*, *63*, 1986–1999.

Hu, X. Y., Yuan, J., Wang, X. D., Vasanthavada, K., Falick, A. M., Jones, P. R., et al. (2007). Analysis of aqueous glue coating proteins on the silk fibers of the cob weaver, *Latrodectus hesperus*. *Biochemistry*, *46*, 3294–3303.

Iridag, Y., & Kazanci, M. (2006). Preparation and characterization of *Bombyx mori* silk fibroin and wool keratin. *Journal of Applied Polymer Science*, *100*, 4260–4264.

Ito, H., Muraoka, Y., Yamazaki, T., Imamura, T., Mori, H., Ichida, M., et al. (1995). Structure and chemical composition of silk proteins in relation to silkworm diet. *Textile Research Journal*, *65*, 755–759.

Ittah, S., Barak, N., & Gat, U. (2010). A proposed model for dragline spider silk self-assembly: insights from the effect of the repetitive domain size on fiber properties. *Biopolymers*, *93*, 458–468.

Ittah, S., Cohen, S., Garty, S., Cohn, D., & Gat, U. (2006). An essential role for the C-terminal domain of a dragline spider silk protein in directing fiber formation. *Biomacromolecules*, *7*, 1790–1795.

Ittah, S., Michaeli, A., Goldblum, A., & Gat, U. (2007). A model for the structure of the C-terminal domain of dragline spider silk and the role of its conserved cysteine. *Biomacromolecules*, *8*, 2768–2773.

Jackson, C., & O'Brien, J. P. (1995). Molecular weight distribution of *Nephila clavipes* dragline silk. *Macromolecules*, *28*, 5975–5977.

Jelinski, L. W., Blye, A., Liivak, O., Michal, C., LaVerde, G., Seidel, A., et al. (1999). Orientation, structure, wet-spinning, and molecular basis for supercontraction of spider dragline silk. *International Journal of Biological Macromolecules*, *24*, 197–201.

Karatzas, C. N., Turner, J. D., & Karatzas, A.-L. (1999). Production of biofilaments in transgenic animals. *Canada*, int. patent number: WO 99/47661.

Knight, D., & Vollrath, F. (1999). Hexagonal columnar liquid crystal in the cells secreting spider silk. *Tissue & Cell*, *31*, 617–620.

Knight, D. P., & Vollrath, F. (2001). Changes in element composition along the spinning duct in a *Nephila* spider. *Naturwissenschaften*, *88*, 179–182.

Kohler, K., Thayer, W., Le, T., Sembhi, A., Vasanthavada, K., Moore, A. M. F., et al. (2005). Characterization of a novel class II bHLH transcription factor from the black widow spider, *Latrodectus hesperus*, with silk-gland restricted patterns of expression. *DNA and Cell Biology*, *24*, 371–380.

Kovoor, J., & Zylberberg, L. (1980). Fine structural aspects of silk secretion in a spider (*Araneus diadematus*). I. Elaboration in the pyriform glands. *Tissue Cell*, *12*, 547–556.

Kukuruzinska, M. A., & Lennon, K. (1998). Protein N-glycosylation: molecular genetics and functional significance. *Critical Reviews in Oral Biology and Medicine*, *9*, 415–448.

La Mattina, C., Reza, R., Hu, X., Falick, A. M., Vasanthavada, K., McNary, S., et al. (2008). Spider minor ampullate silk proteins are constituents of prey wrapping silk in the cob weaver *Latrodectus hesperus*. *Biochemistry*, *47*, 4692–4700.

Lammel, A. S., Hu, X., Park, S. H., Kaplan, D. L., & Scheibel, T. R. (2010). Controlling silk fibroin particle features for drug delivery. *Biomaterials*, *31*, 4583–4591.

Lazaris, A., Arcidiacono, S., Huang, Y., Zhou, J. F., Duguay, F., Chretien, N., et al. (2002). Spider silk fibers spun from soluble recombinant silk produced in mammalian cells. *Science*, *295*, 472–476.

Leal-Egana, A., Lang, G., Mauerer, C., Wickinghoff, J., Weber, M., Geimer, S., et al. (2012). Interactions of fibroblasts with different morphologies made of an engineered spider silk protein. *Advanced Engineering Materials*, *14*, B67–B75.

Lee, K. S., Kim, B. Y., Je, Y. H., Woo, S. D., Sohn, H. D., & Jin, B. R. (2007). Molecular cloning and expression of the C-terminus of spider flagelliform silk protein from *Araneus ventricosus*. *Journal of Biosciences*, *32*, 705–712.

Lee, P. A., Tullman-Ercek, D., & Georgiou, G. (2006). The bacterial twin-arginine translocation pathway. *Annual Review of Microbiology*, *60*, 373–395.

Lewis, R. V., Hinman, M., Kothakota, S., & Fournier, M. J. (1996). Expression and purification of a spider silk protein: a new strategy for producing repetitive proteins. *Protein Expression and Purification*, 7, 400–406.

Liebmann, B., Huemmerich, D., Scheibel, T., & Fehr, M. (2008). Formulation of poorly water-soluble substances using self-assembling spider silk protein. *Colloids and Surfaces. A, Physicochemical and Engineering Aspects*, *331*, 126–132.

Liivak, O., Blye, A., Shah, N., & Jelinski, L. W. (1998). A microfabricated wet-spinning apparatus to spin fibers of silk proteins. Structure–property correlations. *Macromolecules*, *31*, 2947–2951.

Lin, Z., Huang, W., Zhang, J., Fan, J. S., & Yang, D. (2009). Solution structure of eggcase silk protein and its implications for silk fiber formation. *Proceedings of the National Academy of Sciences of the United States of America*, *106*, 8906–8911.

Liu, Y., Shao, Z., & Vollrath, F. (2005). Relationships between supercontraction and mechanical properties of spider silk. *Nature Materials*, *4*, 901–905.

Liu, Y., Shao, Z., & Vollrath, F. (2008). Elasticity of spider silks. *Biomacromolecules*, *9*, 1782–1786.

Liu, Y., Sponner, A., Porter, D., & Vollrath, F. (2008). Proline and processing of spider silks. *Biomacromolecules*, *9*, 116–121.

Lombardi, S. J., & Kaplan, D. L. (1990). The amino-acid-composition of major ampullate gland silk (dragline) of *Nephila clavipes* (Araneae, Tetragnathidae). *Journal of Arachnology*, *18*, 297–306.

Macauley-Patrick, S., Fazenda, M. L., McNeil, B., & Harvey, L. M. (2005). Heterologous protein production using the *Pichia pastoris* expression system. *Yeast*, *22*, 249–270.

Madsen, B., Shao, Z. Z., & Vollrath, F. (1999). Variability in the mechanical properties of spider silks on three levels: interspecific, intraspecific and intraindividual. *International Journal of Biological Macromolecules*, *24*, 301–306.

Maeda, S. (1989). Expression of foreign genes in insects using baculovirus vectors. *Annual Review of Entomology*, *34*, 351–372.

Maeda, S., Kawai, T., Obinata, M., Fujiwara, H., Horiuchi, T., Saeki, Y., et al. (1985). Production of human alpha-interferon in silkworm using a baculovirus vector. *Nature*, *315*, 592–594.

Marlovits, T. C., Kubori, T., Lara-Tejero, M., Thomas, D., Unger, V. M., & Galan, J. E. (2006). Assembly of the inner rod determines needle length in the type III secretion injectisome. *Nature*, *441*, 637–640.

Marsano, E., Corsini, P., Arosio, C., Boschi, A., Mormino, M., & Freddi, G. (2005). Wet spinning of *Bombyx mori* silk fibroin dissolved in N-methyl morpholine N-oxide and properties of regenerated fibres. *International Journal of Biological Macromolecules*, *37*, 179–188.

Matsumoto, K., Uejima, H., Iwasaki, T., Sano, Y., & Sumino, H. (1996). Studies on regenerated protein fibers. 3. Production of regenerated silk fibroin fiber by the self-dialyzing wet spinning method. *Journal of Applied Polymer Science*, *60*, 503–511.

Mello, C. M., Senecal, B., Yeung, B., Vouros, P., & Kaplan, D. L. (1994). Initial characterization of *Nephila clavipes* dragline protein. In D. L. Kaplan, W. W. Adams, B. Farmer & C. Viney (Eds.), *Silk polymers, materials science and biotechnology*. Washington, DC: American Chemical Society, *544*, 67–79.

Mello, C. M., Soares, J. W., Arcidiacono, S., & Butlers, M. M. (2004). Acid extraction and purification of recombinant spider silk proteins. *Biomacromolecules*, *5*, 1849–1852.

Menassa, R., Hong, Z., Karatzas, C. N., Lazaris, A., Richman, A., & Brandle, J. (2004). Spider dragline silk proteins in transgenic tobacco leaves: accumulation and field production. *Plant Biotechnology Journal*, *2*, 431–438.

Meyer, D. E., & Chilkoti, A. (1999). Purification of recombinant proteins by fusion with thermally-responsive polypeptides. *Nature Biotechnology*, *17*, 1112–1115.

Miao, Y. G., Zhang, Y. S., Nakagaki, K., Zhao, T. F., Zhao, A. C., Meng, Y., et al. (2006). Expression of spider flagelliform silk protein in *Bombyx mori* cell line by a novel Bac-to-Bac/BmNPV baculovirus expression system. *Applied Microbiology and Biotechnology*, *71*, 192–199.

Michal, C. A., Simmons, A. H., Chew, B. G., Zax, D. B., & Jelinski, L. W. (1996). Presence of phosphorus in *Nephila clavipes* dragline silk. *Biophysical Journal*, *70*, 489–493.

Moloney, M. M., & Holbrook, L. A. (1997). Subcellular targeting and purification of recombinant proteins in plant production systems. *Biotechnology & Genetic Engineering Reviews*, *14*, 321–336.

O'Brien, J. P., Fahnestock, S. R., Termonia, Y., & Gardner, K. C.H. (1998). Nylons from nature: synthetic analogs to spider silk. *Advanced Materials*, *10*, 1185–1195.

Ohgo, K., Kawase, T., Ashida, J., & Asakura, T. (2006). Solid-state NMR analysis of a peptide (Gly-Pro-Gly-Gly-Ala)(6)-Gly derived from a flagelliform silk sequence of *Nephila clavipes*. *Biomacromolecules*, 7, 1210–1214.

Patel, J., Zhu, H., Menassa, R., Gyenis, L., Richman, A., & Brandle, J. (2007). Elastin-like polypeptide fusions enhance the accumulation of recombinant proteins in tobacco leaves. *Transgenic Research*, *16*, 239–249.

Pennock, G. D., Shoemaker, C., & Miller, L. K. (1984). Strong and regulated expression of *Escherichia coli* beta-galactosidase in insect cells with a baculovirus vector. *Molecular Cell Biology*, *4*, 399–406.

Perez-Rigueiro, J., Elices, M., Guinea, G.V., Plaza, G. R., Karatzas, C., Riekel, C., et al. (2011). Bioinspired fibers follow the track of natural spider silk. *Macromolecules*, *44*, 1166–1176.

Perez-Rigueiro, J., Elices, M., Plaza, G. R., & Guinea, G. V. (2007). Similarities and differences in the supramolecular organization of silkworm and spider silk. *Macromolecules*, *40*, 5360–5365.

Prince, J. T., McGrath, K. P., DiGirolamo, C. M., & Kaplan, D. L. (1995). Construction, cloning, and expression of synthetic genes encoding spider dragline silk. *Biochemistry*, *34*, 10879–10885.

Putthanarat, S., Stribeck, N., Fossey, S. A., Eby, R. K., & Adams, W. W. (2000). Investigation of the nanofibrils of silk fibers. *Polymer*, *41*, 7735–7747.

Rauscher, S., Baud, S., Miao, M., Keeley, F.W., & Pomes, R. (2006). Proline and glycine control protein self-organization into elastomeric or amyloid fibrils. *Structure*, *14*, 1667–1676.

Riekel, C., & Vollrath, F. (2001). Spider silk fibre extrusion: combined wide- and small-angle X-ray microdiffraction experiments. *International Journal of Biological Macromolecules*, *29*, 203–210.

Rising, A., Hjalm, G., Engstrom, W., & Johansson, J. (2006). N-terminal nonrepetitive domain common to dragline, flagelliform, and cylindriform spider silk proteins. *Biomacromolecules*, 7, 3120–3124.

Rising, A., Widhe, M., Johansson, J., & Hedhammar, M. (2011). Spider silk proteins: recent advances in recombinant production, structure–function relationships and biomedical applications. *Cellular and Molecular Life Sciences*, *68*, 169–184.

Römer, L., & Scheibel, T. (2007). Basis for new material – spider silk protein. *Chemie in Unserer Zeit*, *41*, 306–314.

Rosenberg, A. H., Goldman, E., Dunn, J. J., Studier, F. W., & Zubay, G. (1993). Effects of consecutive AGG codons on translation in *Escherichia coli*, demonstrated with a versatile codon test system. *Journal of Bacteriology*, *175*, 716–722.

Schacht, K., & Scheibel, T. (2011). Controlled hydrogel formation of a recombinant spider silk protein. *Biomacromolecules*, *12*, 2488–2495.

Scheibel, T. (2004). Spider silks: recombinant synthesis, assembly, spinning, and engineering of synthetic proteins. *Microbial Cell Factories*, *3*.

Scheller, J., & Conrad, U. (2005). Plant-based material, protein and biodegradable plastic. *Current Opinion in Plant Biology*, *8*, 188–196.

Scheller, J., Guhrs, K. H., Grosse, F., & Conrad, U. (2001). Production of spider silk proteins in tobacco and potato. *Nature Biotechnology*, *19*, 573–577.

Scheller, J., Henggeler, D., Viviani, A., & Conrad, U. (2004). Purification of spider silk-elastin from transgenic plants and application for human chondrocyte proliferation. *Transgenic Research*, *13*, 51–57.

Schmidt, F. R. (2004). Recombinant expression systems in the pharmaceutical industry. *Applied Microbiology and Biotechnology*, *65*, 363–372.

Schmidt, M., Romer, L., Strehle, M., & Scheibel, T. (2007). Conquering isoleucine auxotrophy of *Escherichia coli* BLR(DE3) to recombinantly produce spider silk proteins in minimal media. *Biotechnology Letters*, *29*, 1741–1744.

Schulz, S. (2001). Composition of the silk lipids of the spider *Nephila clavipes*. *Lipids*, *36*, 637–647.

Shao, Z. Z., Vollrath, F., Yang, Y., & Thogersen, H. C. (2003). Structure and behavior of regenerated spider silk. *Macromolecules*, *36*, 1157–1161.

Simmons, A. H., Michal, C. A., & Jelinski, L. W. (1996). Molecular orientation and two-component nature of the crystalline fraction of spider dragline silk. *Science*, *271*, 84–87.

Slotta, U. K., Rammensee, S., Gorb, S., & Scheibel, T. (2008). An engineered spider silk protein forms microspheres. *Angewandte Chemie International Edition*, *47*, 4592–4594.

Slotta, U., Tammer, M., Kremer, F., Koelsch, P., & Scheibel, T. (2006). Structural analysis of spider silk films. *Supramolecular Chemistry*, *18*, 465–471.

Sorensen, H. P., & Mortensen, K. K. (2005). Advanced genetic strategies for recombinant protein expression in *Escherichia coli*. *Journal of Biotechnology*, *115*, 113–128.

Sponner, A., Unger, E., Grosse, F., & Weisshart, K. (2005). Differential polymerization of the two main protein components of dragline silk during fibre spinning. *Nature Materials*, *4*, 772–775.

Sponner, A., Vater, W., Monajembashi, S., Unger, E., Grosse, F., & Weisshart, K. (2007). Composition and hierarchical organisation of a spider silk. *PLoS One*, *2*, e998.

Sponner, A., Vater, W., Rommerskirch, W., Vollrath, F., Unger, E., Grosse, F., et al. (2005). The conserved C-termini contribute to the properties of spider silk fibroins. *Biochemical and Biophysical Research Communications*, *338*, 897–902.

Stark, M., Grip, S., Rising, A., Hedhammar, M., Engstrom, W., Hjalm, G., et al. (2007). Macroscopic fibers self-assembled from recombinant miniature spider silk proteins. *Biomacromolecules*, *8*, 1695–1701.

Stauffer, S. L., Coguill, S. L., & Lewis, R. V. (1994). Comparison of physical properties of 3 silks from *Nephila clavipes* and *Araneus gemmoides*. *Journal of Arachnology*, *22*, 5–11.

Stephens, J. S., Fahnestock, S. R., Farmer, R. S., Kiick, K. L., Chase, D. B., & Rabolt, J. F. (2005). Effects of electrospinning and solution casting protocols on the secondary structure of a genetically engineered dragline spider silk analogue investigated via fourier transform Raman spectroscopy. *Biomacromolecules*, *6*, 1405–1413.

Szela, S., Avtges, P., Valluzzi, R., Winkler, S., Wilson, D., Kirschner, D., et al. (2000). Reduction–oxidation control of beta-sheet assembly in genetically engineered silk. *Biomacromolecules*, *1*, 534–542.

Terpe, K. (2006). Overview of bacterial expression systems for heterologous protein production: from molecular and biochemical fundamentals to commercial systems. *Applied Microbiology and Biotechnology*, *72*, 211–222.

Teule, F., Aube, C., Ellison, M., & Abbott, A. (2003). Biomimetic manufacturing of cus-
    tomised novel fibre proteins for specialised applications. *AUTEX Research Journal*, *3*,
    160–165.
Teule, F., Cooper, A. R., Furin, W. A., Bittencourt, D., Rech, E. L., Brooks, A., et al. (2009).
    A protocol for the production of recombinant spider silk-like proteins for artificial fiber
    spinning. *Nature Protocols*, *4*, 341–355.
Teule, F., Furin, W. A., Cooper, A. R., Duncan, J. R., & Lewis, R. V. (2007). Modifications of
    spider silk sequences in an attempt to control the mechanical properties of the synthetic
    fibers. *Journal of Materials Science*, *42*, 8974–8985.
Teule, F., Miao, Y. G., Sohn, B. H., Kim, Y. S., Hull, J. J., Fraser, M. J., Jr., et al. (2012).
    Silkworms transformed with chimeric silkworm/spider silk genes spin composite
    silk fibers with improved mechanical properties. *Proceedings of the National Academy of
    Sciences of the United States of America*, *109*, 923–928.
Thiel, B. L., Guess, K. B., & Viney, C. (1997). Non-periodic lattice crystals in the hierarchical
    microstructure of spider (major ampullate) silk. *Biopolymers*, *41*, 703–719.
Thiel, B. L., & Viney, C. (1996). Beta sheets and spider silk. *Science*, *273*, 1480–1481.
Tillinghast, E. K., Chase, S. F., & Townley, M. A. (1984). Water extraction by the major ampullate
    duct during silk formation in the spider, *Argiope aurantia* Lucas. *Journal of Insect Physiology*,
    30, 591–596.
Tillinghast, E. K., & Townley, M. A. (1994). Silk glands of araneid spiders – selected morpho-
    logical and physiological aspects. *Silk Polymers*, *544*, 29–44.
Urry, D. W., Haynes, B., Zhang, H., Harris, R. D., & Prasad, K. U. (1988). Mechanochemical
    coupling in synthetic polypeptides by modulation of an inverse temperature transi-
    tion. *Proceedings of the National Academy of Sciences of the United States of America*, *85*,
    3407–3411.
van Beek, J. D., Hess, S., Vollrath, F., & Meier, B. H. (2002). The molecular structure of spider
    dragline silk: folding and orientation of the protein backbone. *Proceedings of the National
    Academy of Sciences of the United States of America*, *99*, 10266–10271.
Vasanthavada, K., Hu, X., Falick, A. M., La Mattina, C., Moore, A. M. F., Jones, P. R., et al.
    (2007). Aciniform spidroin, a constituent of egg case sacs and wrapping silk fibers
    from the black widow spider *Latrodectus hesperus*. *Journal of Biological Chemistry*, *282*,
    35088–35097.
Viney, C. (1997). Natural silks: archetypal supramolecular assembly of polymer fibres.
    Supramolecular Science, *4*, 75–81.
Vollrath, F. (1994). General properties of some spider silks. In D. Kaplan, W. W. Adams, B.
    Farmer & C. Viney (Eds.), *Silk polymers – materials science and biotechnology* (Vol. 544,
    pp. 17–28). Washington: ACS.
Vollrath, F. (1999). Biology of spider silk. *International Journal of Biological Macromolecules*, *24*,
    81–88.
Vollrath, F. (2006). Spider silk: thousands of nano-filaments and dollops of sticky glue. *Current
    Biology*, *16*, R925–R927.
Vollrath, F., & Porter, D. (2006). Spider silk as archetypal protein elastomer. *Soft Matter*, *2*,
    377–385.
Vollrath, F., & Tillinghast, E. K. (1991). Glycoprotein glue beneath a spider webs aqueous
    coat. *Naturwissenschaften*, *78*, 557–559.
Wen, H. X., Lan, X. Q., Zhang, Y. S., Zhao, T. F., Wang, Y. J., Kajiura, Z., et al. (2010). Trans-
    genic silkworms (*Bombyx mori*) produce recombinant spider dragline silk in cocoons.
    Molecular Biology Reports, *37*, 1815–1821.
Werten, M. W., Moers, A. P., Vong, T., Zuilhof, H., van Hest, J. C., & de Wolf, F. A. (2008).
    Biosynthesis of an amphiphilic silk-like polymer. *Biomacromolecules*, *9*, 1705–1711.
Widmaier, D. M., Tullman-Ercek, D., Mirsky, E. A., Hill, R., Govindarajan, S., Minshull, J.,
    et al. (2009). Engineering the *Salmonella* type III secretion system to export spider silk
    monomers. *Molecular Systems Biology*, *5*, 309.

Widmaier, D. M., & Voigt, C. A. (2010). Quantification of the physiochemical constraints on the export of spider silk proteins by *Salmonella* type III secretion. *Microbial Cell Factories*, *9*, 78.

Winkler, S., & Kaplan, D. L. (2000). Molecular biology of spider silk. *Journal of Biotechnology*, *74*, 85–93.

Winkler, S., Szela, S., Avtges, P., Valluzzi, R., Kirschner, D. A., & Kaplan, D. (1999). Designing recombinant spider silk proteins to control assembly. *International Journal of Biological Macromolecules*, *24*, 265–270.

Winkler, S., Wilson, D., & Kaplan, D. L. (2000). Controlling beta-sheet assembly in genetically engineered silk by enzymatic phosphorylation/dephosphorylation. *Biochemistry*, *39*, 12739–12746.

Wohlrab, S., Muller, S., Schmidt, A., Neubauer, S., Kessler, H., Leal-Egana, A., et al. (2012). Cell adhesion and proliferation on RGD-modified recombinant spider silk proteins. *Biomaterials*, *33*, 6650–6659.

Wong Po Foo, C., Patwardhan, S. V., Belton, D. J., Kitchel, B., Anastasiades, D., Huang, J., et al. (2006). Novel nanocomposites from spider silk-silica fusion (chimeric) proteins. *Proceedings of the National Academy of Sciences of the United States of America*, *103*, 9428–9433.

Xia, X.-X., Qian, Z. -G., Ki, C. S., Park, Y. H., Kaplan, D. L., & Lee, S. Y. (2010). Native-sized recombinant spider silk protein produced in metabolically engineered *Escherichia coli* results in a strong fiber. *Proceedings of the National Academy of Sciences*, *107*, 14059–14063.

Xie, F., Zhang, H. H., Shao, H. L., & Hu, X. C. (2006). Effect of shearing on formation of silk fibers from regenerated *Bombyx mori* silk fibroin aqueous solution. *International Journal of Biological Macromolecules*, *38*, 284–288.

Xu, H. T., Fan, B. L., Yu, S. Y., Huang, Y. H., Zhao, Z. H., Lian, Z. X., et al. (2007). Construct synthetic gene encoding artificial spider dragline silk protein and its expression in milk of transgenic mice. *Animal Biotechnology*, *18*, 1–12.

Yamada, H., Nakao, H., Takasu, Y., & Tsubouchi, K. (2001). Preparation of undegraded native molecular fibroin solution from silkworm cocoons. *Materials Science & Engineering. C Biomimetic and Supramolecular Systems*, *14*, 41–46.

Yang, M., & Asakura, T. (2005). Design, expression and solid-state NMR characterization of silk-like materials constructed from sequences of spider silk, *Samia cynthia ricini* and *Bombyx mori* silk fibroins. *Journal of Biochemistry*, *137*, 721–729.

Yang, J. J., Barr, L. A., Fahnestock, S. R., & Liu, Z. B. (2005). High yield recombinant silk-like protein production in transgenic plants through protein targeting. *Transgenic Research*, *14*, 313–324.

Yao, J. M., Masuda, H., Zhao, C. H., & Asakura, T. (2002). Artificial spinning and characterization of silk fiber from *Bombyx mori* silk fibroin in hexafluoroacetone hydrate. *Macromolecules*, *35*, 6–9.

Zarkoob, S., Eby, R. K., Reneker, D. H., Hudson, S. D., Ertley, D., & Adams, W. W. (2004). Structure and morphology of electrospun silk nanofibers. *Polymer*, *45*, 3973–3977.

Zhang, Y., Hu, J., Miao, Y., Zhao, A., Zhao, T., Wu, D., et al. (2008). Expression of EGFP-spider dragline silk fusion protein in BmN cells and larvae of silkworm showed the solubility is primary limit for dragline proteins yield. *Molecular Biology Reports*, *35*, 329–335.

Zhao, A. C., Zhao, T. F., Nakagaki, K., Zhang, Y. S., SiMa, Y. H., Miao, Y. G., et al. (2006). Novel molecular and mechanical properties of egg case silk from wasp spider, *Argiope bruennichi*. *Biochemistry*, *45*, 3348–3356.

Zhou, Y. T., Wu, S. X., & Conticello, V. P. (2001). Genetically directed synthesis and spectroscopic analysis of a protein polymer derived from a flagelliform silk sequence. *Biomacromolecules*, *2*, 111–125.

Zuo, B., Dai, L., & Wu, Z. (2006). Analysis of structure and properties of biodegradable regenerated silk fibroin fibers. *Journal of Materials Science*, *41*, 3357–3361.

Part 4

To Spin or Not to Spin: Spider Silk Fibers and More

Doblhofer, E.*, Heidebrecht, A.*, and Scheibel, T.

* The authors contributed equally

Published in *Applied Microbiology & Biotechnology*, 99, pp. 9361-9380

Reprinted with kind permission from the publisher Springer Science and Business Media.

CrossMark

MINI-REVIEW

To spin or not to spin: spider silk fibers and more

Elena Doblhofer[1] · Aniela Heidebrecht[1] · Thomas Scheibel[1,2,3,4,5]

Abstract Spider silk fibers have a sophisticated hierarchical structure composed of proteins with highly repetitive sequences. Their extraordinary mechanical properties, defined by a unique combination of strength and extensibility, are superior to most man-made fibers. Therefore, spider silk has fascinated mankind for thousands of years. However, due to their aggressive territorial behavior, farming of spiders is not feasible on a large scale. For this reason, biotechnological approaches were recently developed for the production of recombinant spider silk proteins. These recombinant proteins can be assembled into a variety of morphologies with a great range of properties for technical and medical applications. Here, the different approaches of biotechnological production and the advances in material processing toward various applications will be reviewed.

Elena Doblhofer and Aniela Heidebrecht contributed equally to this work.

✉ Thomas Scheibel
thomas.scheibel@bm.uni-bayreuth.de

[1] Lehrstuhl Biomaterialien, Fakultät für Ingenieurswissenschaften, Universität Bayreuth, 95440 Bayreuth, Germany

[2] Institut für Bio-Makromoleküle (bio-mac), Universität Bayreuth, Universitätsstraße 30, 95440 Bayreuth, Germany

[3] Bayreuther Zentrum für Kolloide und Grenzflächen (BZKG), Universität Bayreuth, Universitätsstraße 30, 95440 Bayreuth, Germany

[4] Bayreuther Zentrum für Molekulare Biowissenschaften (BZMB), Universität Bayreuth, Universitätsstraße 30, 95440 Bayreuth, Germany

[5] Bayreuther Materialzentrum (BayMAT), Universität Bayreuth, Universitätsstraße 30, 95440 Bayreuth, Germany

Introduction

Spider silks represent a class of fibers with a unique combination of strength and flexibility which leads to an outstanding toughness (Gosline et al. 1999). In comparison to one of the strongest man-made fibers, Kevlar, spider silk can absorb three times more energy before breaking (Roemer and Scheibel 2007). Therefore, it is not surprising that ancient Australian aborigines and New Guinean natives utilized spider silk as fishing lines, fishing nets, head gear, and bags (Lewis 1996). Further, until World War II, spider silk was used for crosshairs in optical devices like microscopes, telescopes, and guns because of its extremely small diameters (thickness of 1/40 of a human hair) (Gerritsen 2002; Lewis 1996). By using cobwebs to stanch bleeding wounds, the ancient Greeks unknowingly observed further extraordinary characteristics of this material, like high biocompatibility and low immunogenicity (Altman et al. 2003; Gerritsen 2002; Vollrath et al. 2002). However, the first scientific studies to unravel its biomedical properties were not started until 1710, when it was shown that a spider's web is able to stop bleeding in human wounds and also supports the wound healing (Bon 1710). Two centuries later, Otto G. T. Kiliani investigated spider silk as suture material for surgery (Kiliani 1901).

As illustrated by the long history of spider silk use, the outstanding properties of natural spider silk have been well-known for a long time; however, scientifically, the material attained intensive interest of researchers only in the last decades. The combination of mechanical performance, biodegradability, and ambient processing conditions of the underlying proteins makes spider silk a highly desirable material for

⧜ Springer

applications from biomaterials to high-performance industrial fibers (Rising 2014; Vollrath and Knight 2001).

Spider silk structure

Female orb weaving spiders can produce up to six different types of silk, with each one produced in a specialized gland that provides the name of the corresponding silk type (Fig. 1). Every silk type has to fulfill a certain task either in the structure of the web, the protection of the offspring, or the wrapping of prey. Additionally, a silk-like glue, produced in a seventh gland, is deposited on the web for prey capture. The most frequently investigated silk type is the dragline silk, used to build frame and radii of an orb web. It also is used as the lifeline of the spider and is therefore easy to obtain by forced silking (Andersen 1970; Blackledge and Hayashi 2006; Denny 1976; Heim et al. 2009; Vollrath 2000). Similar to many biological materials, the outstanding (mechanical)

performance of spider silk is based on its hierarchical structure (Brown et al. 2012; Keten and Buehler 2008; Munch et al. 2008; Smith and Scheibel 2013; Sponner et al. 2007). Dragline spider silk fibers exhibit a core-shell structure with proteinaceous fibrils in the core and a three-layered shell of minor ampullate (Mi) silk, glycoproteins, and lipids. While the lipid part of the shell is only loosely attached to the core and does not substantially contribute to the mechanical performance of the fiber, the glyco-layer adheres directly and is a mediator between the fiber and its environment (Sponner et al. 2007). In this context, the shell is thought to be relevant for protection against environmental damage and microbes (Sponner et al. 2007). However, the determinant of the extraordinary mechanical characteristics of spider silk is the proteins which form the core of the fiber. The protein core of dragline silk is composed of two classes of spider silk proteins (spidroins): the highly ordered, hydrophobic spidroin I (Sp1), poor in proline residues, and the less ordered, hydrophilic, proline-rich spidroin II (Sp2), each with a molecular mass of

Fig. 1 Schematic overview of the different types of silk produced by female orb weaving spiders (Araneae); each silk type (highlighted in *red*) is tailored for a specific purpose as depicted
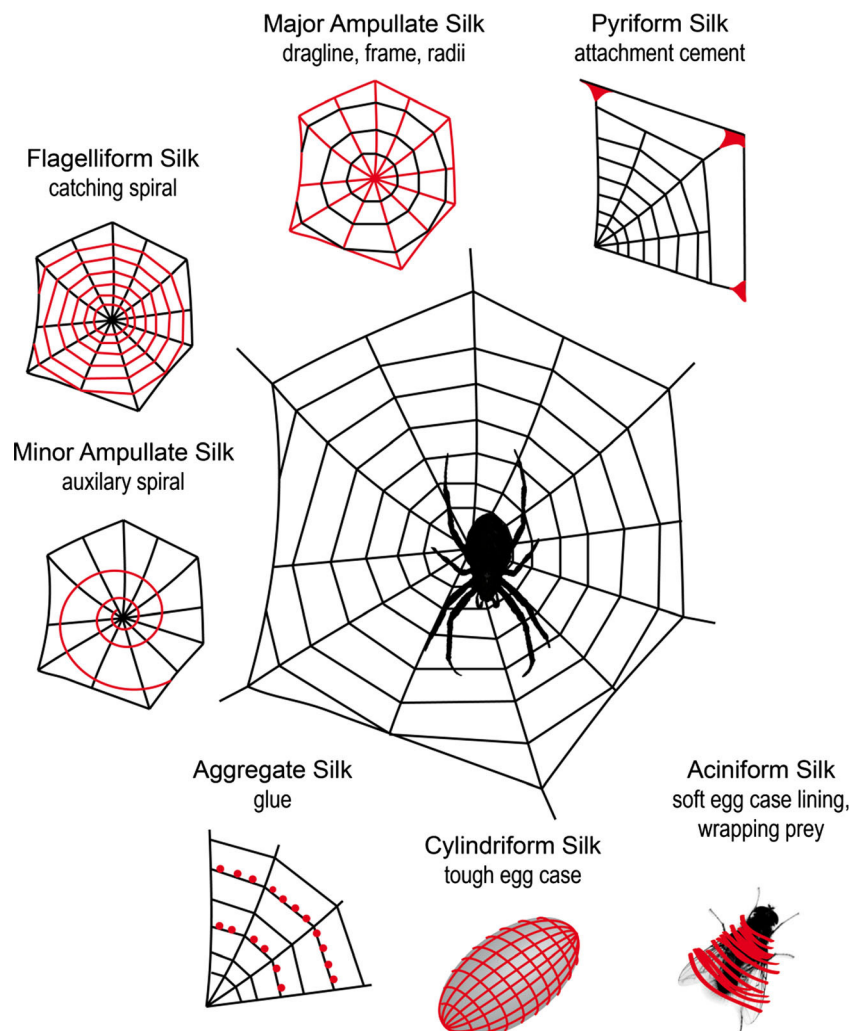
around 300 kDa (Heim et al. 2009; Xu and Lewis 1990) (Ayoub et al. 2007; Hinman and Lewis 1992; Xu and Lewis 1990). As they originate from the major ampullate gland, these proteins are also called major ampullate spidroins (MaSp). All MaSps comprise a highly repetitive core domain (up to 100 repeats of highly conserved sequence motifs, with 40 to 200 amino acids each) flanked by short (around 100–150 amino acids each) nonrepetitive (NR) terminal domains (Fig. 2). Upon fiber assembly, the gain and arrangement of secondary structure elements of the spidroins is responsible for the extraordinary mechanical properties of the fiber. Poly-alanine stretches fold into β-sheets, forming hydrophobic crystallites responsible for a high tensile strength (Kummerlen et al. 1996; Lewis 1992; Simmons et al. 1996); 3_1-helices formed by hydrophilic glycine-rich regions (GGX-motif, where X represents tyrosine, leucine, glutamine) are reflecting the elastic part (Kummerlen et al. 1996); and type II β-turns made of proline-rich GPG motifs are important for the reversible extensibility of a spider silk fiber (Hinman and Lewis 1992). While the latter sequence motif is only present in MaSp2, the first two motifs are ubiquitous (Ayoub et al. 2007; Hayashi et al. 1999; Hinman et al. 2000; Hinman and Lewis 1992; van Beek et al. 2002). All these motifs are repeated several dozen times within a single spidroin core domain. The nonrepetitive terminal motifs which flank the core do-main have an α-helical secondary structure arranged in a five-helix bundle. These domains are responsible for control-ling the storage of the spidroins at high concentrations in the spinning duct (Motriuk-Smith et al. 2005), and they also have an important function during the initiation of fiber formation upon their controlled dimerization and structural arrangement (Challis et al. 2006; Eisoldt et al. 2010, 2011; Hagn et al. 2010, 2011; Hedhammar et al. 2008; Heidebrecht et al. 2015; Huemmerich et al. 2004b; Rising et al. 2006)
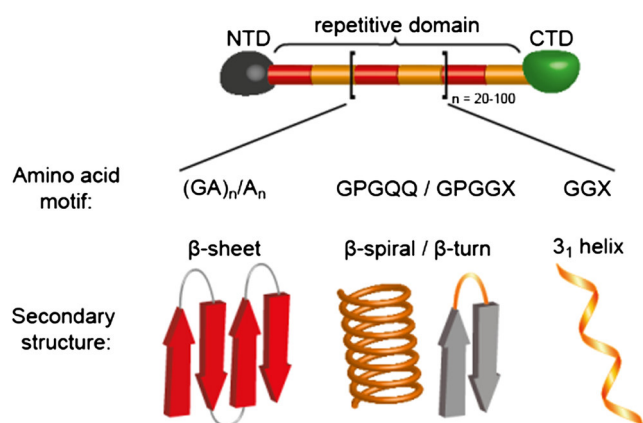

Fig. 2 Schematic structure of major ampullate spidroins including recurring amino acid motifs and the corresponding secondary structure. X: predominantly tyrosine, leucine, glutamine, alanine and serine residues. *NTD* amino-terminal domain, *CTD* carboxy-terminal domain

Biotechnological production of recombinant spider silk proteins

Unfortunately, it is not possible to produce large quantities of spider silk for applications by farming. This is due to the territorial and cannibalistic behavior and lower quality as well as quantity of silk produced by captive spiders (Craig et al. 2000; Fox 1975; Madsen et al. 1999; Vollrath and Knight 1999). Therefore, biotechnological production of the underly-ing spidroins was pursued to enable applications for spider silks.

Recombinant spidroin production has been conducted using a range of organisms including bacteria (Teule et al. 2009), tobacco plants (Menassa et al. 2004), yeast (Fahnestock and Bedzyk 1997), silk worms (Teule et al. 2012), goats (Steinkraus et al. 2012), insect cells (Huemmerich et al. 2004b), and mammalian cells (Lazaris et al. 2002). Each of these host systems has advantages and disadvantages. To begin with, short fragments of unmodified spider silk genes were expressed in a variety of hosts. It turned out that spider silk genes were unstable or the mRNA folded into undesirable secondary structures. Further, rearrange-ments, translation pauses, and problems with PCR amplifica-tion arose due to the highly repetitive character of the genes and the infidelity of template realignment during primer an-nealing (Fahnestock and Irwin 1997; Fahnestock et al. 2000). Additionally, host-derived differences in codon usage, prob-lems with expression of repetitive sequences in various hosts, and insufficient Gly- and Ala-tRNA pools led to only limited success concerning the recombinant production of natural spi-der silk proteins.

To overcome these hurdles, several synthetic genes were designed encoding proteins that resemble the key features of the natural spider silk proteins. Since the gram-negative en-terobacterium *Escherichia coli* is relatively simple, has a well-known genetic composition, and has the capability of fast, high-density cultivation, recombinant protein expression in *E. coli* allows for inexpensive, large-scale production (Sørensen and Mortensen 2005). Likewise, several ap-proaches of recombinant spider silk-like protein production were successful in *E. coli* (for an overview, see Heidebrecht and Scheibel 2013).

In addition to *E coli*, yeast or insect cells have been used to express spider silk constructs with the advantage of the latter of being genetically more closely related to spiders. However, the spidroins produced in these systems showed a quite low solubility (Heim et al. 2009; Huemmerich et al. 2004b). Other hosts such as plants and mammalian cells have been used, too, but showed mostly low expression levels (Barr et al. 2004; Hauptmann et al. 2013; Lazaris et al. 2002).

Finally, transgenic animals were tested as hosts to produce recombinant spidroins in secreted body fluids. The presumed advantage of this approach would be the ease of purification

upon secretion into the milk or urine of the respective animal (Heim et al. 2009; Karatzas et al. 1999). However, it turned out that the purification was more difficult than thought due to contamination with animal-based secreted proteins. Given the fact that the generation of transgenic animals is far more complex and time consuming than that of bacteria or yeast, this approach has been rarely used in the past (Heim et al. 2009; Xu et al. 2007). For example, recombinant spider silk-EGFP fusion proteins were produced using BmN cells and larvae of silkworms as a host organism, but the protein yield was low due to the insolubility of the recombinant spider silk proteins (Zhang et al. 2008). In a more successful approach, chimeric proteins containing sequences of spider silk proteins and silkworm fibroin were designed, including either a H-chain promoter (Kuwana et al. 2014; Teule et al. 2012; Zhu et al. 2010) or a sericin promoter (Wen et al. 2010) locating the chimeric silkworm/spider silk proteins in the core or the sericin shell of the fiber. In both cases, silkworms spun fibers with mechanical properties exceeding that of silkworm silk, but they did not reach the properties of natural spider silk (Teule et al. 2012; Wen et al. 2010). Production of designed short spider silk proteins (50 kDa) resembling MaSp1 and MaSp2 of *Nephila clavipes* in goat milk was also successful, while expression of their partial complementary DNA (cDNA) in transgenic mice was not possible likely due to errors in protein synthesis (Perez-Rigueiro et al. 2011; Xu et al. 2007).

Based on the experience throughout the last three decades, *E. coli* has been established as the host system of choice, given the balance of quality of the silk produced with the scalability of the approach.

"To spin": artificial spider silk fibers

Due to the abovementioned, outstanding mechanical and biomedical properties of spider silk fibers, great efforts have been made to employ these fibers in different technical as well as biomedical applications. For instance, functional recovery of nerve defects was successfully performed in rats and sheep by using natural spider silk fibers as a guiding material (Allmeling et al. 2008; Radtke et al. 2011). Further, native spider dragline silk, directly woven onto steel frames, was used as a matrix for three-dimensional skin cell culture (Wendt et al. 2011). Since natural spider silk fibers are not available at large scale as mentioned above (see section "Biotechnological production of recombinant spider silk proteins"), different approaches have been tested to produce artificial spider silk fibers during the last two decades, which will be discussed in greater detail below.

The natural spinning process

In order to successfully establish a man-made spider silk spinning process, it is at first necessary to understand the natural one. Natural spider silk fiber spinning is a highly complex process involving a number of parameters in a highly regulated environment as exemplarily demonstrated in Fig. 3 for the assembly of major ampullate spidroins. Epithelial cells covering the tail and the ampulla of the major ampullate silk gland produce the spidroins and secrete them into the lumen. There, the spidroins are stored in a soluble state at high concentrations (up to 50 % (*w/v*)) in the presence of sodium and chloride ions. Analysis of major ampullate silk glands by polarized microscopy revealed a liquid-crystal behavior of the spinning dope (Knight and Vollrath 1999; Viney 1997), whereas in vitro experiments showed micellar-like structures both of which are not mutually exclusive (Eisoldt et al. 2010; Exler et al. 2007; Heidebrecht et al. 2015). The combination of the presence of chaotropic ions (stabilizing soluble protein structures) and a pre-assembly of the spidroins enables their storage at concentrations as found in the ampulla of the spinning gland. From the ampulla, the spinning dope passes into an S-shaped tapered duct, which is lined by a cuticular intima layer. In addition to supporting the duct and protecting the epithelial cells, this layer is hypothesized to function as a hollow fiber dialysis membrane, enabling the dehydration of the spinning dope (Vollrath and Knight 1999). During traveling of the spinning dope through the spinning duct, sodium and chloride ions are replaced by the more kosmotropic potassium and phosphate ions inducing salting-out of the proteins (Knight and Vollrath 2001; Papadopoulos et al. 2007). Additionally, acidification (from pH 7.2 to 5.7; Kronqvist et al. 2014) takes place triggered by carbonic anhydrase (Andersson et al. 2014), which has a contrary structural effect on the terminal domains. Upon acidification, glutamic acid residues of the amino-terminal domain are sequentially protonated, leading to structural rearrangements of the domain enabling dimerization in an antiparallel manner (Rising and Johansson 2015). In contrary to the stabilizing effect of the pH reduction on the amino-terminal domain, the carboxy-terminal one is destabilized upon acidification. In addition to the pH-induced destabilization, the presence of phosphate ions initiates the exposition of hydrophobic areas within the C-terminal domain initiating the parallel alignment of the associated two core domains (Eisoldt et al. 2010, 2012; Hagn et al. 2010). Based on the parallel (carboxy-terminal domains) and antiparallel (amino-terminal domains) orientation of the terminal domains, an endless spidroin network is achieved. Finally, water resorption via the cuticular intima layer and shear stress, resulting from the tapering of the spinning duct and the pulling of the fiber from the spider's abdomen, lead to the final alignment of the spidroins followed by solidification of the fiber (Fig. 3) (Hagn et al. 2011; Hardy et al. 2008).

Fig. 3 Overview of natural and
artificial spinning processes
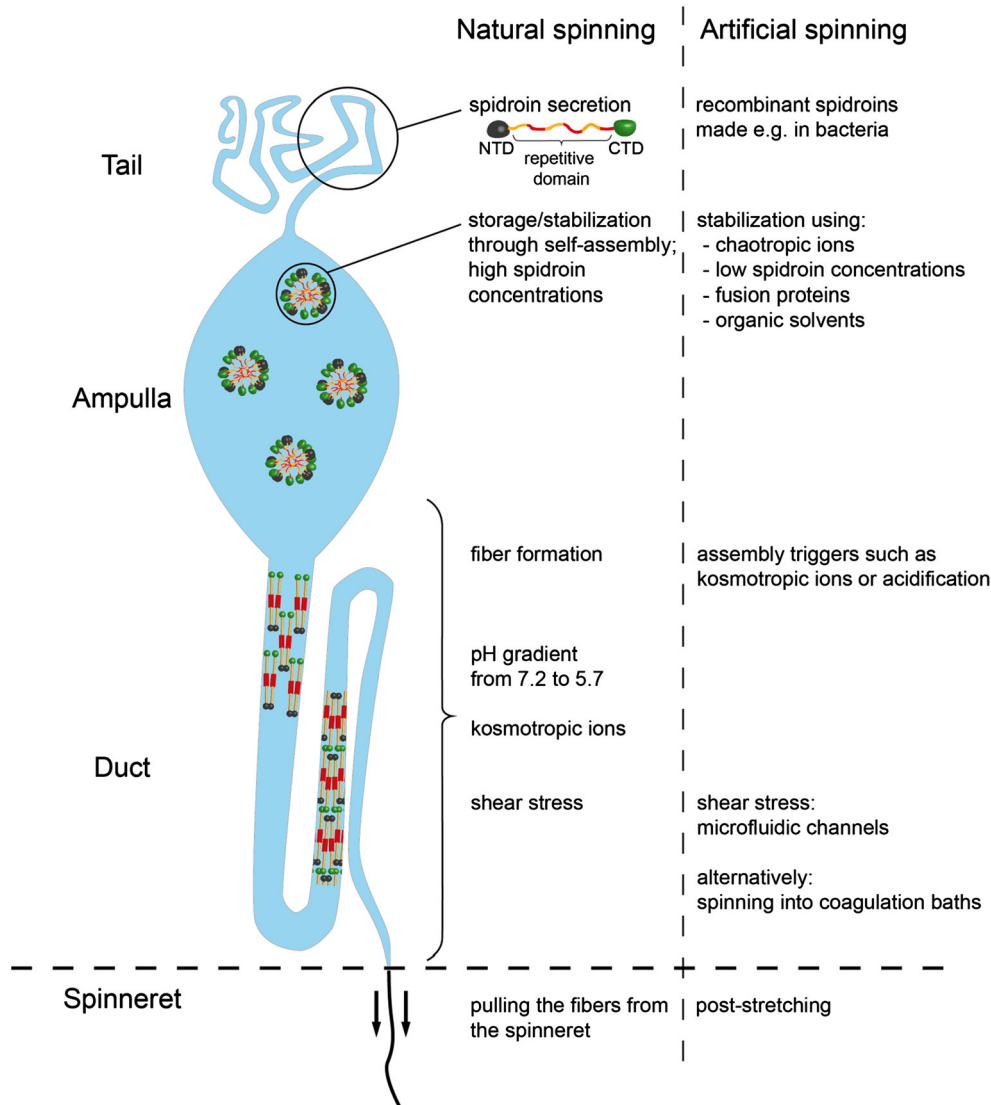
Artificial fiber spinning

Commonly used artificial spinning processes are not like the natural silk spinning one. Typical processes out of solution are wet spinning, dry spinning, and electrospinning. In wet spinning, a polymer solution is extruded into a coagulation bath, where the polymer precipitates and the fibers are formed. For dry spinning and electrospinning, the polymers are solvated in an organic solvent and extruded into the air. Whereas fiber formation in dry spinning relies solely on the fast evaporation of the organic solvent, in electrospinning, the polymer solution is extruded into an electrostatic field. This field yields repulsive forces in the extruded solution, leading to eruption of a thin jet that is stretched toward the collector (i.e., counter electrode); as the solvent evaporates, a solid fiber is formed (Greiner and Wendorff 2007; Smit et al. 2005). This fiber is randomly deposited onto the collector, which results in a non-woven mat (Teo and Ramakrishna 2006). In theory, wet spinning, dry spinning, and electrospinning are suitable methods for spider silk fiber spinning, since organic as well as aqueous spinning dopes can be used. In practice, dry spinning has been shown to be so far not suitable for silk fiber production, since spinning a silk fiber out of an organic solution results in mechanically unstable fibers (unpublished results), while dry spinning from an aqueous solution could not be achieved since this spinning technique relies on a highly volatile solvent for fast fiber formation. Therefore, so far, only wet spinning and electrospinning have been successfully employed for producing artificial spider silk fibers.

Dope preparation

The first step toward the production of artificial spider silk fibers is to solve the spidroins. Therefore, often an organic solvent is used exhibiting strong hydrogen bonding properties in order to guarantee good solvent-protein interactions. A

disadvantage, especially for biomedical applications, of organic spinning solutions is their putative toxicity. However, a high spidroin solubility enables the production of highly concentrated spinning dopes, which simplifies fiber formation (Um et al. 2004). With the objective of high protein solubility, many research groups have used the organic solvent 1,1,1,3,3, 3-hexafluoro-2-propanol (HFIP). In HFIP, spidroin concentrations ranging from 10 to 30 % (*w/v*) can easily be achieved (Adrianos et al. 2013; An et al. 2011; Brooks et al. 2008; Lin et al. 2013; Teule et al. 2007; Xia et al. 2010), with the highest reported spidroin content of 45–60 % (*w/v*) (Albertson et al. 2014). One advantage of HFIP as solvent for spidroins is its volatility. Therefore, HFIP is commonly used for spinning processes which rely on a fast evaporation of the solvent such as electrospinning (Bini et al. 2006; Lang et al. 2013; Stephens et al. 2005; Wong Po Foo et al. 2006; Zhu et al. 2015). In addition to HFIP, formic acid (FA) has been used as an organic solvent of spidroins (Peng et al. 2009).

Seidel et al. (1998, 2000) dissolved dragline silk of *N. clavipes* in HFIP, produced a film out of the reconstituted spidroins, and then solved this film again in HFIP to a concentration of 2.5 % (*w/w*) in order to use it as a spinning dope for wet spinning. Dopes made of reconstituted spidroins did not form fibers in the otherwise commonly used methanol and isopropanol coagulation baths, but only in acetone coagulation baths (Seidel et al. 1998).

At first glance, using an organic solvent to gain solutions with a high protein concentration seems to be beneficial for spinning, but good protein-solvent interactions and, therefore, high protein solubility may also prevent protein assembly. Further, if artificial spider silk fibers are to be used for medical applications like suture materials, health risks caused by toxic solvents have to be avoided. Additionally, organic waste disposal in industrial processes is highly regulated and expensive; thus, the application of organic solvents is not favorable for scale-up processes. In order to avoid organic solvents, three approaches have been used to produce highly concentrated aqueous spidroin solutions: (1) spidroin self-assembly in aqueous buffers (Exler et al. 2007; Grip et al. 2009; Heidebrecht et al. 2015; Stark et al. 2007; Teule et al. 2007), (2) concentration of a diluted aqueous spidroin solution (Arcidiacono et al. 2002; Heidebrecht et al. 2015), and (3) direct solvation at high spidroin concentrations (Bogush et al. 2009; Jones et al. 2015). Protein concentrations typically used for spinning fibers out of aqueous solutions range from 10 to 30 % (*w/v*) (Arcidiacono et al. 2002; Bogush et al. 2009; Exler et al. 2007; Heidebrecht et al. 2015; Jones et al. 2015; Lazaris et al. 2002), and the highest concentration achieved so far has been 30 % (*w/v*) (Bogush et al. 2009). When spidroins are purified by a precipitation step such as salting-out or lyophilization, high spidroin purities are gained, but the spidroins also have to be resolved afterwards.

Heidebrecht et al. (2015) used the strong denaturant guanidinium thiocyanate for spidroin solvation, followed by its removal using dialysis against a 50-mM Tris/HCl buffer (pH 8.0). Additionally, 100 mM NaCl was added to the dialysis buffer in order to stabilize the spidroins in solution. Subsequent dialysis against a phosphate-containing buffer induced a liquid-liquid phase separation of the spidroin solution into a low-density phase and a self-assembled, high-density phase. Such phosphate-induced self-assembly of spidroins in solution resulted in spidroin concentrations ranging between 9 and 11 % (Heidebrecht et al. 2015). Alternatively, spinning dopes were produced by concentrating the protein solution using either ultrafiltration or dialysis against the hygroscopic polyethylene glycol (PEG) (Arcidiacono et al. 2002; Heidebrecht et al. 2015). In this approach, the spidroin molecules are forced into a highly concentrated solution and they cannot self-assemble. However, these spinning dopes are prone to aggregation and are less stable than self-assembled spinning dopes (Heidebrecht et al. 2015). The third approach to achieve highly concentrated aqueous spinning dopes is the direct solvation of spidroins in a medium suitable for spinning. Jones et al. (2015) added a solution containing 0.1 % propionic acid and 10 mM imidazole to spidroins in a glass vial and used sonication and subsequent heating in a microwave oven until complete spidroin solvation (Jones et al. 2015). The spidroin suspension was heated up to 130 °C for more than 48 h, indicating the high energy input that is needed to directly solve a spidroin at high concentration.

Wet spinning

Extrusion of the spinning dope into monohydric alcohols, such as methanol, ethanol, or isopropanol with the exemption of reconstituted spider silks which have to be spun into acetone as mentioned above, initiates fiber formation through dehydration of the spidroins. This technique results in single fibers with a diameter in the micrometer range. An advantage of wet spinning over other techniques such as electrospinning is the rather "slow" fiber formation, which allows a high degree of alignment of the proteins during spinning. This alignment enables the formation of a structural hierarchy necessary to produce fibers with superior mechanical properties. Wet spinning allows the use of different spinning dopes, ranging from inorganic or aqueous solutions to dispersions and liquid crystalline phases, and thus can be used for any polymer/biopolymer. Variation of the spinning dope and the composition of the coagulation bath influence fiber properties, allowing the production of fibers with tunable mechanical properties. One disadvantage of wet spinning is the necessity to remove the solvent or coagulation bath residues after spinning, which requires at least one washing step resulting in a longer and therefore more expensive process compared to dry spinning (Jestin and Poulin 2014).

Besides 100 % of methanol or isopropanol (Adrianos et al. 2013; Albertson et al. 2014; An et al. 2011; Jones et al. 2015; Zhu et al. 2010), mixtures of water with monohydric alcohols are often used as coagulation baths (Arcidiacono et al. 2002; Bogush et al. 2009; Heidebrecht et al. 2015; Lazaris et al. 2002; Teule et al. 2007; Xia et al. 2010). The addition of water to the coagulation bath slows down the coagulation rate of spidroins, and water works as a plasticizer for the fibers, which renders them less brittle and prevents clogging of the spinneret (Lin et al. 2013).

Posttreatment, such as drawing the spun fibers in air or inside a bath, is applied to improve the fibers' mechanical properties. Poststretching of spun fibers has been shown to induce a higher β-sheet content (An et al. 2011) and to align the β-sheet crystals along the thread axis (Heidebrecht et al. 2015). In contrast to the coagulation bath, the poststretching bath needs to contain water because of its plasticizing features for the fibers, which enables the proteins to rearrange and align along the fiber axis. The absence of water results in brittle fibers. An overview of recombinant spider silk fiber wet spinning and posttreatment conditions is given in Table 1.

Electrospinning

Electrospinning of recombinant or reconstituted spider silk protein solutions is possible using an electric field of 4–30 kV with a distance of 2–25 cm between the electrodes (i.e., the capillary tip and the collector) (Bini et al. 2006; Bogush et al. 2009; Lang et al. 2013; Peng et al. 2009; Stephens et al. 2005; Wong Po Foo et al. 2006; Yu et al. 2014; Zhou et al. 2008; Zhu et al. 2015). Parameters influencing the fiber properties (e.g., fiber diameter) of nonwoven mats mostly depend on the properties of the spinning dope, such as the viscosity, surface free energy, protein concentration, and the solvent's intrinsic electrical conductivity and permeability (Greiner et al. 2006). In contrast to wet spinning, electrospinning of comparatively low protein concentrations of 2–6 % (w/v) (Bini et al. 2006; Leal-Egana et al. 2012; Wong Po Foo et al. 2006; Yu et al. 2014; Zarkoob et al. 2004) also yields fibers, but higher protein concentrations of 10–30 % (w/v) (Bogush et al. 2009; Lang et al. 2013; Leal-Egana et al. 2012; Peng et al. 2009; Stephens et al. 2005; Zhou et al. 2008; Zhu et al. 2015) are more commonly used. In general, increasing the spidroin concentration in the dope leads to an increased fiber diameter and a reduction of bead formation, the latter being an unwanted side effect of electrospinning (Lang et al. 2013; Leal-Egana et al. 2012). Structural analysis of nonwoven mats electrospun from HFIP using Fourier-transformed infrared spectroscopy (FTIR) with subsequent Fourier self-deconvolution (FSD) revealed a low β-sheet content (~15 %) (Lang et al. 2013). The electric field interacts with the hydrogen bond dipoles of the protein, stabilizing α-helical segments and thus inhibiting β-sheet formation

(Stephens et al. 2005). Instead of a solid collector, water- or organic solvent-based coagulation baths can be used to collect the spun micro- and nanofibers. In general, the latter approach has the advantage of including a posttreatment within the spinning process. Yu et al. used a coagulation bath containing 90 % (v/v) of organic solutions (acetone or methyl alcohol) as a collector; however, SEM images showed inhomogeneous fibers containing many beads (Yu et al. 2014). Posttreatment of electrospun fibers with organic solvents or alcohols is necessary in order to render the spun α-helical fibers water insoluble (i.e., inducing β-sheet formation) (Lang et al. 2013; Leal-Egana et al. 2012; Slotta et al. 2006). Immersing the fibers into alcohol baths resulted in fused intersections of single fibers (Bini et al. 2006), giving the fibers a "molten" appearance. Therefore, instead of immersing the fibers, Leal-Egana et al. (2012) and Lang et al. (2013) exposed them to methanol or ethanol vapor to render the fibers water insoluble with keeping their original morphology.

Other spinning methods

Besides wet spinning and electrospinning, recombinant spider silk fibers were produced using microfluidic devices (Rammensee et al. 2008). Such devices mimic some aspects of the natural spinning process, such as ion exchange, pH change, and elongational flow conditions. Since only low or medium protein concentrations were used, high flow rates were necessary to induce fiber assembly. Shear forces can also be applied by hand-drawing fibers from pre-assembled spidroins out of aqueous solutions (Exler et al. 2007; Teule et al. 2007). The gained fibers show similar properties as those produced by wet spinning. However, several parameters can be fine-tuned within the microfluidic channels which will allow for more sophisticated spinning processes and, therefore, fibers, in the future.

Transgenic silkworms producing silkworm/spider silk composite fibers

One elegant way to "artificially" spin spider silk fibers is to use transgenic, naturally fiber-producing animals. Silkworms are naturally able to produce and spin silk proteins and they can be genetically modified. Transgenic silkworms were engineered to produce silkworm fibroin/spider silk composite fibers with a spider silk content of 0.4 to 5 % (w/w) (Kuwana et al. 2014; Teule et al. 2012). Importantly, the mechanical properties of silkworm silk (toughness 70 MJ m^{-3}; Gosline et al. 1999) are inferior to those of spider silk (toughness 167 MJ m^{-3}; Heidebrecht et al. 2015), and since the composite material merges the properties of both silks, the mechanical properties of hybrid silkworm/spider silk fibers will always be inferior to those of spider silk. In 2000, Tamura et al. succeeded in a stable germline transformation of the silkworm

Table 1 Overview of wet-spinning conditions used for generating recombinant spider silk fibers

Spinning dope	Max. protein concentration [%]	Coagulation bath	Posttreatment	Source
Aqueous				
160 mM or 1 M urea, 10 mM NaH$_2$PO$_4$, 1 mM Tris, 20 mM NaCl, 10 mM or 100 mM glycine, pH 5.0	25 (after ultrafiltration)	MeOH/H$_2$O mixture	N/A	Arcidiacono et al. (2002)
60 % NaNCS, 20 % acetate solution, mix ratio 8:2 or 10 % LiCl in 90 % formic acid (FA)	30	96 % EtOH	1st draw: 92 % EtOH 2nd draw: 75 % EtOH	Bogush et al. (2009)
50 mM Tris/HCl, pH 8.0 or 50 mM Na-phosphate buffer, pH 7.2	17	IPA/H$_2$O mixture	IPA/H$_2$O mixture	Heidebrecht et al. (2015)
0.1 % propionic acid, 10 mM imidazole; microwaved	12	100 % IPA	1st draw: 80 % IPA 2nd draw: 20 % IPA	Jones et al. (2015)
PBS	28	MeOH/H$_2$O mixture	1st draw: MeOH 2nd draw: H$_2$O	Lazaris et al. (2002)
Organic				
HFIP (5 % v/v added to dope prior to spinning)	15	100 % IPA	80 % IPA	Adrianos et al. (2013)
HFIP (evaporation of HFIP prior to spinning)	60	100 % IPA	85 % IPA, 60 °C	Albertson et al. (2014)
HFIP	30	100 % IPA	75 % IPA	An et al. (2011)
HFIP	12	IPA	N/A	Brooks et al. (2008)
HFIP	10	100 mM ZnCl$_2$, 1 mM FeCl$_3$ in H$_2$O	1st draw: air 2nd draw: 50–70 % EtOH	Lin et al. (2013)
HFIP (addition of 15 % water prior to spinning)	30	90 % IPA	N/A	Teule et al. (2007)
HFIP	15 (10 % silkworm fibroin and 5 % spider silk-like protein)	MeOH	1st: 3 h incubation in MeOH 2nd: drawing in distilled H$_2$O	Zhu et al. (2010)
HFIP	20	90 % MeOH	90 % MeOH	Xia et al. (2010)

MeOH methanol, *EtOH* ethanol, *IPA* isopropyl alcohol, *PBS* phosphate buffered saline, *HFIP* 1,1,1,3,3,3-hexafluoro-2-propanol, *N/A* not applicable

Bombyx mori using a *piggyBac*-derived vector (Tamura et al. 2000). *PiggyBac* is a transposon discovered in the lepidopteran *Trichoplusia ni* (Cary et al. 1989), and vectors based hereon are able to transpose into *B. mori* chromosomes enabling silkworm transformation with various genes encoding fibrous proteins (Tamura et al. 2000). In general, to create transgenic silkworms producing chimeric silkworm/spider silk, genes were designed encoding synthetic spider silk-like sequences, *B. mori* fibroin sequences as well as a *B. mori* promoter, targeting the foreign protein production to the silk gland. Subsequently, these genes were cloned into a *piggyBac*-based vector which was then injected into *B. mori* eggs. Silk fibroin fibers are composed of three proteins, namely fibroin heavy chain (H-chain), fibroin light chain (L-chain), and fibrohexamerin protein (fhx/P25) (Kojima et al. 2007), and they are covered by a sericin layer (Wen et al. 2010). Just like spidroins, silk fibroins consist of a highly repetitive region which is flanked by nonrepetitive amino- and carboxy-terminal domains. Since the H-chain is believed to be mainly

responsible for the mechanical properties of the silk (Kojima et al. 2007), fibroin H-chain genes were modified with spider silk sequences for improved properties (Kuwana et al. 2014; Teule et al. 2012; Zhu et al. 2010). Kuwana et al. (2014) generated three transgenic silkworm strains using a Japanese commercial silkworm strain (C515), two of which contained cDNA of major ampullate spidroins of the spider *Araneus ventricosus*, flanked by the amino- and carboxy-terminal domains of the *B. mori* fibroin H-chain gene. The third strain consisted of a plasmid coding for enhanced green fluorescent protein (EGFP), in order to simplify the analysis of the spun cocoons, subcloned in between the amino- and carboxy-terminal domains of the H-chain gene. After creating transgenic silkworms carrying the modified genes using the *piggyBac*-based vector system, the silkworms produced the modified H-chain/spider silk protein in the silk gland. In the silkworm's gland, the modified H-chain protein dimerized with the fibroin L-chain and was subsequently spun into a cocoon containing the spider dragline protein (Kuwana et al.

2014). Transgenic efficiencies of the strains were 20.0 % for the EGFP-containing strain and 16.7 and 22.6 %, respectively, for the strains containing the spider silk cDNA. Cocoons of the EGFP-transgenic silkworms showed green fluorescence, indicating that the EGFP protein is folded in its functional structure after spinning, suggesting that the spider silk protein may also be present in the cocoon fibers in its natural structure. The maximum amount of the modified H-chain/spider silk protein against the total fibroin was estimated at 0.4–0.6 % (w/w) (Kuwana et al. 2014) and 2-5 % (w/w) (Teule et al. 2012).

Alternatively, the sericin promoter has been used to target spider dragline silk proteins toward the outer sericin layer of the silk fiber (Wen et al. 2010). Whereas the breaking strain of the composite fiber was similar to that of natural spider silk fibers, the breaking stress and toughness were increased compared to that of natural silkworm silk, but the average values were still well below those of natural spider silk fibers (Teule et al. 2012). Theoretically, a breaking stress of cocoon silk equal to that of spider dragline silk could be achieved if the spidroin content was raised to 5–8 % (Kuwana et al. 2014), but this has not been shown experimentally, yet.

Properties of reconstituted vs. recombinant fibers

In order to establish processing technologies for gaining biomimetic spider silk fibers, two research groups used reconstituted *Nephila* spp. dragline silk for fiber spinning (Seidel et al. 2000; Shao et al. 2003). The best performing fibers, in terms of mechanical properties, were obtained by drawing the fibers in air after spinning, soaking them in water, and then drawing them in air again. These fibers exhibited a strength of 320 MPa, a Young's modulus of 8 GPa, and an extensibility of 100 % (Seidel et al. 2000). In comparison to natural dragline fibers, these fibers were much more extensible, but had a lower strength. Hand-drawn fibers of reconstituted *Nephila edulis* dragline silk yielded fibers showed natural dragline-like extensibility (10–27 %) and Young's modulus (6 GPa), but a breaking strength (100–140 MPa) that was well below that of the natural dragline fibers (Shao et al. 2003). Generally, achieving man-made fibers with a breaking stress in the regime of natural spider silk fibers seems to be the greatest challenge. Since the amount of natural and, therefore, also reconstituted, spider silk is quite limited due to the facts as mentioned above, the generation of recombinant (i.e., artificial) silk fibers is the only meaningful route toward large-scale applications. In several attempts, extensibility (1.2–302 %) and Young's modulus (0.04–21 GPa) of artificial spider silk fibers have been highly variable, reaching lower as well as higher values in comparison to natural spider silk fibers (24 % and 8 GPa). On the other hand, the strength even of the best performing fibers achieved values far

below those of natural spider silk fibers. The highest strength (660 MPa) was achieved by silkworm/spider silk composite fibers, but since these fibers were only extensible up to 19 % (Wen et al. 2010), the toughness was far below that of natural spider silk fibers. In comparison, the highest strength (508 MPa) of recombinant spider silk fibers was achieved by wet spinning of proteins with a molecular weight of 285 kDa containing only amino acid motifs based on the core domain of natural spidroins (Xia et al. 2010). The highest toughness (189 MJ m^{-3}), on the other hand, was observed with fibers wet-spun from a self-assembled aqueous spinning dope of a 134-kDa protein containing all three functional domains: the highly repetitive core domain as well as the helical amino- and carboxy-terminal domains (Heidebrecht et al. 2015).

Tensile testing of electrospun, recombinant fibers also showed, not surprisingly, inferior mechanical properties in comparison to those of natural spider silk fibers (Bogush et al. 2009; Zhu et al. 2015). But in this case, mechanics can be neglected, since electrospun fibers are commonly applied as nonwoven meshes used for biomedical or for filter applications without the need of nature-like mechanical properties. In this context, biocompatibility is the more important feature of spider silks. In general, fibers produced from both reconstituted and recombinant spidroins exhibited good biomedical properties. For instance, fibers electrospun from reconstituted *A. ventricosus* major ampullate spidroins revealed a very low degradation rate and showed a good biocompatibility with PC 12 cells (Yu et al. 2014). Cell attachment and proliferation experiments of BALB/3T3 mouse fibroblasts on nonwoven meshes spun from recombinant spidroins showed cell alignment along individual fibers as well as a protrusion of filopodia/lamellipodia through the interstitial space between the fibers (Leal-Egana et al. 2012). Electrospinning of recombinant spidroins hybridized with the cell binding sequence RGD even induced the differentiation of bone marrow-derived, human mesenchymal stem cells (hMSCs) to osteogenic outcomes (Bini et al. 2006). Also, self-assembled recombinant spidroin fibers implanted subcutaneously in rats did not show any negative systemic or local reactions (Fredriksson et al. 2009), suggesting these fibers to be biocompatible. Additionally, fiber bundles thereof seem to support the formation of vascularized tissue formation, since already 1 week after implantation, new capillaries and fibroblast-like cells formed in the center of such fiber bundles (Fredriksson et al. 2009).

"Not to spin": artificial assembly morphologies

Recombinant spider silk proteins can be processed into more than fibers; other morphologies such as particles, foams, films, or hydrogels can also be fabricated, all of which have a high

application potential (Hardy and Scheibel 2010; Hermanson et al. 2007; Slotta et al. 2008; Spiess et al. 2010a, b). Processing of recombinant spider silk proteins in aqueous solutions can be triggered by changes in the pH value, amount and type of additives (e.g., potassium phosphate, alcohols, or polymers), mechanical shear, or temperature changes. Alternatively, organic solvents such as HFIP or FA can be used; however, the choice of solvent has a significant impact on structure formation. While aqueous processing leads mainly to particle and hydrogel formation, water-soluble films are mainly produced using fast-evaporating organic solvents. Here, posttreatment procedures with agents, like potassium phosphate or monohydric alcohols (methanol, ethanol, isopropanol), are necessary to render the films insoluble in water (Exler et al. 2007; Huemmerich et al. 2004a, b; Lammel et al. 2008; Numata et al. 2010; Rammensee et al. 2008; Rising 2014; Scheibel 2004; Slotta et al. 2007; Spiess et al. 2010b).

Particles

Spidroin particles are produced in a simple, aqueous process by the addition of high concentrations of kosmotropic salts, like potassium phosphate, and fast mixing. This procedure results in solid particles with high β-sheet content, a smooth surface (Hofer et al. 2012; Lammel et al. 2008; Slotta et al. 2008), and particle sizes between 250 nm and 3 μm depending on the mixing intensity, protein concentration, and the concentration of kosmotropic salts (Lammel et al. 2008; Slotta et al. 2008; Spiess et al. 2010a). Using ionic liquids instead of aqueous buffers and high potassium phosphate concentrations to induce phase separation and nucleation in the protein solution or ultrasonication for particle production allowed enhanced size control and a reduced polydispersity index (Elsner et al. 2015; Lucke et al. 2015). eADF4(C16) (engineered *Araneus diadematus* fibroin 4) particles show a brush-like outer layer with protruding protein strands and a thickness of 30–50 nm covering a solid inner core (Helfricht et al. 2013). Importantly, no posttreatment with dehydrating agents is necessary to obtain water-insoluble particles, since the β-sheet content is high after the salting-out process (Slotta et al. 2008). Further, it has been shown that particles made of recombinant spider silk proteins exhibit an extraordinary mechanical stability when analyzed in dry state. In a swollen, hydrated state, these particles exhibited a different mechanical behavior: the elastic modulus was three orders of magnitude lower (E modulus dry, 0.8±0.5 GPa; E modulus hydrated, 2.99±0.90 MPa). Further, when dry, the particles deformed in a plastic response, and when hydrated, they showed a reversible, elastic deformation behavior. In both states, dry and hydrated, the mechanical properties were dependent on the molecular weight of the spidroin: The higher the molecular weight, the better the mechanical stability (Neubauer et al. 2013).

Particles made of recombinant spider silk proteins are suitable for a large variety of applications. Due to their enhanced mechanical properties, these particles can be used, for example, as filler for composite materials. Additionally, due to their favorable properties in a physiological environment (nontoxic, biodegradable, etc.), these particles could be used as carriers of different substances, for example in drug delivery. Silk particles retain their properties for a limited period of time in the human body before they gradually decompose into degradation products which can be eliminated (Altman et al. 2003; George and Abraham 2006; Liu et al. 2005; Müller-Herrmann and Scheibel 2015).

Uptake and release studies of small molecules with model drugs showed that these types of molecular entities can be incorporated either by diffusion or by coprecipitation of both the spidroin and the drug substance. While the latter increased the loading efficiency of the particles, it did not significantly influence the release rate. Importantly, drugs can be only loaded into spidroin particles if there is no electrostatic repulsion. In this context, only positively and neutrally charged drugs can be loaded onto negatively charged spider silk protein particles, such as those made of eADF4(C16) (Blüm and Scheibel 2012; Doblhofer and Scheibel 2015; Lammel et al. 2011). Since protein design allowed the production of positively charged spider silk proteins, particles made thereof were also able to uptake negatively charged small molecules as well as large oligonucleotides (Doblhofer and Scheibel 2015).

One important justification for the use of silk-based drug delivery vehicles is the ability to design the underlying proteins for a specific target, for example uptake by a specific cell type. Previous investigations showed that, in general, negatively charged spider silk particles have a low uptake efficiency by mammalian cells. Therefore, cell penetrating peptides (CPP) as well as an Arg8-TAG or a RGD sequence were engineered to the N- and C-termini of eADF4(C16). The presence of CPP increased the number of incorporated particles in HeLa cells; however, the mechanism behind the increased uptake was surprisingly mainly the particle's surface charge, not the presented surface peptide (Elsner et al. 2015).

Films

The first studies on films made of spider silk proteins were reported in 2002 by Chen et al. where the salt-controlled structural conversion of natural spider silk proteins obtained from the major ampullate gland of *Nephila senegalensis* was investigated (Chen et al. 2002). Films made of recombinant spider silk proteins first gained attention in 2005 where it was shown that these spider silk-like proteins undergo a similar structural conversion from random coil to β-sheet rich. Recombinantly produced engineered spider silk protein films turned out to be

transparent and chemically stable under ambient conditions, depending on their processing (Huemmerich et al. 2006; Slotta et al. 2006; Spiess et al. 2010b). Two major components determine the properties of these films: the molecular structure including the secondary structure and intermolecular as well as intramolecular interactions as well as the macroscopic structure reflecting the material's interface with the environment (Spiess et al. 2010a).

Depending on the solvent, spider silk proteins in solution adopt mainly an α-helical or random coil conformation which is often maintained in as-cast films (Borkner et al. 2014; Slotta et al. 2006). These as-cast films are water soluble, as mentioned above, due to the weak intermolecular interactions of spider silk proteins in an α-helical conformation. Upon conversion of the protein structure toward a β-sheet-rich structure by using agents like kosmotropic salts or alcohols, water vapor, or temperature annealing, films can be rendered chemically more stable and thereby water insoluble (Huemmerich et al. 2006; Slotta et al. 2006; Spiess et al. 2010b). This is an important quality, as most potential applications of recombinant spider silk films involve interaction with a humid environment. Structural control over synthetic recombinant spider silk proteins is also given by the variation of the amino acid sequence toward a higher number of β-sheet forming building blocks, and with the control of the β-sheet portion, mechanical properties can be predetermined (Rabotyagova et al. 2009, 2010). While the terminal domains of spider silk proteins play an important role in the fiber spinning process, no significant influence of the nonrepetitive regions could be observed during the film casting from organic protein solutions. Nevertheless, as-cast films made of recombinant spider silk proteins containing the NR regions are slightly more chemically stable than those without, though there are no disulfide bridges present (Slotta et al. 2006). Besides chemical stability, the β-sheet content also determines the mechanical properties of a film. With increasing β-sheet content, elastic modulus and strength increase, and there is a loss of elasticity. High amounts of β-sheets, therefore, can be correlated with stiffness and brittleness in silk films (Spiess et al. 2010b). However, as the content of β-sheets can be adjusted by the posttreatment conditions upon varying incubation times of the films in alcohols or posttreatment with water/alcohol mixtures at various ratios lead to a varying β-sheet content, this is not a challenge for tailoring films to specific applications (Spiess et al. 2010a). The water content in silk films plays also an important role; due to its softening effect, it can work as a plasticizer. Another possibility to overcome the brittleness of silk films is to add plasticizers like glycerol. It was reported that glycerol can alter the intermolecular interactions of silk proteins in a film and, therefore, is able to enhance the films' elasticity. The addition of 40 % *w/w* glycerol to an eADF4(C16) film yielded a 10-fold increased elasticity, but also going

along with a 10-fold decrease of the elastic modulus and a slight decrease in strength (Lawrence et al. 2010; Spiess et al. 2010a).

Spider silk protein films can be envisioned for various applications; however, they are especially promising for use in the biomedical field due to their biocompatibility which has been demonstrated in vitro and in vivo (Allmeling et al. 2006, 2008; Gellynck et al. 2008a, b; Hakimi et al. 2010; Vollrath et al. 2002). Conceivable applications are materials for a controlled substance release at a specific site of action in the human body, biomedical sensors, and cell-supporting scaffolds (Hardy et al. 2013; Minoura et al. 1995; Sofia et al. 2001; Vendrely and Scheibel 2007). It is possible, for example, to directly integrate substances (e.g., drugs) into silk films or to load these substances into microparticles that are then embedded in or coated with a silk layer amenable for delayed release (Wang et al. 2007, 2010). Biomedical or biochemical sensors can be fabricated by covalent binding of biologically active compounds to the silk proteins (Lawrence et al. 2008; Spiess et al. 2010b). Cell adhesion on recombinant spider silk protein scaffolds was shown to be very weak (Baoyong et al. 2010); therefore, chemical or genetic coupling of specific functional groups, for example components of the extracellular matrix, and modification of the surface hydrophilicity have been employed to influence the cellular response to a film's surface concerning adhesion, proliferation, and differentiation (Bini et al. 2006; Karageorgiou et al. 2004; Wohlrab et al. 2012a). As mentioned above, the function of silk films can be also partly controlled by the macroscopic structure they adopt. Changing the surface morphology by patterning or partial roughening of a film under different posttreatment conditions can lead to a deviating behavior of cells thereon (Bauer et al. 2013; Borkner et al. 2014). The hydrophilicity of the film surface can easily be affected by the choice of the template for drop-cast films (Wohlrab et al. 2012b). The influence of the template's surface hydrophilicity can be diminished by spin coating of spidroin solutions, since the duration of solvent evaporation determines the rearrangement of silk protein molecules within the films, and their interaction with the underlying substrate and the film properties are in this case determined by the utilized solvent (Metwalli et al. 2007; Wohlrab et al. 2012b). Applications of films made of silk protein in the medical field include coatings for medical devices (Bettinger and Bao 2010; Kim et al. 2010; Zeplin et al. 2014a, b) and skin grafts (Baoyong et al. 2010; Jiang et al. 2007).

In the context of biomedical applications, it is important to mention that recombinant spider silk protein films undergo partial degradation in the presence of wound proteases (~10 %) in a timescale of 15 days, which is in the range of

the initial phase of wound healing (Müller-Herrmann and Scheibel 2015).

Hydrogels

Hydrogels are three-dimensional polymer networks that absorb over 95 % (w/w) of water (Knight et al. 1998; Lee and Mooney 2001; Rammensee et al. 2006; Schacht and Scheibel 2011; Shin et al. 2003). Their porous structure and mechanical properties make them candidates for applications in tissue engineering, drug delivery, or as functional coatings (Rammensee et al. 2006). The mechanical properties of a specific hydrogel are determined by the properties of its individual constituents, and many different polymers, synthetic and natural ones, have been utilized to form hydrogels. Spidroin hydrogels are built upon self-assembly of nanofibrils by a mechanism of nucleation-aggregation followed by a concentration-dependent gelation in which β-sheet-rich spider silk fibrils become entangled to build a stable three-dimensional network (Hu et al. 2010; Rammensee et al. 2006; Schacht et al. 2015; Schacht and Scheibel 2011; Slotta et al. 2008). Spider silk proteins can be processed into stable hydrogels in a controlled manner by adjusting the protein concentration, pH, temperature, ion composition, and concentration (Jones et al. 2015; Schacht and Scheibel 2011; Vepari and Kaplan 2007). Each of these inputs influences the hydrogel's morphology, mechanical properties, and pore size. In particular, increasing the protein concentration and increasing the addition of chemical crosslinkers lead to an increase in mechanical strength, accompanied by a decrease in pore sizes (Schacht and Scheibel 2011). It has been recently shown that recombinant spidroin hydrogels, like many biopolymer hydrogels, show a viscoelastic behavior with stress changes proportional to the linear increasing strain (Mackintosh et al. 1995). In the special case of eADF4 hydrogels, the elastic behavior dominates over the viscous behavior, with low-viscosity flow behavior, good form stability, and a shear thinning effect, allowing their use as bioink in a biofabrication setup. Eukaryotic cells were embedded within the hydrogel prior to printing with a bioplotter and they survived for at least 7 days after printing. The addition of cells did not considerably influence the print-ability of the spider silk protein gels (Schacht et al. 2015).

Foams and sponges

Foams are defined as material containing small bubbles formed on or in a liquid. To produce foams made of spidroin solutions, gas bubbles remain stable when using a high protein concentration, and the foam is established upon drying. In comparison, sponges are, like foams, three-dimensional porous scaffolds, but differ in their production technique and their mechanical properties. Sponges can be produced by

gas foaming, lyophilization, or using porogens. It has been shown for silkworm silk fibroin that porogens like sodium chloride and sugar can be used to produce sponges with defined pore sizes due to silk β-sheet formation around the porogen. Therefore, the pores are the size of the porogen in case of organic protein solutions and 80–90 % of the size of the porogen in aqueous solutions (Kim et al. 2005). As a consequence, it is even possible to produce pore size gradients by stacking porogens with different diameters (Kim et al. 2005; Nazarov et al. 2004; Vepari and Kaplan 2007). Foams and sponges are both qualified for cell culture applications due to the ability of good transportation of nutrients and metabolic waste through the material in combination with a good structural and mechanical stability (Kluge et al. 2008). While a number of studies on silkworm silk fibroin foams and sponges have been published, spider silk protein foams and sponges remain largely unexplored. Widhe et al. showed in 2010 that their recombinant miniature spider silk protein 4RepCT can be processed into foams which stay microscopically stable in a cell culture medium. The surface of these foams showed heterogeneous pores with diameters between 30 and 200 μm. However, in this pore size range, foams lack a characteristic surface topography which influences cell adhesion (Widhe et al. 2010).

Concerning spider silk sponges, Jones et al. developed a method in which hydrogels were frozen in an aqueous medium and subsequently thawed, resulting in a highly elastic, three-dimensional morphology. Such sponges could uptake water to the extent of hydrogels as well as maintain their form upon compression and drying. That is, the effect of dehydration was completely reversible by the addition of water. The high elasticity of these sponges is based on a lower content of stiffening β-sheet crystals and a higher amount of the elastic random coil and helical structures in comparison to other spider silk scaffolds (Jones et al. 2015).

Composite materials including spider silk

Composites provide the opportunity to produce materials with extraordinary properties by complementation of at least two different kinds of materials. In this context, natural as well as recombinant spider silk materials can play a role due to their outstanding mechanical and biocompatible properties. In some studies, naturally spun spider dragline silks were used to assemble composites with inorganic nanoparticles to reinforce the fibers. Recently, it was shown that feeding spiders with carbon nanotubes or graphene dispersions led to carbon-reinforced silk threads (Lepore et al. 2015). Despite that, most approaches to enhance mechanical strength of spider dragline silk were employed after collection of the silk by forced silking. Dragline silk was used as template for the insertion of zinc (Zn), titanium (Ti), and aluminum (Al) by multiple pulsed vapor-phase infiltration (MPI). This treatment

increased the toughness of the spider silk fibers by almost 10-fold and the E moduli of the fibers from 9.7 to 68 GPa, in the best case (Lee et al. 2009).

Spider silk composite production allows not only to increase its mechanical strength but also to extend the range of applications. Dragline silk fibers, for instance, were incubated in chloroauric acid to assemble gold nanoparticles on their surface with the goal of producing water and methanol vapor sensors with a response time of about 10 s and 150-fold change of conductivity. Their supercontraction behavior in the presence of water and methanol vapor led to a change in the distance of the gold nanoparticles and, therefore, altered the electrical conductivity of the fibers (Hardy and Scheibel 2010; Singh et al. 2007). Electrical conductivity was also introduced into spider silk fibers by deposition of amine-functionalized multiwalled carbon nanotubes (MWCNT) onto their surface. In this study, additionally, an increase in mechanical strength was observed for the composite fibers. The combination of properties allowed an extended application of the material in various technical approaches (Steven et al. 2013). The accumulation of calcium carbonate or hydroxyapatite (HAP) on naturally spun fibers enabled producing new scaffolds for bone tissue engineering or building blocks for bone replacement materials (Cao and Mao 2007; Mehta and Hede 2005). In the case of hydroxyapatite deposition, oriented crystal growth was obtained being consistent with the orientation of β-sheet crystals in the silk fibers (Cao and Mao 2007). In another approach, naturally spun spider silk was solubilized in FA for electrospinning. By mixing the resulting protein solution with a poly(D,L-lactic acid) (PDLLA) FA solution and subsequent electrospinning, nonwoven meshes with core-shell structured fibers with a diameter range of about 90–1000 nm were produced. The size of the fibers was tuned by the weight ratio of the two material components in the spinning solution (Zhou et al. 2008).

Recombinant spider silk proteins have been used in blends with polycaprolactone (PCL) and thermoplastic polyurethane (TPU) to cast films with a higher elasticity than nonblended spider silk protein films. Good cell adhesion, proliferation, and the possibility to incorporate drugs in these composite films endorse them as candidates for implant coatings or as scaffolds for tissue engineering (Hardy et al. 2013). Another filler material used in spider silk protein films were carbon nanotubes. Composite films made of recombinant spider silk proteins and single-walled carbon nanotubes led to excellent mechanical properties as a result of the transfer of stress in the matrix to the filler and of the potential for extensive reorganization of the matrix at applied high stress (Blond et al. 2007).

Blended dopes of recombinant spider silk with collagen or gelatin have also been used for electrospinning processes. The resulting composite nonwoven meshes were predominantly used in tissue engineering. Electrospinning of a mixture of spider silk proteins and collagen led to unidirectional, partially crosslinked fiber scaffolds usable in stem cell differentiation and in neural tissue engineering. Collagen-dominant scaffolds were found to provide unique structural, mechanical, and biochemical cues; stem cells were directed to neural differentiation, and the development of long neural filaments along the fibers was facilitated. These neural tissue-like constructs are promising candidates for transplantation in cellular replacement therapies for neurodegenerative disorders such as Alzheimer's or Parkinson's disease (Sridharan et al. 2013; Zhu et al. 2015). Tubular scaffolds made of a blend of recombinant spider silk proteins and gelatins, supported by a polyurethane outer layer, were produced to be used in tissue-engineered vessel grafts (TEVG). The morphological and mechanical characterization of the tubular structures showed strong similarities with the structure of native arteries, both in strength and elasticity. The appearance of RGD sequences in spider silk used for this purpose supported the growth of adult stem cells, yielding a higher cellular content prior to prospective implantation than without the cellular recognition sequence (Zhang et al. 2014).

Modification of recombinant spider silk proteins with specific binding motifs for HAP (Huang et al. 2007), titanium dioxide, germania, and gold could be assembled into various morphologies and provided the control of organic-inorganic interfaces and composite structural features (Belton et al. 2012; Foo et al. 2006; Mieszawska et al. 2010). Silica binding sequences (e.g., R5 from *Cylindrotheka fusiformis*) were used to control silica particle formation and assembly on the surfaces of spider silk films, fibers, and particles. Mineral phase formation, morphology, chemistry, and, therefore, composite properties could be influenced by varying the processing conditions or by sequence alteration. Silica is a critical osteoconductive element, which can be processed under ambient conditions, and has the potential to control the tissue remodeling rate, making this composite a possible scaffold for bone regeneration. Studies with human mesenchymal stem cells (hMSCs) attached to silica/silk films showed upregulation of osteogenic gene markers at high silica contents (Belton et al. 2012; Foo et al. 2006; Mieszawska et al. 2010).

Summary and outlook

Biotechnological production of spider silk proteins and their processing into diverse morphologies (Fig. 4) allow for applications in textile, automotive, and biomedical industries. Concerning the production of artificial spider silk fibers, significant progress has been made in the last years. Since reconstituted spider silk fibers did not show nature-like mechanical properties after spinning, various techniques for biotechnological production (i.e., proteins, transgenic animals, etc.) have been investigated to gain proteins enabling fibers with such features. Regarding the biotechnological production
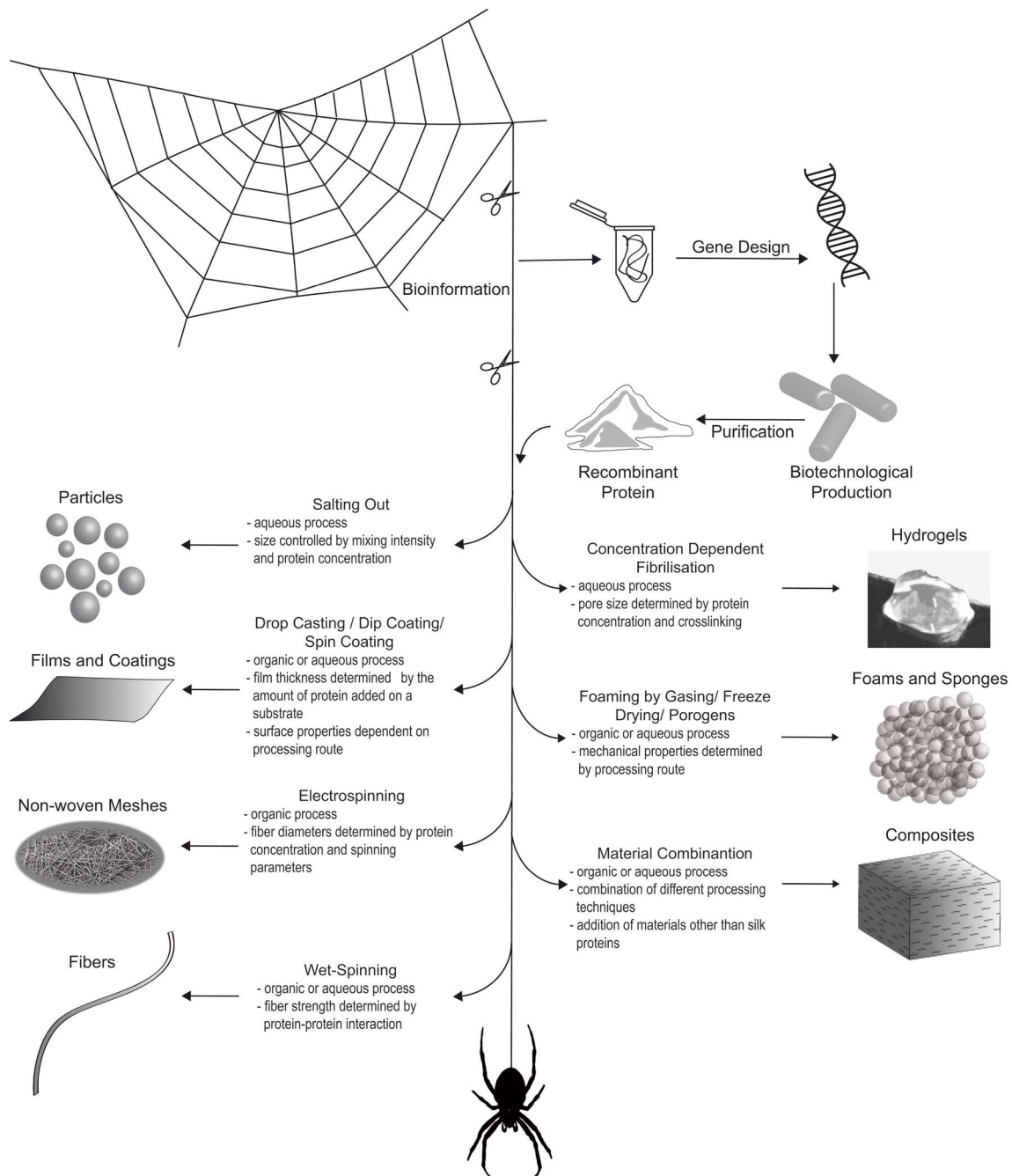
Fig. 4 Design, production, and processing of recombinant spider silk proteins: from identification of the bioinformation given by the natural material produced by a spider, to genetic design of its recombinant counterpart, to possible morphologies

and artificial fiber spinning, great progress was made by analyzing the natural spinning process and the role of the amino- and carboxy-terminal domains. Inclusion of the nonrepetitive terminal domains into the recombinantly produced spider silk proteins and wet spinning these proteins into fibers resulted in a toughness comparable to that of natural fibers. This emphasized the importance of the nonrepetitive terminal domains in the proper alignment of the spidroins, which was neglected in earlier trials. By fine-tuning the composition of the recombinant proteins and the spinning process, artificial spider silk fibers with mechanical properties exceeding those of the natural fibers will be likely possible in the future.

Recombinant production of spider silk proteins does not only offer the option to mimic nature and produce fibers that are similar to their natural counterparts, but it also enables the production of different morphologies. These different structures are biodegradable and biocompatible just like the natural equivalents, but still comprise new properties that lead to

applications in both the medical and the technical field. Particles and films/coatings have already been well-investigated, and this paves the way toward the first applications in drug delivery and cell culture. On the other hand, hydrogels, foams, and sponges require further exploration before they can be used directly in applications. Nevertheless, in all cases, recombinant spider silk protein research tends to explore new tailor-made materials by adapting the morphology's properties to a specific application. The potential of recombinant spider silk proteins in different fields is thereby essentially limitless.

Compliance with ethical standards

Conflict of interest The authors declare that they have no competing interests.

Ethics approval This article does not contain any studies with human participants or animals performed by any of the authors.

References

Adrianos SL, Teule F, Hinman MB, Jones JA, Weber WS, Yarger JL, Lewis RV (2013) *Nephila clavipes* flagelliform silk-like GGX motifs contribute to extensibility and spacer motifs contribute to strength in synthetic spider silk fibers. Biomacromolecules 14:1751–1760. doi:10.1021/bm400125w

Albertson AE, Teule F, Weber W, Yarger JL, Lewis RV (2014) Effects of different post-spin stretching conditions on the mechanical properties of synthetic spider silk fibers. J Mech Behav Biomed Mater 29:225–234. doi:10.1016/j.jmbbm.2013.09.002

Allmeling C, Jokuszies A, Reimers K, Kall S, Vogt PM (2006) Use of spider silk fibres as an innovative material in a biocompatible artificial nerve conduit. J Cell Mol Med 10:770–777. doi:10.2755/jcmm010.003.18

Allmeling C, Jokuszies A, Reimers K, Kall S, Choi CY, Brandes G, Kasper C, Scheper T, Guggenheim M, Vogt PM (2008) Spider silk fibres in artificial nerve constructs promote peripheral nerve regeneration. Cell Prolif 41:408–420. doi:10.1111/j.1365-2184.2008.00534.x

Altman GH, Diaz F, Jakuba C, Calabro T, Horan RL, Chen J, Lu H, Richmond J, Kaplan DL (2003) Silk-based biomaterials. Biomaterials 24:401–416. doi:10.1016/S0142-9612(02)00353-8

An B, Hinman MB, Holland GP, Yarger JL, Lewis RV (2011) Inducing beta-sheets formation in synthetic spider silk fibers by aqueous post-spin stretching. Biomacromolecules 12:2375–2381. doi:10.1021/bm200463e

Andersen SO (1970) Amino acid composition of spider silks. Comp Biochem Physiol 35:705–711. doi:10.1016/0010-406X(70)90988-6

Andersson M, Chen G, Otikovs M, Landreh M, Nordling K, Kronqvist N, Westermark P, Jornvall H, Knight S, Ridderstrale Y, Holm L, Meng Q, Jaudzems K, Chesler M, Johansson J, Rising A (2014) Carbonic anhydrase generates CO2 and H+ that drive spider silk formation via

opposite effects on the terminal domains. PLoS Biol 12:e1001921. doi:10.1371/journal.pbio.1001921

Arcidiacono S, Mello CM, Butler M, Welsh E, Soares JW, Allen A, Ziegler D, Laue T, Chase S (2002) Aqueous processing and fiber spinning of recombinant spider silks. Macromolecules 35:1262–1266. doi:10.1021/Ma011471o

Ayoub NA, Garb JE, Tinghitella RM, Collin MA, Hayashi CY (2007) Blueprint for a high-performance biomaterial: full-length spider dragline silk genes. PLoS ONE 2:e514. doi:10.1371/journal.pone.0000514

Baoyong L, Jian Z, Denglong C, Min L (2010) Evaluation of a new type of wound dressing made from recombinant spider silk protein using rat models. Burns 36:891–896. doi:10.1016/j.burns.2009.12.001

Barr LA, Fahnestock SR, Yang JJ (2004) Production and purification of recombinant DP1B silk-like protein in plants. Mol Breed 13:345–356. doi:10.1016/j.burns.2009.12.001

Bauer F, Wohlrab S, Scheibel T (2013) Controllable cell adhesion, growth and orientation on layered silk protein films. Biomater Sci 1:1244–1249. doi:10.1039/C3bm60114e

Belton DJ, Mieszawska AJ, Currie HA, Kaplan DL, Perry CC (2012) Silk-silica composites from genetically engineered chimeric proteins: materials properties correlate with silica condensation rate and colloidal stability of the proteins in aqueous solution. Langmuir 28:4373–4381. doi:10.1021/La205084z

Bettinger CJ, Bao Z (2010) Biomaterials-based organic electronic devices. Polym Int 59:563–567. doi:10.1002/pi.2827

Bini E, Foo CW, Huang J, Karageorgiou V, Kitchel B, Kaplan DL (2006) RGD-functionalized bioengineered spider dragline silk biomaterial. Biomacromolecules 7:3139–3145. doi:10.1021/bm0607877

Blackledge TA, Hayashi CY (2006) Silken toolkits: biomechanics of silk fibers spun by the orb web spider *Argiope argentata* (Fabricius 1775). J Exp Biol 209:2452–2461. doi:10.1242/jeb.02275

Blond D, McCarthy DN, Blau WJ, Coleman JN (2007) Toughening of artificial silk by incorporation of carbon nanotubes. Biomacromolecules 8:3973–3976. doi:10.1021/Bm700971g

Blüm C, Scheibel T (2012) Control of drug loading and release properties of spider silk sub-microparticles. J Bionanosci 2:67–74. doi:10.1007/s12668-012-0036-7

Bogush VG, Sokolova OS, Davydova LI, Klinov DV, Sidoruk KV, Esipova NG, Neretina TV, Orchanskyi IA, Makeev VY, Tumanyan VG, Shaitan KV, Debabov VG, Kirpichnikov MP (2009) A novel model system for design of biomaterials based on recombinant analogs of spider silk proteins. J Neuroimmune Pharmacol 4:17–27. doi:10.1007/s11481-008-9129-z

Bon M (1710) A discourse upon the usefulness of the silk of spiders. By Monsieur Bon, President of the Court of Accounts, Aydes and Finances, and President of the Royal Society of Sciences at Montpellier. Communicated by the author. Philos Trans R Soc London 27:2–16. doi:10.1098/rstl.1710.0001

Borkner CB, Elsner MB, Scheibel T (2014) Coatings and films made of silk proteins. ACS Appl Mater Interfaces 6:15611–15625. doi:10.1021/Am5008479

Brooks AE, Stricker SM, Joshi SB, Kamerzell TJ, Middaugh CR, Lewis RV (2008) Properties of synthetic spider silk fibers based on *Argiope aurantia* MaSp2. Biomacromolecules 9:1506–1510. doi:10.1021/bm701124p

Brown CP, Harnagea C, Gill HS, Price AJ, Traversa E, Licoccia S, Rosei F (2012) Rough fibrils provide a toughening mechanism in biological fibers. ACS Nano 6:1961–1969. doi:10.1021/nn300130q

Cao B, Mao C (2007) Oriented nucleation of hydroxylapatite crystals on spider dragline silks. Langmuir 23:10701–10705. doi:10.1021/la7014435

Cary LC, Goebel M, Corsaro BG, Wang HG, Rosen E, Fraser MJ (1989) Transposon mutagenesis of baculoviruses: analysis of *Trichoplusia ni* transposon IFP2 insertions within the FP-locus of nuclear

polyhedrosis viruses. Virology 172:156–169. doi:10.1016/0042-6822(89)90117-7

Challis RJ, Goodacre SL, Hewitt GM (2006) Evolution of spider silks: conservation and diversification of the C-terminus. Insect Mol Biol 15:45–56. doi:10.1111/j.1365-2583.2005.00606.x

Chen X, Knight DP, Shao ZZ, Vollrath F (2002) Conformation transition in silk protein films monitored by time-resolved Fourier transform infrared spectroscopy: effect of potassium ions on *Nephila* spidroin films. Biochemistry 41:14944–14950. doi:10.1021/Bi026550m

Craig CL, Riekel C, Herberstein ME, Weber RS, Kaplan D, Pierce NE (2000) Evidence for diet effects on the composition of silk proteins produced by spiders. Mol Biol Evol 17:1904–1913

Denny M (1976) Physical properties of spiders silk and their role in design of orb-webs. J Exp Biol 65:483–506

Doblhofer E, Scheibel T (2015) Engineering of recombinant spider silk proteins allows defined uptake and release of substances. J Pharm Sci 104:988–994. doi:10.1002/jps.24300

Eisoldt L, Hardy JG, Heim M, Scheibel TR (2010) The role of salt and shear on the storage and assembly of spider silk proteins. J Struct Biol 170:413–419. doi:10.1016/j.jsb.2009.12.027

Eisoldt L, Smith A, Scheibel T (2011) Decoding the secrets of spider silk. Mater Today 14:80–86. doi:10.1016/S1369-7021(11)70057-8

Eisoldt L, Thamm C, Scheibel T (2012) The role of terminal domains during storage and assembly of spider silk proteins. Biopolymers 97:355–361. doi:10.1002/bip.22006

Elsner MB, Herold HM, Muller-Herrmann S, Bargel H, Scheibel T (2015) Enhanced cellular uptake of engineered spider silk particles. Biomater Sci 3:543–551. doi:10.1039/C4bm00401a

Exler JH, Hummerich D, Scheibel T (2007) The amphiphilic properties of spider silks are important for spinning. Angew Chem Int Ed 46:3559–3562. doi:10.1002/anie.200604718

Fahnestock SR, Bedzyk LA (1997) Production of synthetic spider dragline silk protein in *Pichia pastoris*. Appl Microbiol Biotechnol 47:33–39

Fahnestock SR, Irwin SL (1997) Synthetic spider dragline silk proteins and their production in *Escherichia coli*. Appl Microbiol Biotechnol 47:23–32

Fahnestock SR, Yao Z, Bedzyk LA (2000) Microbial production of spider silk proteins. Rev Mol Biotechnol 74:105–119. doi:10.1016/S1389-0352(00)00008-8

Foo CWP, Patwardhan SV, Belton DJ, Kitchel B, Anastasiades D, Huang J, Naik RR, Perry CC, Kaplan DL (2006) Novel nanocomposites from spider silk-silica fusion (chimeric) proteins. Proc Natl Acad Sci U S A 103:9428–9433. doi:10.1073/pnas.0601096103

Fox LR (1975) Cannibalism in natural populations. Annu Rev Ecol Syst 6:87–106

Fredriksson C, Hedhammar M, Feinstein R, Nordling K, Kratz G, Johansson J, Huss F, Rising A (2009) Tissue response to subcutaneously implanted recombinant spider silk: an in vivo study. Materials 2:1908–1922. doi:10.3390/Ma2041908

Gellynck K, Verdonk P, Forsyth R, Almqvist KF, Van Nimmen E, Gheysens T, Mertens J, Van Langenhove L, Kiekens P, Verbruggen G (2008a) Biocompatibility and biodegradability of spider egg sac silk. J Mater Sci Mater Med 19:2963–2970. doi:10.1007/s10856-007-3330-0

Gellynck K, Verdonk PCM, Van Nimmen E, Almqvist KF, Gheysens T, Schoukens G, Van Langenhove L, Kiekens P, Mertens J, Verbruggen G (2008b) Silkworm and spider silk scaffolds for chondrocyte support. J Mater Sci Mater Med 19:3399–3409. doi:10.1007/s10856-008-3474-6

George M, Abraham TE (2006) Polyionic hydrocolloids for the intestinal delivery of protein drugs: alginate and chitosan—a review. J Control Release 114:1–14. doi:10.1016/j.jconrel.2006.04.017

Gerritsen VB (2002) The tiptoe of an airbus. Protein Spotlight Swiss Prot 24:1–2

Gosline JM, Guerette PA, Ortlepp CS, Savage KN (1999) The mechanical design of spider silks: from fibroin sequence to mechanical function. J Exp Biol 202:3295–3303

Greiner A, Wendorff JH (2007) Electrospinning: a fascinating method for the preparation of ultrathin fibres. Angew Chem Int Ed 46:5670–5703. doi:10.1002/anie.200604646

Greiner A, Wendorff JH, Yarin AL, Zussman E (2006) Biohybrid nanosystems with polymer nanofibers and nanotubes. Appl Microbiol Biotechnol 71:387–393. doi:10.1007/s00253-006-0356-z

Grip S, Johansson J, Hedhammar M (2009) Engineered disulfides improve mechanical properties of recombinant spider silk. Protein Sci 18:1012–1022. doi:10.1002/Pro.111

Hagn F, Eisoldt L, Hardy JG, Vendrely C, Coles M, Scheibel T, Kessler H (2010) A conserved spider silk domain acts as a molecular switch that controls fibre assembly. Nature 465:239–242. doi:10.1038/Nature08936

Hagn F, Thamm C, Scheibel T, Kessler H (2011) pH-dependent dimerization and salt-dependent stabilization of the N-terminal domain of spider dragline silk—implications for fiber formation. Angew Chem Int Ed 50:310–313. doi:10.1002/anie.201003795

Hakimi O, Gheysens T, Vollrath F, Grahn MF, Knight DP, Vadgama P (2010) Modulation of cell growth on exposure to silkworm and spider silk fibers. J Biomed Mater Res A 92:1366–1372. doi:10.1002/jbm.a.32462

Hardy JG, Scheibel TR (2010) Composite materials based on silk proteins. Prog Polym Sci 35:1093–1115. doi:10.1016/j.progpolymsci.2010.04.005

Hardy JG, Romer LM, Scheibel TR (2008) Polymeric materials based on silk proteins. Polymer 49:4309–4327. doi:10.1016/j.polymer.2008.08.006

Hardy JG, Leal-Eganã A, Scheibel T (2013) Engineered spider silk protein-based composites for drug delivery. Macromol Biosci 13:1431–1437. doi:10.1002/mabi.201300233

Hauptmann V, Weichert N, Rakhimova M, Conrad U (2013) Spider silks from plants—a challenge to create native-sized spidroins. Biotechnol J 8:1183–1192. doi:10.1002/biot.201300204

Hayashi CY, Shipley NH, Lewis RV (1999) Hypotheses that correlate the sequence, structure, and mechanical properties of spider silk proteins. Int J Biol Macromol 24:271–275. doi:10.1016/S0141-8130(98)00089-0

Hedhammar M, Rising A, Grip S, Martinez AS, Nordling K, Casals C, Stark M, Johansson J (2008) Structural properties of recombinant nonrepetitive and repetitive parts of major ampullate spidroin 1 from *Euprosthenops australis*: implications for fiber formation. Biochemistry 47:3407–3417. doi:10.1021/bi702432y

Heidebrecht A, Scheibel T (2013) Recombinant production of spider silk proteins. Adv Appl Microbiol 82:115–153

Heidebrecht A, Eisoldt L, Diehl J, Schmidt A, Geffers M, Lang G, Scheibel T (2015) Biomimetic fibers made of recombinant spidroins with the same toughness as natural spider silk. Adv Mater 27:2189–2194. doi:10.1002/adma.201404234

Heim M, Keerl D, Scheibel T (2009) Spider silk: from soluble protein to extraordinary fiber. Angew Chem Int Ed 48:3584–3596. doi:10.1002/anie.200803341

Helfricht N, Klug M, Mark A, Kuznetsov V, Blum C, Scheibel T, Papastavrou G (2013) Surface properties of spider silk particles in solution. Biomater Sci 1:1166–1171. doi:10.1039/c3bm60109a

Hermanson KD, Huemmerich D, Scheibel T, Bausch AR (2007) Engineered microcapsules fabricated from reconstituted spider silk. Adv Mater 19:1810–1815. doi:10.1002/adma.200602709

Hinman MB, Lewis RV (1992) Isolation of a clone encoding a second dragline silk fibroin. *Nephila clavipes* dragline silk is a two-protein fiber. J Biol Chem 267:19320–19324

Hinman MB, Jones JA, Lewis RV (2000) Synthetic spider silk: a modular fiber. Trends Biotechnol 18:374–379. doi:10.1016/S0167-7799(00)01481-5

Hofer M, Winter G, Myschik J (2012) Recombinant spider silk particles for controlled delivery of protein drugs. Biomaterials 33:1554–1562. doi:10.1016/j.biomaterials.2011.10.053

Hu X, Lu Q, Sun L, Cebe P, Wang X, Zhang X, Kaplan DL (2010) Biomaterials from ultrasonication-induced silk fibroin-hyaluronic acid hydrogels. Biomacromolecules 11:3178–3188. doi:10.1021/bm1010504

Huang J, Wong C, George A, Kaplan DL (2007) The effect of genetically engineered spider silk-dentin matrix protein 1 chimeric protein on hydroxyapatite nucleation. Biomaterials 28:2358–2367. doi:10.1016/j.biomaterials.2006.11.021

Huemmerich D, Helsen CW, Quedzuweit S, Oschmann J, Rudolph R, Scheibel T (2004a) Primary structure elements of spider dragline silks and their contribution to protein solubility. Biochemistry 43:13604–13612. doi:10.1021/Bi048983q

Huemmerich D, Scheibel T, Vollrath F, Cohen S, Gat U, Ittah S (2004b) Novel assembly properties of recombinant spider dragline silk proteins. Curr Biol 14:2070–2074. doi:10.1016/j.cub.2004.11.005

Huemmerich D, Slotta U, Scheibel T (2006) Processing and modification of films made from recombinant spider silk proteins. Appl Phys A Mater Sci Process 82:219–222. doi:10.1007/s00339-005-3428-5

Jestin S, Poulin P (2014) Chapter 6—wet spinning of CNT-based fibers. In: Yin Z, Schulz MJ, Shanov VN (eds) Nanotube superfiber materials. William Andrew Publishing, Boston, pp 167–209. doi:10.1016/B978-1-4557-7863-8.00006-2

Jiang C, Wang X, Gunawidjaja R, Lin YH, Gupta MK, Kaplan DL, Naik RR, Tsukruk VV (2007) Mechanical properties of robust ultrathin silk fibroin films. Adv Funct Mater 17:2229–2237. doi:10.1002/adfm.200601136

Jones JA, Harris TI, Tucker CL, Berg KR, Christy SY, Day BA, Gaztambide DA, Needham NJ, Ruben AL, Oliveira PF, Decker RE, Lewis RV (2015) More than just fibers: an aqueous method for the production of innovative recombinant spider silk protein materials. Biomacromolecules 16:1418–1425. doi:10.1021/acs.biomac.5b00226

Karageorgiou V, Meinel L, Hofmann S, Malhotra A, Volloch V, Kaplan D (2004) Bone morphogenetic protein-2 decorated silk fibroin films induce osteogenic differentiation of human bone marrow stromal cells. J Biomed Mater Res A 71A:528–537. doi:10.1002/jbm.a.30186

Karatzas CN, Turner JD, Karatzas A-L (1999) Production of biofilaments in transgenic animals. Canada Patent

Keten S, Buehler MJ (2008) Geometric confinement governs the rupture strength of H-bond assemblies at a critical length scale. Nano Lett 8:743–748. doi:10.1021/nl0731670

Kiliani OG (1901) II. On traumatic keloid of the median nerve, with observations upon the absorption of silk sutures. Ann Surg 33:13

Kim U-J, Park J, Joo Kim H, Wada M, Kaplan DL (2005) Three-dimensional aqueous-derived biomaterial scaffolds from silk fibroin. Biomaterials 26:2775–2785. doi:10.1016/j.biomaterials.2004.07.044

Kim D-H, Viventi J, Amsden JJ, Xiao J, Vigeland L, Kim Y-S, Blanco JA, Panilaitis B, Frechette ES, Contreras D, Kaplan DL, Omenetto FG, Huang Y, Hwang K-C, Zakin MR, Litt B, Rogers JA (2010) Dissolvable films of silk fibroin for ultrathin conformal bio-integrated electronics. Nat Mater 9:511–517. doi:10.1038/nmat2745

Kluge JA, Rabotyagova O, Leisk GG, Kaplan DL (2008) Spider silks and their applications. Trends Biotechnol 26:244–251. doi:10.1016/j.tibtech.2008.02.006

Knight DP, Vollrath F (1999) Liquid crystals and flow elongation in a spider's silk production line. Proc R Soc London, Ser B 266:519–523. doi:10.1098/rspb.1999.0667

Knight DP, Vollrath F (2001) Changes in element composition along the spinning duct in a *Nephila* spider. Naturwissenschaften 88:179–182

Knight DP, Nash L, Hu XW, Haffegee J, Ho MW (1998) In vitro formation by reverse dialysis of collagen gels containing highly oriented arrays of fibrils. J Biomed Mater Res 41:185–191. doi:10.1002/(sici)1097-4636(199808)41:2<185::aid-jbm2>3.0.co;2-e

Kojima K, Kuwana Y, Sezutsu H, Kobayashi I, Uchino K, Tamura T, Tamada Y (2007) A new method for the modification of fibroin heavy chain protein in the transgenic silkworm. Biosci Biotechnol Biochem 71:2943–2951. doi:10.1271/bbb.70353

Kronqvist N, Otikovs M, Chmyrov V, Chen G, Andersson M, Nordling K, Landreh M, Sarr M, Jornvall H, Wennmalm S, Widengren J, Meng Q, Rising A, Otzen D, Knight SD, Jaudzems K, Johansson J (2014) Sequential pH-driven dimerization and stabilization of the N-terminal domain enables rapid spider silk formation. Nat Commun 5:3254. doi:10.1038/ncomms4254

Kummerlen J, vanBeek JD, Vollrath F, Meier BH (1996) Local structure in spider dragline silk investigated by two-dimensional spin-diffusion nuclear magnetic resonance. Macromolecules 29:2920–2928

Kuwana Y, Sezutsu H, Nakajima K, Tamada Y, Kojima K (2014) High-toughness silk produced by a transgenic silkworm expressing spider (*Araneus ventricosus*) dragline silk protein. PLoS ONE 9:e105325. doi:10.1371/journal.pone.0105325

Lammel A, Schwab M, Slotta U, Winter G, Scheibel T (2008) Processing conditions for the formation of spider silk microspheres. ChemSusChem 1:413–416. doi:10.1002/cssc.200800030

Lammel A, Schwab M, Hofer M, Winter G, Scheibel T (2011) Recombinant spider silk particles as drug delivery vehicles. Biomaterials 32:2233–2240. doi:10.1016/j.biomaterials.2010.11.060

Lang G, Jokisch S, Scheibel T (2013) Air filter devices including non-woven meshes of electrospun recombinant spider silk proteins. J Vis Exp e50492 doi:10.3791/50492

Lawrence BD, Cronin-Golomb M, Georgakoudi I, Kaplan DL, Omenetto FG (2008) Bioactive silk protein biomaterial systems for optical devices. Biomacromolecules 9:1214–1220. doi:10.1021/Bm701235f

Lawrence BD, Wharram S, Kluge JA, Leisk GG, Omenetto FG, Rosenblatt MI, Kaplan DL (2010) Effect of hydration on silk film material properties. Macromol Biosci 10:393–403. doi:10.1002/mabi.200900294

Lazaris A, Arcidiacono S, Huang Y, Zhou JF, Duguay F, Chretien N, Welsh EA, Soares JW, Karatzas CN (2002) Spider silk fibers spun from soluble recombinant silk produced in mammalian cells. Science 295:472–476. doi:10.1126/science.1065780

Leal-Egana A, Lang G, Mauerer C, Wickinghoff J, Weber M, Geimer S, Scheibel T (2012) Interactions of fibroblasts with different morphologies made of an engineered spider silk protein. Adv Eng Mater 14:B67–B75. doi:10.1002/adem.201180072

Lee KY, Mooney DJ (2001) Hydrogels for tissue engineering. Chem Rev 101:1869–1879. doi:10.1021/cr000108x

Lee S-M, Pippel E, Gösele U, Dresbach C, Qin Y, Chandran CV, Bräuniger T, Hause G, Knez M (2009) Greatly increased toughness of infiltrated spider silk. Science 324:488–492. doi:10.1126/science.1168162

Lepore E, Bonaccorso F, Bruna M, Bosia F, Taioli S, Garberoglio G, Ferrari A, Pugno NM (2015) Silk reinforced with graphene or carbon nanotubes spun by spiders. arXiv preprint arXiv:150406751

Lewis RV (1992) Spider silk: the unraveling of a mystery. Acc Chem Res 25:392–398. doi:10.1021/ar00021a002

Lewis R (1996) Unraveling the weave of spider silk. Bioscience 46:636–638

Lin Z, Deng Q, Liu XY, Yang D (2013) Engineered large spider eggcase silk protein for strong artificial fibers. Adv Mater 25:1216–1220. doi:10.1002/adma.201204357

Liu X, Sun Q, Wang H, Zhang L, Wang JY (2005) Microspheres of corn protein, zein, for an ivermectin drug delivery system. Biomaterials 26:109–115. doi:10.1016/j.biomaterials.2004.02.013

Lucke M, Winter G, Engert J (2015) The effect of steam sterilization on recombinant spider silk particles. Int J Pharm 481:125–131. doi:10.1016/j.ijpharm.2015.01.024

Mackintosh FC, Kas J, Janmey PA (1995) Elasticity of semiflexible biopolymer networks. Phys Rev Lett 75:4425–4428

Madsen B, Shao ZZ, Vollrath F (1999) Variability in the mechanical properties of spider silks on three levels: interspecific, intraspecific and intraindividual. Int J Biol Macromol 24:301–306

Mehta N, Hede S (2005) Spider silk calcite composite. Hypothesis 3:21. doi:10.1021/nn204506d

Menassa R, Hong Z, Karatzas CN, Lazaris A, Richman A, Brandle J (2004) Spider dragline silk proteins in transgenic tobacco leaves: accumulation and field production. Plant Biotechnol J 2:431–438. doi:10.1111/j.1467-7652.2004.00087.x

Metwalli E, Slotta U, Darko C, Roth SV, Scheibel T, Papadakis CM (2007) Structural changes of thin films from recombinant spider silk proteins upon post-treatment. Appl Phys A Mater Sci Process 89:655–661. doi:10.1007/s00339-007-4265-5

Mieszawska AJ, Fourligas N, Georgakoudi I, Ouhib NM, Belton DJ, Perry CC, Kaplan DL (2010) Osteoinductive silk-silica composite biomaterials for bone regeneration. Biomaterials 31:8902–8910. doi:10.1016/j.biomaterials.2010.07.109

Minoura N, Aiba S, Gotoh Y, Tsukada M, Imai Y (1995) Attachment and growth of cultured fibroblast cells on silk protein matrices. J Biomed Mater Res 29:1215–1221

Motriuk-Smith D, Smith A, Hayashi CY, Lewis RV (2005) Analysis of the conserved N-terminal domains in major ampullate spider silk proteins. Biomacromolecules 6:3152–3159. doi:10.1021/bm050472b

Müller-Herrmann S, Scheibel T (2015) Enzymatic degradation of films, particles, and nonwoven meshes made of a recombinant spider silk protein. ACS Biomater Sci Eng 1:247–259. doi:10.1021/ab500147u

Munch E, Launey ME, Alsem DH, Saiz E, Tomsia AP, Ritchie RO (2008) Tough, bio-inspired hybrid materials. Science 322:1516–1520. doi:10.1126/science.1164865

Nazarov R, Jin H-J, Kaplan DL (2004) Porous 3-D scaffolds from regenerated silk fibroin. Biomacromolecules 5:718–726. doi:10.1021/bm034327e

Neubauer MP, Blum C, Agostini E, Engert J, Scheibel T, Fery A (2013) Micromechanical characterization of spider silk particles. Biomater Sci 1:1160–1165. doi:10.1039/c3bm60108k

Numata K, Hamasaki J, Subramanian B, Kaplan DL (2010) Gene delivery mediated by recombinant silk proteins containing cationic and cell binding motifs. J Control Release 146:136–143. doi:10.1016/j.jconrel.2010.05.006

Papadopoulos P, Solter J, Kremer F (2007) Structure-property relationships in major ampullate spider silk as deduced from polarized FTIR spectroscopy. Eur Phys J E: Soft Matter Biol Phys 24:193–199. doi:10.1140/epje/i2007-10229-9

Peng H, Zhou S, Jiang J, Guo T, Zheng X, Yu X (2009) Pressure-induced crystal memory effect of spider silk proteins. J Phys Chem B 113:4636–4641. doi:10.1021/jp811461b

Perez-Rigueiro J, Elices M, Guinea GV, Plaza GR, Karatzas C, Riekel C, Agullo-Rueda F, Daza R (2011) Bioinspired fibers follow the track of natural spider silk. Macromolecules 44:1166–1176. doi:10.1021/ma102291m

Rabotyagova OS, Cebe P, Kaplan DL (2009) Self-assembly of genetically engineered spider silk block copolymers. Biomacromolecules 10:229–236. doi:10.1021/bm800930x

Rabotyagova OS, Cebe P, Kaplan DL (2010) Role of polyalanine domains in beta-sheet formation in spider silk block copolymers. Macromol Biosci 10:49–59. doi:10.1002/mabi.200900203

Radtke C, Allmeling C, Waldmann K-H, Reimers K, Thies K, Schenk HC, Hillmer A, Guggenheim M, Brandes G, Vogt PM (2011) Spider silk constructs enhance axonal regeneration and remyelination in long nerve defects in sheep. PLoS ONE 6:e16990. doi:10.1371/journal.pone.0016990

Rammensee S, Huemmerich D, Hermanson KD, Scheibel T, Bausch AR (2006) Rheological characterization of hydrogels formed by recombinantly produced spider silk. Appl Phys A Mater Sci Process 82:261–264. doi:10.1007/s00339-005-3431-x

Rammensee S, Slotta U, Scheibel T, Bausch AR (2008) Assembly mechanism of recombinant spider silk proteins. Proc Natl Acad Sci U S A 105:6590–6595. doi:10.1073/pnas.0709246105

Rising A (2014) Controlled assembly: a prerequisite for the use of recombinant spider silk in regenerative medicine? Acta Biomater 10:1627–1631. doi:10.1016/j.actbio.2013.09.030

Rising A, Johansson J (2015) Toward spinning artificial spider silk. Nat Chem Biol 11:309–315. doi:10.1038/nchembio.1789

Rising A, Hjalm G, Engstrom W, Johansson J (2006) N-terminal nonrepetitive domain common to dragline, flagelliform, and cylindriform spider silk proteins. Biomacromolecules 7:3120–3124. doi:10.1021/bm060693x

Roemer L, Scheibel T (2007) Basis for new material—spider silk protein. Chem Unserer Zeit 41:306–314

Schacht K, Scheibel T (2011) Controlled hydrogel formation of a recombinant spider silk protein. Biomacromolecules 12:2488–2495. doi:10.1021/bm200154k

Schacht K, Jüngst T, Schweinlin M, Ewald A, Groll J, Scheibel T (2015) Biofabrication of cell-loaded 3D spider silk constructs. Angew Chem Int Ed 54:2816–2820. doi:10.1002/anie.201409846

Scheibel T (2004) Spider silks: recombinant synthesis, assembly, spinning, and engineering of synthetic proteins. Microb Cell Factories 3:14. doi:10.1186/1475-2859-3-14

Seidel A, Liivak O, Jelinski LW (1998) Artificial spinning of spider silk. Macromolecules 31:6733–6736. doi:10.1021/Ma9808880

Seidel A, Liivak O, Calve S, Adaska J, Ji GD, Yang ZT, Grubb D, Zax DB, Jelinski LW (2000) Regenerated spider silk: processing, properties, and structure. Macromolecules 33:775–780. doi:10.1021/Ma990893j

Shao ZZ, Vollrath F, Yang Y, Thogersen HC (2003) Structure and behavior of regenerated spider silk. Macromolecules 36:1157–1161. doi:10.1021/Ma0214660

Shin H, Jo S, Mikos AG (2003) Biomimetic materials for tissue engineering. Biomaterials 24:4353–4364

Simmons AH, Michal CA, Jelinski LW (1996) Molecular orientation and two-component nature of the crystalline fraction of spider dragline silk. Science 271:84–87

Singh A, Hede S, Sastry M (2007) Spider silk as an active scaffold in the assembly of gold nanoparticles and application of the gold–silk bioconjugate in vapor sensing. Small 3:466–473. doi:10.1002/smll.200600413

Slotta U, Tammer M, Kremer F, Koelsch P, Scheibel T (2006) Structural analysis of spider silk films. Supramol Chem 18:465–471. doi:10.1080/10610270600832042

Slotta U, Hess S, Spiess K, Stromer T, Serpell L, Scheibel T (2007) Spider silk and amyloid fibrils: a structural comparison. Macromol Biosci 7:183–188. doi:10.1002/mabi.200600201

Slotta UK, Rammensee S, Gorb S, Scheibel T (2008) An engineered spider silk protein forms microspheres. Angew Chem Int Ed 47:4592–4594. doi:10.1002/anie.200800683

Smit E, Buttner U, Sanderson RD (2005) Continuous yarns from electrospun fibers. Polymer 46:2419–2423. doi:10.1016/j.polymer.2005.02.002

Smith A, Scheibel T (2013) Basis for new material—spider silk protein. In: Fratzl P, Dunlop J, Weinkamer R (eds) Materials design inspired by nature: function through inner architecture. RSC smart materials,

vol 4. RSC Publishing, Cambridge, pp 256–281. doi:10.1039/9781849737555-00256

Sofia S, McCarthy MB, Gronowicz G, Kaplan DL (2001) Functionalized silk-based biomaterials for bone formation. J Biomed Mater Res 54:139–148. doi:10.1002/1097-4636(200101)54:1<139

Sørensen HP, Mortensen KK (2005) Advanced genetic strategies for recombinant protein expression in *Escherichia coli*. J Biotechnol 115:113–128. doi:10.1016/j.jbiotec.2004.08.004

Spiess K, Lammel A, Scheibel T (2010a) Recombinant spider silk proteins for applications in biomaterials. Macromol Biosci 10:998–1007. doi:10.1002/mabi.201000071

Spiess K, Wohlrab S, Scheibel T (2010b) Structural characterization and functionalization of engineered spider silk films. Soft Matter 6:4168–4174. doi:10.1039/b927267d

Sponner A, Vater W, Monajembashi S, Unger E, Grosse F, Weisshart K (2007) Composition and hierarchical organisation of a spider silk. PLoS ONE 2:e998. doi:10.1371/journal.pone.0000998

Sridharan I, Kim T, Strakova Z, Wang R (2013) Matrix-specified differentiation of human decidua parietalis placental stem cells. Biochem Biophys Res Commun 437:489–495. doi:10.1016/j.bbrc.2013.07.002

Stark M, Grip S, Rising A, Hedhammar M, Engstrom W, Hjalm G, Johansson J (2007) Macroscopic fibers self-assembled from recombinant miniature spider silk proteins. Biomacromolecules 8:1695–1701. doi:10.1021/Bm070049y

Steinkraus HB, Rothfuss H, Jones JA, Dissen E, Shefferly E, Lewis RV (2012) The absence of detectable fetal microchimerism in nontransgenic goats (*Capra aegagrus hircus*) bearing transgenic offspring. J Anim Sci 90:481–488. doi:10.2527/jas.2011-4034

Stephens JS, Fahnestock SR, Farmer RS, Kiick KL, Chase DB, Rabolt JF (2005) Effects of electrospinning and solution casting protocols on the secondary structure of a genetically engineered dragline spider silk analogue investigated via Fourier transform Raman spectroscopy. Biomacromolecules 6:1405–1413. doi:10.1021/Bm049296h

Steven E, Saleh WR, Lebedev V, Acquah SFA, Laukhin V, Alamo RG, Brooks JS (2013) Carbon nanotubes on a spider silk scaffold. Nat Commun 4:2435. doi:10.1038/ncomms3435

Tamura T, Thibert C, Royer C, Kanda T, Abraham E, Kamba M, Komoto N, Thomas JL, Mauchamp B, Chavancy G, Shirk P, Fraser M, Prudhomme JC, Couble P (2000) Germline transformation of the silkworm *Bombyx mori* L. using a *piggyBac* transposon-derived vector. Nat Biotechnol 18:81–84. doi:10.1038/71978

Teo WE, Ramakrishna S (2006) A review on electrospinning design and nanofibre assemblies. Nanotechnology 17:R89–R106. doi:10.1088/0957-4484/17/14/R01

Teule F, Furin WA, Cooper AR, Duncan JR, Lewis RV (2007) Modifications of spider silk sequences in an attempt to control the mechanical properties of the synthetic fibers. J Mater Sci 42:8974–8985. doi:10.1007/s10853-007-1642-6

Teule F, Cooper AR, Furin WA, Bittencourt D, Rech EL, Brooks A, Lewis RV (2009) A protocol for the production of recombinant spider silk-like proteins for artificial fiber spinning. Nat Protoc 4:341–355. doi:10.1038/nprot.2008.250

Teule F, Miao YG, Sohn BH, Kim YS, Hull JJ, Fraser MJ, Lewis RV, Jarvis DL (2012) Silkworms transformed with chimeric silkworm/spider silk genes spin composite silk fibers with improved mechanical properties. Proc Natl Acad Sci U S A 109:923–928. doi:10.1073/pnas.1109420109

Um IC, Ki CS, Kweon H, Lee KG, Ihm DW, Park YH (2004) Wet spinning of silk polymer. II. Effect of drawing on the structural characteristics and properties of filament. Int J Biol Macromol 34:107–119. doi:10.1016/j.ijbiomac.2004.03.011

van Beek JD, Hess S, Vollrath F, Meier BH (2002) The molecular structure of spider dragline silk: folding and orientation of the protein backbone. Proc Natl Acad Sci U S A 99:10266–10271. doi:10.1073/pnas.152162299

Vendrely C, Scheibel T (2007) Biotechnological production of spider-silk proteins enables new applications. Macromol Biosci 7:401–409. doi:10.1002/mabi.200600255

Vepari C, Kaplan DL (2007) Silk as a biomaterial. Prog Polym Sci 32:991–1007. doi:10.1016/j.progpolymsci.2007.05.013

Viney C (1997) Natural silks: archetypal supramolecular assembly of polymer fibres. Supramol Sci 4:75–81

Vollrath F (2000) Strength and structure of spiders' silks. J Biotechnol 74:67–83. doi:10.1016/S1389-0352(00)00006-4

Vollrath F, Knight DP (1999) Structure and function of the silk production pathway in the spider *Nephila edulis*. Int J Biol Macromol 24:243–249. doi:10.1016/S0141-8130(98)00095-6

Vollrath F, Knight DP (2001) Liquid crystalline spinning of spider silk. Nature 410:541–548. doi:10.1038/35069000

Vollrath F, Barth P, Basedow A, Engstrom W, List H (2002) Local tolerance to spider silks and protein polymers in vivo. In vivo 16:229–234

Wang X, Wenk E, Matsumoto A, Meinel L, Li C, Kaplan DL (2007) Silk microspheres for encapsulation and controlled release. J Control Release 117:360–370. doi:10.1016/j.jconrel.2006.11.021

Wang X, Yucel T, Lu Q, Hu X, Kaplan DL (2010) Silk nanospheres and microspheres from silk/PVA blend films for drug delivery. Biomaterials 31:1025–1035. doi:10.1016/j.biomaterials.2009.11.002

Wen HX, Lan XQ, Zhang YS, Zhao TF, Wang YJ, Kajiura Z, Nakagaki M (2010) Transgenic silkworms (*Bombyx mori*) produce recombinant spider dragline silk in cocoons. Mol Biol Rep 37:1815–1821. doi:10.1007/s11033-009-9615-2

Wendt H, Hillmer A, Reimers K, Kuhbier JW, Schafer-Nolte F, Allmeling C, Kasper C, Vogt PM (2011) Artificial skin—culturing of different skin cell lines for generating an artificial skin substitute on cross-weaved spider silk fibres. PLoS ONE 6:e21833. doi:10.1371/journal.pone.0021833

Widhe M, Bysell H, Nystedt S, Schenning I, Malmsten M, Johansson J, Rising A, Hedhammar M (2010) Recombinant spider silk as matrices for cell culture. Biomaterials 31:9575–9585. doi:10.1016/j.biomaterials.2010.08.061

Wohlrab S, Müller S, Schmidt A, Neubauer S, Kessler H, Leal-Egaña A, Scheibel T (2012a) Cell adhesion and proliferation on RGD-modified recombinant spider silk proteins. Biomaterials 33:6650–6659. doi:10.1016/j.biomaterials.2012.05.069

Wohlrab S, Spieß K, Scheibel T (2012b) Varying surface hydrophobicities of coatings made of recombinant spider silk proteins. J Mater Chem 22:22050–22054. doi:10.1039/C2JM35075K

Wong Po Foo C, Patwardhan SV, Belton DJ, Kitchel B, Anastasiades D, Huang J, Naik RR, Perry CC, Kaplan DL (2006) Novel nanocomposites from spider silk-silica fusion (chimeric) proteins. Proc Natl Acad Sci U S A 103:9428–9433. doi:10.1073/pnas.0601096103

Xia X-X, Qian Z-G, Ki CS, Park YH, Kaplan DL, Lee SY (2010) Native-sized recombinant spider silk protein produced in metabolically engineered *Escherichia coli* results in a strong fiber. Proc Natl Acad Sci U S A 107:14059–14063. doi:10.1073/pnas.1003366107

Xu M, Lewis RV (1990) Structure of a protein superfiber: spider dragline silk. Proc Natl Acad Sci 87:7120–7124

Xu HT, Fan BL, Yu SY, Huang YH, Zhao ZH, Lian ZX, Dai YP, Wang LL, Liu ZL, Fei J, Li N (2007) Construct synthetic gene encoding artificial spider dragline silk protein and its expression in milk of transgenic mice. Anim Biotechnol 18:1–12. doi:10.1080/10495390601091024

Yu Q, Xu S, Zhang H, Gu L, Xu Y, Ko F (2014) Structure-property relationship of regenerated spider silk protein nano/microfibrous scaffold fabricated by electrospinning. J Biomed Mater Res Part A 102:3828–3837. doi:10.1002/jbm.a.35051

Zarkoob S, Eby RK, Reneker DH, Hudson SD, Ertley D, Adams WW (2004) Structure and morphology of electrospun silk nanofibers. Polymer 45:3973–3977. doi:10.1016/j.polymer.2003.10.102

Zeplin PH, Berninger AK, Maksimovikj NC, van Gelder P, Scheibel T, Walles H (2014a) Verbesserung der Biokompatibilität von Silikonimplantaten durch Spinnenseidenbeschichtung: Immunhistochemische Untersuchungen zum Einfluss auf die Kapselbildung. Handchir Mikrochir Plast Chir 46:336–341. doi:10.1055/s-0034-1395558

Zeplin PH, Maksimovikj NC, Jordan MC, Nickel J, Lang G, Leimer AH, Römer L, Scheibel T (2014b) Spider silk coatings as a bioshield to reduce periprosthetic fibrous capsule formation. Adv Funct Mater 24:2658–2666. doi:10.1002/adfm.201302813

Zhang Y, Hu J, Miao Y, Zhao A, Zhao T, Wu D, Liang L, Miikura A, Shiomi K, Kajiura Z, Nakagaki M (2008) Expression of EGFP-spider dragline silk fusion protein in BmN cells and larvae of silkworm showed the solubility is primary limit for dragline proteins yield. Mol Biol Rep 35:329–335. doi:10.1007/s11033-007-9090-6

Zhang C-Y, Zhang D-C, Chen D, M L (2014) A bilayered scaffold based on RGD recombinant spider silk proteins for small diameter tissue engineering. Polym Compos. doi:10.1002/pc.23208

Zhou S, Peng H, Yu X, Zheng X, Cui W, Zhang Z, Li X, Wang J, Weng J, Jia W, Li F (2008) Preparation and characterization of a novel electrospun spider silk fibroin/poly(D, L-lactide) composite fiber. J Phys Chem B 112:11209–11216. doi:10.1021/jp800913k

Zhu ZH, Kikuchi Y, Kojima K, Tamura T, Kuwabara N, Nakamura T, Asakura T (2010) Mechanical properties of regenerated *Bombyx mori* silk fibers and recombinant silk fibers produced by transgenic silkworms. J Biomater Sci Polym Ed 21:395–412. doi:10.1163/156856209x423126

Zhu B, Li W, Lewis RV, Segre CU, Wang R (2015) E-spun composite fibers of collagen and dragline silk protein: fiber mechanics, biocompatibility, and application in stem cell differentiation. Biomacromolecules 16:202–213. doi:10.1021/bm501403f

(EIDESSTATTLICHE) VERSICHERUNGEN UND ERKLÄRUNGEN

(§ 8 S. 2 Nr. 6 PromO)

Hiermit erkläre ich mich damit einverstanden, dass die elektronische Fassung meiner Dissertation unter Wahrung meiner Urheberrechte und des Datenschutzes einer gesonderten Überprüfung hinsichtlich der eigenständigen Anfertigung der Dissertation unterzogen werden kann.

(§ 8 S. 2 Nr. 8 PromO)

Hiermit erkläre ich eidesstattlich, dass ich die Dissertation selbstständig verfasst und keine anderen als die von mir angegebenen Quellen und Hilfsmittel benutzt habe.

(§ 8 S. 2 Nr. 9 PromO)

Ich habe die Dissertation nicht bereits zur Erlangung eines akademischen Grades anderweitig eingereicht und habe auch nicht bereits diese oder eine gleichartige Doktorprüfung endgültig nicht bestanden.

(§ 8 S. 2 Nr. 10 PromO)

Hiermit erkläre ich, dass ich keine Hilfe von gewerblichen Promotionsberatern bzw. –vermittlern in Anspruch genommen habe und auch künftig nicht nehmen werde.

....

Ort, Datum, Unterschrift